SEVENTH CONFERENCE ON NONLINEAR VIBRATIONS, STABILITY, AND DYNAMICS OF STRUCTURES

July 26-30, 1998

Program

Chairmen:

Ali H. Nayfeh and Dean T. Mook

Department of Engineering Science and Mechanics

Virginia Polytechnic Institute and State University

Blacksburg, Virginia 24061

19990616 067

1. AGENCY USE ONLY (Leave Blank)	2. REPORT DATE May 11, 1999	3. REPORT TYPE AND DATES COVERED Final Report

4. TITLE AND SUBTITLE
Seventh Conference on Nonlinear Vibrations, Stability, and Dynamics of Structures

5. FUNDING NUMBERS
DAAG55-98-1-0411

6. AUTHOR(S)
Ali H. Nayfeh, principal investigator

7. PERFORMING ORGANIZATION NAME(S) AND ADDRESS(ES)
Virginia Polytechnic Institute and State University
Blacksburg, VA 24061

8. PERFORMING ORGANIZATION REPORT NUMBER

9. SPONSORING / MONITORING AGENCY NAME(S) AND ADDRESS(ES)

U. S. Army Research Office
P.O. Box 12211
Research Triangle Park, NC 27709-2211

10. SPONSORING / MONITORING AGENCY REPORT NUMBER

ARO 38534.1-EG-CF

11. SUPPLEMENTARY NOTES
The views, opinions and/or findings contained in this report are those of the author(s) and should not be construed as an official Department of the Army position, policy or decision, unless so designated by other documentation.

12 a. DISTRIBUTION / AVAILABILITY STATEMENT

Approved for public release; distribution unlimited.

12 b. DISTRIBUTION CODE

13. ABSTRACT (Maximum 200 words)

14. SUBJECT TERMS

15. NUMBER OF PAGES

16. PRICE CODE

17. SECURITY CLASSIFICATION OR REPORT UNCLASSIFIED	18. SECURITY CLASSIFICATION ON THIS PAGE UNCLASSIFIED	19. SECURITY CLASSIFICATION OF ABSTRACT UNCLASSIFIED	20. LIMITATION OF ABSTRACT UL

DTIC QUALITY INSPECTED 4

FINAL REPORT
SEVENTH CONFERENCE ON
NONLINEAR VIBRATIONS,
STABILITY, AND DYNAMICS OF
STRUCTURES
DAAG55-98-1-0411

July 26-30, 1998
Ali H. Nayfeh and Dean T. Mook
University Distinguished Professor and N. Waldo Harrison Professor
Department of Engineering Science and Mechanics, MC 0219
Virginia Polytechnic Institute and State University
Blacksburg, VA 24061
540-231-5453/540-231-6841/FAX 540-231-2290/EMAIL sallys@vt.edu

May 11, 1999

Objectives

The Seventh conference was held on July 26-30, 1998 and had the following basic objectives:

1. Development of a better understanding of nonlinear dynamical phenomena,

2. Assessment of the state of the art of experimental, computational, and analytical techniques for nonlinear dynamics, including presentations from some of the leading international researchers,

3. Exchange of ideas among some of the leading national researchers,

4. Suggestions for directions of future research, and

5. Bringing graduate students in contact with the experts in nonlinear dynamics, giving some of them an opportunity to present their research, and helping them to know the state of the art.

Scope

The Seventh conference focused on the following topics:

1. Multibody dynamics,

2. Vehicle dynamics,

3. Rotorcraft dynamics,

4. Modal interactions

5. Nonlinear modes and localization,

6. Parametrically excited vibrations: single- and multi-frequency excitations of single- and multi-degree-of-freedom systems,

7. Analytical methods,

8. Computational techniques: efficient algorithms, use of symbolic manipulators, integration of symbolic manipulation and numerical methods, and use of parallel processors,

9. Experimental methods: benchmark experiments, measurements in hostile environments, and instrumentation techniques,

10. Structural control,

11. Identification of nonlinear systems,

12. Dynamics of composite structures,

13. Dynamics of adaptive structures, and

14. Fluid/structure interactions.

Report

The program consisted of invited and contributed papers. The leading researchers were identified and invited to give presentations. Potential contributors were asked to submit a two-page abstract by January 15, 1998. They were notified of their acceptance by March 31, 1998. Full-length papers were due on April 1, 1998. There were one hundred oral presentations. Two-page extended abstracts of the invited and the contributed presentations were published in a Proceedings that was available at the time of the conference. Please find attached ten copies of the Proceedings, including the Program.

The conference was well-received and attended by many prominent researchers. It provided a forum for many fruitful exchanges of ideas and for an assessment of the state of the art. The participants agreed that it was also very successful in: a) contributing to the development of a better understanding of nonlinear phenomena, b) providing an assessment of the state of the art of experimental, computational, and analytical techniques for nonlinear dynamics, and c) fostering an exchange of ideas among leading researchers and a discussion of priorities for future research.

One hundred forty participants came from many countries, including Canada, Germany, Italy, France, Japan, Greece, Turkey, Jordan, The Netherlands, Ukraine, Norway, Lithuania, Sweden, Czech Republic, Israel, Austria, Russia, Poland, Hong Kong, and Brazil. The papers were uniformly good; many were submitted for publication in the journal **Nonlinear Dynamics** and the **Journal of Vibration and Control**. Many papers were reviewed by participants who were in the audience during the presentation. This review process contributed to the lively discussions following many of the presentations and considerably reduced the time needed to evaluate submitted papers.

SEVENTH CONFERENCE ON NONLINEAR VIBRATIONS, STABILITY, AND DYNAMICS OF STRUCTURES

July 26-30, 1998

Program

Sponsored by

The United States Army Research Office
Dr. Gary Anderson, Contract Monitor
and
Virginia Polytechnic Institute and State University

Chairmen:

Ali H. Nayfeh and Dean T. Mook

Department of Engineering Science and Mechanics

Virginia Polytechnic Institute and State University

Blacksburg, Virginia 24061

Schedule for the Seventh Conference on Nonlinear Vibrations, Stability, and Dynamics of Structures

in Blacksburg, Virginia 24061
at the Donaldson-Brown Continuing Education Center on the Campus of the
Virginia Polytechnic Institute and State University
July 26-30, 1998

	Sunday	*Monday*	*Tuesday*	*Wednesday*	*Thursday*
08:00		3.	7.	11.	15.
09:30		*Break*	*Break*	*Break*	*Break*
10:00		4.	8.	12.	16.
11:30		*Lunch*	*Lunch*	*Lunch*	*Lunch*
13:30	Conference begins. 1.	5.	9.	13.	17.
15:00	*Break*	*Break*	*Break*	*Break*	*Break*
15:30	2.	6A. 6B.	10A. 10B.	14.	18.

Sunday, July 26

1320-1330　　　　　**Opening Remarks**

Session 1.

Co-Chairs: V. J. Modi, University of British Columbia, Vancouver, British Columbia, CANADA and **S. W. Smith**, University of Kentucky, Lexington, KY

Sunday, July 26
1330-1500

Deterministic and Stochastic Responses of Nonlinear Coupled Bending-Torsion Modes in a Cantilever Beam
R. A. Ibrahim and M. Hijawi, Wayne State University, Detroit, MI

Dynamics of a Flexible Structure with Pendulum Studied at Various Angles Between Vertical and the Horizontal Positions
A. Ertas, O. Cuvalci, and **S. Ekwaro-Osire**, Texas Tech University, Lubbock, TX

The Effects of Combination Resonance on the Performance of a Nonlinear Vibration Absorber
S. G. Kelly, The University of Akron, Akron, OH and T. Rohde, SES, Inc., Alliance, OH

Nonlinear Nonplanar Dynamics of a Parametrically Excited Inextensional Rotating Elastic Shaft
C. D. Morgan, Kumho Technical Center, Akron, OH and C. M. Krousgrill, Purdue University, West Lafayette, IN

A Fuzzy Chip Controller for Nonlinear Vibrations
F. Casciati, L. Faravelli, F. Giorgi, and G. Torelli, University of Pavia, Pavia, ITALY

Sunday, July 26
1500-1530　　　　　Break

Session 2.

Co-Chairs: R. A. Ibrahim, Wayne State University, Detroit, MI and **M. Yoshizawa,** Keio University, Yokohama, JAPAN

Sunday, July 26
1530-1700

Localization Phenomena in Flexible Systems with Nonlinear Joints
T. A. Nayfeh and A. F. Vakakis, University of Illinois at Urbana-Champaign, Urbana, IL

Regions of Instability of Satellite's Vibrations Parametrically Excited with Harmonics of Gravity Potential
A. **Chigirev,** Crosna Space Communications, Moscow, RUSSIA and J. Volkova, Moscow University of Electronics and Mathematics, Moscow, RUSSIA

Identification of PV Array Nonlinearities from On-Orbit Optical Measurements
K. D. Dippery and S. W. Smith, University of Kentucky, Lexington, KY

Dynamics of an Orbiting Platform-Based Flexible Manipulator System
M. Caron, **V. J. Modi**, C. W. de Silva, University of British Columbia, Vancouver, British Columbia, CANADA, and A. K. Misra, McGill University, Montreal, Quebec, CANADA

Parametric Excitation and Internal Resonance of a Flexible Solar Array
K. Mei and S. W. Smith, University of Kentucky, Lexington, KY

Sunday, July 26
1900-2100 Reception

Monday, July 27

Session 3.

Co-Chairs: F. Vestroni, Università di Roma "La Sapienza", Roma, ITALY and **K. Yasuda**, Nagoya University, Nagoya, JAPAN

Monday, July 27
0800-0930

Response of a Parametrically Excited Rectangular Metallic Plate to a One-to-One Internal Resonance
M. Üstertuna, Ö. Elbeyli, and **G. Anlaş,** Bogaziçi University, Istanbul, TURKEY

One-to-One Internal Resonance of Laminated Shallow Shells
A. Abe, Y. Kobayashi, and G. Yamada, Hokkaido University, Sapporo, JAPAN

Nonlinear Modal Interaction of Liquid Impact-Structural Dynamic under Parametric Excitation
M. A. El-Sayad and R. A. Ibrahim, Wayne State University, Detroit, MI

Internal Resonance in Wire Electro-Discharge Machining
K. D. Murphy, University of Connecticut, Storrs, CT

Effects of the Lorentz Force on Lateral Vibration of a Conducting and Nonmagnetic Cable
S. Shimokawa, H. Kawamoto, T. Sugiura, and M. Yoshizawa, Keio University, Yokohama, JAPAN

Monday, July 27
930-1000   **Break**

Co-Chairs: S. Hanagud, Georgia Institute of Technology, Atlanta, GA and **P. Sniady**, Wroclaw Technical University, Wroclaw, POLAND

Monday, July 27
1000-1130

Vibration Conveyor Dynamics
F. Pfeiffer and P. Wolfsteiner, Technische Universität München, Garching, GERMANY

Computing Analysis of Dynamic Properties of Interactive Drive Systems
C. Kratochvíl and V. Kotek, Technical University of Brno, Brno, CZECH REPUBLIC

Sway Control for Trolley with Pendulum Load
G. Roberson and G. Tao, University of Virginia, Charlottesville, VA

Nonlinear and Experimental Analyses of the Hunting Motion in a Railway Wheelset
H. Yabuno, M. Nunokawa, and N. Aoshima, University of Tsukuba, Tsukuba-City, JAPAN

Prediction of Incipient "Ground Resonance" Instability in a Physical Model of a Rotorcraft
P. V. Bayly, C. M. Cueman, and M. E. Clark, Washington University, St. Louis, MO

Monday, July 27
1130-1330   Lunch

Session 5.

Co-Chairs: F. Pfeiffer, Technische Universität München, Garching, GERMANY and **F. Casciati**, University of Pavia, Pavia, ITALY

Monday, July 27
1330-1500

On the Reconstitution Problem in the Multiple Time Scale Method
A. Luongo and A. Paolone, University of L'Aquila, L'Aquila, ITALY

Escape Criteria for Imperfection Sensitive Single Degree of Freedom Structures Under External Harmonic Loading
D. M. Santee and P. B. Gonçalves, Pontifícia Universidade Católica, Rio de Janeiro, BRAZIL

Response and Stability of Piecewise Linear Oscillators under Parametric and External Excitations
S. Theodossiades, I. Goudas, and **S. Natsiavas**, Aristotle University, Thessaloniki, GREECE

On Applying Special Non-Smooth Temporal Transformations to Systems Parametrically
Excited by Discontinuous Forces
V. N. Pilipchuk, State Chemical and Technological University of Ukraine,
Dnepropetrovsk, UKRAINE

Delaminated Beam Nonlinear Dynamic Response Calculation and Visualization
H. Luo and **S. Hanagud**, Georgia Institute of Technology, Atlanta, GA

Monday, July 27
1500-1530   **Break**

Session 6A.

Co-Chairs: H. G. Davies, University of New Brunswick, Fredericton, New Brunswick,
CANADA and **F. Petrone**, Università di Catania, Catania, ITALY

Monday, July 27
1530-1700

Self-Excited Oscillations of Machine Tools
T. Kalmár-Nagy, F. C. Moon, Cornell University, Ithaca, NY, and G. Stépán, Technical
University of Budapest, Budapest, HUNGARY

Stability of Diamond Turning Processes that use Round Nosed Tools
D. E. Gilsinn, M. A. Davies, National Institute of Standards and Technology,
Gaithersburg, MD, and B. Balachandran, University of Maryland, College Park, MD

Milling of Flexible Structures: Dynamics of Workpiece-Tool Interactions
M. X. Zhao and B. Balachandran, University of Maryland, College Park, MD

Session 6B.

Co-Chairs: S. C. Sinha, Auburn University, Auburn, AL and **L. N. Virgin,** Duke
University, Durham, NC

Monday, July 27
1530-1700

Active Flow Control for Twin-Tail Buffet Alleviation
E. F. Sheta and **O. A. Kandil**, Old Dominion University, Norfolk, VA

Nonlinear Panel Flutter Phenomena in Supersonic and Transonic Flow
B. A. Grohmann, Universität Stuttgart, Stuttgart, GERMANY and **D. Dinkler,**
Universität Braunschweig, Braunschweig, GERMANY

Numerical Prediction of Response Characteristics of a Vortex-Excited Cylinder
E. Guilmineau, Ecole Centrale de Nantes, Nantes, FRANCE

Prediction of the Initial Stage Slamming Force in Rigid and Elastic Systems Impacting on the Water Surface
A. Carcaterra, INSEAN, Rome, ITALY and E. Ciappi, University of Rome 'La Sapienza', Rome, ITALY

Self-Excited Oscillations of Dual Cylindrical Flexible Weir Shells due to the Overflow of Fluid
S. Tanaka and **S. Kaneko**, The University of Tokyo, Tokyo, JAPAN

Tuesday, July 28

Session 7.

Co-Chairs: **Y. Tsujioka**, Keio University, Yokohama, JAPAN and **S. Natsiavas**, Aristotle University, Thessaloniki, GREECE

Tuesday, July 28
0800-0930

Quadratic Map Approximations to Vector Fields
H. G. Davies and K. Karagiozis, University of New Brunswick, Fredericton, New Brunswick, CANADA

Nonplanar Vibrations of Two Phase Cables due to the Alternating Currents
M. Yoshizawa, T. Sugiura, H. Kawamoto, S. Shimokawa, and T. Kawaguchi, Keio University, Yokohama, JAPAN

Bottlenecking Phenomenon Near a Saddle-Node Remnant in an Experimental Duffing Oscillator
S. T. Trickey and L. N. Virgin, Duke University, Durham, NC

Versal Deformation and Local Bifurcation Analysis of Time-Periodic Nonlinear Systems
A. Dávid and S. C. Sinha, Auburn University, Auburn, AL

Dynamic Response and Stability of a Rotating Asymmetrical Shaft Mounted on a Flexible Base
T. Ikeda and S. Murakami, Shimane University, Matsue, JAPAN

Tuesday, July 28
930-1000   **Break**

Co-Chairs: O. A. Kandil, Old Dominion University, Norfolk, VA and **B. T. Nohara**, Mitsubishi Heavy Industries, Nagoya, JAPAN

Tuesday, July 28
1000-1130

Using Karhunen Loeve Decomposition to Analyze the Vibroimpact Response of a Rotor
M. F. A. Azeez and A. F. Vakakis, University of Illinois at Urbana-Champaign, Urbana, IL

Efficient CFD Applications using Discrete-Time Volterra Kernels
W. A. Silva, NASA Langley Research Center, Hampton, VA

Some Computer Assisted Studies in Nonlinear Dynamics
K. Yagasaki, Gifu University, Gifu, JAPAN

An Efficient, Hybrid Frequency-Time Domain Method for the Dynamics of Large-Scale Dry-Friction Damped Structural Systems
J. Guillen and C. Pierre, The University of Michigan, Ann Arbor, MI

Accurate Prediction of the Nonlinear Dynamic Behaviour of an Impact Oscillator
A. Stensson, Lulea University of Technology, Lulea, SWEDEN

Tuesday, July 28
1130-1330   **Lunch**

Session 9.

Co-Chairs: G. Rega, Università di Roma "La Sapienza", Roma, ITALY and **A. F. Vakakis**, University of Illinois at Urbana-Champaign, Urbana, IL

Tuesday, July 28
1330-1500

On Choosing Inputs for System Identification in Nonlinear Systems
T. Doughty, **P. Davies**, and A. K. Bajaj, Purdue University, West Lafayette, IN

An Iterative Approach to Decomposing Harmonics for Nonlinear Systems
S. O'F. Fahey, Electric Boat Corporation, Groton, CT

Experimental Identification Technique in Time Domain for Nonlinear Rotating Shaft Systems
K. Yasuda and K. Kamiya, Nagoya University, Nagoya, JAPAN

Nonparametric Nonlinear System Identification of a Nonlinear Flexible System Using Proper Orthogonal Mode Decomposition
X. Ma, M. A. F. Azeez, and A. F. Vakakis, University of Illinois at Urbana-Champaign, Urbana, IL

Identification of Non-Linear Free Vibration: Time Domain Hilbert Transform Approach
M. Feldman, Israel Institute of Technology, Haifa, ISRAEL

Tuesday, July 28
1500-1530   Break

Session 10A.

Co-Chairs: A. Luongo, University of L'Aquila, L'Aquila, ITALY and **Y. Kobayashi**, Hokkaido University, Sapporo, JAPAN

Tuesday, July 28
1530-1700

Dynamics of a Flexible Cantilever Beam Carrying a Moving Mass
S. A. Q. Siddiqui, M. F. Golnaraghi, and G. R. Heppler, University of Waterloo, Waterloo, Ontario, CANADA

Nonlinear Oscillations in Coriolis Based Gyroscopes
D. Kristiansen and O. Egeland, Norwegian University of Science and Technology, Trondheim, NORWAY

Measurement of Displacements using Nonlinear Systems
A. Mozuras, Research Laboratory, Akustika, Vilnius, LITHUANIA

Electromagnetic Levitation Modeling and Control
B. O. Ciocirlan, D. B. Marghitu, D. G. Beale, and R. A. Overfelt, Auburn University, Auburn, AL

Modal Analysis of Jointed Plates of Composites
M. Lacagnina, F. Petrone, and R. Sinatra, Università di Catania, Catania, ITALY

Tuesday, July 28
1500-1530   Break

Co-Chairs: P. Davies, Purdue University, West Lafayette, IN and **R. Sinatra**, Università di Catania, Catania, ITALY

Tuesday, July 28
1530-1700

Perturbation Analysis of Bifurcations in a Model of Phase Transitions with Order Parameter
J. P. Cusumano and **J. Sikora**, Penn State University, University Park, PA

Implementation of Genetic Algorithm and Simulated Annealing in Layout Optimization of Space Trusses
M. H. Kadivar, M. R. Pourghassem, K. Samani, and **F. Daneshmand**, Shiraz University, Shiraz, IRAN

Modeling and Analysis of Panel Rattle Noise in Automobiles
J. Qiu and **Z. C. Feng**, Massachusetts Institute of Technology, Cambridge, MA

Modeling General, Unsteady, Nonlinear, Aeroelastic Behavior
S. Preidikman and D. Mook, Virginia Polytechnic Institute and State University, Blacksburg, VA

Control of Rolling in Ships by Means of Active Fins Governed by a Neural-Network Controller
D. Liut, D. Mook, H. VanLandingham, and A. Nayfeh, Virginia Polytechnic Institute and State University, Blacksburg, VA

1900   Banquet

Wednesday, July 29

Session 11.

Co-Chairs: A. K. Bajaj, Purdue University, West Lafayette, IN and **K-i. Nagai**, Gunma University, Gunma, JAPAN

Wednesday, July 29
0800-0930

Parametric Identification of an Experimental Magneto-Elastic Oscillator
B. F. Feeny, Michigan State University, East Lansing, MI, C.-M. Yuan, Taoyuan Institute, Taiwan, REPUBLIC OF CHINA, and J. P. Cusumano, Pennsylvania State University, State College, PA

Identification of Viscoelastic Properties of Foam Used in Car Seats
S. White, S. K. Kim, A. K. Bajaj, P. Davies, Purdue University, West Lafayette, IN, and D. K. Showers, Johnson Controls, Milwaukee, WI

Tracking Slowly-Varying Hidden Variables Using Phase Space Reconstruction
J. P. Cusumano, **D. Chelidze**, and A. Chatterjee, Penn State University, University Park, PA

Robust Control of Adaptive Structures with Embedded Sensors and Actuators
D. G. Wilson, C. T. Abdallah, G. P. Starr, University of New Mexico, Albuquerque, NM, and R. D. Robinett, Sandia National Laboratories, Albuquerque, NM

Simulation of Structure Control and Controller Design for Smart Structures within a Finite Element Code
M. W. Zehn and M. Enzmann, Otoo-von-Guericke-Universität Magdeburg, Magdeburg, GERMANY

Wednesday, July 29
930-1000   **Break**

Session 12.

Co-Chairs: S. G. Kelly, The University of Akron, Akron, OH and **J.M. Balthazar**, UNESP, Rio Claro-SP-BRAZIL

Wednesday, July 29
1000-1130

On a Particles-System-Model Representing the Motion of the Generated Wave - A Suitable Model for Control System Design
T. Kobayashi, K. Osuka, Osaka Prefecture University, Nagoya, JAPAN, B. T. Nohara, Mitsubishi Heavy Industries, Nagoya, JAPAN, and T. Ono, Osaka Prefecture University, Nagoya, JAPAN

Neural Networks used for Dynamic Systems Simulation and Neurocontrollers Design
T. Brezina and J. Krejsa, Technical University of Brno, Brno, CZECH REPUBLIC

Control of Large-Scale Linear Time-Periodic Dynamical Systems
S. C. Sinha and **V. Deshmukh**, Auburn University, Auburn, AL

Suppress Chaos in Mathieu's Equation by the System Variable Substitution
F. Wu and Q. Li, Zhejiang University of Technology, Hangzhou, PEOPLES REPUBLIC OF CHINA

Non-Linear Vibration of an Elasto-Plastic Beam with Damage
L. F. P. Franca, M. A. Savi, Instituto Militar de Engenharia, Rio de Janeiro, BRAZIL, and **P. M. C. L. Pacheco**, CEFET/RJ, Rio de Janeiro, BRAZIL

Wednesday, July 29
1130-1330   **Lunch**

Session 13.

Co-Chairs: **O. A. Bauchau**, Georgia Institute of Technology, Atlanta, GA and **S. Kaneko**, University of Tokyo, Tokyo, JAPAN

Wednesday, July 29
1330-1500

Synchronization by Linear Feedback in Chaotic Systems and Lyapunov Exponent
M. Nakai and N. Tsukamoto, Kyoto University, Kyoto, JAPAN

Stabilization of the Parametric Resonance of a Cantilever Beam by Boundary and Bifurcation Control
J. Kawazoe, H. Yabuno, and N. Aoshima, University of Tsukuba, Tsukuba-City, JAPAN

Stabilization of the Parametric Resonance in a Magnetically Levitated Body by a Bifurication Control
H. Sakai, H. Yabuno, and N. Aoshima, University of Tsukuba, Tsukuba-City, JAPAN

Vibration and Control by Parametric Excitation for Driving Belt
H. Okubo, K. Takano, O. Matsushita, K. Watanabe, and Y. Hirase, National Defense Academy, Kanagawa, JAPAN

Seismic Response Mitigation by a Nonlinear Sliding Mode Controller
M. P. Singh, E. E. Matheu, and **L. M. Moreschi**, Virginia Polytechnic Institute and State University, Blacksburg, VA

Wednesday, July 29
1500-1530   **Break**

Session 14.

Co-Chairs: **P. Hagedorn**, Darmstadt University of Technology, Darmstadt, GERMANY and **C. Kratochvíl**, Technical University of Brno, Brno, CZECH REPUBLIC

Wednesday, July 29
1530-1700

Influence of Static Nonlinearity to Resonances Due to a Crack (Superharmonic Resonance)
Y. Ishida and **F. Lu**, Nagoya University, Nagoya, JAPAN

Simulation Study of Orbits with Impacts Between a Rotor and a Backup Bearing
H. Ecker, Vienna University of Technology, Vienna, AUSTRIA

Perturbed Rotations of a Rigid Body, Close to the Lagrange Case
L. D. Akulenko and **D. D. Leshchenko,** Odessa State Academy, Odessa, UKRAINE

Dimensionality and Spatial Coherence in the Complex Finite Dynamics of an
Experimental Continuous Elastic System
R. Alaggio, Universitá dell'Aquila, L'Aquila, ITALY, **G. Rega**, Università di Roma "La
Sapienza", Roma, ITALY, and F. Benedettini, Universitá dell'Aquila, L'Aquila, ITALY

Modeling and Analysis of Switching-Mode DC-DC Regulators
M. Alfayyoumi, A. H. Nayfeh, and D. Borojevic, Virginia Polytechnic Institute and State
University, Blacksburg, VA

Thursday, July 30

Session 15.

Co-Chairs: **D. Dinkler**, Universität Braunschweig, Braunschweig, GERMANY and **D. D. Leshchenko,** Odessa State Academy, Odessa, UKRAINE

Thursday, July 30
0800-0930

The Characterization of Stochastic Layers in Duffing Oscillators
A. C. J. Luo, University of California, Berkeley, CA and R. P. S. Han, University of
Iowa, Iowa City, IA

Instant Chaos and Hysteresis in Beam-Pendulum Systems
I. B. Schwartz, Naval Research Laboratory, Washington, DC and I. T. Georgiou,
Science Applications International Corporation, McLean, VA

Synchronization and Chaos in a Parametrically and Self-Excited System with Two
Degrees of Freedom
J. Warmiński, G. Litak, and K. Szabelski, Technical University of Lublin, Lublin,
POLAND

Experiments on the Chaotic Vibrations of a Cylindrical Shell-Panel: Influence of
Boundary Condition on Chaotic Responses
K-i. Nagai, Gunma University, Gunma, JAPAN, T. Hata, ANEST IWATA, Co., Ltd.,
Yokohama, JAPAN, and T. Yamaguchi, SUBARU Research Center, Co., Ltd., Gunma,
JAPAN

On the Appearance of Chaos in a Nonideal System
D. Belato, UNICAMP, Campinas-SP-BRAZIL, **J.M. Balthazar**, UNESP, Rio Claro-
SP-BRAZIL, H.I. Weber, PUC, Rio de Janeiro-RJ-BRASIL, and D.T. Mook, Virginia
Polytechnic Institute and State University, Blacksburg, VA

Thursday, July 30
0930-1000   **Break**

Session 16.

Co-Chairs: B. Balachandran, University of Maryland, College Park, MD and **F. Lu**, Nagoya University, Nagoya, JAPAN

Thursday, July 30
1000-1130

Sweep Tests on Non-Linearly Damped Vibrating Systems
B. Ravindra and **P. Hagedorn**, Darmstadt University of Technology, Darmstadt, GERMANY

Stick-Slip Vibrations Induced by Alternate Friction Models
R. I. Leine, D. H. van Campen, A. de Kraker, Eindhoven University of Technology, Eindhoven, THE NETHERLANDS, and L. van den Steen, Shell International Exploration and Production B.V., Rijswijk, THE NETHERLANDS

Harmonic Balancing Approach for Hysteretic Multi-Degree of Freedom Oscillators of Masing Type
D. Capecchi, Universitá di Napoli "Federico II", Napoli, ITALY, R. Masiani, and **F. Vestroni**, Università di Roma "La Sapienza", Roma, ITALY

Approximate Model for the Dynamics of Belt/Pulley Frictional Contact
M. J. Leamy, J. R. Barber, and N. C. Perkins, The University of Michigan, Ann Arbor, MI

Dynamics of Rotating Piezoelectric Rings Subjected to Radial Pressure Load
J. Wauer, Universität Karlsruhe, Karlsruhe, GERMANY

Thursday, July 30
1130-1330   **Lunch**

Session 17.

Co-Chairs: H. W. Haslach, Jr., University of Maryland Baltimore Country, Baltimore, MD and **M. Santee**, Pontifícia Universidade Católica, Rio de Janeiro, BRAZIL

Thursday, July 30
1330-1500

Rotor Drop Nonlinear Transient Analysis of Magnetic Bearing Rotors on Auxiliary Bearings
P. E. Allaire and **W. C. Foiles**, University of Virginia, Charlottesville, VA

Modeling and Analysis of a Self -Centering Auxiliary Bearing
G. T. Flowers and A. George, Auburn University, Auburn, AL

Effects of Flux Saturation in a Magnetic Bearing on Rotor Motion
M. Chinta and A. B. Palazzolo, Texas A & M University, College Station, TX

Analysis of Flexible Multi-Body Systems with Intermittent Contacts
O. A. Bauchau, Georgia Institute of Technology, Atlanta, GA

Dynamics of Self-Excited Oscillators with 1:2 Internal Resonance
G. Verros and **S. Natsiavas**, Aristotle University, Thessaloniki, GREECE

Thursday, July 30
1500-1530 **Break**

Session 18.

Co-Chairs: J. Wauer, Universität Karlsruhe, Kaiserstraße, Karlsruhe, GERMANY and
G. T. Flowers, Auburn University, Auburn, AL

Thursday, July 30
1530-1700

Applying the POD Method for Modal Analysis and Modal Interaction in Coupled Structural/Mechanical Systems
I. T. Georgiou, Science Applications International Corporation, McLean, VA and I. B. Schwartz, Naval Research Laboratory, Washington, DC

Multi-Body Analysis of a Tilt-Rotor Configuration
G. L. Ghiringhelli, **P. Masarati**, P. Mantegazza, Politecnico di Milano, Milano, ITALY, and M. W. Nixon, NASA Langley Research Center, Hampton, VA

Periodic Internal Pressurization of a Nonlinear Elastic Sphere in an External Fluid
H. W. Haslach, Jr., University of Maryland Baltimore Country, Baltimore, MD

Motion Reduction in Systems with Uncontrollable Modes and/or Noncollocated Inputs: A Perturbation-Based Approach
R. R. Soper, W. Lacarbonara, C-M. Chin, A. H. Nayfeh, and D. T. Mook, Virginia Polytechnic Institute and State University, Blacksburg, VA

Post-Buckling Analysis of Nonlinear Dynamical Thick Beam Model and Dual Variational Principles
D. Y. Gao, Virginia Polytechnic Institute and State University, Blacksburg, VA

Sunday, July 26
1320-1330 Opening Remarks
1330-1500
Session 1.

Deterministic and Stochastic Responses of Nonlinear Coupled Bending-Torsion Modes in a Cantilever Beam

R. A. IBRAHIM AND M. HIJAWI
Wayne State University, Department of Mechanical Engineering, Detroit, MI 48202

Abstract. The purpose of this study is to understand the main differences between the deterministic and random response characteristics of an inextensible cantilever beam (with a tip mass) in the neighborhood of combination parametric resonance. The excitation is applied in the plane of largest rigidity such that the bending and torsion modes are cross-coupled through the excitation. In the absence of excitation, the two modes are also coupled due to nonlinear inertia forces. This means that both linear generalized and normal coordinates are the same. For sinusoidal parametric excitation, the beam experiences instability in the neighborhood of the combination parametric resonance $\Omega = \omega_u + \omega_\phi$, where Ω is the excitation frequency, and ω_u and ω_ϕ are the first bending and torsion mode natural frequencies, respectively. The dependence of the response amplitude on the excitation level reveals three distinct regions: nearly linear behavior, jump phenomena, and energy transfer. In the absence of nonlinear coupling, the stochastic stability boundaries are obtained in terms of sample Lyapunov exponent. The response statistics are estimated using Monte Carlo simulation and measured experimentally. The excitation center frequency is selected to be close to the sum of the bending and torsion mode frequencies. The beam is found to experience a single response, two possible responses, or non-stationary responses, depending on excitation level. Experimentally, it is possible to obtain two different responses for the same excitation level by providing a perturbation to the beam during the test.

DYNAMICS OF A FLEXIBLE STRUCTURE WITH PENDULUM STUDIED AT VARIOUS ANGLES BETWEEN VERTICAL AND THE HORIZONTAL POSITIONS

Atila Ertas, Olkan Cuvalci and S. Ekwaro-Osire
Texas Tech University,   Dept. of Mech. Engineering,   Lubbock, TX 79401

ABSTRACT

A passive vibration absorber for large flexible structures is modeled by a column/beam with an appendage consisting of a mass-pendulum attached at its tip. The model is rotated from the vertical position to the horizontal and vise versa at 5 degrees increments to investigate energy interaction between the system (column/beam) and the absorber (appendage). Autoparametric conditions are only tuned in the horizontal or in the vertical position of the model. Experimental dynamics indicate that the motion is quasiperiodic when the system is around the vertical position. In the quasiperiodic motion, there are some windows which include periodic motions. If the system is oriented in the horizontal position, it shows periodic motion and one-to-two and one-to-one relation between the modes. The objective of this study is to show the effect of the energy absorption phenomenon at various column/beam positions in the x-y plane.

INTRODUCTION

Nayfeh [1] examined the response of the two-degree-of-freedom system to multifrequency parametric excitations for different resonance combinations. Ibrahim [2] investigated two mode interaction in a structure containing liquid as a model of an autoparametric absorber. It was shown that energy transfer could occur when the lower mode frequency is equal to one-half of the higher mode frequency. Autoparametric vibration has been investigated among others by including Zavodney and Nayfeh [3], and Sprysl [4].

Mustafa and Ertas [5] investigated a flexible column with an appendage consisting of a mass-pendulum attached to its tip, and Cuvalci and Ertas [6] studied the beam-tip mass-pendulum model as a vibration absorber devices. In this present study, the models studied by the previous authors, were rotated from vertical position to horizontal position and vise versa at 5 degrees increments. Internal frequency ratio was tuned in the vertical or in the horizontal position just before starting experiments, such that

$$\Omega = \omega_s = 2\omega_a \tag{1}$$

The above ratio remained unchanged for each rotation. From the experimental data, frequency response curves, time series, phase planes, FFT and two and one dimensional sections of the torus were plotted. The aforementioned plots offered an insight in the dynamics of the system.

EXPERIMENTAL RESULTS AND DISCUSSIONS

Experiments were performed for two main setups. First, the model was setup as a beam-tip mass-pendulum system. Then it was rotated in 5 degrees increments to the vertical position. Second, the model was set up as a column-tip mass-pendulum system. Then it was rotated in 5 degrees increments to the horizontal position. For both cases, internal frequency ratio was tuned in the initial position (vertical or horizontal) as described in Equation (1).

To observe the dynamics of the experimental system, four sets of plots were extracted from experimental data. The first set of plots were frequency response curves. The second set of plots includes time histories, phase planes, and Fast Fourier Transforms. The third set of plots show the cover of the two-torus and , specified section on it, and the first return map of the specified section. The fourth set of plots show maximum displacements of the system and the absorber, the response relation between the two modes and the absorption regions with respect to the rotating angel.

CONCLUSION

The system in vertical direction (column-tipmass-pendulum) shows more complex dynamics than the system in horizontal direction (beam-tipmass-pendulum). The column-tip mass-pendulum system has quasiperiodic motion interrupted by webs of periodic windows. This dynamic was not changed by rotation of the system. However, after a critical angle of rotation, the autoparametric interaction disappeared. Therefore, beyond this critical angle the energy interaction between the system and absorber was not

observed. The same phenomenon was valid for the beam-tip mass-pendulum system. Experiments show that the relation between the system and absorber was also related to the forcing amplitude. The autoparametric interaction region becomes larger by increasing the forcing amplitude. Hence, when autoparametric condition for the system was tuned in the horizontal or the vertical position, the energy transfer between the modes was perfectly observed in the neighborhood of the resonance at the current positions. The energy absorption effect on the system was observed to gradually decrease by rotating the angle of rotation. The absorber device absorbs energy from the system until the critical boundary was reached. The critical boundary angel depends on the forcing amplitude and is increased or decreased by increasing or decreasing the forcing amplitude, respectively. At the internal frequency ratio 0.5 (1/2), a perfect absorption was observed. In the close neighborhood of 0.5 (i.e.. 0.48-0.52) the absorption decreases and for the values more diverging from 0.5 the absorption was completely unobservable and the system behaved as an uncoupled system.

REFERENCES

[1]   Nayfeh, A. H., (1983), " Response of the two-degree-of-freedom System to Multifrequency Parametric Excitations", Journal of Sound and Vibration, Vol. 88, No. 1, pp. 1 - 10.

[2]   Ibrahim, R. A., (1975), "Autoparametric Resonance in a Structure Containing Liquid - Part 1: Two Mode Interaction", Journal of Sound and Vibration, Vol. 2, No. 2, pp. 159 - 179.

[3]   Zavodney, L. D. and Nayfeh, A. H., (1986), "The Nonlinear Response of a Slender Beam Carrying a Lumped Mass to a Principle Parametric Excitation: Theory and Experiment," Int. Journal of Non-Linear Mechanics, Vol. 24(2), pp. 105 - 125.

[4]   Sprysl, H., (1987), "Internal Resonance of Non-Linear Autonomous Vibrating Systems with two-degrees-of-freedom," Journal of Sound and Vibration, Vol. 112(1), pp. 63 - 67.

[5]   Mustafa, G. and Ertas, A., (1995), "Experimental Evidence of Quasiperiodicity and Its Breakdown in the Column-Pendulum Oscillator", Journal of Dynamic Systems, Measurement and Control, Vol. 117, pp. 218 - 225.

[6]   Cuvalci, O. and Ertas, A., (1996), "Pendulum as Vibration Absorber for Flexible Structures: Experiments and Theory", Journal of Vibration and Acoustic, Vol. 118, pp. 558 - 566.

The Effects of Combination Resonance on the Performance of a Nonlinear Vibration Absorber

S. Graham Kelly
Department of Mechanical Engineering
The University of Akron

Tim Rohde
SES, Inc.
Alliance, Oh

A dynamic vibration absorber can be used to alleviate the large amplitude response of a system when it is subject to a harmonic excitation at a frequency near one of the system's natural frequencies. Addition of a correctly tuned linear vibration absorber to a n-degree-of-freedom system (the primary system) leads to a n+1-degree-of-freedom system with natural frequencies away from the excitation frequency. If both the primary system and the absorber are undamped then the steady-state amplitude of the primary system is zero at the frequency to which the absorber is tuned. However the frequency response of the system is such that a small deviation in frequency from the tuned frequency can lead to a large steady-state amplitude in the primary system. In addition one of the natural frequencies of the resulting system is less than the tuned frequency, leading to the possibility of large amplitude during start up and shut down.

If a nonlinear elastic element is used in the vibration absorber the above concerns are reduced. If an elastic element with a cubic nonlinearity is used a jump phenomenon occurs during start up and shut down, reducing the maximum amplitudes during these periods from those attained using a linear absorber. The presence of the backbone curve also leads to a frequency response curve that is nearly flat near the excitation frequency.

Previous investigator [1], [2], and [3] using the Galerkin method or the Duffing method to analyze the frequency response of the primary system using an elastic element with a cubic nonlinearity in the absorber. However these methods do not capture combination resonance effects that may be present. Consider a one-degree-of-freedom linear system excited by a harmonic excitation of frequency ω. When an absorber is added the natural frequencies of the linearized two-degree-of-freedom system are ω_1 and ω_2. Since the excitation frequency is near

$$\omega_1 + \omega_2 \approx 2\omega$$

the primary system's natural frequency it can be shown that
Since this is the case a combination resonance exists in the resulting system. The purpose of this paper is to analyze the system in the presence of this combination resonance.

The primary system is an undamped mass-spring system exited by a single frequency harmonic excitation whose frequency is near the primary system's natural frequency. The absorber added to the primary system is a mass-spring-viscous damper system in which the nondimensional

$$F = x + \varepsilon x^3$$

force-displacement relationship for the elastic element is
where ε is a small dimensionless parameter. The damping ratio of the absorber is also of order ε. The method of multiple scales is used to solve the coupled nonlinear nondimensional differential equations relating the displacements of the primary mass and the absorber mass. The presence of the combination resonance is apparent only when a transformation is made to the system's principal coordinates. A detuning parameter is introduced to capture the essence of the

$$\varepsilon\sigma = 2\omega - \omega_1 - \omega_2$$

combination resonance
Equations for the amplitudes and phases of the principal coordinates are derived. These equations are solved using Runge-Kutta. Transformation is made to the set of original coordinates. Frequency response of the primary mass in terms of the detuning parameter is obtained for various values of the damping ratio. The effect of the combination resonance on the performance of the absorber is discussed.

[1] Arnold, F.R., *Journal of Applied Mechanics*, Vol.22, pp487-492, 1955.
[2] Pipes, L.A., *Journal of Applied Mechanics*, Vol. 75., pp515-58, 1953.
[3] Roberson, R.E. *Journal of the Franklin Institute*, Vol. 254, pp205-220, 1952.

Equations for the amplitude and phase of th

NONLINEAR NONPLANAR DYNAMICS OF A
PARAMETRICALLY EXCITED
INEXTENSIONAL ROTATING ELASTIC SHAFT

Christopher D. Morgan, Kumho Technical Center and Charles M. Krousgrill, Purdue University

ABSTRACT

The nonlinear dynamics of a clamped-clamped/sliding inextensional rotating elastic shaft subject to a harmonically varying axial load is investigated by means of a perturbation method, numerical integration, and Floquet Theory. The equations of motion that govern the flexural motion about two principal axes and torsion retain the order three nonlinear inertia and geometric terms. The frequency of parametric excitation is set to be nominally 2 times the primary shaft resonance and the primary shaft resonance in orthogonal directions are set to be nominally equal. A stiffness detuning parameter is introduced to quantify the effect of small variations in orthogonal resonance frequencies and a frequency detuning parameter is used to quantify the effect of small variances in parametric excitation frequency.

Divergence and flutter limits are demonstrated as a function of stiffness detuning, frequency detuning, and rotation rate. Where divergence is detected, steady state amplitude motions are shown to exist due to the nonlinear terms. Where flutter is detected, periodic amplitude limit cycles are shown to form. Period-doubling bifurcations and symmetry-breaking bifurcations are demonstrated, as is chaotic motion.

A Fuzzy Chip Controller for NonLinear Vibrations

F. Casciati, L. Faravelli and F. Giorgi
Dept. of Structural Mechanics - University of Pavia
Pavia - 27100, Italy

and

G. Torelli
Dept. of Electronics - University of Pavia
Pavia - 27100, Italy

Abstract. Fuzzy Logic ability in managing nonlinear vibration control problems shows a major drawback: the slow reaction time offered by a software implemented controller. The adoption of integrated chip controllers permits one to overcome it. Nevertheless, designing a fuzzy controller for structural control purposes requires a fine work of tuning. This can be done over an equivalent electronic circuit, rather than by an expensive laboratory environment for testing frame specimen. Conceiving and implementing electronic circuit equivalent to a single degree of freedom system is the topic of this paper.
A case study is finally developed. It discusses the major features of the adopted chip controller. A brief overview of the results of the laboratory tests performed in order to properly tune the fuzzy project for the control of civil structures is also given.

Sunday, July 26
1530-1700
Session 2.

Localization Phenomena in Flexible Systems with Nonlinear Joints

T. A. Nayfeh and A.F. Vakakis
Department of Mechanical and Industrial Engineering
University of Illinois at Urbana-Champaign
Urbana, Illinois

The control of unwanted vibrations in modern lightweight, flexible space structures presents a real challenge to design engineers. Traditional techniques for controlling the vibrational energy include the use of elastomers, vibration isolation padding, damping tapes, springs, rubber mounts, and cork padding, passive vibration absorbers, and, in many instances, active controllers. There are many disadvantages to the use of the above measures. The linear passive elements are effective only in small-predetermined frequency ranges. Active controllers require energy and add to the weight of the structure, which will significantly increase the cost of the use of such devices in space structures. Recent works in the literature have shown that the use of nonlinearities may actually create more desirable dynamic behavior in such structures.

In this work, we show how the use of nonlinearities can enhance the control of unwanted vibrations by passively confining the vibrational energy to substructures. The dynamics of large flexible space trusses subjected to impact and repetitive loading is considered (Figure 1). Each truss element is modeled as a thin beam whose transverse motion is coupled to the axial motion by quadratic nonlinear stretching terms

$$\rho A \frac{\partial^2 u}{\partial t^2} - EA \frac{\partial^2 u}{\partial x^2} = \frac{1}{2} EA \left(1 - 2 \frac{\partial u}{\partial x} \right) \left(\frac{\partial w}{\partial x} \right)^2 + G$$

$$\rho A \frac{\partial^2 w}{\partial t^2} + EI \frac{\partial^{'''} w}{\partial x^4} = EA \frac{\partial}{\partial x} \left(\frac{\partial u}{\partial x} \frac{\partial w}{\partial x} - \left(\frac{\partial u}{\partial x} \right)^2 \frac{\partial w}{\partial x} + \frac{1}{2} \left(\frac{\partial w}{\partial x} \right)^2 \right) + F$$

where ρ is mass per unit length, E is the modulus of elasticity, A is the cross sectional area, I is the mass moment of inertia, G and F are the applied external forces, and u and w are the longitudinal and transverse displacements respectively. Additional nonlinearity is introduced through the use of joints of the preloaded backlash type. These joints behave as tri-linear springs (Figures 2 and 3). The system is modeled using the finite-element

method and the equations of motion are solved by a second-central-difference explicit time integration scheme.
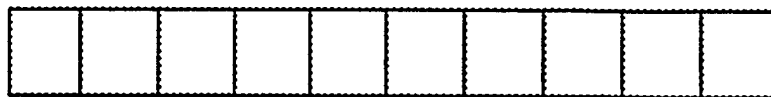

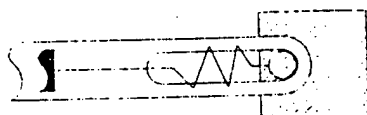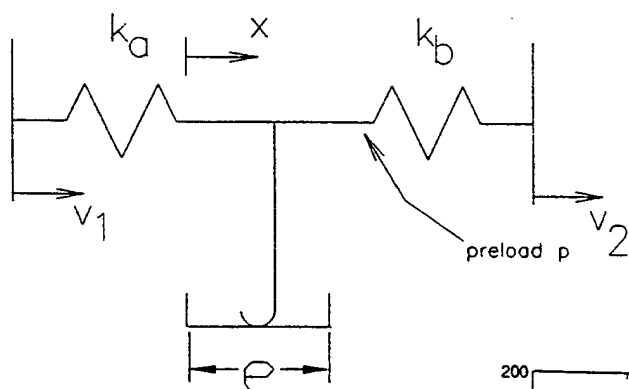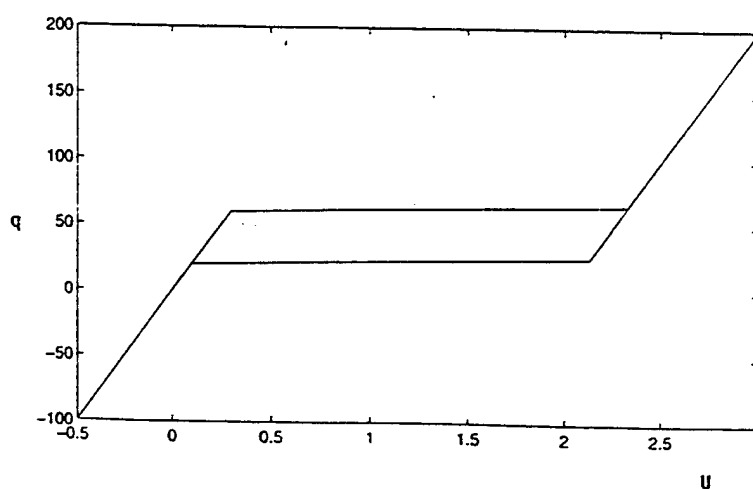Figure 1: A representative truss.

Figure 2: A schematic of the joint with preloaded backlash.

(a)

(b)

Figure 3: Joint with a backlash: (a) equivalent model, (b) a typical load-deflection curve (Modified from: Onoda, Sano, and Minesugi, "Passive Damping of Truss Vibrations Using Preloaded Joint Backlash," *AIAA Journal*, 33, 1995, pp. 1335-1341).

Regions of Instability of Satellite's Vibrations Parametrically Excited with Harmonics of Gravity Potential

A.Chigirev, J.Volkova

The problem under consideration is vibration instability of satellite revolving around a central body with non-central gravitational field. This problem is closely connected with nonlinear vibration dynamics. As a result of the study the asymptotic expressions for boundaries of the instability regions of satellite's vibrations were derived.

It is well-known that the trajectory of a satellite in low orbit differs significantly from expected orbital movement following the Keplerian law, for the effective Earth's gravity potential slightly deviates from a central gravity potential. Moreover, the lower the satellite's orbit the more is discrepancy between the observed satellite's path and the expected Keplerian orbit.

Both global positioning system (GPS) with low-orbit satellites and communication systems based on low-orbit satellite constellations such as "Iridium" are widely put into operation. To operate satellites of the systems properly it is important to predict precisely the satellite's spatial position as well as its trajectory which is perturbed by non-central gravitational field of the Earth. In the paper a special attention is paid to destabilizing effect of the non-central gravitational field on satellite's movement in the resonance cases. Along with mentioned threat of instability just the same destructive resonance effect might be also considered as helpful one to propel the satellites by means of such an unusual non-reactive propulsion technique.

A simple two-dimensional plane model was chosen to estimate the resonance effect of spatial non-uniformity of gravity potential upon a satellite's movement. When the satellite's orbit is close to a circle, its eccentricity can be treated as a small parameter. For this case the linearized equations of satellite's movement in a non-inertial rotating coordinate system are studied. In the coordinate system the equations' yields a solution resulting in ellipse-shaped trajectories both for satellite as well as for central body. Making its oscillation with respect to the rotating coordinate system the satellite moves uniformly in

the ellipse-shaped "suborbit" with center near satellite's equilibrium point expected. The ellipse has a constant eccentricity, with ellipse's center drifting along the unperturbed satellite's orbit at a small constant velocity.

Affected upon the satellite the non-central gravity force is assumed to depend only on an angle variable describing satellite's revolution around the Earth rotating about the same axis of rotation. That is why in this elementary model the gravity force can be expanded into spatial Fourier series of the angle variable only. The motion equations are reduced to Mathieu equation and a linear equation of the second order. The system resembles well-known equations of a pendulum with vibrating suspension.

Dependence of instability regions on the mechanical system parameters is analyzed. An asymptotic solution of Mathieu equation was searched, the ratio of amplitudes of second and zero harmonics being assumed to be a small parameter. Separation of the "slow" and "fast" variables results in a new form of equations, which allows to overcome some difficulties connected with complicated motion of satellites in orbit.

It is found that the second harmonic of transversal component of gravity force applied to low orbital satellite can induct satellite's vibration. Asymptotic calculation of boundary parameters of Mathieu equation were made. A number of instability regions of satellite's vibrations were plotted in term of the calculation.

In the paper is shown that if even taking into consideration atmospheric drag inherited for low orbit satellite the examined resonance phenomenon is able to bring about certain satellite's vibration emerging in mechanical system comprising a lump-shaped rotating planet and its satellite. It is found that on getting significant amplitude in vibration the satellite leaves the boundaries of resonance area. Thus, at exciting these types of oscillations the satellite's vibration amplitude appeared to be practically restricted.

It is reasonable to expand the method developed for circular orbits to orbits with high eccentricity when effect under investigation is manifested essentially stronger. The effect might be made even more powerful by redistributing the satellite's mass periodically in step with satellite's reaching the perigee and apogee of the orbit with high eccentricity.

Identification of PV Array Nonlinearities from On–Orbit Optical Measurements

K. D. Dippery
S. W. Smith
Department of Mechanical Engineering
University of Kentucky
Lexington, Ky 40506–0046
USA

ABSTRACT

Recent investigations into the dynamics of large flexible substructures have revealed a wide variety of complex behaviors. Experiments conducted on a laboratory phenomena model of a solar array mast, for example, revealed nonlinear modal interactions resulting in subharmonic, superharmonic and combination resonances, in addition to jump phenomena, saturation and two–way modal energy exchange [1]. Nonlinear modal interactions are also suspected of playing a role in complex behaviors exhibited by solar arrays on the Hubble Space Telescope [2].

A method of identifying mathematical models for systems which exhibit modal interactions caused by internal resonance has recently been developed [3]. This method combines time–frequency and wavelet transform analysis with the Minimum Model Error state estimation algorithm [4] to produce an optimal model form for the system nonlinearities. A least squares algorithm then produces best–fit estimates of the unknown coefficients in the model.

In this paper, this method is applied to on–orbit measurements to produce a model of the Kvant–II solar array of the Russian Mir space station. These measurements were recorded as part of the PASDE (Photogrammetric Appendage Structural Dynamics Experiment) experiment, flown on space shuttle mission STS–74, in November 1995. In this experiment, six video cameras recorded over 113 minutes of structural response of the Kvant–II solar array to various excitations, including shuttle–Mir docking, shuttle reaction control system firings, and day–to–night / night–to–day transitions. Photogrammetric techniques, including two–dimensional cross–correlation and sub–pixel interpolation methods, were used to produce measurements of displacement at 12 locations on the solar array, in the x–, y– and z–directions [5, 6].

Sample measurements of the solar array response are shown in Figure 1. The lowest–frequency wavelet coefficients for these sample measurements are shown in Figure 2. The varia-

tions in amplitude of the wavelet coefficients in the range 25–70 seconds indicate the possible presence of nonlinear interactions.
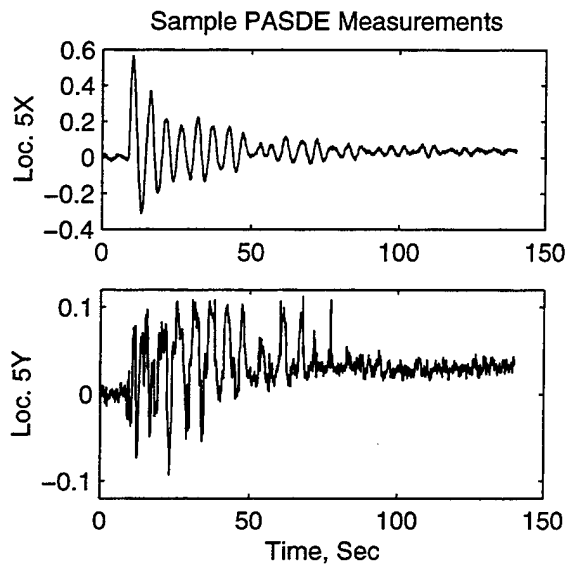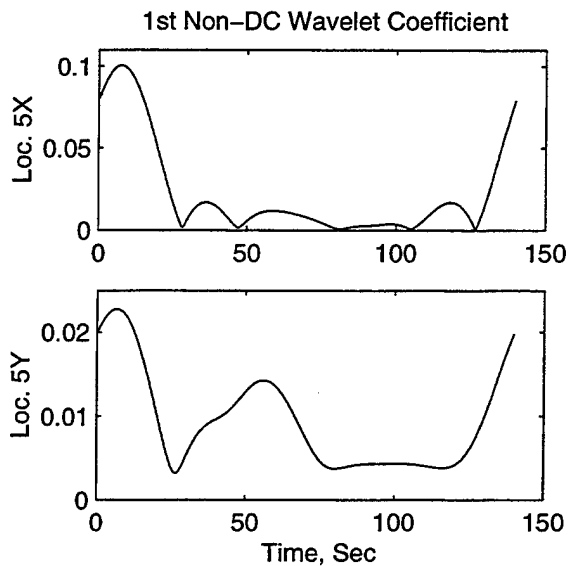

Figure 1. Sample on–orbit optical measurements.

Figure 2. 1st wavelet coefficient of measurements shown in Figure 1.

REFERENCES

1. Smith, S. W, Knowles, G. I. and Farthing, S. R. *Preliminary Survey of Nonlinear Response Behaviors of a Solar Array Phenomena Model*, AIAA–96–1510–CP, Proceedings of the 37th AIAA/ASME/ASCE/AHS/ASC Structures, Structural Dynamics and Materials Conference, Salt Lake City, Utah, pp. 2044–2054, 1996.

2. Smith, S. W., Balachandran, B. and Nayfeh, A. H. *Nonlinear Interactions and the Hubble Space Telescope*, AIAA–92–4617–CP, Proceedings of the AIAA Guidance, Navigation and Control Conference, Hilton Head, South Carolina, pp. 1460–1470, 1992.

3. Dippery, K. D. Model Identification for Systems with Internal Resonance, PhD Dissertation, University of Kentucky, 1998.

4. Mook, D. J. *Estimation and Identification of Nonlinear Dynamic Systems*, AIAA Journal, Vol. 27, No. 7, pp. 968–974, 1989.

5. Gilbert, M. G. and Welch, S. S. *STS–74/MIR Photogrammetric Appendage Structural Dynamics Experiment*, AIAA–96–1493–CP, Proceedings of the 37th AIAA/ASME/ASCE/AHS/ASC Structures, Structural Dynamics and Materials Conference, Salt Lake City, Utah, pp. 1594–1604, 1996.

6. Pappa, R. S., Gilbert, M. G. and Welch, S. S. *Simulation of the Photogrammetric Appendage Structural Dynamics Experiment*, NASA Technical Memorandum 110221, 1995.

DYNAMICS OF AN ORBITING PLATFORM-BASED FLEXIBLE MANIPULATOR SYSTEM

M. CARON[*]
V. J. MODI[**]
C. W. de SILVA[***]
Department of Mechanical Engineering, University of British Columbia, Vancouver, B.C., Canada V6T 1Z4

A. K. MISRA[†]
Department of Mechanical Engineering, McGill University, Montreal, Quebec, Canada H3A 2K6

Space manipulators present several features uncommon to ground-based robots: they operates in a microgravity environment; are highly flexible; often mobile; and have a degree of redundancy (Caron, 1996). The space platform, which supports the manipulator and negotiates a prescribed trajectory, can have its attitudes affected by the manipulator's maneuvers. On the other hand, libration of the platform can influence the performance of the manipulator, thus making the platform and the manipulator dynamics highly coupled (Xu and Shum, 1994; Caron, 1996).

In general, the links of space manipulators tend to be long, light, and consequently highly flexible. The mobile manipulator system abode the proposed International Space Station will be 17.6m long, even without an end-effector. The manipulator will be able to handle payload with a mass two orders of magnitude greater than its own (payload mass $\approx$ 100,000kg, manipulator mass $\approx$ 1,000kg; Robert, 1997). Moreover, the platform supporting the manipulator can be highly flexible, as is the case for the Space Station (Modi and Suleman, 1989). The combination of these factors can result in large structural vibrations.

An important aspect of the space system design is the built-in redundancy to cope with possible failure (Kimura, Tsuchiya and Suzuki, 1995). This implies a greater number of degrees of freedom than required to execute a given task. The redundancy is also important for obstacle avoidance, performance optimization, and introduction of desired constraints.

With this as background, the paper studies, using an O(N) Lagrangian formulation, dynamics of a novel mobile flexible manipulator system, operating abode an elastic platform in a given orbit around the Earth. The manipulator consists of an arbitrary number of interconnected modules forming a chain geometry. Each module comprises of two links, one free to slew while the other can deploy and retrieve. Such a manipulator with a combination of revolute and prismatic joints is able to change its geometry (Figure 1), has relatively simple kinematics, a marked decrease in dynamic coupling, and a

[*] NSERC Graduate Fellow
[**] Professor Emeritus; Fellow ASME, AIAA
[***] NSERC Chair Professor; Fellow ASME; Senior Member IEEE
[†] Professor; Associate Fellow AIAA

reduction in the number of singularity conditions. This class of problems are of contemporary interest and have never been encountered before.

An extensive parametric study assesses the effect of initial disturbances, system flexibility, admissible functions for discretization, number modules, payload and maneuver profiles. Results suggest significant coupling between the rigid body motion and structural vibrations, with the system flexibility substantially affecting the manipulator's performance .

REFERENCES

[1] Caron, M., 1996, "Planar dynamics and control of space-based flexible manipulators with slewing and deployable links," M.A.Sc. thesis, Department of Mechanical Engineering, University of British Columbia, Vancouver, B.C., Canada, pp.1-14, 56-108.

[2] Kimura, S., Tsuchiya, S., and Suzuki, Y., 1995, "Fault-adaptive kinematic control of a hyper-redundant manipulator system for a Geostationary Servicing Vehicle (GSV)," Paper No. IAF-95-A·7·09, *46th International Astronautical Congress*, Oslo, Norway, October.

[3] Modi, V. J. and Suleman, A., 1989, "A dynamic study of the proposed space station type configuration," *Acta Astronautica* **19**(5), 377-391.

[4] Robert, O. L., 1997, "Canada and the ISS," *SpaceFlight* **39**, 113.

[5] Xu, Y. and Shum, H. Y., 1994, "Dynamic control and coupling of a free-flying space robot system," *Journal of Robotic Systems* **11**(7), 573-589.
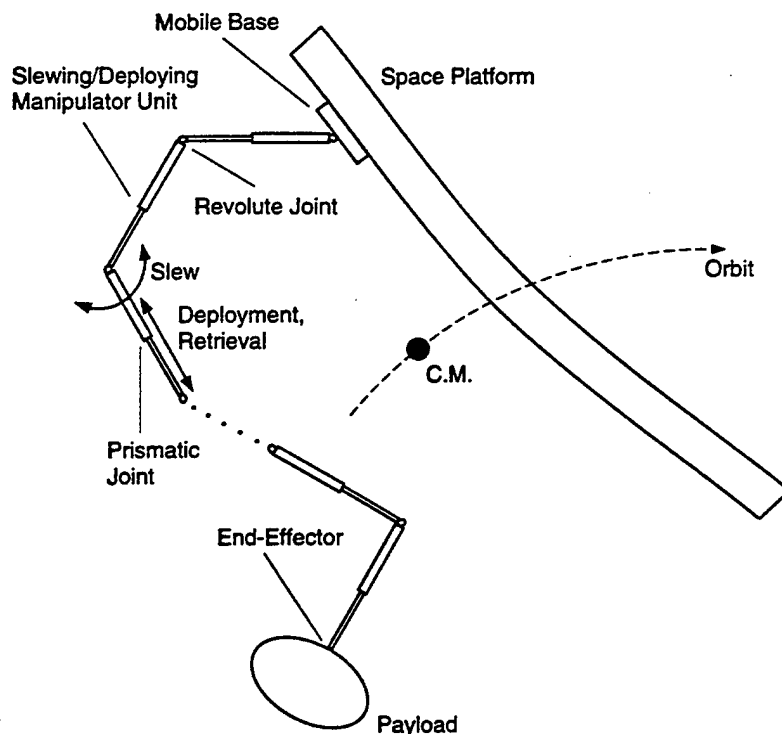
Figure 1   A schematic diagram of the mobile flexible deployable manipulator, based on an elastic space platform, considered for study.

PARAMETRIC EXCITATION AND INTERNAL RESONANCE OF A FLEXIBLE SOLAR ARRAY

Kuiyin Mei and Suzanne Weaver Smith
Department of Mechanical Engineering
University of Kentucky
Lexington, KY 40506-0046

Orbiting platforms of the size and complexity of the impending International Space Station (ISS) present many challenges. Among these is anticipating and understanding the dynamics of the large, flexible, deployable solar arrays. An experimental survey with a laboratory model solar array (support structure only as shown in Figure 1 left) revealed nonlinear behaviors including subharmonic and combination resonances, jumps, and modal energy exchanges. A smaller benchtop model array exhibited similar phenomena [1]. With longitudinal base excitation of the arrays representing vibrational motion of the spacecraft, repeated failures of the lower crossbars of the models occurred (Figure 1 right). This was unexpected due to the small-amplitude motion of the mast at the lower crossbar attachment point.

Linear and nonlinear analytical models were previously developed for the laboratory solar array. These models were correlated to experimental modal results [2]. In this paper, a new analysis is undertaken, following the approach of Nayfeh, Nayfeh, and Mook for a "T-shaped" structure [3]. Deflection functions are first expressed as an expansion with the third (primarily mast second bending) and fifth (primarily lower crossbar first bending) linear free-vibration modes of the solar array structure. This expansion is substituted into the kinetic and potential energy expressions and the result is integrated over the lengths of the beams. Nonlinear differential equations of motion are then obtained by substitution of the result into Lagrange's equations.

To analyze the parametric response of the out-of-plane coupled motion, the method of multiple scales is used. Two detuning parameters are defined to represent the relationships between the crossbar and mast mode frequencies ($\omega_5 \approx 3\omega_3$) and the excitation and mast frequencies ($\Omega \approx 2\omega_3$). The final equations for steady-state motion are as follows:

$$\omega_3 C_1 X_1 - \frac{1}{4}(\omega_3^2 E_{61} + \omega_3^2 E_{71} - \omega_3\omega_5 E_{81} + \omega_5^2 E_{91} - E_{141})X_1^2 X_2 \sin(\beta_1) + E_{171}A_0 X_1 \sin(\beta_2) = 0 \tag{1}$$

$$\omega_3 X_1 \sigma_2 + \frac{1}{4}(-2\omega_5^2 E_{21} + 2\omega_3^2 E_{31} + 2\omega_3^2 E_{121} - 2E_{151})X_1 X_2^2 + \frac{1}{4}(-\omega_3^2 E_{101} + 3\omega_3^2 E_{111} - 3E_{131})X_1^3$$
$$+ \frac{1}{4}(\omega_3^2 E_{61} + \omega_3^2 E_{71} - \omega_3\omega_5 E_{81} + \omega_5^2 E_{91} - E_{141})X_1^2 X_2 \cos(\beta_1) - E_{171}A_0 X_1 \cos(\beta_2) = 0 \tag{2}$$

$$\omega_5 C_2 X_2 + \frac{1}{4}(\omega_3^2 E_{102} + \omega_3^2 E_{112} - E_{132})X_1^3 \sin(\beta_1) + E_{172}A_0 X_1 \sin(\beta_2 - \beta_1) = 0 \tag{3}$$

$$\omega_5 X_2(3\sigma_2 - 2\sigma_1) + \frac{1}{4}(-\omega_5^2 E_{42} + 3\omega_5^2 E_{52} - 3E_{162})X_2^3 + \frac{1}{4}(-2\omega_3^2 E_{62} + 2\omega_3^2 E_{72} + 2\omega_5^2 E_{92} - 2E_{142})X_1^2 X_2$$
$$+ \frac{1}{4}(\omega_3^2 E_{102} + \omega_3^2 E_{112} - E_{132})X_1^3 \cos(\beta_1) - E_{172}A_0 X_1 \cos(\beta_2 - \beta_1) = 0 \tag{4}$$

where $X_1, X_2, \beta_1, \beta_2$ are unknown; ω_3 and ω_5 are the 3th and 5th natural circular frequencies; C_1 and C_2 are damping constants; σ_1 and σ_2 are frequency detuning; A_0 is excitation acceleration amplitude; and E_{ij} are constants, i=1...17, j=1...2.

These equations are identical in form to those obtained in Reference 4 for a system with cubic nonlinearities, internal resonance and parametric excitation. They can be solved for X_1, X_2, β_1, and β_2 using a Newton-Raphson technique. Several cases are considered with various detuning and damping values. Figures 2 and 3 present the results for two of these. The amplitudes of the modes are plotted with respect to the amplitude of the excitation. The crossbar motion is smaller than the mast motion, but as the detuning increases, the amplification of the crossbar motion increases as well. Crossbar response acceleration amplitudes are an order of magnitude larger than those of the mast. Parametric excitation combined with internal resonance is therefore a possible explanation for the lower crossbar failures.

1. Knowles, G.I., "Effects of Parameter Variation on the Nonlinear Response of a Solar Array Phenomena Model," Masters Thesis, University of Kentucky, November 1996.

2. Mei, K., "Analytical Models for the Nonlinear Response of a Flexible Solar Array," Masters Thesis, University of Kentucky, August 1997.

3. Nayfeh, T.A., A.H. Nayfeh, and D.T. Mook, "A Theoretical and Experimental Investigation of a Three-Degree-of-Freedom Structure," *Nonlinear Dynamics*, Vol. 6, pp. 353-374, 1994.

4. Nayfeh, A.H. and D.T. Mook, *Nonlinear Oscillations*, John Wiley and Sons, New York, 1979.
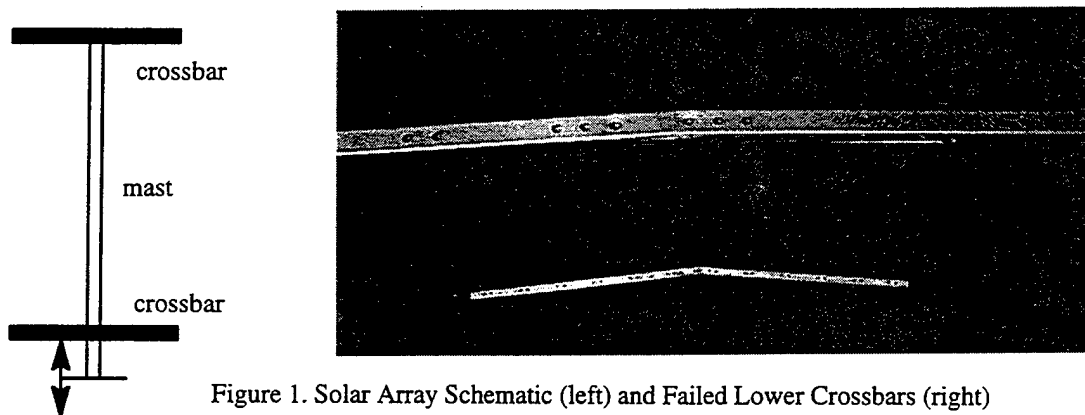
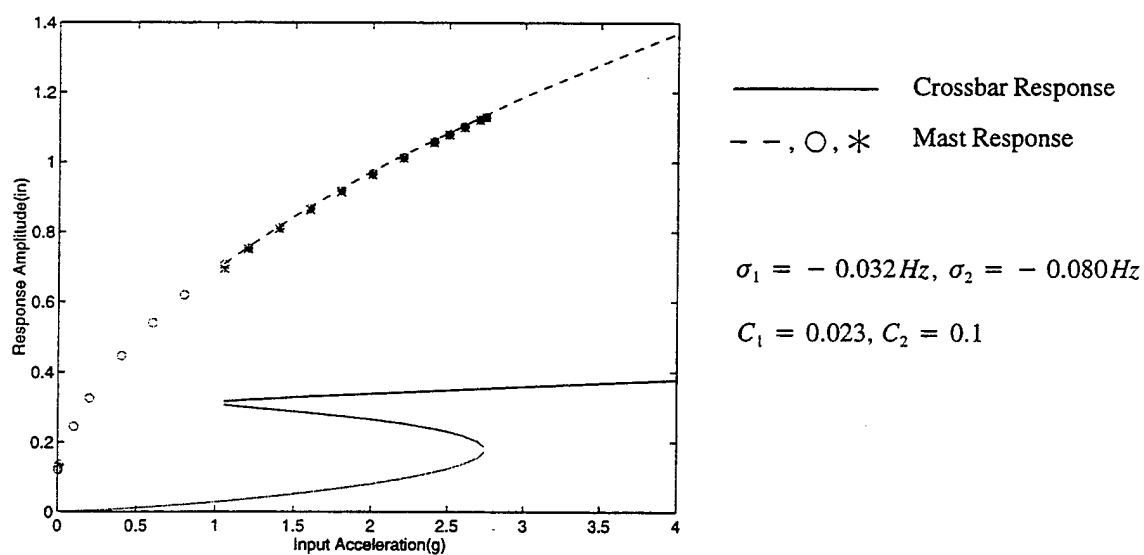Figure 1. Solar Array Schematic (left) and Failed Lower Crossbars (right)

Crossbar Response

$- -, \bigcirc, *$ Mast Response

$\sigma_1 = -0.032\,Hz, \quad \sigma_2 = -0.080\,Hz$

$C_1 = 0.023, \quad C_2 = 0.1$

Figure 2. Amplitude of the Modes versus Amplitude of the Excitation

Crossbar Response

$- -, \bigcirc, *$ Mast Response

$\sigma_1 = -0.1\,Hz, \quad \sigma_2 = -0.2\,Hz$

$C_1 = 0.05, \quad C_2 = 0.05$
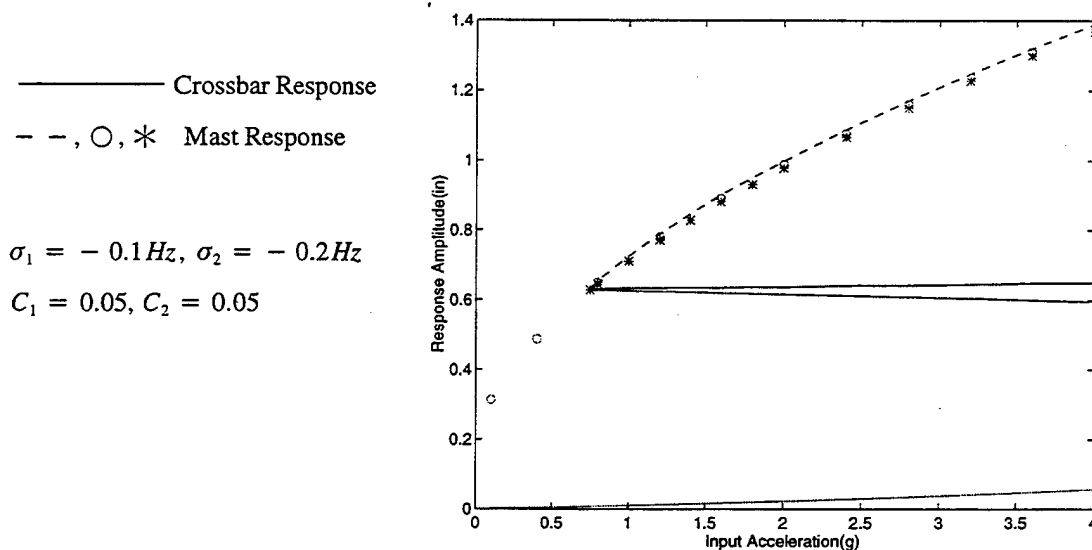
Figure 3. Amplitude of the Modes versus Amplitude of the Excitation

Monday, July 27
0800-0930
Session 3.

Response of a Parametrically Excited Rectangular Metallic Plate to a One-to-one Internal Resonance

M. Üstertuna, Ö. Elbeyli and G. Anlaş

Department of Mechanical Engineering Bogaziçi University,
80815 Bebek, Istanbul, TURKEY

EXTENDED ABSTRACT

The study of nonlinear vibrations of plates includes the study of free vibrations, forced vibrations with an external forcing normal to the midplane of the plate, and parametric vibrations as a result of parametric in-plane excitations. There are many physical examples of parametrically excited systems: cylindrical shells and plates subjected to time dependent axial (in-plane) loads, moving belts, vertical cables in suspension bridges. In the case of externally excited systems, the excitations appear as in-homogeneties in the governing differential equation; whereas in the case of the parametric excitation, the excitation appears as time varying coefficients in the governing differential equation. When the excitations appear as parameters in the governing equations, these excitations are called "parametric excitations" as discussed by Nayfeh & Mook (1979) .

There are a number of recent investigations that deal with parametrically excited dynamic systems: The response of two-degree-of-freedom systems with quadratic nonlinearities to a combination parametric resonance, where the excitation frequency is the sum of the natural frequencies, in the presence of two-to-one internal resonances is investigated by Nayfeh and Zavodney (1985). They used the method of multiple scales to obtain the equations governing the modulation of the amplitudes and the phases of the two interacting modes. Nayfeh and Jebril (1986), determined the response of two-degree-of-freedom systems with quadratic and cubic nonlinearities to multifrequency parametric excitations by using the method of multiple scales. Zavodney, Nayfeh and Sanchez (1988), investigated the response of a one-degree-of-freedom system with quadratic and cubic nonlinearities to a principal parametric resonance. They used the method of multiple scales to determine the modulation equations and determined the fixed points and their stability. The nonlinear response of a slender cantilever beam carrying a lumped mass to a principal

parametric base excitation was observed by Zavodney and Nayfeh (1988) both theoretically and experimentally. They used the Euler-Bernoulli beam theory to derive the governing nonlinear partial differential equation for an arbitrary position of the lumped mass. The method of multiple scales was then used to determine an approximate solution of the temporal equation for the case of a single mode. Nayfeh and Chin (1993), investigated the transfer of energy from high- to low-frequency modes in a two-degree-of-freedom system with widely spaced frequencies and cubic nonlinearities in the presence of a principal parametric resonance of the high-frequency mode. Nayfeh, Chin and Mook (1994) used the method of normal forms to study the nonlinear response of two-degree-of-freedom systems with repeated natural frequencies and cubic nonlinearity to a principal parametric excitation. They analyzed the character of the stability and various types of bifurcation. The nonlinear nonplanar response of cantilever inextensional metallic beams to a principal parametric excitation of two of its flexural modes was investigated by Arafat, Nayfeh and Chin (1997). They used the method of time-averaged Lagrangian to derive four first order nonlinear ordinary-differential equations governing the modulation of the amplitudes and phases of the two interacting modes.

Yang and Sethna (1990), studied nonlinear flexural vibrations of nearly square plates subject to parametric excitations. Their theoretical results are based on the analysis of a fourth order system of nonlinear ordinary differential equations in normal form derived from Von Karman equations. They used a variation of the constants procedure and the method of averaging to obtain the modulation equations. They also analyzed the local and global bifurcation. Yang and Sethna's work is a special and simpler application of the study presented here, because this analysis considers the general rectangular metallic plate subjected to in-plane parametric loading. In Yang & Sethna's work the sides are equal, and most of the terms simplify.

One-to-one Internal Resonance of Laminated Shallow Shells

Akira Abe, Yukinori Kobayashi and Gen Yamada

Division of Mechanical Science, Hokkaido University, Sapporo, Japan

Abstract — This paper presents the response of laminated shallow shells with an internal resonance of $\omega_2 \approx \omega_3$, where ω_2 and ω_3 are linear natural frequencies of asymmetric vibration modes (2,1) and (1,2). Galerkin's procedure is applied to the governing equation based on the first order shear deformation theory, and the shooting method is used to analyze the steady-state response when the driving frequency Ω is near ω_2. In order to take the effect of quadratic nonlinearities into account, we consider (1,1) mode in addition to (2,1) and (1,2) modes. The effect of quadratic nonlinearities due to (1,1) mode on the response are studied.

ANALYSIS

Consider a laminated shallow shell as shown in Fig.1. When a symmetric cross-ply laminated shallow shell is subjected to a harmonic excitation, the equation of motion and the compatibility condition for the shell based on the first order shear deformation theory can be expressed as

$$
\left.
\begin{aligned}
\rho\ddot{w} - \phi_{,yy}\, w_{,xx} + 2\phi_{,xy}\, w_{,xy} - \phi_{,xx}\, w_{,yy} - S_{44}(w_{,yy} + \psi_{y,yy}) - S_{55}(w_{,xx} + \psi_{x,xx}) = q(x,y)\cos\Omega' t \\
D_{11}^*\psi_{x,xx} + D_{66}^*\psi_{x,yy} + (D_{12}^* + D_{66}^*)\psi_{y,xy} - S_{55}(w_{,x} + \psi_x) = 0 \\
(D_{12}^* + D_{66}^*)\psi_{x,xy} + D_{66}^*\psi_{y,xx} + D_{22}^*\psi_{y,yy} - S_{44}(w_{,y} + \psi_y) = 0
\end{aligned}
\right\}, \quad (1)
$$

$$
A_{22}^*\phi_{,xxxx} + (2A_{12}^* + A_{66}^*)\phi_{,xxyy} + A_{11}^*\phi_{,yyyy} = w_{,xy}^2 - w_{,xx}\, w_{,yy} + w_{,yy}/R_x + w_{,xx}/R_y, \quad (2)
$$

where w is the transverse displacement, ϕ is the stress function, ψ_x and ψ_y are the rotations of midsurface about the y and x axes, respectively. Constants A_{ij}^*, D_{ij}^* and S_{ij} correspond to the stiffness coefficients of the shell.

In the following analysis, the boundary conditions for the shell are considered as simply supported along its four edges. The displacement functions are expressed using the eigenfunction of the linear vibration as

$$
\left.
\begin{aligned}
w = h\sum_m\sum_n W_{mn}(t)\sin(m\pi x/a)\sin(n\pi y/b) \quad \psi_x = \sum_m\sum_n X_{mn}(t)\cos(m\pi x/a)\sin(n\pi y/b) \\
\psi_y = \sum_m\sum_n Y_{mn}(t)\sin(m\pi x/a)\cos(n\pi y/b)
\end{aligned}
\right\}, \quad (3)
$$

where m and n are the number of half waves in the x and y directions, respectively. The stress function satisfying the boundary conditions is assumed to be of the form

$$
\phi = \sum_p\sum_q B_{pq}\cos(p\pi x/a)\cos(q\pi y/b) + \sum_r\sum_s C_{rs}\sin(r\pi x/a)\sin(s\pi y/b). \quad (4)
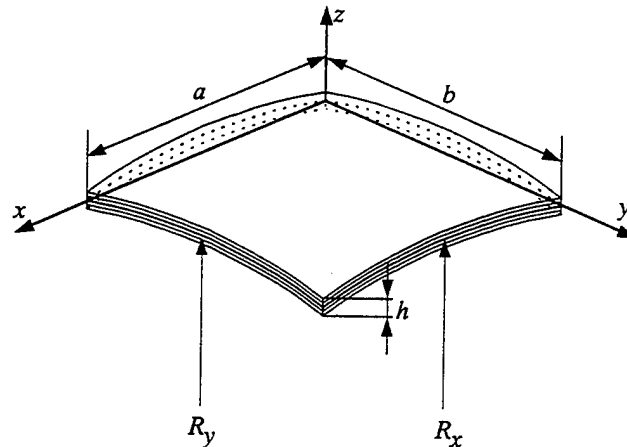$$

Fig.1 Coordinate system of a shallow shell

Substituting Eqs.(3) and (4) into the compatibility condition (2), the coefficients B_{pq} and C_{rs} can be determined by comparing the coefficients of trigonometric functions in both sides of Eq.(2). Further we assume that only the vibration mode (2,1) is directly excited by the transverse force. Therefore $q(x,y)$ is defined as

$$q(x, y) = q_0 \sin(2\pi x/a) \sin(\pi y/b). \tag{5}$$

By substituting Eqs.(3), (4) and (5) into (1) and applying to Galerkin's procedure, we obtain the following simultaneous nonlinear ordinary differential equations in terms of the vibration modes (1,1), (2,1) and (1,2):

$$\left.\begin{array}{l} \ddot{W}_1 + \mu\omega_1\dot{W}_1 + \omega_1^2 W_1 + G_{a1}W_1^2 + G_{a2}W_2^2 + G_{a3}W_3^2 + G_{a4}W_1^3 + G_{a5}W_1W_2^2 + G_{a6}W_1W_3^2 = 0 \\[2mm] \ddot{W}_2 + \mu\omega_2\dot{W}_2 + \omega_2^2 W_2 + G_{b1}W_1W_2 + G_{b2}W_1^2 W_2 + G_{b3}W_2^3 + G_{b4}W_2W_3^2 = F\cos\Omega\tau \\[2mm] \ddot{W}_3 + \mu\omega_3\dot{W}_3 + \omega_3^2 W_3 + G_{c1}W_1W_3 + G_{c2}W_1^2 W_3 + G_{c3}W_2^2 W_3 + G_{c4}W_3^3 = 0 \end{array}\right\}, \tag{6}$$

where μ, ω, G, τ, F and Ω are the non-dimensional damping coefficient, the non-dimensional linear natural frequencies, the non-dimensional coefficients of the nonlinear terms, the non-dimensional time, the non-dimensional amplitudes and frequency of the load, respectively. Subscript i of the non-dimensional displacements is redefined as $\{W_1, W_2, W_3\} = \{W_{11}, W_{21}, W_{12}\}$. As can be seen from Eq.(6), W_1 is activated by the nonlinear term $G_{a2}W_2^2$ when W_2 is excited. Therefore the amplitude of (1,1) mode affects the response for (2,1) mode through the nonlinear terms $G_{b1}W_1W_2$ and $G_{b2}W_1^2 W_2$. However, the effect of the quadratic nonlinear terms as $G_{b1}W_1W_2$ is not considered in the case of W_1 is negligible. The steady-state response is obtained by applying the shooting method to Eq.(6).

RESULTS AND DISCUSSION

A symmetric cross-ply laminated shallow shell ($\theta = 90°/0°/90°$) is treated in the following numerical examples. Each lamina is assumed to be made of graphite/epoxy which is a highly orthotropic fiber-reinforced material, and the material properties are $E_L = 138$(GPa), $E_T = 8.96$(GPa), $G_{LT} = G_{LZ} = 7.10$(GPa), $G_{TZ} = E_T/2$, $\nu_{LT} = 0.30$. Other parameters are

$$\left.\begin{array}{l} R_x/a = R_y/a = 5, \quad h/a = 0.01, \quad b/a = 1.22, \\[2mm] \omega_1 = 34.52, \quad \omega_2 = 45.85, \quad \omega_3 = 46.08, \quad \mu = 0.01, \quad F/\omega_2^2 = 0.01 \end{array}\right\} \tag{7}$$

Figure 2 (a) and (b) show frequency-response curves by two-mode analysis (W_1 is negligible) and three-mode analysis, respectively. In each figure, solid and broken lines denote stable and unstable responses, respectively. In the case of two-mode analysis, a stable two-mode response occurs at $\Omega/\omega_2 \approx 1.014$ via a pitchfork bifurcation, and then the single-mode response loses its stability. As the excitation frequency is increased from low frequency (e.g., $\Omega/\omega_2 = 0$), the single-mode response change into a two-mode response through the bifurcation point continuously. As seen from Fig.2 (b), the responses for three-mode analysis are quite different from those for two-mode analysis. In contrast to the result for two-mode analysis, a stable response of (1,2) mode occurs at $\Omega/\omega_2 \approx 0.985$ via a saddle-node bifurcation. Although the response curve of (1,1) mode is omitted due to space restriction, the amplitude of W_1 is very small compared with that of W_2.
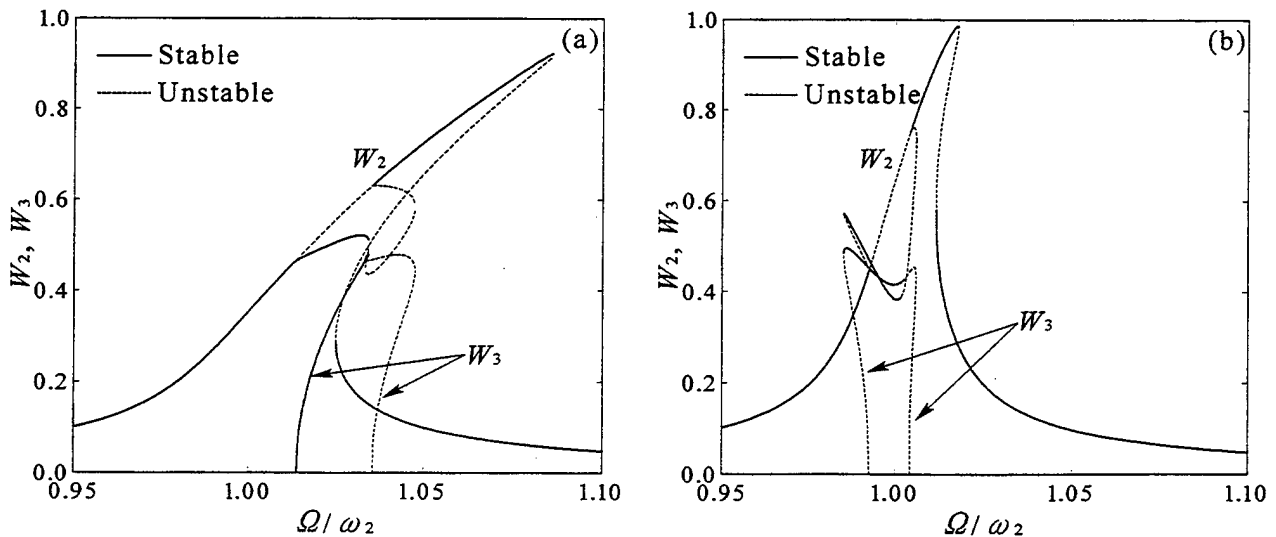

Fig.2 Frequency-response curves for the shell, (a) two-mode analysis, (b) three-mode analysis

NONLINEAR MODAL INTERACTION OF LIQUID IMPACT-STRUCTURAL DYNAMIC UNDER PARAMETRIC EXCITATION

By Mohamed A. El-Sayad and Raouf A. Ibrahim
Wayne State University
Department of Mechanical Engineering
Detroit, MI 48202

ABSTRACT:
The nonlinear modal interaction of liquid sloshing hydrodynamic impact with an elastic support structure subjected to parametric excitation is examined for three parametric resonance conditions. The liquid sloshing mass is represented by a pendulum experiencing impacts with the tank walls. The impact loads are modeled based on a phenomenological representation in the form of a power function with a higher exponent. In this case the system equations of motion included two types of nonlinearities; impact nonlinearities (taken to be of order five) and structural geometric nonlinearities (of order three). The method of multiple scales is used to determine the response amplitude characteristics in the absence and in the presence of impact loading. When the first mode is parametrically excited the system experiences hard nonlinear behavior and the impact loading reduces the response amplitude. On the other hand, when the second mode is parametrically excited, the impact loading results in creating more fixed points and the response switches from soft to hard nonlinear characteristics. Under combination parametric resonance, the system behaves like a soft system in the absence of impact and like a hard system in the presence of impact. The system geometric nonlinearities may also give rise to the occurrence of internal resonance.

Internal Resonance in Wire Electro-Discharge Machining

Kevin D. Murphy
Department of Mechanical Engineering
University of Connecticut
Storrs, CT 06269-3139

Wire electro-discharge machining (wire EDM) is a manufacturing technique in which material is eroded from a workpiece by producing an electrical discharge between the workpiece and a translating wire electrode that is in close proximity, see Figure 1a. While there are numerous benefits to wire EDM, wire vibrations and instabilities detract from the precision of the cut, reduce productivity, and may lead to wire rupture resulting in prolonged downtime.

The translating wire fits in the broad classification of an *axially moving material*. Axially moving systems have been studied for a number of years and have been shown to be susceptible to vibrations and various instabilities, particularly at high transport speeds [1]. In the case of the EDM wire, it has been shown that the wire undergoes both pitchfork and Hopf bifurcations [2]. This is evident from Figure 1b and 1c which shows the behavior of the eigenvalues, generated by linearizing the equations of motion about the stable equilibrium configuration (Figure 1d), as a function of nondimensional transport speed.

In the present study, Hamilton's principle is used to develop the nonlinear equations governing the displacements in the a_1, a_2, and a_3 directions along with the associated boundary conditions. These equations are then discretized using a Galerkin projection resulting in the following equations for forced, undamped motion:

$$\ddot{\alpha} + K_1 A_1 \dot{\alpha} + (K_2 - K_3) A_2 \alpha - K_3 A_3 \beta^2 - K_3 A_4 \gamma^2 = 0 \tag{1}$$

$$\ddot{\beta} + K_1 B_1 \dot{\beta} + (K_2 - K_4) B_2 \beta + B_3 \beta - K_3 B_4 \alpha\beta - K_3 B_5 \gamma^2 \beta - K_3 B_6 \beta^3 = F \sin(\omega t) \tag{2}$$

$$\ddot{\gamma} + K_1 C_1 \dot{\gamma} + (K_2 - K_4) C_2 \gamma + C_3 \gamma - K_3 C_4 \alpha\gamma - K_3 C_5 \beta^2 \gamma - K_3 C_6 \gamma^3 = 0 \tag{3}$$

where α, β and γ are the modal amplitudes in the a_1, a_2 and a_3 directions, respectively. Note that these equations are gyroscopically coupled and contain both quadratic and cubic nonlinearities. The external excitation in the a_2 direction arises from the periodic electrical discharges which momentarily repel the wire from the workpiece.

As is evident from Figure 1b and 1c, the eigenvalues are sensitive functions of the transport speed. At a nondimensional transport speed of approximately $c\sqrt{mL^2/(EI)} = 5.1$, the imaginary parts of the β and γ eigenvalues are equal creating the necessary conditions for a 1:1 internal resonance [3], [4]. Using a second order perturbation analysis, the 1:1 internally resonant response and its stability are examined. In addition, the implications for large amplitude, steady state motion in γ are explored. Specifically, the possibility of large amplitude "snap-through" motion is considered via numerical integration of the equations of motion.
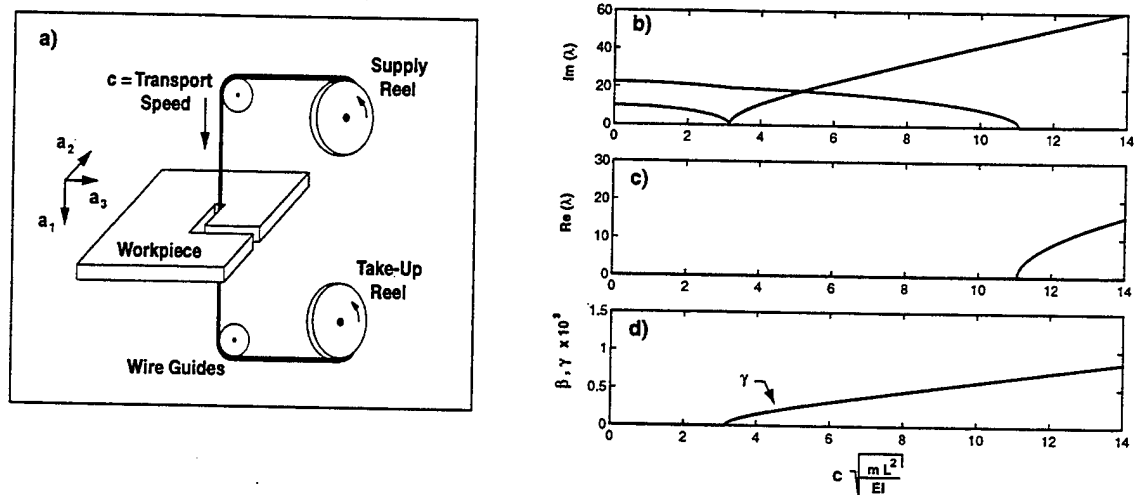
Figure 1: a) A schematic of the wire electro-discharge machining (wire EDM) process. b) The imaginary parts of the β and γ eigenvalues (i.e., the natural frequencies) as a function of nondimensional axial transport speed. c) The real part of the β and γ eigenvalues. d) The stable, static modal amplitudes (the deflected state of the wire). This figure is taken from reference [2].

Acknowledgments

References

[1] Wickert, J.A. and Mote, C.D., 1988, "Current Research on the Vibration and Stability of Axially-Moving Materials," *Shock and Vibration Digest.* **20**. 3-13.

[2] Murphy, K.D., and Lin, Z., 1998, "Natural Frequencies, Mode Shapes and Predictions of Instability in Wire EDM," *Journal of Manufacturing Science and Engineering*, submitted for publication.

[3] Nayfeh, A.H., and Balachandran, B., 1989, "Modal Interactions in Dynamical and Structural Systems," *Applied Mechanics Review*, **42**(11), S175-S201.

[4] Murphy, K.D., and Lee, C.L., 1998, "The 1:1 Internally Resonant Response of a Cantilever Beam Attached to a Rotating Body," *Journal of Sound and Vibration*, to appear.

EFFECTS OF THE LORENTZ FORCE ON LATERAL VIBRATION
OF A CONDUCTING AND NONMAGNETIC CABLE

S.Shimokawa, H.Kawamoto, T. Sugiura, and M. Yoshizawa

Department of Mechanical Engineering, Faculty of Science and Technology, Keio University,

3-14-1 Hiyoshi, Kouhoku-ku, Yokohama, Kanagawa, 223, Japan

Abstract. There are many problems of cable vibrations due to the Lorentz force in the power transmission systems using high voltage cables or superconducting cables [1]. This paper discusses the effects of the Lorentz force on a lateral vibration of a conducting and nonmagnetic cable. Finally we observe the dynamic behaviors of a copper cable under the Lorentz force.
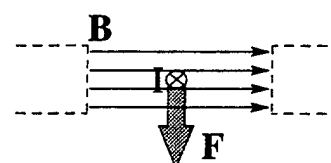
Fig.1

When a conductor carrying an electric current I is in a magnetic field B, the Lorentz force, expressed as F=I×B, acts on the conductor as shown in Fig.1. This force has two types as follows.

First, the unsteady magnetic field B(t) is applied to a nonmagnetic and conducting cable which is a part of a closed electric circuit [2]as shown in Fig.2. In this case the induced current occurs in the cable which is a part of a closed electric circuit. According to Faraday's law, the induced current is expressed as follows:
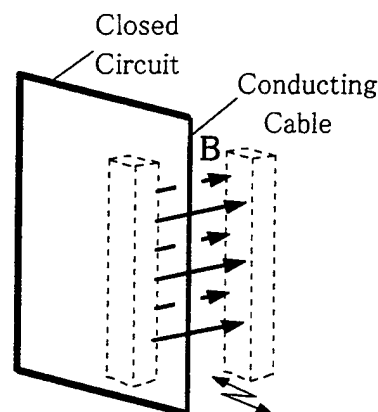

$$I = \frac{1}{R}\left[-\int_S \frac{\partial \mathbf{B}}{\partial t} \cdot d\mathbf{S} + \oint (\mathbf{v} \times \mathbf{B}) \cdot d\mathbf{l} \right]$$

Fig.2

where R is the electric resistance of the closed circuit, S is a surface enclosed with the closed electric circuit and v is the velocity of the cable in a plane perpendicular to S . The first component of the induced current expressed by the first term in the right-hand side of the above equation, yields due to the periodically changed magnetic field, and the second one due to the movement of the cable. The

Lorentz force for the first one acts on a lateral vibration of a cable as an exciting force, as shown in Fig.3.   While that for the second one acts as a damping force as shown in Fig.4.
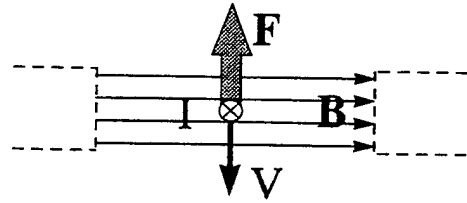
due to Time-Varying Magnetic Field   **due to Lateral Motion of a Cable**

Exciting Force

Fig.3

Damping Force

Fig.4

We observe the nonplanar cable vibration (Fig.5), in a system as shown in Fig.2.

Second, the alternating current I(t) is applied to a nonmagnetic conducting cable in a magnetic field [3]as shown in Fig. 6 . Then the Lorentz force occurs in the cable. We estimate theoretically the Lorentz force acting on the cable, which is produced by I(t).

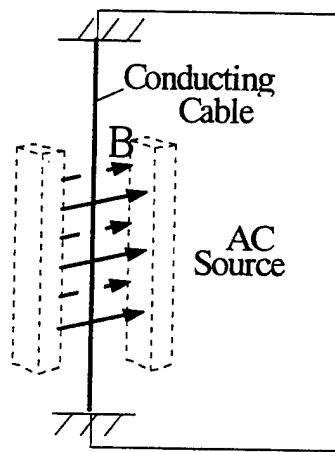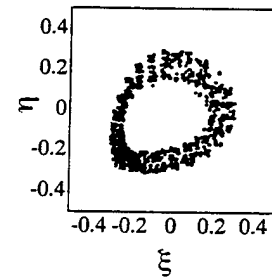We observe the nonplanar cable vibration (Fig.7), in a system as shown in Fig.6.
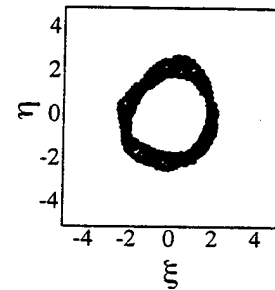

Fig.6

Fig.5

Fig.7

References
[1]M.N. Zervas and E.E.Kriezis, "Integral formulation for the calculation of the field and the forces in a system of conducting cylindrical shells: a general approach" *IEE PROCEEDINGS, Vol.134,Pt.B No.5,* pp.269-275, 1987
[2]B.-L. Ma and I-T. Lu, "Electromagnetic Excitation of a Wire Enclosed in a Rectangular Cavity by Plane Wave Incident on a Small Aperture" *Journal of Electromagnetic Waves and Applications , Vol. 4,* pp.311-324, 1990
[3]Jeffrey L. Young and James R. Wait, "Electromagnetic Response of Two Crossing, Infinitely Long, Thin Wires" *IEEE Trans. Antennas Propagat., Vol.39, No. 6,* pp.732-739

Monday, July 27
1000-1130
**Session 4.**

VIBRATION CONVEYOR DYNAMICS

Friedrich Pfeiffer, Peter Wolfsteiner, Garching

Vibration conveyors are used in mass production facilities for providing automated manufacturing processes with parts like screws, bolts or electronic devices. They store, feed, orientate and isolate such parts. Due to the complex mechanics of the feeding process the design of the feeders is still depending on trial and error. This paper presents a complete dynamical model of the transportation process including unilateral constraints and multiple impacts, both with Coulomb Friction. Simulation results, computed with a three dimensional model, explain the practical benefit of the proposed tool.

Compared with other machines applied in the automated assembly vibratory feeders are quite uncomplex. The high number of different variants of devices based on the vibratory feeding-principle, and the large amount of applications give the impression that we deal with a well developed and reliable tool. This impression is wrong. Especially errors that occur in part feeders are mostly responsible for troubles in the automated assembly. The reason is the exclusively experimental tuning of the feeders which is often done without a theoretical background, especially as far as the mechanics of the transportation process is concerned.

The transportation process in a vibratory feeder (see Figure) is based on a micro ballistic principle that is driven by an oscillating track. The mechanical model can be splitted in the dynamics of the base device, mostly represented by an electro magnetically excited oscillator, and the dynamic of the transportation process. This does not mean that there is no reaction from the parts on the track, but the modeling is quite different. In contrast to the transportation process, the base device can be modeled as a bilaterally coupled system with well-known standard techniques. Due to the highly sensitive contact mechanics all oscillating frequencies and flexible structures have to be well analysed. Furthermore interconnections to an oscillating environment must be taken into consideration.

Nevertheless, this paper focuses more on the modeling of the transportation process.
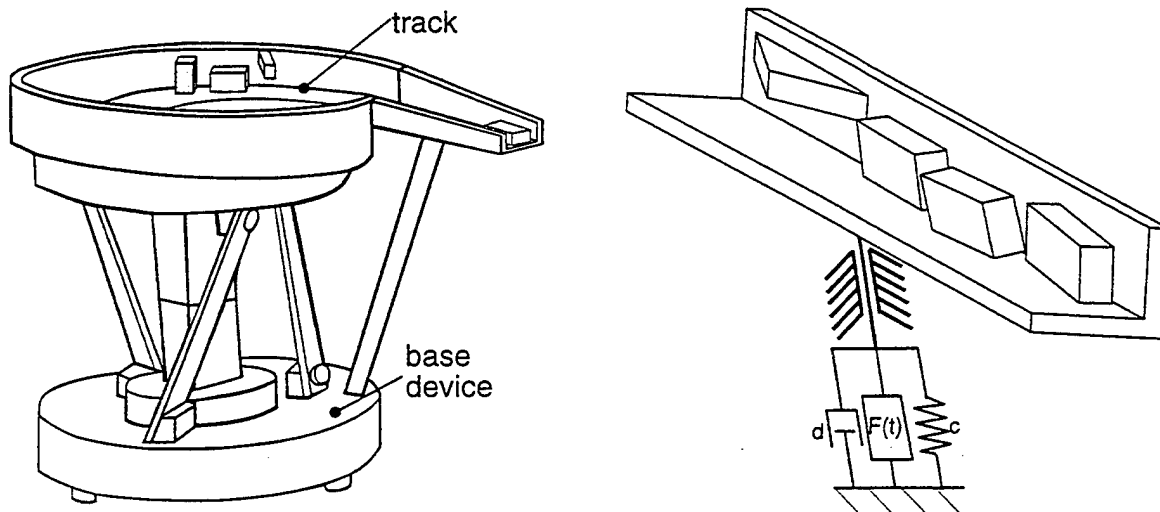
Changing contact configurations between the transported parts and the track and the parts themselves are characteristic for the feeding process. These contacts appear either continuously for a certain time interval, or for a discrete moment (impact). Friction has a fundamental importance for the transportation process. It would not work without it. Consequently the modeling must be done with respect to the friction effects. Therefore a structure- variant multibody system with unilateral constraints and Coulomb Friction is an optimal tool. It's formulation results in a set of differential equations with inequality constraints that require a special mathematical and numerical treatment. The geometric model has three dimensions, thus the contact model is twodimensional. The formulation of the inequality constraints is also capable to treat time-discrete multibody impacts with Coulomb Friction. The assumption of rigid bodies realizes a wide variety of different parts.

The shape of the contact surfaces is modeled by flat plane-elements, so that any geometric objects can be approximated. Point-contacts are therefore between *point-plane* and *line-line*. Line- and plane-contacts are composed by single point-contacts.

Theory is verified by experiments with very good correspondance. Simulations provide detailed informations on the transportation rate, the influence of different parameters, the stability of the process which means its sensitivity to unsafe parameters, the performance of the orienting devices, and the influence of different base-devices. They can therefore either support the experiment-based design, or replace it completely by theoretical

methods.

Literature

Berkowitz, D.R.; Canny, J.: *Designing Parts Feeders Using Dynamic Simulations*, in: International Conference on Robotic and Automation. IEEE, 1996.

Boothroyd, G.; Poli, C.R.; Murch, L.E.: *Handbook for Feeding and Orienting Techniques for Small Parts*, Department of Mechanical Engineering, University of Massachusetts, Amherst, MA, 1976.

Glocker, Ch.; Pfeiffer, F.: *Stick-slip phenomena and application*, in: Nonlinearity and Chaos in Engineering Dynamics, IUTAM Symposium, UCL, July 1993. John Wiley, New York, 103-113.

Pfeiffer, F.; Glocker, Ch.: *Multibody Dynamics with Unilateral Contacts*, John Wiley & Sons, Inc., New York, 1996.

Wösle, M.; Pfeiffer, F.: *Dynamics of Multibody Systems Containing Dependent Unilateral Constraints with Friction*, in: Journal of Vibration and Control 2, Sage Publications, Inc., 1996, 161-192.

Yeong, M.I.; De Vries, W.R.: *A Methodology for Part Feeder Design*, in: Annals of the CIRP, Vol 43/1/1994.

Computing analysis of dynamic properties of interactive drive systems

Ctirad Kratochvíl, Vladimír Kotek

Introduction

Methods of mathematical modeling have spread widely in all fields of human activity. Engineering practice requires therefore a complete and consistent system of qualitative analysis of mathematical models and their quantitative processing. The problem of the system approach utilization for the solution of concrete technical problems is related to the problems of modeling methods, to the possibilities and usefulness of mathematical methods, and is connected with the problems of simplicity or alternatively of complexity, too.

Drive systems as a dynamical system

With respect to the fact that the most of factual technical systems have their hierarchy-oriented structure represented by more or less wide set of inside and outside interactions, for example the drive system of working machine - see fig. 1, it is necessary to study these internal interactions in more details, especially when they are the concrete reflections of mutual connections among the substructures of often different physical nature. In these cases the utilization of dynamic systems general theory results may be very useful.
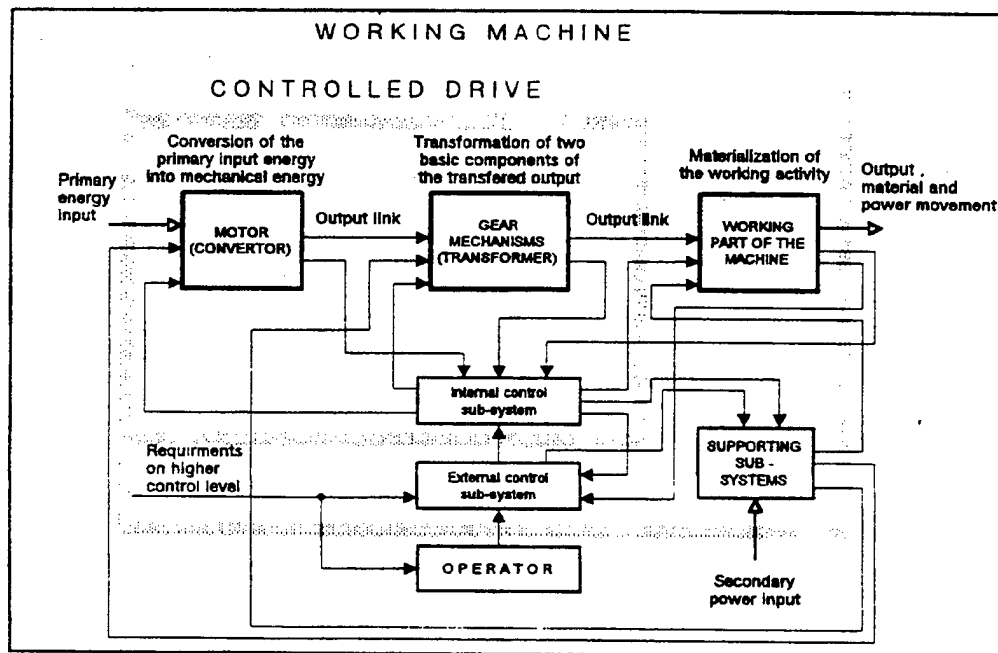

Figure 1: Drive system of working machine

If we came from the definition of the dynamic system (according to ZADEH) in the sense of the identification of real technical object (primary object) and abstract model formed by the dynamic system (secondary object), we may create on primary objects with respect to the solution of concrete problems (i.e. for the given purpose) on the selected or prescribed differentiating level. At the very beginning the designer determines the degree of the structural complexity of the dynamic system, decides the transient from the lower types of models to the higher ones and influences on the target, working and informative functions on the system and on the higher degree even the control functions. So we define the specialized and partially structured dynamic systems.

Professor Ctirad Kratochvíl, Vladimír Kotek, M.Sc
TU Brno, Faculty of Mechanical Engineering, Institute of Solid Mechanics, Czech Republic

Models of real machine drives

Example 1:

We can see results of structural analysis of controlled electromechanical drive systems – rolling mills and trains (one-motor drive models and multi-motor drive models); time courses of frequency response functions at working, transition and failure overload states.
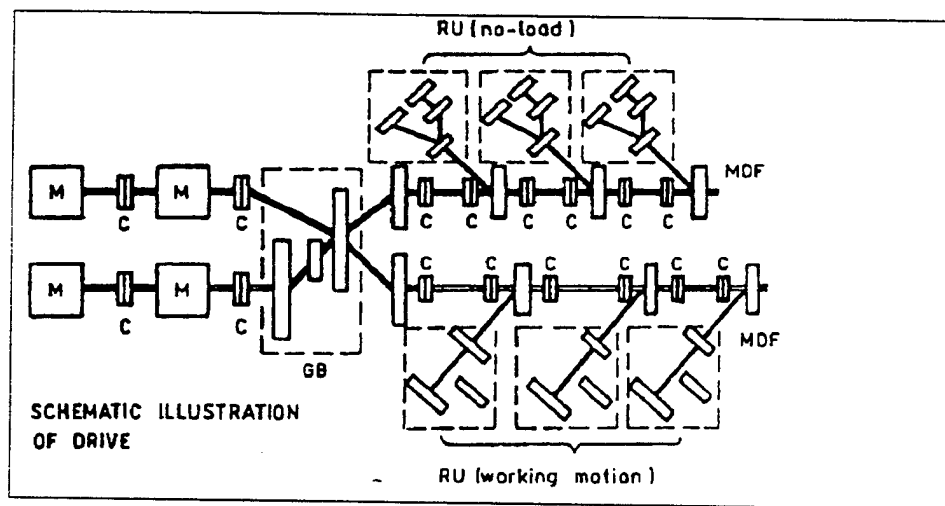

Figure 2: Dynamic of the rolling train drive (M-el. motor, C-coupling, GB-gear box, RU-rolling unit, MDF-main distribution frame)

Example 2:

We can see result of structural analysis of gearbox system, e.g. epicyclical gearbox used in off-the-road vehicles.
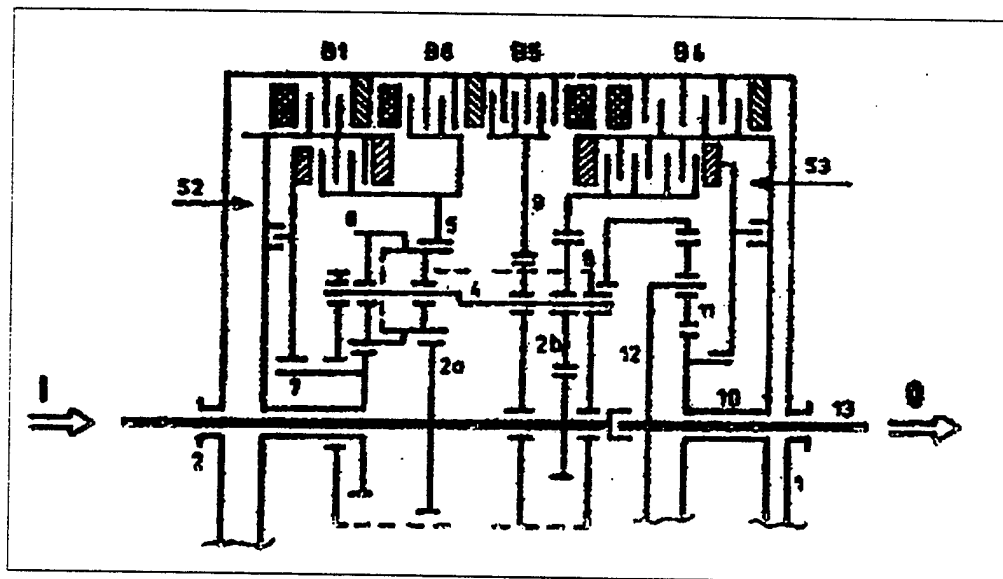

Figure 3: Schematic representation of gear box structure (B-brake, S-coupling, I-input, O-output)

Conclusion

The aim of our paper is to reveal one of less used methods of computing models establishment by means of analogies i.e., by electroanalogy concretely. Furthermore experiments in modeling using drives models design enable analysis of dynamic properties under so called nonstandard serviceable conditions first of all emergency ones, also they allow to find the evaluations of expected extreme loads or deformations, etc.

Sway Control for Trolley with Pendulum Load

Gray Roberson and Gang Tao
Department of Electrical Engineering
University of Virginia
Charlottesville, VA 22903
E-mail: roberson-dg@salem.ge.com

The paper will describe the results of the authors' investigation into the control of a trolley and pendulum system. The research includes the following areas of investigation: evaluation of a sway controller presently used in industry, improvements in the response of the present controller, design of a new sway control system using a more accurate model for the trolley and pendulum, analysis of various reference conditioning schemes, compensation for noise in measured system feedbacks, online identification of pendulum frequency, and final position control for the pendulum load.

Sway control for the trolley and pendulum is important to industry. A prevalent application of the trolley and pendulum system is the crane system that moves large containers from one location to another. The trolley in the crane system is generally operated by a person who provides a speed reference with a joystick or other control mechanism. Crane operation is expensive, so the application demands a short cycle time. The containers must be stacked accurately on the receiving end of the process. Control of load position and speed must be realized without sudden and violent trolley movements which could endanger the operator. The control must be effective over a range of system parameters. Considerations such as these must be made when designing the sway controller.

Evaluation of a present industry controller shows that improvements can be made by a different selection of closed loop poles. Simulation of the system shows that without any degradation in the time it takes the load speed to change from one steady state value to another, trolley acceleration and jerk can be decreased significantly. Trolley acceleration and jerk indicate how uncomfortable the trolley movement is for the operator in the crane application. The improvements are observable over the specified operating range. Justification of a particular set of closed loop poles will be pursued.

The present industry controller makes simplifying assumptions about the physics of the trolley and pendulum system. A more accurate model of the system has been developed and simulated. Controller design using the improved model is proceeding. The goal of this area of research is to produce a controller that improves the response of the trolley and load to the operator reference but that does not add much complexity to the implementation of the control.

In the crane application, the reference input that the operator provides to the sway controller is often conditioned using a rate limiter or a filter. The reference conditioning

provides a smoother trolley ride for the operator. The effects of the reference conditioning on the overall response of the trolley and load will be analyzed.

The present industry controller controls the speed response of the pendulum load to a reference signal. Currently no load position control is being performed. One of the objectives of the research is to design a position regulator for the trolley and pendulum system.

Feedback measurements in the trolley and pendulum system are often corrupted by noise. Especially bothersome is DC noise in the load position measurement, which causes the feedback to have a constant offset. The DC noise introduces inaccuracies in load position control. Methods for eliminating noise from the feedback measurements will be investigated.

In the present system the pendulum frequency is not measured, and an estimate for frequency is used in the controller. Using the measured frequency as a system feedback will improve the accuracy of the control. A goal of the research is to develop a method for online identification of pendulum frequency.

Simulations of the trolley and pendulum system will be performed to demonstrate the effectiveness of the control design in each of the research areas. Any conclusive improvements to the present sway controller will be implemented in a forthcoming industry product.

Nonlinear and Experimental Analyses of the Hunting Motion in a Railway Wheelset

Hiroshi YABUNO,
Institute of Applied Physics, University of Tsukuba,
Tsukuba-Science-City 305 Japan, Email: yabuno@aosuna.esys.tsukuba.ac.jp

Masato NUNOKAWA,
Doctoral Program in Engineering, University of Tsukuba,

Nobuharu AOSHIMA,
Institute of Applied Physics, University of Tsukuba,

Recently, significant attention has been focused on nonlinear dynamics on railway vehicle dynamics [1]. It is known that wheelset rolling on a railway track loses its stability above a critical speed due to creep forces. This phenomenon called hunting motion is a kind of self-excited oscillation due to a flutter instability. The critical speed which has been obtained by the eigenvalue analysis (linearized stability analysis) often gives a higher critical speed than the experimental one. It is therefore necessary to perform the non-linear analysis. Jensen and True showed the chaos and the bifurcations in a speed range by numerically solving the governing equations including nonlinear creep forces [2]. Xu, Troger, and Steindl investigated the governing equations whose friction force is approximated by the fifth order polynomial by using the center manifold reduction and classified the nonlinear characteristics of the hunting motion by using the method of normal form [3]. It is analytically shown that the wheelset loses its stability through a subcritical Hopf bifurcation at the critical speed obtained by the linear analysis. However, there are few experiments on the nonlinear phenomena in the hunting motion and are few studies on comparison between the experimentally and theoretically obtained phenomena.

In this paper, the theoretically and experimentally obtained nonlinear phenomena are qualitatively compared in a test apparatus of a wheelset rolling on a railway track as shown in Fig. 1. Experiment shows that the hunting motion occurs depending the lateral disturbance, even if the speed is below the experimental critical speed which is assumed to be the experimentally obtained critical speed in the case of no artificial disturbance, i.e., in the case with only fluctuation noise due to the roughness of the rail, the wheelset and etc. Figure 2 shows the limitations of the lateral disturbance in some cases when the speed is below the experimental critical speed; the hunting motion occurs and does not occur in the cases when the lateral disturbance is smaller than the symbol o and larger than the symbol ×, respectively. Also, it follows from this figure that the limitation increases as the speed decreases. Next, the above experimentally obtained nonlinear characteristics of the hunting motion is analytically explained by considering only linear component of

the creep forces and the restoring forces including the geometrical nonlinearity by the springs attached to the wheelset. The dimensionless equations governing the yow and lateral motions are derived as follows:

$$\ddot{y} + \mu_y(1-\epsilon)\dot{y} + \alpha_y y - \alpha_\psi \psi + \alpha_{yyy}y^3 - \alpha_{y\psi\psi}y\psi^2 + \alpha_{\psi\psi\psi}\psi^3 = 0$$
$$\ddot{\psi} + \mu_\psi(1-\epsilon)\dot{\psi} + \beta_y y + \psi - \beta_{yy\psi}y^2\psi + \beta_{y\psi\psi}y\psi^2 - \beta_{\psi\psi\psi}\psi^3 = 0, \qquad (1)$$

where μ_y, μ_ψ, α, and β are positive constants. The method to obtain the values of the independent dimensionless parameters corresponding to the apparatus is shown. The above dynamical system is reduced by the center manifold theory. It is furthermore clarified that the the bifurcation at the critical speed (the bifurcation from the trivial solution) is a subcritical Hopf bifurcation. Therefore the hunting motion can occur depending on the disturbance even if the speed is below the critical speed. By expressing the unstable limit cycle in the vicinity of the bifurcation point, one can show the disturbance such that the wheelset loses its stability in the case when the speed is lower than the critical speed. Figure 3 shows the limitation of the lateral disturbance; the hunting motion occurs in the case when the disturbance is lager than the limitation, even if the speed is below the critical speed obtained by the eigenvalue analysis (linearized stability analysis). Also the limitation increases as the speed decreases. These theoretical results are qualitative agreements with the above experimental ones.

References

1. True, H., 'Dynamics of a rolling wheelset', *Appl Mech Rev*, 46, 1993, 438-444.
2. Jensen. C.N., and True, H., 'On a New Route to Chaos in Railway Dynamics', *Nonlinear Dynamics*, 13, 1997, 117-129.
3. Xu, G., Troger, H., and Steindl, A., 'Global Analysis of the Loss of Stability of a Special Railway Body' in W. Schiehlen, (ed), Nonlinear Dynamics in Engineering Systems, 1990, 345-352, Springer-Verlag, Berlin.
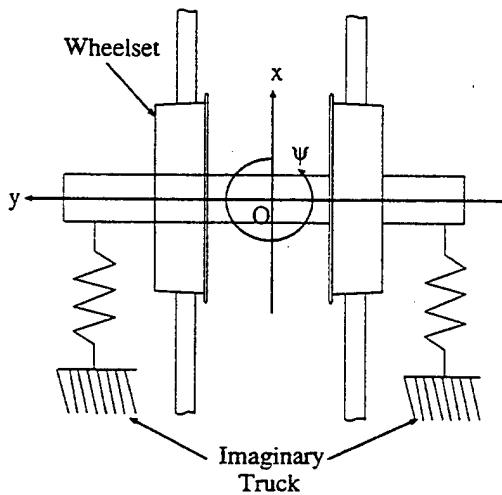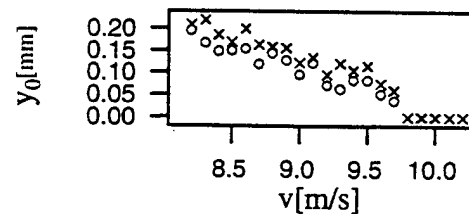
Fig.1: Top View of Wheelset Model

Fig.2: Bifurcation Diagram(Experimental)
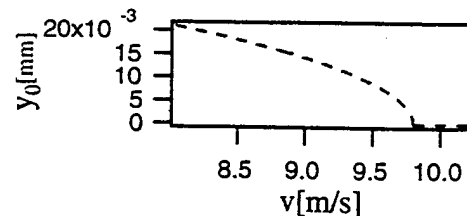(Experimental Critical Speed=9.8[m/s])

Fig.3: Bifurcation Diagram(Theoretical)
(Critical Speed=9.8[m/s])

Prediction of incipient "ground resonance" instability in a physical model of a rotorcraft

Philip V. Bayly, Christopher M. Cueman, Melissa E. Clark
Mechanical Engineering
Washington University, St. Louis, MO

Introduction The stability of periodic motion in a physical model of a rotorcraft is investigated as the system approaches a ground resonance instability. Stability is characterized by the eigenvalues of discrete, linearized models fitted to points on the Poincare section.

Ground resonance is a well-known instability in rotorcraft caused by the coupling between fuselage motion and rotor blade dynamics [1. Ground resonance remains an important prototypical instability, and may involve both nonlinearity and periodic coefficients depending on the configuration of the rotor and fuselage. For several reasons, a ground resonance model is an attractive test bed for evaluating stability measurement techniques. The phenomenon does not depend on aerodynamic forces, and hence can be studied experimentally without a wind tunnel. In addition, the theory governing the instability [1] is well known and accurate, although the system has multiple degrees-of-freedom.

The ability to measure stability and predict instability of rotorcraft behavior in real time is potentially very useful. The stability of periodic behavior in systems with periodic coefficients and nonlinearity can be determined from the eigenvalues of a local Poincare map [2,3]. This approach has been applied to nonlinear single degree-of-freedom (1-DOF) oscillators [2] and 2-DOF systems [3]. Measurement of stability and prediction of instability in a physical ground resonance model represents an important extension and application of these methods to a practical, multi-degree-of-freedom (N-DOF) system.

Ground resonance model A photograph of the physical model is shown in Figure 1. The model is based on a similar experiment designed in the 1960s by R. Bielawa, and used recently by Flowers [4]. The "fuselage" of the model is an aluminum plate mounted on a two-axis gimball assembly. Stiffness is provided by extension springs attached to the underside of the fuselage. Viscous damping (as well as some additional stiffness) is provided by adjustable air dashpots. A brush-type DC-servo motor drives the rotor directly at a commanded speed. Two or four cylindrical "blades" with lead-lag hinges are mounted symmetrically on the rotor hub. Thin, cantilevered music wire beams attached to the blades serve as centering springs. Bearings at the blade hinges and on the gimball are all low-friction (ABEC-5 or higher) ball bearings. The entire assembly is housed in a steel-frame box with panels of Lexan safety glass.

Angular displacements of the fuselage (θ, ϕ) and blades (ξ_1, ξ_2, ξ_3, ξ_4) are measured by RVDTs. Signals from the hub are transmitted through a slip-ring to the data acquisition system. To obtain Poincare sections, a signal from the motor encoder is used to trigger the acquisition of data once per revolution. Since only displacement is measured, time-delayed measurements ($\theta(t+dt)$, $\phi(t+dt)$, etc.) are also acquired once per revolution.

Measurements and stability analysis At a given rotor speed the model exhibits small oscillations. A small perturbation is applied to the system at a random phase in the forcing cycle, and 20-30 points on the Poincare section are obtained. Typical transients of the discrete points on the Poincare section are shown in Figure 2. All the measurements taken at the start of the nth

revolution are stored in a pseudo-state vector $\mathbf{x}_n$; a total of N of these vectors are stored. A linearized map is assumed to approximate the transient dynamics of points on the Poincare section:

$$\mathbf{x}_{n+1} = A\mathbf{x}_n + \mathbf{b} \tag{1}$$

A least-squares fitting procedure [2] is used to estimate the matrix A (the Floquet transition matrix) and the constant vector $\mathbf{b}$, and the eigenvalues of A are found numerically. The inverse map ($\mathbf{x}_{n-1} = C\mathbf{x}_n + \mathbf{d}$) is also estimated, and the eigenvalues of C are compared those of A to eliminate spurious estimates. The eigenvalues with largest magnitude describe the stability of the system.

Both the magnitude and phase of the eigenvalues may be used to track changes in stability as a function of rotor speed. Experimental trajectories of eigenvalues in the complex plane as rotor speed approaches the ground resonance condition will be presented and compared to theory.

References

1. R.P. Coleman and A. M. Feingold, "Theory of self-excited mechanical oscillations of helicoper rotors with hinged blades," NACA TR-1351 (1958).
2. K.D. Murphy, P.V. Bayly, L.N. Virgin and J.A. Gottwald, "Measuring the stability of periodic attractors using perturbation-induced transients: application to two nonlinear oscillators," *Journal of Sound and Vibration*, 172:85-102, 1994.
3. P.V. Bayly and L.N. Virgin, "An empirical investigation of the stability of periodic motion in the forced spring-pendulum," *Proceedings of the Royal Society of London*, 443A:391-408, 1993.
4. G.T. Flowers, "A study on the effects of nonlinearities on the behavior of rotorcraft in ground and air resonance," PhD Thesis, Mechanical Engineering, Georgia Institute of Technology, Dec. 1988.
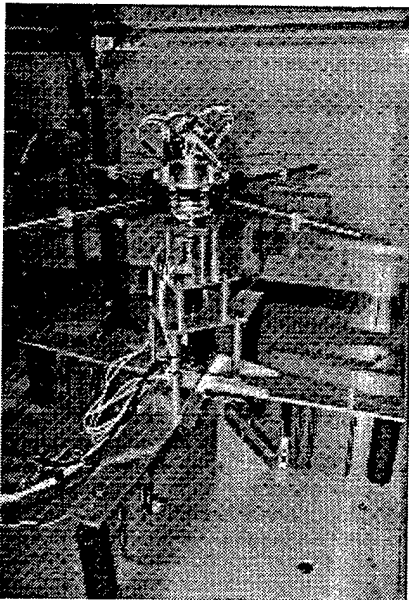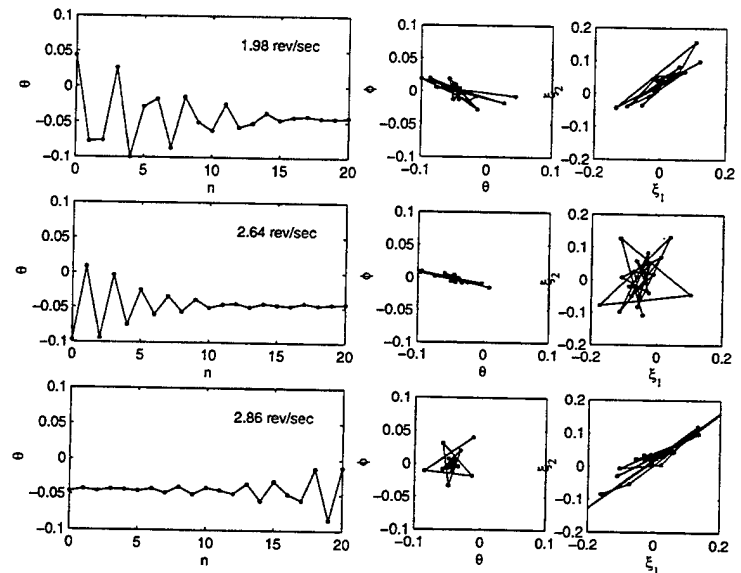
Figure 1: Ground resonance model

Figure 2: Points on the Poincare section plotted vs iteration number and in state space. Eigenvalues are (respectively at 1.98, 2.64, and 2.86 rev/sec): $\lambda = -0.57 \pm 0.65$, $\lambda = -0.58 \pm 0.58$, and $\lambda = -1.00 \pm 0.78$.

Monday, July 27
1330-1500
Session 5.

On the Reconstitution Problem
in the Multiple Time Scale Method

A. Luongo   A. Paolone

Dipartimento di Ingegneria delle Strutture, delle Acque e del Terreno,
University of L'Aquila, 67040 Monteluco di Roio (L'Aquila), Italy

The multiple time scale method has been widely used to analyze the dynamical response of weakly nonlinear mechanical systems, both in free oscillations and in forced oscillations regime [1]. More recently, it has been also used in the description of non-linear normal modes [2] and in the analysis of the local post-critical behavior in bifurcation problems [3, 4]. Furthermore, it has been applied to discrete-time dynamical systems [5]. Similarly to other reduction methods, the multiple time scale method reconducts the analysis of the evolution of a multidimensional dynamical system to that of an equivalent dynamical problem of dimension less than the original one, and equal to the number of amplitudes and/or phases that characterize the response at regime.

The multiple time scale method often implies a minor computational effort if compared with other reduction methods. For example, in the description of nonlinear normal modes, it is simpler and involves less algebra than the normal form method [2]. Analogous result is found in the analysis of local bifurcations, when comparison is made with the center manifold reduction method [3, 4]. Nevertheless, the cases in which the equivalent dynamical system equation is obtained through a unique non-trivial step of the perturbative procedure, should be distinguished from those in which more non-trivial steps have to be performed. In fact, in the former case, the method brings to motion amplitude equations already reduced in normal form [2]–[4], while in the latter the presence of additional extraneous terms is possible.

As shown in [6]–[7], spurious solutions can arise when a reconstitution of the time scale [8] is performed. This inconvenient can be avoided if the steady-state solutions are determined by separately vanishing the different amplitudes time-derivatives at each order of the perturbation procedure [9], thus giving up to obtain the equivalent dynamical system. These solvability conditions can be satisfied if a suitable number of control parameters are expanded in series of the perturbation parameter or, less conveniently, if the homegeneous solutions of the perturbative equations are accounted for at each step. In problems of local bifurcation, the number of the parameters to be expanded turns out to be equal to the co-dimension of the bifurcation itself [4].

Notwithstanding this circumstance seems to be well known in literature, due to computational reasons, a strong interest is still devoted to obtain a dynamical system equivalent to the original one and, obviously, exempt from additional extraneous steady-state solutions. This has given rise to a great deal of proposals alternative to the reconstitution method, which

often are confusing [10]-[11].

In this paper, after an analysis of the state of art on the subject, two classes of methods employed in literature are individuated. In the first class the reconstituted system is "ε-dependent", while in the second one the perturbation parameter "ε" is absorbed (e.g. by imposing "$\varepsilon = 1$"). The first class of method is here called "coherent", the second class "incoherent", since in the latter the logic on which the asymptotic method is based is violated. It is shown that incoherent methods sometimes furnish wrong results, since the "exact" numerical solution of the reconstituted equations contains ε-terms which are of higher order than the highest order term present in the equations. Moreover, in each class of methods applied in literature, two different procedures are followed. In the first one all the time-derivatives on the slower scales are retained in the solvability conditions at each step; in the second (simplified) procedure such derivatives are instead neglected by invoking questionable reasons [10]-[11]. Obviously the neglected terms do not influence the steady-state solutions; however they can affect the eigenvalues of the linearized problem and therefore to play a non-trivial role on the stability of the stead! y-state solutions. By evaluating t he eigenvalues with respect to the concept of "coherence", the limits of validity of the simplified procedure are discussed.

Finally the particular cases in which the "incoherent" reconstitution method together with the simplified procedure do not involve spurious solutions neither errors on stability are illustrated.

References

[1] A.H. Nayfeh and Mook, D.T., *Nonlinear Oscillations*, Wiley, New York, 1979.

[2] A.H. Nayfeh 1995 *Journal of Vibration and Control* 1, 389-430. On direct methods for constructing nonlinear normal modes of continuous systems.

[3] A.H. Nayfeh and B. Balachandran 1995 *Applied Nonlinear Dynamics*. Wiley-Interscience, New York.

[4] A. Luongo and A. Paolone 1997 *Nonlinear Dynamics* 14, 193-210. Perturbation Methods for Bifurcation Analysis from Multiple Nonresonant Complex Eigenvalues.

[5] A. Luongo 1996 *Nonlinear Dynamics* Perturbation methods for nonlinear autonomous discrete-time dynamical systems, 10, 317-331.

[6] Z. Rahman and T.D. Burton 1989 *Journal of Sound and Vibration* , 133, 369-379. On Higher Order Methods of Multiple Scales in Non-Linear Oscillations-Periodic Steady State Response.

[7] A. Hassan 1994 *Journal of Sound and Vibration*, 178, 1-19. Use of transformations with the higher order method of multiple scales to determine the steady state periodic response of harmonically excited nonlinear oscillators, Part I: transformation of derivative; 178, 21-40, Part II: transformation of detuning.

[8] A.H. Nayfeh 1985 Topical course on nonlinear dynamics, *Società italiana di Fisica, Santa Margherita di Pula, Sardinia*. Perturbation methods in nonlinear dynamics.

[9] A. Luongo, G. Rega, F. Vestroni 1986 *Journal of Applied Mechanics*, 53, 619-624. On nonlinear dynamics of planar shear indeformable beams.

[10] C.L. Lee and C.T. Lee 1997 *Journal of Sound and Vibration*, 202, 284-287. A higher order method of multiple scales.

[11] F. Benedettini, G. Rega and R. Alaggio 1995 *Journal of Sound and Vibration*, 182, 775-798. Non-linear oscillations of a four-degree-of-freedom model of a suspended cable under multiple internal resonance conditions.

Escape Criteria For Imperfection Sensitive Single Degree Of Freedom Structures Under External Harmonic Loading

D. M. Santee and P. B. Gonçalves
Pontifícia Universidade Católica - PUC-Rio
Civil Engineering Department
Rio de Janeiro CEP 22453-900 - Brazil

Imperfection sensitive structures, under externally applied loading, when reduced to one degree of freedom, and assuming small amplitude vibrations can be expressed by the ordinary differential equation (1), for structures liable to an asymmetric bifurcation, and (2), for structures liable to an unstable symmetric bifurcation. The dots on expressions (1) and (2) mean time (t) derivatives, $\zeta > 0$ is a viscous damping parameter, ω_0^2 is the effective stiffness, ε is an imperfection parameter, β and $\gamma > 0$ are non-linearity parameters, finally F and Ω are the maximum intensity and frequency of the externally applied driving force.

$$\ddot{x} + 2\zeta\omega_0\dot{x} + \omega_0^2 x + \varepsilon + \beta x^2 = F\cos(\Omega t) \tag{1}$$

$$\ddot{x} + 2\zeta\omega_0\dot{x} + \omega_0^2 x + \varepsilon - \gamma x^3 = F\cos(\Omega t) \tag{2}$$

Solutions to particular cases of these equations have been studied both numerically and analytically by several authors [1,2,3,4,5], and been found to be very complex. Generally from the engineers point of view, the main concern is with the unbounded solutions or escape from a safe potential well. Physically this means the ruin or failure of the structure. In this sense it is important to engineering design the existence of analytical criteria to predict these unbounded, or escaping, solutions.

The objective of this work is to study different criteria to predict the minimum value of F that leads to escaping solutions of equations (1) - for structures liable to asymmetric bifurcation, and (2) - for structures liable to unstable symmetric bifurcations, considering all the other parameters fixed. The following criteria are compared:

a) **The Melnikov Criterion:**. This criterion is based on the fact that when the stable manifold of a saddle point crosses transversally its unstable manifold, they cross at infinitely many points. This in turn makes the boundary of the basin of attraction become fractal, making the whole basin loose its integrity. The value of the forcing parameter F that makes the stable and unstable manifolds cross is the escape force can be considered as a safe lower-bound of the escape load.

b) **The Criteria of Maximum Displacement, Maximum Velocity or Potential Barrier:** These criteria are based on an approximate analytical solution. The value of the forcing amplitude parameter F that makes the maximum displacement, maximum velocity or maximum energy of the approximate analytical solution, become greater then the maximum displacement, velocity or potential energy of the conservative basin of attraction, is the escape force. The precision of the results are dependent on the quality of the approximate solution.

c) **The Bifurcation Criterion:**. For this criterion the escape force is the value of F that makes the approximate solution loose its stability, either by a fold or a flip bifurcation.

Most of these criteria depends strongly on the analytical expression of the approximate solution, this means that for different frequency regions, where different approximate solution expressions are needed lead to different escape expressions. figure a shows the results of the different escape criteria, and the numerical solution, for a structure liable to asymmetric bifurcation (1) with the following parameters: $\varepsilon = 0$, $\omega_0 = 1$, $\beta = -1$ and $\zeta = 0.05$, on the vicinity of the natural frequency.
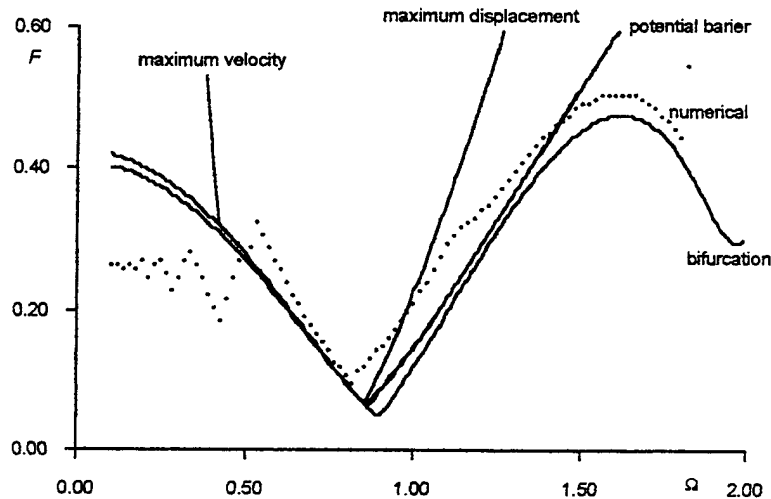

Figure A

References.

1. W. Szemplińska-Stupnicka 1995 *Nonlinear Dynamics* 7,129-147. The Analytical Predictive Criteria for Chaos and Escape in Nonlinear Oscillators: A Survey

2. M. S. Soliman 1993 *Journal of Applied Mechanics* 60, 669-676. Jumps to Resonance: Long Chaotic Transients, Unpredictable Outcome, and the Probability of Restabilization

3. J. A. Gottwald, L. N. Virgin and E. H. Dowell 1995 *Journal of Sound and Vibration* 187(1), 133-144. Routes to Escape from an Energy Well.

4. W. Szemplińska-Stupnicka and P. Niezgodzki 1990 Journal of Sound and Vibration 141(2), 181-192. The Approximate Approach to Chaos Phenomena in Oscillators Having Single Equilibrium Position.

5. P. B. Gonçalves and D. M. Santee 1997 "Non-Linear Vibrations and Instabilities of Structural Systems Liable to Asymmetric Bifurcation". In: Structural Dynamics: Recent Advances, vol. 1, Fergunson, Wolve and Mei eds., University of Southampton

RESPONSE AND STABILITY OF PIECEWISE LINEAR OSCILLATORS UNDER PARAMETRIC AND EXTERNAL EXCITATION

S. Theodossiades, I. Goudas and S. Natsiavas

Department of Mechanical Engineering

Aristotle University

54006 Thessaloniki

Greece

(Phone: +30 31 996088, Fax: +30 31 996078, e-mail: natsiava@ccf.auth.gr)

ABSTRACT

Dynamical systems with piecewise linear characteristics are frequently encountered in many engineering applications. When the coefficients appearing in the equations of motion of these systems are constant, it may be possible to apply methodologies which locate exact solutions of these equations. However, in cases of oscillators with time-varying coefficients it is no longer possible to obtain exact analytical solutions.

The main objective of the present study is to develop a methodology which determines approximate periodic steady-state solutions for a general class of piecewise linear systems. The equations of motion of these systems involve weakly periodic coefficients and periodic external forcing terms. The method of analysis combines characteristics of classical perturbation approaches applied to oscillators with time-varying coefficients as well as of exact methods employed for piecewise linear systems with constant coefficients. Through the application of a proper analytical scheme, the task of locating periodic steady-state motions of such systems under parametric and external excitation is reduced to the solution of relatively small sets of algebraic equations. In addition, the analytical part of the method is complemented by appropriate methodologies for investigating the stability properties of the various types of located periodic solutions.

In the second part of the study, a gear-pair model with backlash is employed as an example mechanical oscillator. First, the accuracy of the new analytical procedure is confirmed with numerical results obtained by direct integration of the equations of motion. Then, numerical results are presented in the form of frequency-response diagrams, showing the effect of the variable stiffness, the damping and the external load parameters on the system response. In places where branches of periodic solutions lose stability, the resulting dynamic response is captured by direct integration. This reveals the coexistence of multiple solutions, the appearance of boundary crises phenomena and the existence of period doubling and trippling sequences leading to a repeated interchange of periodic and chaotic responses of the system.

ON APPLYING SPECIAL NON-SMOOTH TEMPORAL TRANSFORMATIONS TO SYSTEMS PARAMETRICALLY EXCITED BY DISCONTINUOUS FORCES

Valery N. Pilipchuk

Department of Applied Mathematics
State Chemical and Technological University of Ukraine
Gagarin Ave., 8, Dnepropetrovsk, Ukraine 320005

Current mailing address: Mechanical Engineering, WSU, Detroit, MI 48202
E-mail: pylyp@me1.eng.wayne.edu

The action of instantaneous impulses on a mechanical system is frequently simulated using one of the two methods. The first one imposes special conditions for the velocities in the neighborhoods of the impulses location, while the second one requires an introducing the Dirac's function into the equations. An advantage of the first approach is that the differential equations describing the system are the same as when there are no impulses acting. However, these equations are treated separately in each of the intervals between the impulses, and hence, instead of a single system, a whole sequence of systems must be analyzed. The second method gives a single set of equations over the whole time interval without introducing the above-mentioned conditions imposed on the variables. However, in this case the analysis can be carried out correctly within the framework of the theory of generalized functions (distributions). This requires additional mathematical proofs in non-linear cases and cases of the parametric loading of a mechanical system as well. Both of the mentioned above ways of analysis are fruitfully employed for different quantitative and qualitative considerations of mechanical systems under pulsed excitations.

A method is described in this paper which enables one, on the one hand, to eliminate the singular terms in the equations of motion and, on the other hand, to obtain solutions as a single analytic expression over the whole time interval. The analytical technique related is based on an idea of non-smooth transformations of variables. At least two different ways by which the idea of non-smooth transformations can be realized are

possible. The first realization deals with the spatial coordinates of the so-called vibroimpact systems. This kind of transformations enables one to eliminate absolutely rigid constrains that the vibroimpact systems must include by its definition. The second way does not necessarily imply that a system includes any rigid constrains. Instead of the spatial coordinates, the parameter of time is transformed by means of a non-smooth function. As a result the spatial coordinates get a special algebraic structure with a series of mathematically suitable properties. This kind of transformations is applied to systems subjected to the impulsive and discontinuous excitations. It is suggested that the solutions of differential equations of motion for mechanical systems with periodic impulsive excitation can be found in a special form that contains a standard pair of non-smooth periodic functions and possesses the structure of an algebra without division. This form is also suitable in the case of excitation with a periodic series of the first kind of discontinuities. The transformations are illustrated on the series of examples. An explicit form of analytical solutions has been obtained for periodic regimes. In the case of parametric impulsive excitation, it is shown that a dipole-like shift in the periodic series of impulses has an impotent mechanical meaning. For example, the sequence of instability zones loses its different subsequences dependently on a parameter of the shift.

The pair of non-smooth functions plays an important role in the proposed method. In the symmetric case these functions are associated in a natural way with the motion of a free point mass between two fixed arresting devices, that is, with one of two simplest mechanical oscillators. The functions belong to the set of elementary ones and can be treated as the sawtooth sine and rectangular cosine. Hence, the technique applied in this work also has a certain physical meaning.

DELAMINATED BEAM NONLINEAR DYNAMIC RESPONSE CALCULATION AND VISUALIZATION

H. Luo[*] and S. Hanagud
School of Aerospace Engineering
Georgia Institute of Technology
Atlanta, Georgia 30332

One of the earliest models for vibration analysis of composite beams with delaminations was proposed by Ramkumar et al.[1]. This model simply used four Timoshenko beams connected at the delamination edges to model a composite beam with one through-width delamination. The predicted frequencies based on this model were consistently lower than the results of experimental measurements. Wang et al.[2] improved the analytical solution by including coupling between flexural and axial vibrations of the delaminated sublaminates. Using an isotropic beam with splits and the classical beam model, they found that the calculated natural frequencies were closer to experimental results. With similar considerations, Nagesh and Hanagud[3] formulated a finite element solution for arbitrary composite beams. In the finite element models, they considered a classical composite beam model as well as the beam model with high order shear deformations. Later, Mujumdar and Suryanarayan[4] proposed a model which imposed a constraint between the delaminated sublaminates to force them to have the same flexural displacement. This model was unable to predict the delamination opening mode observed in experiments.

Experimental research on delaminations can be found in a paper by Shen and Grady[5]. In their report, opening modes were found even in the first mode for some cases of delaminated beams. Experimental research conducted by Hanagud and Luo[6-7] has indicated that the delamination modes can also be found in combination with higher order modes for through-width as well as embedded delamination cases.

The existence of delamination modes in delaminated composites has been corroborated by analytical and experimental research. Due to the change of effective stiffness caused by delamination opening and closing, we expect nonlinear effects in the dynamic response of delaminated structures. The purpose of this paper is to develop a procedure that is able to calculate the dynamic response of a delaminated structure by using the analytical modes obtained by a delamination analysis method proposed by the authors. The analysis is used for nondestructive examination of damaged composite structures.

References

[1] Ramkumar, R. L., Kulkami, S. V. and Pipes, R. B., "Free Vibration Frequencies of a Delaminated Beam," 34th Annual Technical Conference, 1979 Reinforced Plastics/Composites Institute, The Society of the Plastics Industry, Inc., Section 22-E, pp. 1-5.
[2] Wang, J. T. S., Liu, Y. Y. and Gibby, J. A., "Vibration of Split Beams," Journal of Sound and Vibrations, Vol. 84, No. 4, 1982, pp. 491-502.
[3] Nagesh Babu, G. L. and Hanagud, S., "Delamination in Smart Structures - A Parametric Study on Vibrations", 31st SDM Conference, 1990, pp. 2417-2426.
[4] Mujumdar, P. M. and Suryanarayan, S., "Flexural Vibrations of Beams with Delaminations," Journal of Sound and Vibrations, Vol. 125, No. 3, 1988, pp. 441-461.
[5] Shen, M,-H, H and Grady, J. E., "Free Vibrations of Delaminated Beams," AIAA Journal, Vol. 30, No. 5, May 1992, pp. 1361-1370.
[6] Hanagud, S. and Luo, H., "Modal Analysis of a Delaminated Beam," Proceedings of SEM Spring Conference on Experimental Mechanics, June 1994, pp. 880-887.
[7] Luo, H. and Hanagud, S., "Delamination Detection Using Dynamic Characteristics of Composite Plates," Proceedings of 36th AIAA/ASME/ASCEI AHS SDM Conference, 1995, pp. 129-139.

[*] H. Luo is currently with G. E. Schenectady, NY

Monday, July 27
1530-1700
Session 6A.

SELF-EXCITED OSCILLATIONS OF MACHINE TOOLS

Tamás Kalmár-Nagy[1], Francis C. Moon[2] and Gábor Stépán[3]

[1]Department of Theoretical and Applied Mechanics
Cornell University, Ithaca, NY 14853, USA
email:nagy@tam.cornell.edu
[2]Sibley School of Aerospace&Mechanical Engineering
Cornell University, Ithaca, NY 14853, USA
email:fcm3@cornell.edu
[3]Department of Applied Mechanics
Technical University of Budapest, Budapest H-1521, Hungary
email:stepan@mm.bme.hu

Recently, there has been an increased interest in vibrations in material removal processes such as cutting and drilling. Some of these vibrations arise due to a regenerative effect. This study concerns regenerative machine tool oscillations in cutting.

During machining the tool may start a damped oscillation relative to the workpiece. This motion will make the surface of the workpiece uneven. Thus the chip thickness will vary at the tool after a revolution. The cutting force therefore not only depends on the current position of the tool and the workpiece but also on a delayed value of the displacement. This is the so-called regenerative effect. The corresponding mathematical model is a delay-differential equation.

Recent experiments as well as the earlier results of Shi and Tobias ([6]) clearly show the existence of unstable periodic motion of the tool around its asymptotically stable position related to the stationary cutting. These observations strengthen the possibility of a Hopf bifurcation. The PhD theses Johnson ([3]) and Fofana ([2]), as well as the paper of Nayfeh, Chin, Pratt ([5]) presented the analysis of the Hopf bifurcation in different models using different methods, like the method of multiple scales, harmonic balance, Floquet Theory and of course, numerical simulations.

Here we study a simple 1 degree of freedom (DOF) damped oscillator model of orthogonal cutting. By doing so, we hope we are able to isolate and study the effects related to the delay. The model is

$$\ddot{x} + 2\kappa\alpha\dot{x} + \alpha^2 x = -\frac{1}{m}\Delta F_x(\Delta f) \tag{1}$$

with α and κ being the natural angular frequency of the undamped system and the relative damping factor, respectively. ΔF_x is the cutting force variation and given by a truncated power series expansion around the zero value of the chip thickness variation $\Delta f = f - f_0 = x(t) - x(t - \tau)$

$$\Delta F_x(\Delta f) = \begin{cases} k_1 \left(\Delta f - \frac{1}{8f_0} \Delta f^2 + \frac{5}{96f_0^2} \Delta f^3 \right) & \text{if } \Delta f > -f_0 \\ -\frac{4}{3} k_1 f_0 & \text{if } \Delta f \le -f_0 \end{cases} \tag{2}$$

where k_1 is the so-called cutting force coefficient, while τ is the time of one revolution of the workpiece.

The aim of this paper is to give a rigorous analytical investigation of the Hopf bifurcation present in the regenerative machine tool vibration model using computer algebra (see also [4]).

We also consider nonlinear phenomena when the tool leaves the material (as in [1], [6]). In this case the regenerative effect disappears, and the result of the local analysis is not valid anymore. We show that in this case there exists an attractor (see also [7]).

References

[1] S. Doi and S. Kato, Chatter vibration of lathe tools, *Transactions of the ASME* **78**(5), 1956, 1127-1134.

[2] M. Fofana, Nonlinear Dynamics of Cutting Process, PhD thesis, University of Waterloo, Waterloo, 1993.

[3] M. A. Johnson, Nonlinear differential equations with delay as models for vibrations in the machining of metals, PhD Thesis, Cornell University, 1996.

[4] T. Kalmár-Nagy, G. Stépán and F. C. Moon, Regenerative machine tool oscillations, Submitted to Dynamics of Continuous, Discrete and Impulsive Systems, 1998.

[5] A. H. Nayfeh, C. Chin and J. Pratt, Perturbation methods in nonlinear dynamics - applications to machining dynamics, *J. Manuf. Sci. Eng.*, 1997.

[6] H. M. Shi and S. A. Tobias, Theory of finite amplitude machine tool instability, *Int. J. of Machine Tool Design and Research* **24**, 1984, 45-69.

[7] G. Stépán, Delay-differential equation models for machine tool chatter, *Nonlinear Dynamics of Material Processing and Manufacturing* (Ed.: F. C. Moon), Wiley, New York, 1997.

Stability of Diamond Turning Processes that use Round Nosed Tools

D.E. Gilsinn, M.A. Davies, National Institute of Standards and Technology, Gaithersburg, MD 20899-0001

B. Balachandran, Dept. of Mechanical Engineering, University of Maryland, College Park, MD 20742-3035

In this article, a multi-mode model is developed for a boring bar in a diamond-turning process. The model takes into account the cutting forces that result from the geometry of the chip area cut by a round nosed tool. An underlying assumption of this model is that during one feed pass of the round nosed tool it produces a helical groove in the workpiece that overlaps with itself depending on the feed rate and spindle speed. The current model assumes that the feed rate is slow relative to the spindle speed so that the grooves overlap and can lead to regenerative effects. This leads to a system of retarded differential equations that is studied to determine the stability of the cutting process with respect to parameters such as feed rate, depth of cut, and spindle speed. These cutting forces are assumed proportional to the uncut chip area. The chip area, A_c, generated during the cutting action is approximately modeled as a parabolic segment that is a function of the tool feed rate, the depth of cut, and the current and previous tool-displacement histories. In order to study the stability of the system the linear approximation to A_c was computed as

$$A_c = \alpha_0 + \alpha_1 v + \beta_1 v_\tau \tag{1}$$

where

$$\alpha_0 = \frac{24dfR - f^3 - 12d^2 f}{24R - 12d}, \alpha_1 = \frac{f}{2} + z_0, \beta_1 = \frac{f}{2} - z_0 \tag{2}$$

The delay differential equations take the form

$$\ddot{a}_i + 2\xi_i\omega_i\dot{a}_i + \omega_i^2 a_i = -W_i(L-R)K(\alpha_0$$
$$+\alpha_1 \sum_{j=1}^{N} a_j(t)W_j(L-R) + \beta_1 \sum_{j=1}^{N} a_j(t-\tau)W_j(L-R)) \tag{3}$$

where $\omega_i^2 \approx \frac{EI}{\rho A}\left(\frac{(2i-1)\pi}{2}\right)^4$, $\xi_i\omega_i = \gamma/\rho A$ for $i = 1,...N$, the spatial mode shapes $W_i(z)$ are approximated by the spatial modes associated with the free vibrations of an undamped, isotropic cantilever beam and $a_i(t)$ represents the time dependent amplitudes. L is the length of the boring bar, R the radius of the tool tip, τ the time for one spindle revolution and K aparameter related to the workpiece cutting energy. The right hand side of equation (3) contains a constant that represents the static cutting force that would be experienced under nonoscillatory cutting conditions. For the purpose of stability analysis this term can be eliminated. Because this problem is somewhat different than that of simple orthogonal cutting, calculation of stability boundaries is somewhat more involved. However, for feeds, f, and depths of cut, d, much smaller than the tool tip radius, R, the equations are amenable to analytic solution. Following the orthogonal cutting analysis, let s be a complex variable. Then the characteristic equation becomes

$$1 + K(\alpha_1 + \beta_1 e^{-s\tau}) \sum_{m=1}^{N} \Phi_m(s)W_m^2 = 0 \tag{4}$$

where

$$\Phi_m(s) = \frac{1}{s^2 + 2\xi_m \omega_m s + \omega_m^2} \tag{5}$$

For the stability boundary analysis, let $s = i\omega$, $\Phi_m(i\omega) = G_m(\omega) + iH_m(\omega)$ and $G(\omega) = \sum_{m=1}^{N} W_m^2 G_m(\omega)$, $H(\omega) = \sum_{m=1}^{N} W_m^2 H_m(\omega)$. From the imaginary part of (4), one can obtain $\frac{H(\omega)}{G(\omega)} = \frac{\frac{\beta_1}{\alpha_1} \sin \omega \tau}{1 + \frac{\beta_1}{\alpha_1} \cos \omega \tau}$. The method of perturbations can be used in two steps to show that the right hand side of this equation can be put into a form similar to one that arises in the stability analysis of orthogonal cutting. From (2), one obtains $\frac{\beta_1}{\alpha_1} = \frac{-1+\epsilon}{1+epsilon} \approx -1 + 2\epsilon$, $\epsilon = \frac{f}{2z_0}$, where z_0 is the half-chip width. To be meaningful the feed must be less than the denominator, which is the chip width. In the case of diamond turning ϵ is often very small. This implies that $\frac{\frac{\beta_1}{\alpha_1} \sin \omega \tau}{1 + \frac{\beta_1}{\alpha_1} \cos \omega \tau} \approx \frac{(-1+2\epsilon) sin \omega \tau}{1 + (-1+2\epsilon) cos \omega \tau}$. As a first step, if we consider a perturbed frequency $\omega(\epsilon) = \omega_0 + \epsilon \omega_1 + \epsilon^2 \omega_2 + \cdots$, then, to a first order ϵ approximation, we can solve for the coefficient ω_1 so that, using the Taylor series, sum of angles formulas and the assumption that $\epsilon \omega_1 \tau$ is small,

$$\frac{H(\omega_0) + \epsilon \omega_1 H'(\omega_0)}{G(\omega_0) + \epsilon \omega_1 G'(\omega_0)} \approx \frac{-\sin \omega_0 \tau_0 + \epsilon(2 \sin \omega_0 \tau_0 - \omega_1 \tau_0 \cos \omega_0 \tau_0)}{(1 - \cos \omega_0 \tau_0) + \epsilon(2 \cos \omega_0 \tau_0 - \omega_1 \tau_0 \sin \omega_0 \tau_0)} \tag{6}$$

where ω_0 and τ_0 are obtained as a first term generator for $\omega(\epsilon)$ by an orthogonal cutting argument. In order to use the methods from orthogonal cutting to develop stability charts for round nosed tools we must, in the second step, find a function $\tau(\epsilon)$, defined on an interval about $\epsilon = 0$, such that $\tau(0) = \tau_0$ and

$$\frac{(-1+\epsilon) \sin \omega(\epsilon) \tau_0}{(1+\epsilon) + (-1+\epsilon) \cos \omega(\epsilon) \tau_0} = \frac{-\sin \omega_0 \tau(\epsilon)}{1 - \cos \omega_0 \tau(\epsilon)} \tag{7}$$

Then $\frac{H(\omega(\epsilon))}{G(\omega(\epsilon))} = \frac{-sin \omega_0 \tau(\epsilon)}{1 - cos \omega_0 \tau(\epsilon)} = \tan \psi$, where ψ is the phase of the transfer function that is given by $\psi = \arctan \left(\frac{H(\omega(\epsilon))}{G(\omega(\epsilon))} \right)$. To solve for $\omega_0 \tau(\epsilon)$, half angle formulas are used to show that $\omega_0 \tau(\epsilon) = 2(\psi + p\pi) + 3\pi$ for $p = 0, 1, 2, \ldots$. The spindle rotation rate is computed as $\Omega(\epsilon) = \frac{1}{\tau(\epsilon)}$. Finally, using the real part of the characteristic equation,

$$K(\epsilon) \approx \frac{-1}{2\alpha_1 G(\omega_0) + \epsilon \alpha_1 P(\omega_0)} \tag{8}$$

where $P(\omega_0)$ is a perturbation term computed by assuming first order approximation in terms of ϵ. As $\epsilon \to 0$, the cutting energy parameter $K(\epsilon)$ approaches the form for orthogonal cutting. The results can be presented as a graphs of $K(\epsilon)$ versus $\Omega(\epsilon)$, which form the stability charts. For round nosed tools, these charts are found to be perturbed forms of those obtained for orthogonal cutting tools. For a given fixed feed rate, the two most significant parameters that affect the stability regions are found to be the tool nose radius and the material damping ratio. The predicted stability results are found to be consistent with observations made during experiments. This work also points to the importance of considering a multi-mode formulation for high-speed turning processes since the boundary lobes for the higher modes can interleave the stable regions for lower modes. This occurs most prominently at higher spindle rotation rates.

Milling of Flexible Structures: Dynamics of Workpiece-Tool Interactions

M. X. Zhao
Graduate Research Assistant

and

B. Balachandran
Assistant Professor
Department of Mechanical Engineering
University of Maryland
College Park, MD 20742-3035

Analytical and experimental investigations into workpiece-tool interactions during milling of flexible structures are conducted in this study. A first generation mechanics based model is developed and numerically implemented. The various aspects of this model include the following: a) the workpiece and the tool each have two degrees of freedom (see Figure 1), b) inclusion of process damping along the lines of Tlusty (1985), c) a refined orthogonal cutting model inclusive of the effects of the helix angle of the tool, and d) accommodation of partial engagement of the tool with the workpiece and regenerative effects. The approach used for describing the cutting forces along the tool is similar to a certain extent to the approach followed by Kline, DeVor, and Lindberg (1982). Numerical simulations are conducted for milling operations carried out with a high-speed steel helical tool on a flexible aluminum workpiece. The results are analyzed by using the following tools: a) time histories, b) phase portraits, c) power spectra, and d) dimension calculations. Bifurcation diagrams on Poincaré sections are also presented.
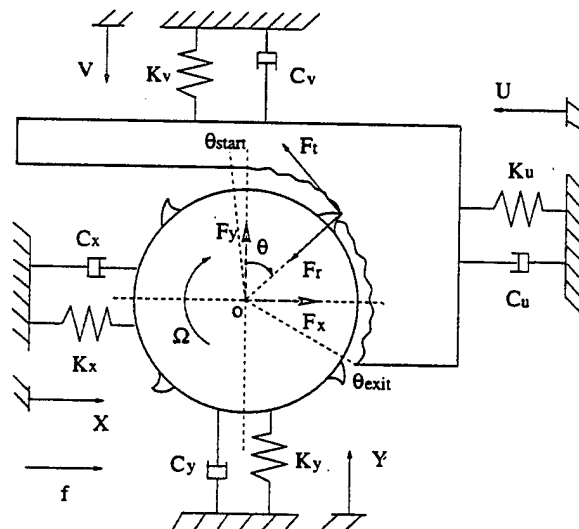

Figure 1: Model of workpiece-tool system

The results obtained in the numerical simulations are compared to observations made in experiments, which were conducted by using the set up illustrated in Figure 2.

1 SPINDLE
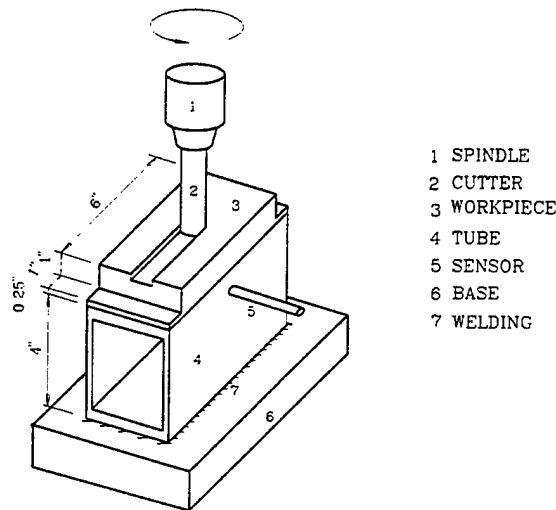2 CUTTER
3 WORKPIECE
4 TUBE
5 SENSOR
6 BASE
7 WELDING

Figure 2: Experimental arrangement

The numerical results are found to be in good agreement with the experimental observations presented in the reports of Balachandran (1996–1997). Stability charts obtained by using the current model are also compared with those obtained by Altintas and Budak (1995). It is believed that the current model, which is unique in terms of description of cutting forces, is applicable to a wide range of cutting operations including partial immersion cuts, high immersion cuts, and slotting cuts. Unlike the other available models, the current model allows us to study cases where both regenerative effects and nonlinearities due to intermittent engagement of the cutter are likely to have a significant influence on the dynamics of workpiece-tool interactions.

References

1. Tlusty, J., "Machine Dynamics," in *Handbook of High-speed Machining Technology*, R. I. King, ed., pp. 48-153, Chapman and Hall, New York, 1985.

2. Kline, W. A., DeVor, R. E., and Lindberg, J. R., "The prediction of cutting forces in end milling with application to cornering cuts," *Int. J. Mach. Tool Des. Res.*, Vol. 22, No. 1, pp. 7-22, 1982.

3. Balachandran, B., "Modeling of Dynamics for Milling of Thin Walled Structures," *Progress Reports to the National Institute of Standards and Technology*, Gaithersburg, Maryland, May 1996 to December 1997.

4. Altintas, Y. and Budak, E., "Analytical prediction of stability lobes in milling," *Annals of the CIRP*, Vol. 44, No. 1, pp. 357–362, 1995.

Monday, July 27
1530-1700
Session 6B.

ACTIVE FLOW CONTROL FOR TWIN-TAIL BUFFET ALLEVIATION*

Essam F. Sheta[†]and Osama A. Kandil[‡]
Aerospace Engineering Department
Old Dominion University, Norfolk, VA 23529

ABSTRACT

Effectiveness of active flow control for twin-tail buffet alleviation is investigated. Tangential leading-edge blowing and flow suction along the path of the wing leading-edge vortices are used to alter the vortex breakdown flow upstream of the twin tail. The tangential leading-edge blowing (TLEB) alters the path and breakdown location of the leading-edge vortices, and moves the leading-edge vortices laterally towards the twin tail, which increases the aerodynamic damping on the tails. The flow suction from the core of the wing leading-edge vortices effectively delays the breakdown location at high angles of attack. The computational model consists of a sharp-edged delta wing of aspect ratio one and swept-back flexible twin tail with taper ratio of 0.23. This complex multidisciplinary problem is solved sequentially using three sets of equations on a dynamic multi-block grid structure. The first set is the unsteady, compressible, full Navier-Stokes equations which are solved accurately in time using the implicit, upwind, flux-difference splitting, finite volume scheme. The second set is the coupled bending and torsion aeroelastic equations of cantilevered beams which are solved accurately in time using fifth-order accurate Runge-Kutta scheme. The third set is the grid-displacement equations which are used for updating the grid coordinates due to the tails deflections. The computational model is pitched at 30° angle of attack. The freestream Mach number and Reynolds number are 0.3 and 1.25 million, respectively.

INTRODUCTION AND BACKGROUND

· The maneuver capabilities of the F/A-18 fighter are achieved through the combination of the leading-edge extension (LEX) with a delta wing and the use of vertical tails. At some flight conditions, the vortices emanating from the highly-swept LEX of the delta wing breakdown before reaching the vertical tails which get bathed in a wake of unsteady highly-turbulent, swirling flow, which produces severe buffet on the tails and has led to their premature fatigue failure.

Experimental investigation of vertical tail buffet models have been conducted by several investigators such as the extensive work by Washburn, et al.[1]. Recently, Moses and Ashley[2] conducted extensive wind tunnel tests on a refurbished 16% , rigid, full-span model of the F/A-18 A/B aircraft with three flexible and two rigid vertical tails.

Kandil, et al.[3] studied the buffet response of twin-tail models in turbulent flow over wide range of angles of attack. The computational results were in good quantitative agreement with the experimental data of Washburn, et al.[1]. In a recent paper by Sheta and Kandil[4], the effects of dynamic pitching-up motion of the configuration model on twin tail buffet response were investigated.

In this paper, the fundamental issue of twin-tail buffet alleviation is investigated using two methods of flow control; tangential leading-edge blowing[5] and flow suction from the vortex cores along the vortex path[6]. Details of the formulation of the multidisciplinary problem, the solution methodology, and the configuration geometrical, aerodynamical, and structural parameters specifications are given in Ref. 3.

RESULTS AND DISCUSSION

Figure 1 shows the buffet excitation spectra of the inner and outer surfaces of the right tail. The buffet excitation parameter is defined by $\sqrt{nF(n)}$, where F(n) is the contribution to power spectrum of $\bar{p}^2/q_\infty^2$ in a frequency band Δn. The TLEB has shown a reduction of up to 23% on the inner surface, and a reduction of up to 33% on the outer surface in favorable of TLEB case. The flow suction has shown a reduction in the buffet parameter of up to 23% on the inner surface, and a reduction of up to 30% on the outer surface in favorable of flow suction case.

In summary, the vortex-core flow suction shows some improvements in the buffet excitation spectra, torsion acceleration spectra, root twisting moment, and an appreciatable reduction in the bending deflection. However, it also shows an increase in the bending acceleration spectra and in the root bending moment. On the other hand, the TLEB shows improvements in the buffet excitation spectra, root bending and twisting moments, and torsion deflections and accelerations. Thus, a combination between the TLEB and vortex-core flow suction may be suggested to combine between the reduction of the bending deflection gained by the flow suction and the lower root moments gained by the TLEB to effectively alleviate the buffet responses of the tails.
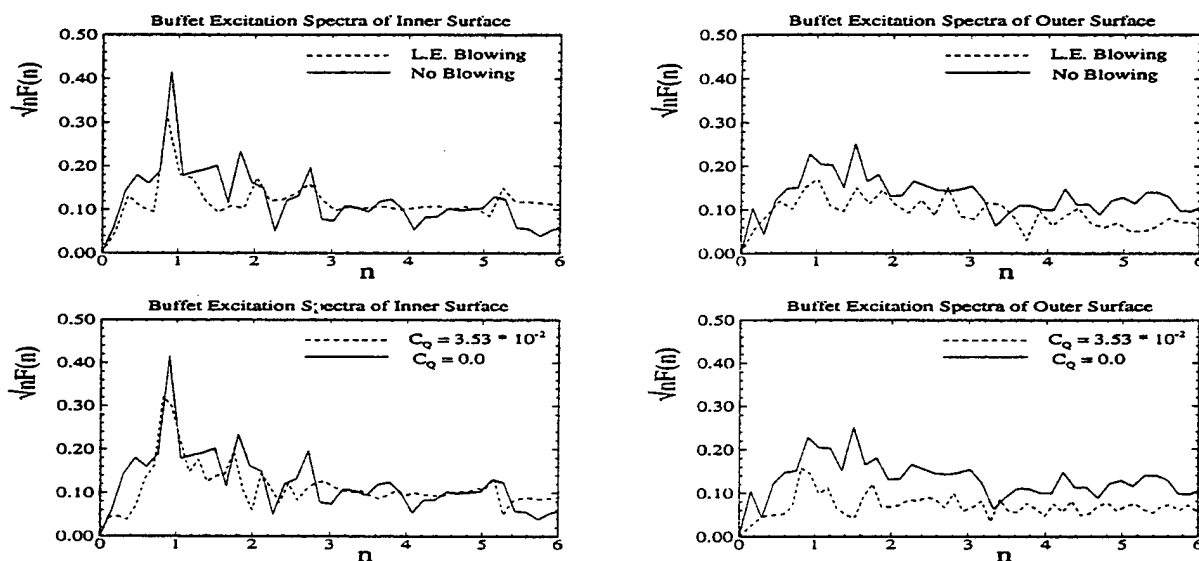

Figure 1: Effects of Leading-edge blowing and flow suction on buffet excitation spectra of the right-tail-tip transducer, 50% chord and 90% span. $M_\infty = 0.3$, $\alpha = 30°$, $R_e = 1.25 \times 10^6$.

REFERENCES

1. Washburn, A. E., Jenkins, L. N. and Ferman, M. A., "Experimental Investigation of Vortex-Fin Interaction," AIAA 93-0050, AIAA 31st ASM, Reno, NV, January 1993.

2. Moses, R. W. and Ashley, H., "Spatial Characteristics of the Unsteady Differential Pressures on 16% F/A-18 Vertical Tails," AIAA-98-0519, AIAA 36th Aerospace Sciences Meeting and Exhibit, Reno, NV, January 1998.

3. Kandil, O. A., Sheta, E. F. and Massey, S. J., "Fluid/Structure Twin Tail Buffet Response Over A Wide Range of Angles of Attack," AIAA 97-2261-CP, 15th AIAA Applied Aerodynamics Conference, Atlanta, GA, June 23-25, 1997.

4. Sheta, E. F. and Kandil, O A., "Effect of Configuration Pitching Motion on Twin Tail Buffet Response," AIAA-98-0520, 36th AIAA Aerospace Sciences Meeting and Exhibit, Reno, NV, January 12-15, 1998.

5. Wong, G. S., Rock, S. M., Wood, N. J. and Roberts, L., "Active Control of Wing Rock Using Tangential Leading-Edge Blowing," Journal of Aircraft, Vol. 31, No. 3, May-June 1994.

6. Hummel, D., "On the Vortex Formation over A Slender Wing at Large Angles of Incidence," AGARD-CP-247, Oct. 1978.

Nonlinear Panel Flutter Phenomena in Supersonic and Transonic Flow

BORIS A. GROHMANN *
Institut für Statik und Dynamik der Luft- und Raumfahrtkonstruktionen
Universität Stuttgart, Pfaffenwaldring 27,
70550 Stuttgart, Germany

DIETER DINKLER †
Institut für Statik
Universität Braunschweig, Beethovenstr. 51
38106 Braunschweig, Germany

The present work deals with nonlinear panel flutter phenomena in supersonic and transonic flow. For this purpose, a high order accurate and efficient method for computational aeroelasticity has been developed. Aerodynamics are modeled using the inviscid, compressible Euler equations and nonlinear Timoshenko beam elements are employed for the structure. Time-discontinuous Galerkin least-squares finite elements are employed for both the transonic fluid flow [3] and the elastic aircraft wing structure [4]. Time dependent deformations of fluid domains are modeled using space-time mappings for the finite element geometry [6]. A least-squares term is applied to stabilize the convective term. In order to get sharp resolution of discontinuities without spurious oscillations, a consistent high order shock-capturing operator is added. The resulting implicit time marching scheme is unconditionally stable and 1st or 3rd order accurate.

Based on the discretization of equal type for fluids and structures, an overall iterative solver strategy for the fully coupled problem analogous to [1] has been developed. For this purpose, a modified Newton iteration of the fluid nonlinearity, a structure iterative solver and the fluid-structure coupling iteration are combined in one common loop. This leads to a significant reduction of the overall computer time without any convergence problems of the present scheme.

The algorithms are proofed by the following two applications:

For supersonic flow at $M = 2$ influences of the structures curvature on flutter stability have been investigated. The comparison of results obtained by the present CFD methodology to earlier works [5] employing different versions of the aerodynamic piston theory shows very

*Phone: +49/711-685-3625, Fax: +49/711-685-3706, Email: grohmann@isd.uni-stuttgart.de
†Phone: +49/531-391-3667, Fax: +49/531-391-8116, Email: d.dinkler@tu-bs.de

good agreement. It is shown, that even moderate surface curvature reduces flutter boundaries significantly. This is caused by nonlinear buckling mechanisms of the shell, which are not present for plane structures. With increasing amplitude interaction of structure and flow may lead to very complex, partly chaotic oscillations.

While structural nonlinearities are the driving factors for flutter in supersonic regions, nonlinear shock motions in fluid domain are the governing effect in transonic flow and may lead to limit cycle oscillations. Comparison to results obtained by [2] shows very good agreement.
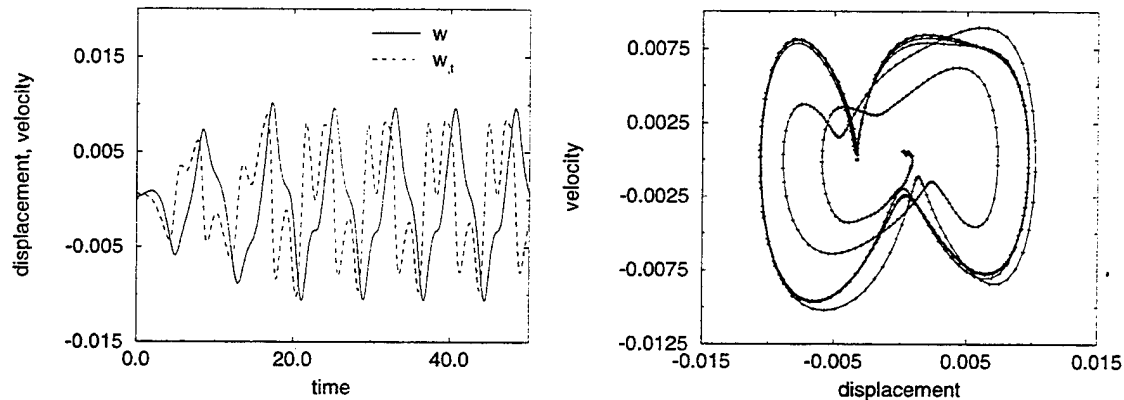
Figure 1: Transonic panel flutter at $M = 1.1$, $\lambda = 314$, $\mu = 0.1$ and $h/t = 0$: time history (left) and phase diagram (right) of deformation $w(t)$ and velocity $w_{,t}(t)$ at $x/l = 0.75$.

References

[1] J. J. ALONSO, A. JAMESON: *Fully-Implicit Time-Marching Aeroelastic Solutions.* 32nd Aeroespace Sciences Meeting & Exhibit, AIAA, Reno, NV, 1994

[2] G. A. DAVIS, O. O. BENDIKSEN: *Transonic Panel Flutter.* AIAA/ASME/ASCE/AHS/ASC Structures, Dtructural Dynamics and Materials Conference, La Jolla, CA, 1993

[3] T. J. R. HUGHES, G. HAUKE, K. JANSEN, Z. JOHAN: *Stabilized Finite Element Methods in Fluids: Inspirations, Origins, Status and Recent Developments.* in: Recent Developments in Finite Element Analysis – A Book dedicated to Robert L. Taylor. T. J. R. Hughes, E. Onate and O. C. Zienkiewicz, CIMNE, Barcelona 1994

[4] G. M. HULBERT: *Time Finite Element Methods for Structural Dynamics.* International Journal for Numerical Methods in Engineering 33 (1992), 307-331

[5] H. KRAUSE: *Flattern Flacher Schalen bei Überschallanströmung.* Dissertation, Universität Stuttgart, 1997

[6] T. E. TEZDUYAR, M. BEHR: *A new strategy for finite element computations involving moving boundaries and interfaces – The deforming-spatial-domain/space-time procedure: I. The concept and the preliminary numerical tests.* Computer Methods in Applied Mechanics and Engineering 94 (1992) 339-351

Numerical prediction of response characteristics of a vortex-excited cylinder

E. Guilmineau

CFD Group, LMF CNRS UMR 6598, ECN, B.P. 92101,
44321 Nantes Cedex 3, FRANCE
Emmanuel.Guilmineau@ec-nantes.fr

Abstract

In this paper, the incompressible viscous flow past cylinder is numerically simulated by solving the incompressible Navier-Stokes equations. These equations are written in primitive formulation of the partial transformation and in a conservation form. The Cartesian velocity components and pressure share the same location at the center of the control volume. The numerical method uses a consistent physical reconstruction for the mass and momentum fluxes: the so-called CPI approach. This method is presented in details by Deng et al. [1] for laminar problems and extended to turbulent flow problems by Deng et al. [2] and more recently by Guilmineau et al. [3]. The momentum and continuity equations are solved in a segregated way, using the PISO algorithm. A second-order accurate three-level fully implicit time discretisation is used.

The structural model allows motion with two-degrees-of-freedom: pitch and vertical displacement (Fig. 1). The equations of motion for the airfoil incorporate linear and torsional springs, structural damping in both axes and structural coupling effects [4]. These equations equations are integrated in time using a fourth-order Runge-Kutta algorithm.

To start a fluid-structure interaction, aeroelastic response analyses are carried out for a NACA 0012 airfoil which is considered as single or two degrees of freedom systems. In all case, the airfoil pitches about mid-chord and the initial incidence is $\alpha_0 = 0.1$ rad. The Reynolds number , based on the airfoil length, is 1000. Therefore, the flow is laminar. The mesh is generated using a conformal mapping technique and we use a 100×60 grid with a time step $\Delta t = 0.01$. The first case is those of airfoil pitching only with the mass moment of inertia is one, the natural frequency $\pi/2$ and the damping zero (2). The response for the pitching displacement corresponds to the neutrally stable condition. This motion is dominated by a simple harmonic motion which have a period T=4.55. The second case corresponds to an airfoil with two degrees of freedom. The mass is ten, the mass moment of inertia one, the plunging frequency 2π, the pitching frequency $pi/2$ and both damping coefficients zero. The computed response is presented in figure 3. The pitching motion is dominated by a simple harmonic motion and it is not true for the plunging motion.

In contrast to the dynamic stall, we want to point out the dramatic lack of experimental data bases for such computations, specially for incompressible flows around airfoils. In order to validate the model of fluid-structure interaction, comparison with experimental results is necessary. Anagnostopoulos and Bearman [5] conducted a series of experiments on vortex-induced cross-flow oscillations of a circular cylinder mounted elastically in a water channel. They intended to capture 'lock-in' in fully laminar wakes; the Reynolds number ranged from 90 to 150. They captured the 'lock-in' phenomenon over the Reynolds number range 102-130.

The first case computed corresponds to a Reynolds number equal to 106 and a reduced velocity of 5.90. The solution of vortex shedding behind a fixed cylinder is attempted first. When the lift force becomes periodic, the elastically mounted cylinder is allowed to oscillate. The oscillograms of the cylinder displacement and of the lift and drag forces are presented in figure 4.The increase of the mean drag and of the fluctuation of the drag force as the oscillation amplitude increases are apparent from figure 4. The vortex-shedding frequency when the cylinder remains fixed is $f_s = 0.1710$ and when it oscillates $f_v = 0.1709$. These frequencies are higher than the natural frequency $f_n = 0.1695$. The frequency of cylinder oscillations is equal to the natural frequency. Anagonstopoulos [6] does not found this result, the frequency of cylinder oscillations is slightly higher (100.64%) than f_n.

In the final paper, other Reynolds number will be investigated to plot the parameters of the cylinder oscillation versus to the Reynolds number.

References

[1] G. Deng, E. Guilmineau. J. Piquet. P. Queutey, and M. Visonneau. "Computation of Unsteady Laminar Viscous Flow Past an Aerofoil." *International Journal for Numerical Methods in Fluids*, vol. 19, pp. 765–794, 1994.

[2] G. Deng, J. Piquet. P. Queutey. and M. Visonneau, "2-D Computations of Unsteady Flow Past a Square Cylinder With the Baldwin-Lomax Model," *Journal of Fluids and Structures*. vol. 8, pp. 663–680, 1994.

[3] E. Guilmineau. J. Piquet, and P. Queutey, "Two-Dimensional Turbulent Viscous Flow Simulation Past Airfoils at Fixed Incidence," *Computers & Fluids*, vol. 26, pp. 135–162. 1997.

[4] R. Blevins, *Flow-Iinduced Vibrations.* New-York: Van Nostrand Reinhold Company, 1977.

[5] P. Anagnostopoulos and P. Bearman, "Response Characteristics of a Vortex-Excited Cylinder at Low reynolds Numbers." *Journal of Fluids and Structures*, vol. 6, pp. 39–50, 1992.

[6] P. Anagnostopoulos. "Numerical Investigations of Response and Wake Characteristics of a Vortex-Excited Cylinder in a Uniform Stream." *Journal of Fluids and Structures*, vol. 8, pp. 367–390, 1994.
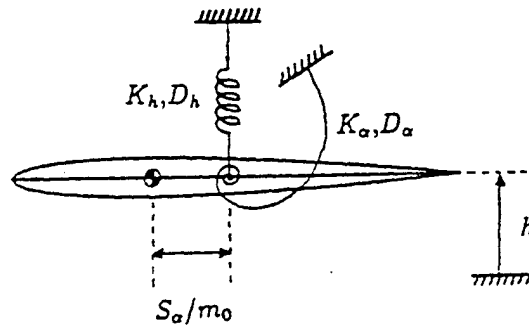
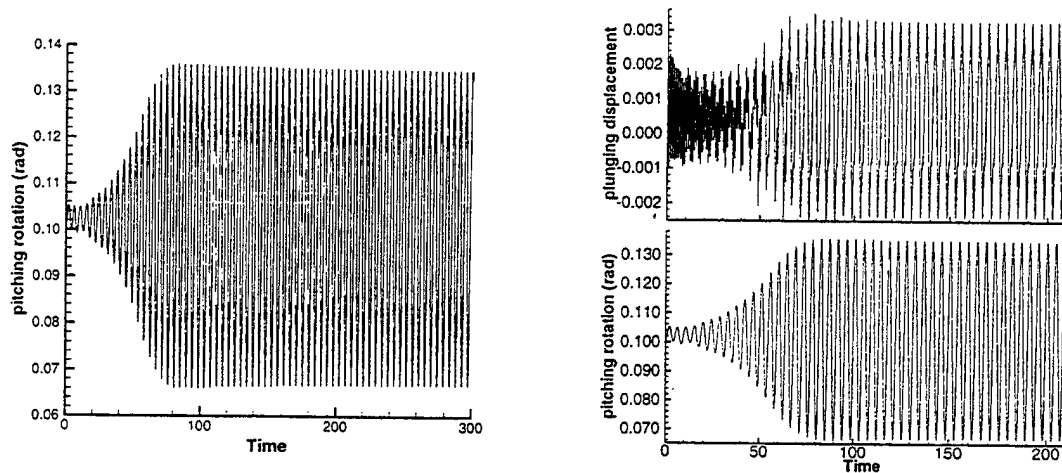Figure 1: Airfoil with linear and torsional springs

Figure 2: Pitching rotation with $I_\alpha = 1., \omega_\alpha = \pi/2, \zeta_\alpha = 0$ and $m_0 = 10$

Figure 3: Plunging and pitching with $m_0 = 10, I_\alpha = 1., \omega_h = \pi/2, /, \omega_\alpha = \pi/2, \zeta_h = \zeta_\alpha = 0$
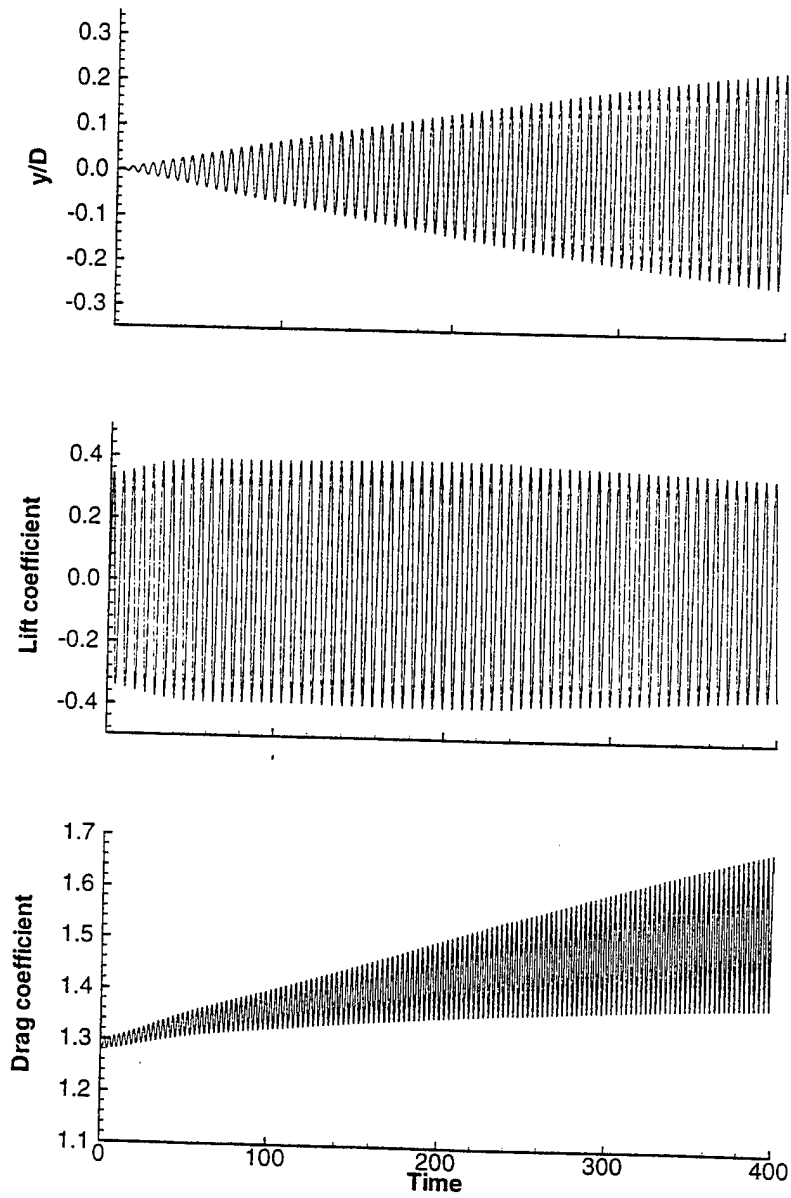
Figure 4: Time history of the cylinder displacement and of the forces exerted on the cylinder

Prediction of the initial stage slamming force

in rigid and elastic systems impacting on the water surface

[1]A. Carcaterra, [2]E. Ciappi

[1]INSEAN,
Istituto Nazionale per Studi ed Esperienze di Architettura Navale
Via di Vallerano, 139, Rome, Italy

[2]Department of Mechanics and Aeronautics
University of Rome 'La Sapienza'
Via Eudossiana, 18, Rome, Italy

ABSTRACT

The present paper addresses the attention to a particular phenomenon in fluid-structure interaction.

The new arising requirements in the field of high speed marine vehicles impose a careful investigation of the impact phenomena of the hull over the water. In fact very large force and stress are induced in the ship's structure and a correct evaluation of them is needed.

A general solution of the problem is particularly difficult involving the coupling between the fluid and structural equations. Although in recent time the problem has been investigated by several authors [1,...,7] by theoretical and numerical models, it seems to be still open.

Two different stages in the water entry process can be identified [2]. In a very early stage of the impact, the fluid response is dominated by compressibility effects and small particle displacements take place and elastic waves are radiated into the liquid [3]. A second stage follows in which the fluid motion is characterized by large displacements and compressibility effects can be definitely neglected [4,5,6].

During the first impact phase the value of the water pressure on the entering body surface assumes very large values that cannot be correctly predicted when using incompressible models.

In this paper some general features of the slamming forces, arising under variable impact velocity, are accounted for and it is assumed that the acoustic approximation can be used [3]. Three simple impact models are considered.

The first model consists in analysing the water entry of a blunt shaped rigid body. The general relationship between the hydrodinamic force and body shape equation is determined in closed form. The characteristic time evolution of the slamming force is analitically recovered for both the wedge and the cylinder case and the expression of its maximum is given. Two dimensionless parameters affect the maximum of the slamming force: the edge Mach number, related to the velocity of propagation of the intersection between the water line and body surface, and the mass ratio, related to body mass and water density.

Moreover the theoretical correlation between the hydrodynamic force and the body geometry, allows to control the time evolution of the slamming force acting on the body's shape. The inverse problem of determining the shape associated with a constant slamming force is analitically solved.

A second model consists of a two degrees of freedom system (fig.1). An external blunt body, directely impacting on the water, is elastically connected to an inner second body. Two different forces are accounted for. The first is the hydrodinamic force, the second the induced elastic force. A systematic numerical analysis of this system is performed by investigating the maximum induced stress versus the characteristic dimensionless parameters of the problem. Moreover a comparison of the obtained results with those related to the rigid body impact is considered.

The last model consists of an elastically deformable wedge impacting on water (two degrees of freedom system, fig.2). In this case the body shape change under the hydrodynamic load arising during the impact. Both the maximum slamming force and the elastic induced stress are investigated versus the dimensionless involved quantities.

Fig. 1

Fig. 2
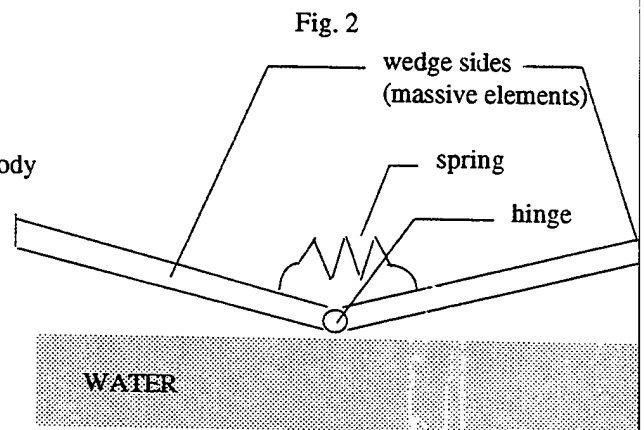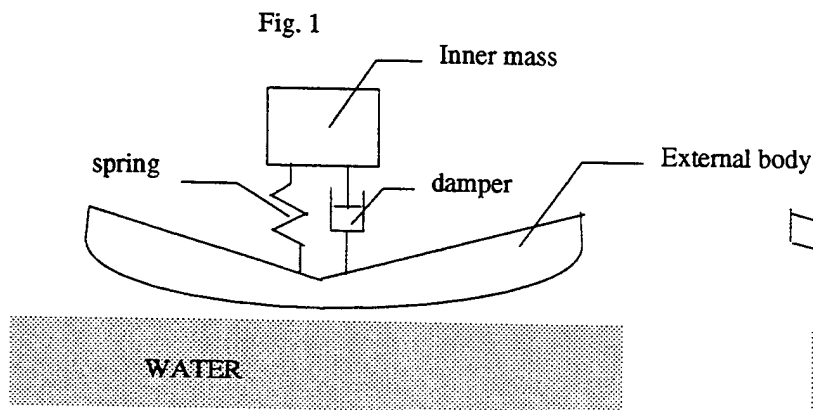
REFERENCES

[1] Wagner, H. 'Uber stoss gleitvergange an oberflache von flussigkeiten', Zeitschr. f. Angewendte Mathematik und Mechanik, 12, pp.192-215, 1932.

[2] Korobkin, A.A., Pukhnachov, V.V:, 'Initial stage of water impact', Ann. Rew. Fluid Mech., vol.20, pp.159-185, 1988.

[3] Skalak, R., Feit, D., ?Impact on the surface of a compressible fluid', Trans. ASME, J. Eng. Ind., vol. 88B, pp. 325-331, 1966.

[4] Kvalsvold, J, Faltinsem, O., 'Hydroelastic modeling of wet deck slamming on multihull vessels', J. of Ship Research, vol. 39, pp. 225-239, 1995.

[5] Yim, B. 'Numerical solution for two-dimensional wedge slammingwith a non-linear free-surface condition', 4-th Int. Conf. On Numerical Ship Hydrodynamics, pp. 107-116, 1985.

[6] Zhao, R., Faltinsen, O., 'Water entry of arbitrary two-dimensional bodies', J. of Fluid Mech., vol. 246, pp.593-612, 1993.

[7] Kim, D.-J., Vorus, W., Troesch, A., Gollwitzer, R., 'Coupled Hydrodynamic Impact and Elastic Response', 21-thSymp. On Naval Hydrodynamics, pp. 424-437,1997.

ABSTRACT for SEVENTH CONFERENCE ON NONLINEAR VIBRATIONS,
STABILITY, AND DYNAMICS OF STRUCTURES

Self-excited Oscillations of Dual Cylindrical Flexible Weir Shells
due to the Overflow of Fluid

Shigehiko TANAKA[1] and Shigehiko KANEKO[2]

[1]Graduate student, Department of Mechanical Engineering, The University of Tokyo
7-3-1 Hongo, Bunkyo-ku, Tokyo, 113, Japan
Phone: +81 3 3812-2111 ext.6428   Fax: +81 3 5689-8054
E-mail:tanaka@fiv.t.u-tokyo.ac.jp
[2] Associate Professor, Department of Mechanical Engineering,
The University of Tokyo

Correspondence: Prof.Shigehiko KANEKO
Department of Mechanical Engineering, The University of Tokyo
7-3-1 Hongo, Bunkyo-ku, Tokyo, 113, Japan
Phone: +81 3 3812-2111 ext.6429   Fax: +81 3 5802-2946
E-mail: kaneko@ingram.mech.t.u-tokyo.ac.jp

Keywords: *Fluid/Structure interactions, Sloshing, Shell vibration, Time delay system*

ABSTRACT

Self-exited oscillations of the structure coupled with inner fluid occurred in the insulation wall cooling system of the fast breeder reactor Super-Phoenix -1(SPX-1) in France during test operations. In this system, the lower temperature sodium in the feeding plenum goes up along the wall of main vessel and brims over the cylindrical flexible weir shell and then flows into the restitution plenum. It is reported that the self-exited oscillation were found to occur at the same natural frequency of the sloshing in the restitution plenum; the free surface of the fluid in both feeding and restitution plenum oscillated at large amplitudes; and the cylindrical shell oscillated with an oval vibration mode, which are called "coupled sloshing mode instability".

In connection with this instability problem, the research on fluid-structure coupling system by the analysis using FEM code was first performed by Aita, where he pointed out that the unstable vibration is excited only at the specific combination of the flow rate and the distance between the feeding and restitution plenum liquid level.

Successively, many studies on the coupled sloshing mode were carried out by Eguchi et al., and Kaneko et al. The excitation mechanism of the self-excited oscillation is basically understood by the previous studies as follows; at first a weir begins to oscillate due to a small disturbance, and then the free surface of the feeding plenum and the fluid

discharge rate fluctuates; as a result the flow rate flowing into the restitution plenum changes accompanied with the time lag generated by the fluid moving from the surface of the feeding plenum to that of the restitution plenum, which excites the restitution plenum sloshing, finally, an oscillatory force acting on the internal and external of the weir shell due to the sloshing of both plenums makes the weir oscillate. In this way, a self-excited vibration loop can be described.

Nagakura and Kaneko, furthermore, set up governing equations of the weir motion taking the effect of fluid force due to the sloshing of the fluid in both restitution and feeding plenums and the added mass of the weir into consideration. Then, they analyzed the instability taking account of the shearing stress at the wall of the weir where the fluid is falling to calculate out the time lag generated by the fluid moving from the surface of the feeding plenum to that of the restitution plenum precisely.

In SPX-1, countermeasures were taken against self-excited oscillations of the fluid-structure coupling system, however, it is difficult to say that the excitation mechanism of its vibration is fully elucidated dynamically. Most studies on analyses have been undertaken so far were on a single cylindrical flexible weir shell, in spite of the fact that the wall cooling system of actual fast breeder reactors is composed of multiple shells. Therefore, the study on the case of multiple shells is necessary.

In this study, we will analyze and perform experiments on the instability of multiple cylindrical structure system with dual cylindrical flexible weir shells. The analysis was done on the basis of the theory developed for the case of a single cylindrical weir by Nagakura and Kaneko. In a set of experiments, it was found that dual cylindrical shell oscillation with anti-phase oval vibration mode was excited under the specific experimental conditions.

Tuesday, July 28
0800-0930
Session 7.

Quadratic map approximations to vector fields

Huw G. Davies, and Konstantinos Karagiozis

Department of Mechanical Engineering
University of New Brunswick
P.O. Box 4400, Fredericton, NB   E3B 5A3

Introduction

Vector fields are often analysed by sampling the field on a suitable Poincaré section. Limit cycles of vector fields, for example, became fixed points of the Poincaré map. Additional information can be obtained by sampling the transient response, for example as the field asymptotes to a stable limit cycle, and plotting successive Poincaré points on a return map. In some cases the map may have a simple smooth character (for example, the one-dimensional map that characterises the Rössler oscillator, (Thompson and Stewart [1] or Jackson [2]). Floquet theory gives, in suitably chosen coordinates, the slope of the map at the fixed point, and hence gives information on the local stability of the associated limit cycle. Standard Floquet theory is based on a linear approximation to perturbations of the limit cycle. Here a quadratic approximation is used to find a quadratic form of the return map in the vicinity of the fixed point.

General case

Consider the vector field described by $\dot{\underline{y}} = f(\underline{y}, \mu)$ or $\dot{y}_i = f_i(\underline{y}, \mu)$, where μ is a control parameter. Suppose $\underline{y}^*(t)$ is a stable limit cycle with period T. The transformation $y_i = y_i^* + \zeta_i$ yields the perturbation equations.

$$\dot{\zeta}_i = \frac{\partial f_i}{\partial y_j}\zeta_j + \frac{1}{2}\frac{\partial^2 f_i}{\partial y_p \partial y_k}\zeta_j\zeta_k + O(\zeta^3) \tag{1}$$

The coefficients are evaluated at $y^*(t)$ and are periodic. It is convenient to diagonalise the equations in the following manner, using just the linear term. The monodrony matrix M obtained from the linear approximation has eigenvalues λ_k, one of which is unity. Suppose C is the matrix that diagonalises M. Then the transformation $\zeta_i = C_i v_j$ gives

$$\dot{v}_i = D_{ij}v_j + E_{ijk} v_j v_k + O(v^3). \tag{2}$$

Both D and E are periodic. Note that D is not diagonal; it is the map not the vector field that has been diagonalised. Note also that if f includes only linear and quadratic terms, as is often the case, the perturbation equations (2) are exact.

Now choose a suitable Poincaré plane, define time t=0 when y^* intersects the plane, and impose perturbations v_i° at this point. Assume a quadratic approximation

$$v_j(t) = a_{jl}(t)v_l^\circ + b_{jlm}(t) v_l^\circ v_m^\circ \tag{3}$$

Then, on substituting (3) into (2):

$$\dot{a}_{il}(t) = D_{ij}(t)a_{jl}(t) \quad \text{with} \quad a_{il}(o) = \delta_{il} \tag{4}$$

$$\dot{b}_{ilm} = D_{ij} \, b_{jlm} + \frac{1}{2}E_{ijk} \, a_{jl} \, a_{km} \quad \text{with} \quad b_{ilm}(0) = 0$$

The solutions $a_{jl}(T) = \lambda_j \delta_{jl}$ and $b_{jlm}(T)$ are the required parameters of the quadratic map.

Rössler oscillator

The Rössler oscillator
$$\dot{y}_1 = -y_1 - y_3$$
$$\dot{y}_2 = y_1 + ay_3 \tag{5}$$
$$\dot{y}_3 = a + y_3 (y_1 - \mu)$$

with ($y_2 = 0$, $y_1 < 0$) chosen as the Poincaré plane yields a smooth one-dimensional map in $y_1[1,2]$. Figure (1) shows results for $a = 0.2$, $\mu = 2.2$, values giving a stable period -1 limit cycle. A one-dimensional map seems to emerge because one of the Floquet eigenvalues is very close to zero. An approximate linear diagonalisation is $\zeta_1 = v_1$, $\zeta_2 = v_2 - \delta v_1$, $\zeta_3 = v_3$, where for this value of μ, $\delta \approx 1.3566$. It is sufficient to consider only perturbations of the y_1 variable v_1° and write $v_i(t) = a_i(t)v_1^\circ + b_i(t)(v_1^\circ)^2$. The resulting map shown in Figure (1) is
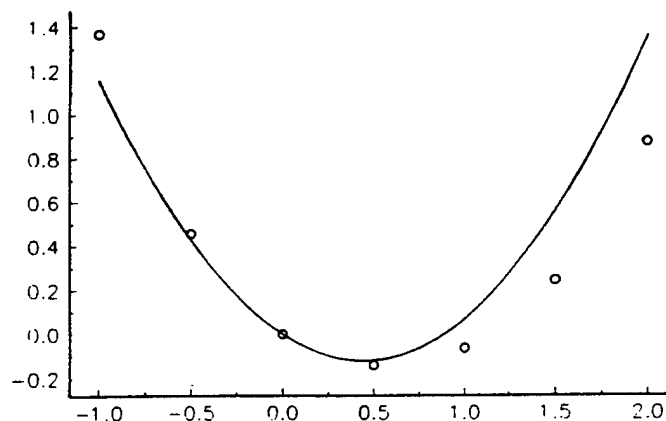
$$v_1(T) = a_1(T)v_1^\circ + b_1(T)(v_1^\circ)^2 \tag{6}$$

with $a_1(T) = -0.5455$ and $b_1(T) = 0.6132$. The circles are values obtained from the exact perturbation equations.

References

1. J.M.T. Thompson and H.B. Stewart, Nonlinear Dynamics and Chaos, Wiley, 1986.
2. E.A. Jackson, Perspectives on Nonlinear Dynamics, Cambridge University Press, 1991.

Figure 1

$v_1(T)$ versus v_1°

Nonplanar Vibrations of Two Phase Cables due to the Alternating Currents

Masatsugu YOSHIZAWA, Toshihiko SUGIURA, Hideo KAWAMOTO
Shingo SHIMOKAWA and Takashi KAWAGUCHI

Department of Engineering, Keio University
3-14-1 Hiyoshi Kouhokuku Yokohama Japan

In the new power electric transmission systems using SF6 gas insulation or superconducting cables, it is predicted that the lateral vibrations of the cable with very high current densities are excited due to the Lorents force in the high magnetic field which is occurred by other current-carrying cables. Moreover the nonlinear coupling oscillations of the current-carrying cables will be occurred in the two-phase or three-phase cables.

The main purpose of this paper is to investigate the induced lateral vibrations of the current-carrying cables in a system of two phase current-carrying cables as shown in Fig.1. The two phase cables are placed at a distance R_0 from the origin in the $x - y$ plane of the orthogonal coordinates, respectively . Compared with R, the length l of the cables is sufficiently long and their radius is negligible.
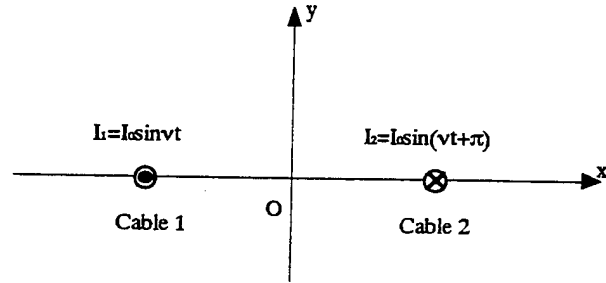

Fig.1 Two Phase Cables

The electromagnetic force F_1 acting on Cable 1, which is caused by the interaction between the current $I_0 \sin Nt$ in Cable 1 and $I_0 \sin(Nt + \pi)$ in Cable 2, is expressed as follows:

$$F_{1x} = \frac{\mu_0 I_0^2}{16\pi R_0}\{\cos 2Nt - 1\}\left(2 + \frac{u_1 - u_2}{R_0}\right) \tag{1}$$

$$F_{1y} = \frac{\mu_0 I_0^2}{16\pi R_0}\{\cos 2Nt - 1\}\left(\frac{-v_1 + v_2}{R_0}\right) \tag{2}$$

where F_{1x} and F_{1y} are the x and y component of F_1, respectively. $u_i(z,t)$ and $v_i(z,t)$ are the x and y components of the displacement of the cable $i(i = 1, 2)$,respectively. The force acting on the cable 2 is expressed in the same manner from the symmetry.

Then the basic equations governing the nonplanar lateral vibrations of the two current-carrying cables are derived as follows:

$$\rho A\frac{\partial^2 u_i}{\partial t^2} + C\frac{\partial u_i}{\partial t} = \left\{T_{0i} + \frac{EA}{2l}\int_{-l}^{l}\left[\left(\frac{\partial u_i}{\partial z}\right)^2 + \left(\frac{\partial v_i}{\partial z}\right)^2\right]dz\right\}\frac{\partial^2 u_i}{\partial z^2} + F_{ix} \tag{3}$$

$$\rho A\frac{\partial^2 v_i}{\partial t^2} + C\frac{\partial v_i}{\partial t} = \left\{T_{0i} + \frac{EA}{2l}\int_{-l}^{l}\left[\left(\frac{\partial u_i}{\partial z}\right)^2 + \left(\frac{\partial v_i}{\partial z}\right)^2\right]dz\right\}\frac{\partial^2 v_i}{\partial z^2} + F_{iy} \tag{4}$$

$$u_i(-l, t) = u_i(l, t) = v_i(-l, t) = v_i(l, t) = 0 \tag{5}$$

where ρ, E, A and T_{0i} are the mass density, Young's modulus, the cross-sectional area and the initial tension of the cable respectively, and $i = 1, 2$.

As a theoretical main result, it is cleared from the analytical solutions of the above equations that there are basically three vibration patterns of the two phase cables for the case when the frequency of the alternating current N is close to half of the fundamental natural frequency of the cable.

The experiments have been conducted to observe the induced lateral vibrations of the two phase cables due to the alternating currents. The three vibration patterns of the two phase cables were observed as shown in Fig.2.
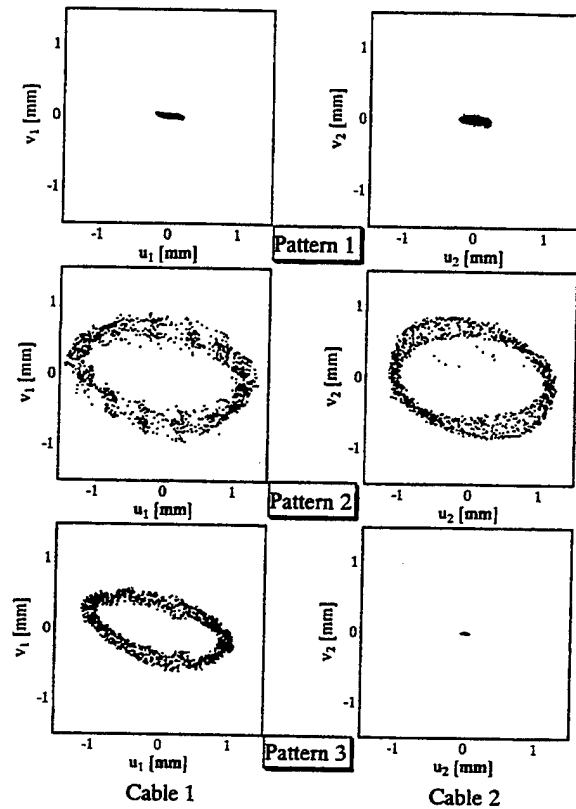
Fig.2 Motions of Two Phase Cables in $x - y$ Plane
(Experimental Results)

References

[1] M.N.Zervas and E.E.Kriezis, Integral for the field and the forces in a system of conducting cylindrical shell: a general approach, IEE PROCEEDINGS, Vol. 134, Pt.B, No.5, pp.269-275,September 1987.

[2] A.Safigianni and Prof.D.Tsanakas, Short-circuit electromagnetic forces in three-phase gas insulated systems with aluminum enclosure, IEE PROCEEDINGS, Vol.133, Pt.B, No.5, pp.331-340, September 1986.

[3] Moon.F.C., *Magneto-Solid Mechanics*, John-Wiley & Sons, Inc., 1984.

[4] A.H.Nayfeh and D.T.Mook, *Nonlinear Oscillations*, Wiley, 1979.

Bottlenecking Phenomenon near a Saddle-node Remnant in an Experimental Duffing Oscillator

Stephen T. Trickey and Lawrence N. Virgin
Department of Mechanical Engineering and Material Science
Duke University, Durham, N.C. 22706

Abstract

The bottlenecking phenomenon near a saddle node remnant or ghost is discussed for an electronic circuit modeling Duffing's equation. Numerical simulation and a useful experimental perturbation method, stochastic interrogation, are used to confirm the analytic inverse square root scaling law associated with saddle-node bifurcations.

Significant advances have been made in the study of nonlinear phenomenon by examining the local dynamics of systems. Local analysis near bifurcations can provide great insight into transitions from one characteristic type of behavior to another. Using this type of local approach and then extending the view of the analysis, a greater understanding of the system's global dynamics can be achieved. The emphasis in this talk is placed on the dynamics near a saddle node bifurcation and the resulting bottlenecking phenomenon.

Originally observed inadvertently on an oscilloscope during automated data acquisition, the bottlenecking phenomenon piqued our curiosity. The analytic result, derived and discussed for generic saddle-node bifurcations in [1,2] and in the context of intermittency [3,4,5] states that the time required to pass through a bottleneck induced by a saddle-node remnant scales with the inverse root of the change in bifurcation parameter

$$T \propto \frac{1}{\sqrt{p_c - p}}.$$

A trivial matter to confirm numerically, experimental confirmation provides more of a challenge. How can initial conditions be generated that lead the system into the bottlenecking region? The answer is an experimental perturbation method called stochastic interrogation [6]. The talk will be comprised of a description of the experimental setup, a review of the scaling law, and a presentation of experimental procedures and results.

The following figure shows preliminary results. Of note is the fact that there is considerable scatter near the critical frequency which will be addressed in the talk and the constant of proportionality is approximately π in accordance with theory.
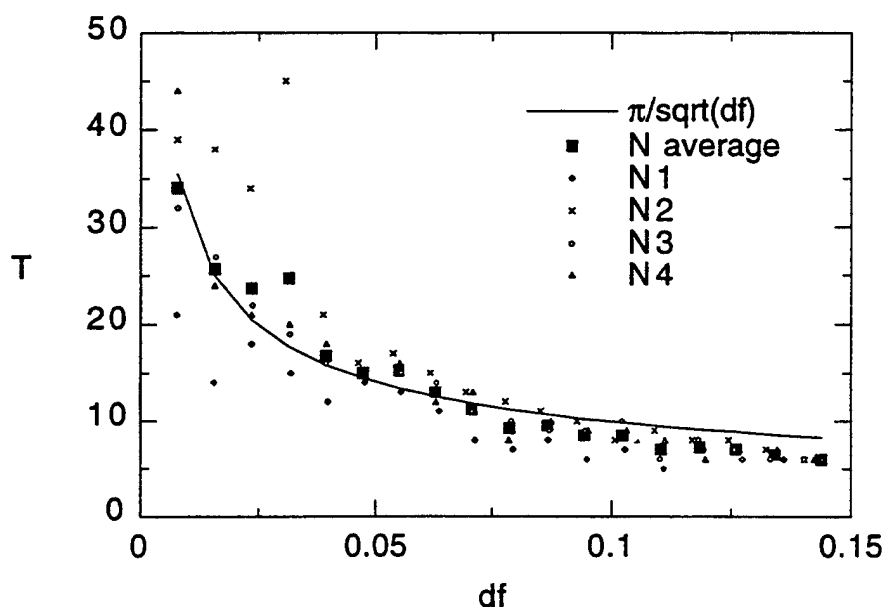
References

[1] S. H. Strogatz. *Nonlinear Dynamics and Chaos.* Addison-Wesley Publishing Company, 1994.

[2] S. Wiggins. *Introduction to applied nonlinear dynamical systems and chaos.* Springer-Verlag, 1990.

[3] F. C. Moon. *Chaotic and Fractal Dynamics.* John Wiley & Sons,Inc.,1992

[4] E. Ott. *Chaos in Dynamical Systems.* Cambridge University Press, 1993.

[5] Y. Pomeau and P. Manneville. Intermittent transition to turbulence in dissipative dynamical systems. *Comm. Math. Phys.,* 74(189),1980.

[6] J. P. Cusumano and B. W. Kimble. A stochastic interrogation method for experimental measurement of global dynamics and basin evolution: application to a two-well oscillator. *Nonlinear Dynamics,* 8:213-235,1995.

Versal deformation and local bifurcation analysis of time-periodic nonlinear systems

Alexandra Dávid and S. C. Sinha
Nonlinear Systems Research Laboratory,
Department of Mechanical Engineering,
Auburn University, AL 36849, USA
E-Mail: ssinha@eng.auburn.edu

Abstract

In this study an analytical method for local bifurcation analysis for time-periodic nonlinear systems is presented. In the neighborhood of a local bifurcation point the systems equations are simplified via Lyapunov-Floquet transformation which transforms the linear part of the equation into a dynamically equivalent time-invariant form. Then time-periodic center manifold reduction is used to separate the "critical" variables and reduce the dimension of the system to a possible minimum. On the center manifold the equations can be simplified further via time-dependent normal form theory. The normal forms for the cases of codimension one bifurcations become completely time-invariant and can be solved in a closed form . Then, for the time-invariant normal forms, versal deformation analysis can be carried out and the bifurcation phenomenon can be studied in the neighborhood of the critical point. Closed form post-bifurcation steady-state solutions can be obtained for the case of flip and secondary Hopf bifurcations. As physical examples, a simple and a double pendulum subjected to periodic parametric excitation are considered. A comparison with results obtained from the traditional averaging method is also made illustrated by a simple two degrees of freedom example. All results are verified by numerical integration.

Dynamic Response and Stability of a Rotating Asymmetrical Shaft Mounted on a Flexible Base

Takashi IKEDA and Shin MURAKAMI

Department of Electronic and Control Systems Engineering
Shimane University
Nishikawatsu, Matsue, JAPAN 690-8504

1. Introduction

The dynamic response of a rotating asymmetrical shaft supported by a flexible base is investigated. The unstable regions of the system and the resonance curves for the steady state oscillations due to a rotor imbalance and gravity forces are presented. Finally, the theoretical resonance curves are compared with the experimental results.

2. Equations of Motion and Natural Frequencies

Figure 1 shows a theoretical model where an asymmetrical shaft system is installed on a base with mass M. The base is supported by a structure that has a spring stiffness k_0 and a damping coefficient c_0. Let x_0 be the displacement of the base and define a moving coordinate system O-xy which is fixed on the base. The rotor with mass m is mounted in the middle of the asymmetrical shaft S(x, y). The damping coefficient of the shaft is designated by c. The axes x_1 and y_1 represent the directions of the minimum and maximum bending stiffness of the shaft, k-Δk and k+Δk, respectively. The coordinate system O-x_1y_1 rotates with angular velocity of the shaft ω. We define the time t=0 when the x_1 axis coincides with the x axis. X (=x+x_0) represents the absolute displacement of the midpoint of the shaft in the x_0 direction. Define e as the distance between point S and the center of gravity of the rotor G, and α as the angular position between the x_1 axis and the line SG. Then, we can write the equations of motion as follows:

Fig.1 Theoretical model.

$$\left.\begin{aligned}
m\ddot{x} + m\ddot{x}_0 + c\dot{x} + kx - \Delta k(x\cos 2\omega t + y\sin 2\omega t) &= me\omega^2 \cos(\omega t + \alpha) \\
m\ddot{y} + c\dot{y} + ky - \Delta k(x\sin 2\omega t - y\cos 2\omega t) &= me\omega^2 \sin(\omega t + \alpha) - mg \\
M\ddot{x}_0 - c\dot{x} + c_0\dot{x}_0 - kx + k_0 x_0 + \Delta k(x\cos 2\omega t + y\sin 2\omega t) &= 0
\end{aligned}\right\} (1)$$

where g is the acceleration of gravity.

Fig.2 Natural frequency diagram.

Figure 2 shows the natural frequency diagram [$p^*(\equiv p/\sqrt{k/m}$): the natural frequency], which is enlarged near (ω^*, p^*)=(1, 1) (where $\omega^* \equiv \omega/\sqrt{k/m}$) when μ ($\equiv m/M$)=10, $\Delta_s(\equiv \Delta k/k$)=0.15, and $k_0^*(\equiv k_0/k$)=10. We name each group of unstable regions seen in Fig.2 as A_1, B_2, $\cdots$, E_1. Here, region A_1 is not seen, but it exists near (ω^*, p^*)=(1, -1). The subscript "1" indicates the type of unstable region (we call this a *one-mode type* with frequencies $\pm\omega$) where the value of p becomes a complex number on the straight line $p=\pm\omega$. The subscript "2" represents an alternative unstable region (we call this a *two-mode type* with frequencies $\pm\omega \pm \beta$).

3. Width of Unstable Regions and Resonance Curves

In this section, we will investigate the above system in more in detail by considering the damping. We assume the solutions of steady state oscillations in Eq.(1) near the major critical speed as follows:

$$\left.\begin{aligned}
x &= r_1 + R_1\cos(\omega t + \delta_1) + R_2\cos(-\omega t + \delta_2) + \varepsilon \cdot f_1(\omega, -\omega) \\
y &= r_2 + R_1\sin(\omega t + \delta_1) + R_2\sin(-\omega t + \delta_2) + \varepsilon \cdot f_2(\omega, -\omega) \\
x_0 &= r_3 + R_3\cos(\omega t + \delta_3) + \varepsilon \cdot f_3(\omega)
\end{aligned}\right\} (2)$$

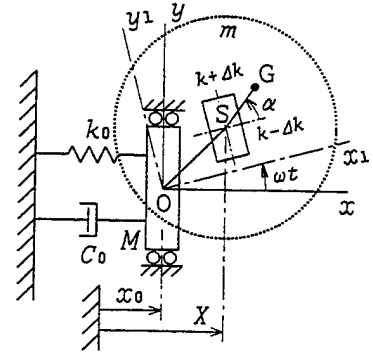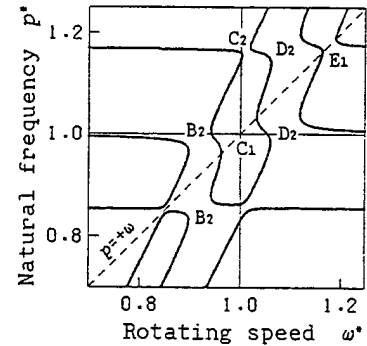where ε is a small parameter. Substituting Eq.(2) into Eq.(1) leads
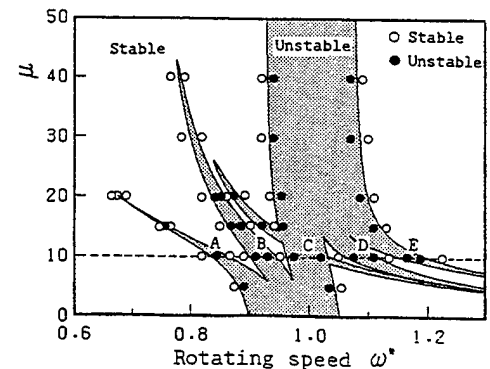

Fig.3 Influence of the mass ratio μ on the width of unstable subregion.

to the simultaneous differential equations. Then, the width of unstable regions and the resonance curves can be numerically obtained.

Figure 3 shows the influence of the mass ratio μ ($\equiv m/M$) on the width of unstable regions when Δ_s ($\equiv \Delta k/k$)=0.15, $k_0{}^*$($\equiv k_0/k$)=10, c^*($\equiv c/\sqrt{km}$)=0.02, and $c_0{}^*$($\equiv c_0/\sqrt{km}$)=0.07. As the value of μ changes, it is found that the unstable region can be divided into one to six subregions. For example, five unstable subregions appear when μ =10. We call these subregions A, B, C, D, and E in order of increasing ω^*. Each of these corresponds to the region with the same name as that shown in Fig.2.

Figure 4 shows an example of resonance curves. The parameter values are μ =10, e^*($\equiv e/x_{st}$; x_{st} $=mg/k$)=0.02, and α =10 deg, and the others are the same as those treated in Fig.3. The solid line represents a stable solution, and the dotted line an unstable one. The ordinate in Fig.4 represents the amplitude of absolute displacement of the shaft X^*($\equiv X/x_{st}$). Subregions A through E in Fig.4 correspond to those for μ =10 in Fig.3. Near the boundaries of subregions A and E (which are of one-mode type), the amplitude is infinite. On the contrary, the amplitude does not become infinite at the boundaries of subregion B and D (which are of two-mode type), but changes continuously from a stable solution to an unstable one. The symbols ● in Fig.4 represent the amplitude of the waveform calculated by integrating Eq.(1) numerically and by using the FFT analysis.

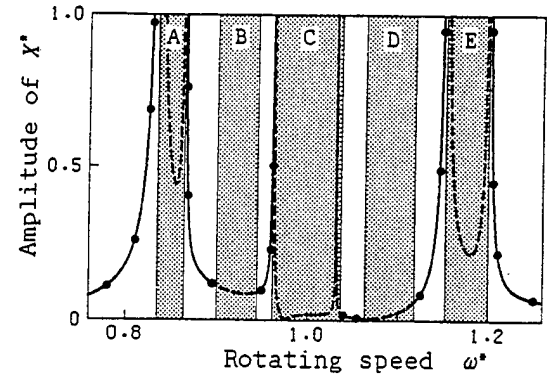Fig.4 Resonance curves for μ =10, e^*=0.02, and α =10 deg.

4. Experimental Results

Figure 5 shows the resonance curves when the values of the base mass M (including the bearing pedestals) were 86.16 kg (μ $\equiv M/m$=15.81). Y represents y. Now, we can see the existence of five unstable subregions in Fig.5, where one-mode type unstable vibrations appeared in subregions A, C, and E, and two-mode type appeared in subregions B and D. In addition, the resonance curves correspond to those of Fig.4, and the shape outside of the unstable region is very similar between the two figures.
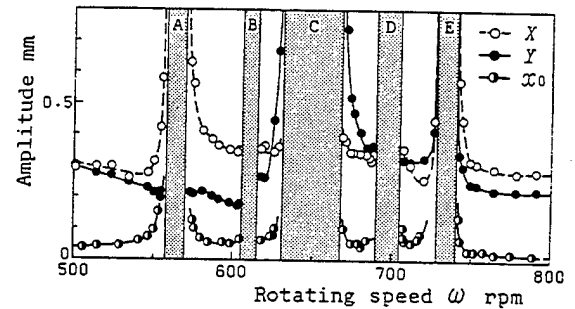
Figure 6 shows a comparison of theoretical and experimental results. The theoretical boundaries of unstable regions are plotted in thin lines, and the widths of unstable subregions found by experimentation are drawn in the thicker horizontal lines. This comparison shows that the theoretical width of the unstable subregions coincides well with those measured in the experiments.

Fig.5 Experimental resonance curves when the base was flexibly supported.

Fig.6 Comparison of theoretical and experimental unstable subregions.

5. Conclusions

The conclusions are summarized below:

(1) The unstable region for the system treated here is divided into six subregions at most.

(2) The modes of vibration in these divided unstable subregions are classified into two types; a one-mode type and a two-mode type.

(3) As for the shape of the resonance curves, the amplitude becomes infinite at the boundary of a one-mode type of unstable region, while the amplitude is finite at the boundary of a two-mode type of an unstable region changing continuously from a stable solution to an unstable one.

(4) It was also found that the experimental results coincided well with the corresponding theoretical results when comparing the widths of unstable subregions and the shapes of the resonance curves.
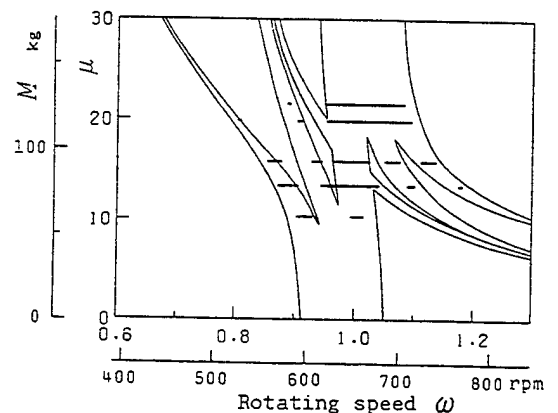
Tuesday, July 28
1000-1130
Session 8.

Using Karhunen Loeve Decomposition to Analyze the Vibroimpact Response of a Rotor

M.F.A. Azeez and **A.F. Vakakis**
Department of Mechanical and Industrial Engineering
University of Illinois at Urbana-Champaign, Urbana, Illinois - 61801, U.S.A.

The method of Proper Orthogonal Decomposition (POD) also known as Karhunen Loeve (KL) method has been used successfully to create lower dimensional models in fluid mechanics ([1]) and heat transfer systems. The KL Method can extract dominant modes of the underlying dynamics of the system, from random experimental or numerical data. These modes are useful since they can be used as trial functions, in Galerkin-type procedures ([2]), to reconstruct the dynamics of the original system, using a lower order model. The KL modes of the system can also be used for non-parametric system identification ([3]). The KL method can be applied to nonlinear as well as dissipative systems.

In this presentation, the application of the KL method to study the dynamics of an overhung rotor undergoing vibroimpacts (Fig. 1 (a)) is discussed. This system has already been considered where comparisons between experiments and numerical simulations have been performed, in an earlier work by the authors ([4]). In the current work, the KL modes are obtained for various speeds of rotation and different clearances. It is found that in regions of periodic response a single KL mode is sufficient to capture nearly all the energy of the system; in chaotic, subharmonic and quasiperiodic regions, more than one KL modes are needed. The degree of nonlinearity is manifested as high energy transfer between the KL modes(Fig. 1 (b),2(a)) and changes in their shapes.

Once the KL modes are obtained they can be used for reconstructing the response of the system. It was reported in [4] that several physical modes are needed to obtain accurate transient responses, as the degree of the nonlinearity is high. It will be shown that only a few KL modes can capture the transient responses accurately. This is demonstrated for a few cases of nonlinearities. The advantage of the KL modes, is that the data required for their computation need not be very closely spaced in time and only a few cycles of simulation are sufficient. The advantage is immediate, because any large scale structure with nonlinearities, can be simulated using Finite Elements Method, for only a few cycles and the KL modes can then be obtained and used to reconstruct the original system response in a profitable manner. One such reconstruction using 3 and 4 KL modes, is shown in Fig. 2 (b) and there is an excellent match of the time responses. Hence, the KL method provides a promising way to develop low-dimensional modes for systems with even strong or nonlinearizable nonlinearities.

Keywords: Karhunen Loeve method, system identification, rotor, impacts,

References

[1] L. Sirovich, B. W. Knight and J. D. Rodriguez, Optimal Low-Dimensional Dynamic Approximation, *Quart. Appl. Math.*, XLVIII(3), pp 535-548,1990

[2] B.A. Finlayson, The Method of Weighted Residuals and Variational Principles, *Math. in Science and Engg.*, Volume 87, 1972.

[3] H. M. Park and D. H. Cho, The Use of Karhunen-Loeve Decomposition for the Modeling of Distributed Parameter Systems, *Chem. Engg. Sci.* 51(1), pp 81-98, 1996

[4] M.F.A. Azeez and A.F. Vakakis, Numerical and Experimental Analysis of the Nonlinear Dynamics Due to Impacts of a Continuous Overhung Rotor, *Proceedings of the ASME Design Engg. Tech. Conf.* Sacramento, September 1997
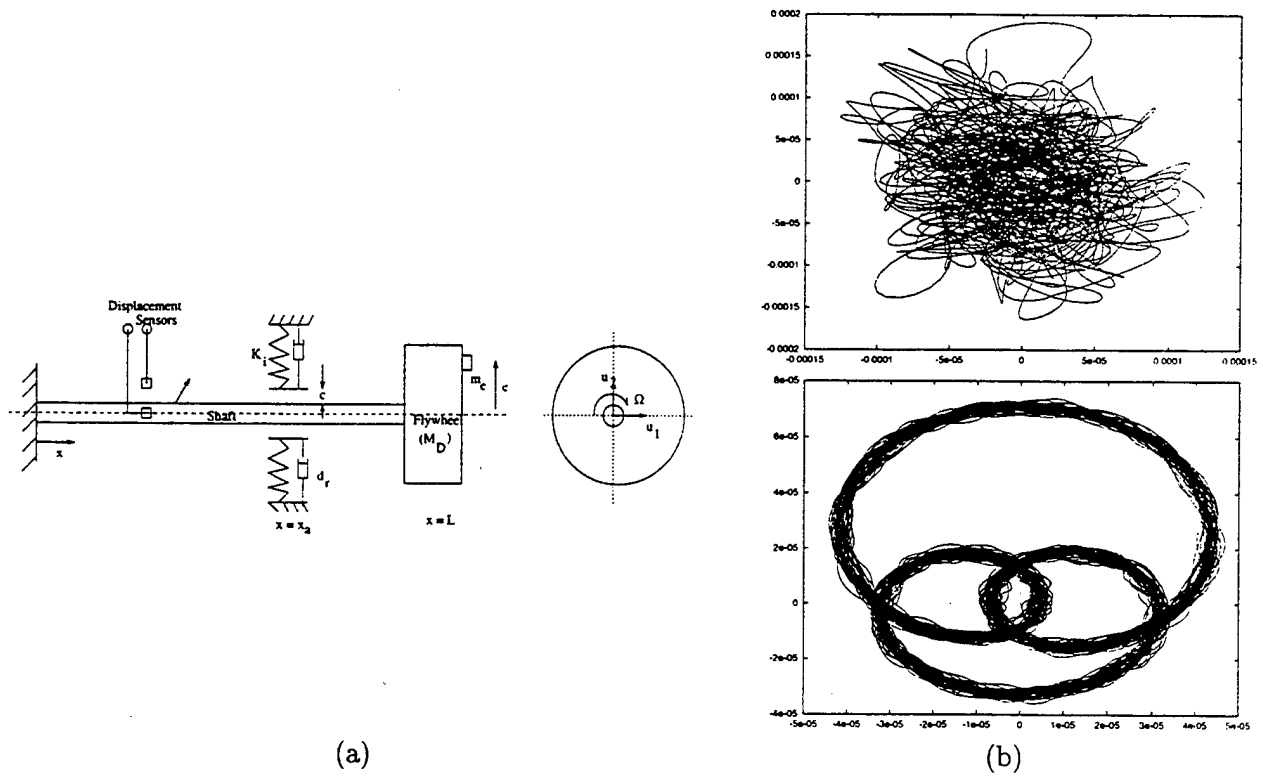
Figure 1: (a) Schematic of the rotor; (b) sample chaotic (800 rpm) and higher period (1300 rpm) rotor orbits [correspond to points 5 and 6 of Fig (2)]
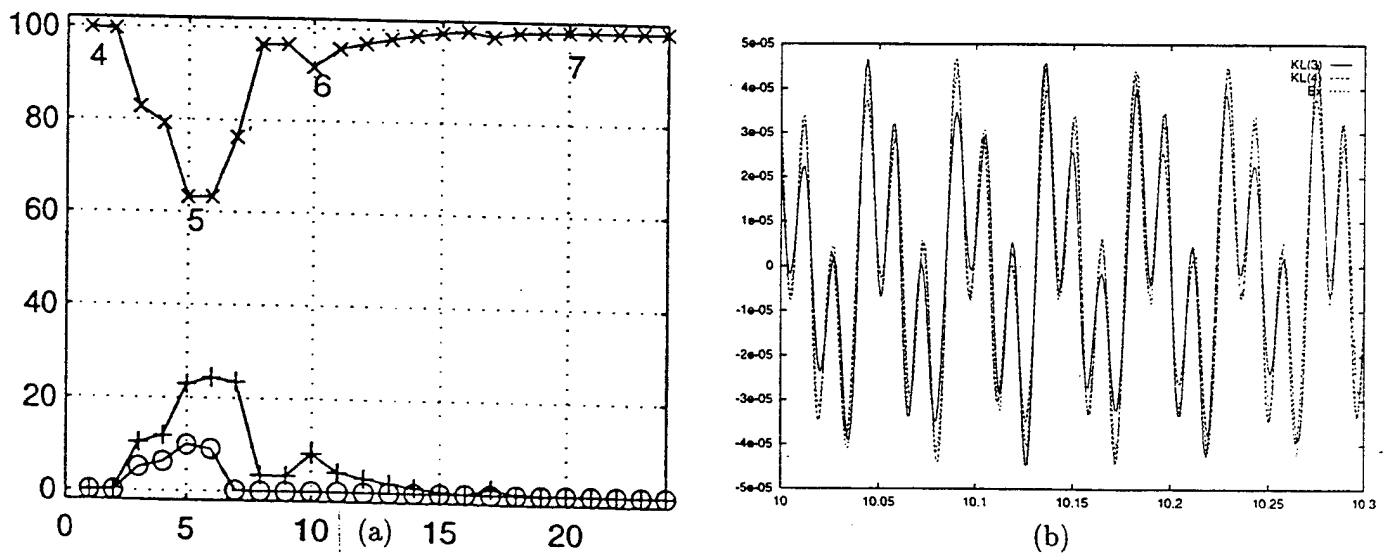

Figure 2: (a) The percentage of energy vs the frequency index in the first three KL modes as the speed is varied for a given clearance of 0.2 mm; (b) comparison of Exact (Ex) and reconstructed (KL) responses (horizontal displacements at x=0.302m), for point 6 of Fig 2 (a)

EFFICIENT CFD APPLICATIONS USING DISCRETE-TIME VOLTERRA KERNELS

Walter A. Silva
Aeroelasticity Branch
NASA Langley Research Center

INTRODUCTION

During the early development of mathematical models of unsteady aerodynamic responses, the efficiency and power of superposition of scaled and shifted fundamental responses, or convolution, was quickly recognized. This led to the classical Wagner's function, which is the response of a two-dimensional airfoil, in incompressible flow, to a unit step variation in angle of attack. Similar functions such as Kussner's function, which is the response of a two-dimensional airfoil to a sharp-edged gust in incompressible flow, were developed as well.

As geometric complexity increased, however, the analytical derivation of these time-domain fundamental functions became quite difficult and, therefore, impractical. As a result, frequency-domain aerodynamics for three-dimensional configurations became the method of choice for computing linear unsteady aerodynamic responses. For the case where geometry- and/or flow-induced nonlinearities are significant in the aerodynamic response, time integration of the nonlinear equations is necessary, as is done in aeroelastic CFD codes. As CFD codes and models have grown in complexity, there is a very real need to develop alternative and efficient nonlinear models for use in preliminary design. Research in this area, combined with the relatively new fields of digital filter design and digital signal processing (DSP), has led to a new method for numerically defining the classical fundamental aerodynamic functions for any configuration in compressible flow, and to the existence of an even more fundamental aerodynamic function: the aerodynamic impulse response function.

This paper will address the mathematical existence and the numerically-correct identification of linear and nonlinear aerodynamic impulse response functions. Differences between continuous-time and discrete-time sytem theories, which permit the identification and efficient use of this function, will be detailed. Important input/output definitions and the concept of linear and nonlinear systems with memory will also be discussed. It will be shown that indicial (or step) responses (such as Wagner's function), forced harmonic responses (such as those from Doublet Lattice theory), and responses to random inputs (such as gusts) can all be obtained from an aerodynamic impulse response function. This will establish the aerodynamic impulse response function as the most fundamental aerodynamic function that can be extracted from any given discrete-time, aerodynamic system. These results help to unify our understanding of classical two-dimensional continuous-time theories with modern three-dimensional, discrete-time theories and applications.

First, the method is applied to the nonlinear viscous Burger's equation. Then the method is applied to three-dimensional aeroelastic models using the CAP-TSD (Computational Aeroelasticity Program - Transonic Small Disturbance) code and the CFL3D Navier-Stokes code. Comparisons of accuracy and computational cost savings will be also presented. Because of its mathematical generality, an important attribute of this methodology is that it is applicable to a wide range of nonlinear, discrete-time problems.

CONCLUSIONS

The mathematically correct and numerically-accurate identification of linear and nonlinear aerodynamic impulse responses was presented. For the linear case, the

aerodynamic impulse response functions were used to reproduce exactly the responses of a linearized three-dimensional aeroelastic CFD model to arbitrary inputs consisting of aeroelastic motions at a fraction of the computational cost and time. The relationship between classical time-domain aerodynamic functions (Wagner's and Kussner's) and the discrete-time, linear aerodynamic impulse responses identified was demonstrated. It was shown that the classical functions can be computed from the impulse response functions, establishing the aerodynamic impulse response function as the most fundamental aerodynamic function that can be extracted from a discrete-time aerodynamic system.

For the nonlinear case, the existence, identification, and application of nonlinear, discrete-time, aerodynamic impulse responses was presented. Applications of the method to the nonlinear viscous Burger's equation revealed the existence of well-behaved first- and second-order impulse response functions. These functions represent an alternative input-output mapping of the nonlinear discrete-time equations that can be used to predict the response of the system to arbitrary inputs. The method was then applied to nonlinear aeroelastic CFD models using the CAP-TSD and CFL3D codes. The results prove the existence of these functions for complex, three-dimensional numerical models and their application proves their usefulness in terms of accuracy and computational efficiency.

Some Computer Assisted Studies in Nonlinear Dynamics

Kazuyuki YAGASAKI

Department of Mechanical and Systems Engineering, Gifu University, Gifu, Gifu 501-1193, Japan

1. Introduction

Recently, the author and his coworker [1] developed a package of the computer algebra system, Mathematica [2], to implement necessary computations for higher-order approximations of the averaging method (e.g., [3]). They used the package for some specific examples and showed that the higher-order averaging results can not only quantitatively but also qualitatively improve the lower-order ones. Moreover, the package and its improved version were used to perform higher-order averaging analyses for ultra-subharmonics as well as higher-order superharmonics and subharmonics [4, 5].

On the other hand, some computer softwares have been developed for numerical analysis of bifurcations. In particular, the computer software AUTO [6] has been widely used and its usefulness has been demonstrated for numerous examples. A driver to AUTO was also developed for numerical analysis of homoclinic and heteroclinic behavior of maps and periodically forced systems [7]. The effectiveness of the driver was proven for several examples there.

In this talk, we review the series of computer assisted researches [1, 4, 5, 7]. We consider some examples, for which the usefulness of the Mathematica package and AUTO driver is demonstrated. Their latest versions are available from the author (email: yagasaki@cc.gifu-u.ac.jp) on request. See the original papers for details on the results.

2. Higher-Order Averaging

Higher-order averaging can be easily performed by means of the Lie transformation [3]. The developed Mathematica package, haverage.m, includes two programs implementing the higher-order averaging procedure and van der Pol transformation for periodically forced, multi-degree-of-freedom weakly nonlinear systems.

As an example, we consider the periodically forced, standard Duffing oscillator,

$$\ddot{x} + \bar{\delta}\dot{x} + x + x^3 = \bar{\gamma}\cos\omega t, \tag{1}$$

where $\bar{\delta}$, $\bar{\gamma}$ and ω are positive constants. We set $\bar{\delta} = \epsilon^d\delta$ and $\bar{\gamma} = \sqrt{\epsilon}\gamma$, where δ, $\gamma = O(1)$ and d is a positive integer. Letting $x = \sqrt{\epsilon}(z - \Gamma\cos\omega t)$ with $\Gamma = \gamma/(\omega^2 - 1)$ in equation (1), we obtain a weakly nonlinear oscillator

$$\ddot{z} + z = \epsilon(z - \Gamma\cos\omega t)^3 + \epsilon^d\delta(\dot{z} + \omega\Gamma\sin\omega t). \tag{2}$$

The (higher-order) averaging analyses for equation (2) were performed with the assistance of the package haverage.m. See [5]. The obtained approximate bifurcation sets are shown in Fig. 1. Numerical simulation results by AUTO are also plotted as broken curves in the figure.

3. Homoclinic Behavior

The developed AUTO driver, HomMap, can treat three- or more dimensional problems and detect loci of homoclinic and heteroclinic points if the unstable or stable manifolds are one-dimensional. The user only has to prepare a simple Fortran source and data files for a new problem as in the standard version of AUTO.

We first consider the forced Duffing oscillator with double well potential,

$$\dot{x}_1 = x_2, \quad \dot{x}_2 = x_1 - x_1^3 - \delta x_2 + \gamma\cos\omega t, \tag{3}$$

where δ, ω and γ are positive constants. For δ, $\gamma > 0$ sufficiently small, there is a hyperbolic periodic orbit near the origin. Running AUTO with HomMap found several types of homoclinic orbits and produced homoclinic bifurcation curves in the (ω, γ)-space for $\delta = 0.1$, as shown in Fig. 2.

We next consider the forced, coupled Duffing oscillators,

$$\dot{x}_1 = x_3, \quad \dot{x}_2 = x_4, \quad \dot{x}_3 = x_1 - (x_1^2 + x_2^2)x_1 - \delta x_3 + \gamma_1\cos\omega t, \quad \dot{x}_4 = ax_2 - (x_1^2 + x_2^2)x_2 - \delta x_4 + \gamma_2\cos\omega t, \tag{4}$$
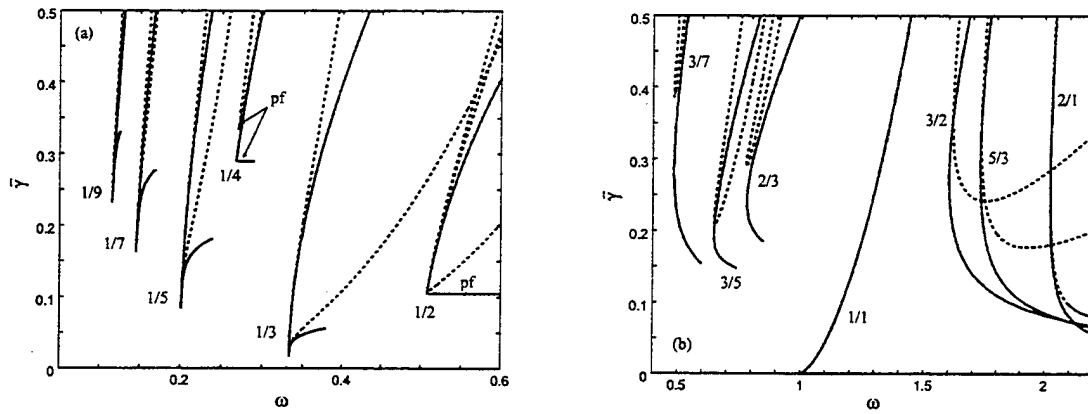
Fig. 1. Bifurcation sets of the Duffing oscillator (1) for $\bar{\delta} = 0.0001$. The theoretical results are shown solid and the numerical simulation results shown broken. The curves indicate a pitchfork bifurcation set if it is labeled "pf", and a saddle-node bifurcation set otherwise. The rational number m/n represent the results for ultra-subharmonic resonances of order m/n.
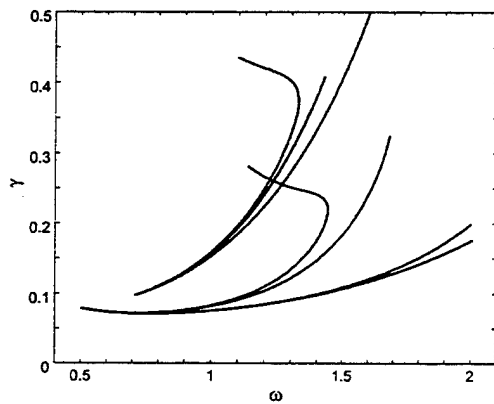

Fig. 2. Homoclinic bifurcation sets of the Duffing oscillator (3) for $\bar{\delta} = 0.1$.
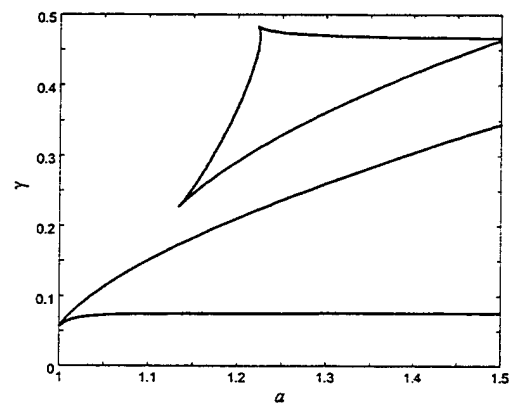

Fig. 3. Homoclinic bifurcation sets of the coupled Duffing oscillators (4) for $\bar{\delta} = 0.1$, $\omega = 1$ and $\gamma_2 = 0.05$.

where δ, ω, a and γ_j, $j = 1, 2$, are positive constants. When δ and γ_j, $j = 1, 2$, are sufficiently small, equation (4) has a hyperbolic periodic orbit near the origin. Running AUTO with HomMap found three types of homoclinic orbits and produced homoclinic bifurcation curves in the (a, γ_1)-space for $\delta = 0.1$, $\omega = 1$ and $\gamma_2 = 0.05$, as shown in Fig. 3.

REFERENCES

[1] K. Yagasaki and T. Ichikawa, Higher-order averaging for periodically forced, weakly nonlinear systems, to appear in *Int. J. Bifurcation Chaos*.

[2] S. Wolfram,, *The Mathematica Book*, 2nd ed., Addison-Wesley, Redwood City, 1991; 3rd ed., Wolfram Media/Cambridge University Press, Champaign/Cambridge, 1996.

[3] A. Nayfeh, *Perturbation Methods*, Wiley, New York, 1973.

[4] K. Yagasaki, Higher-order averaging and ultra-subharmonics in forced oscillators, to appear in *J. Sound Vib.*

[5] K. Yagasaki, Detection of bifurcation structures by higher-order averaging for Duffing's equation, submitted for publication.

[6] E. Doedel, A. R. Champneys, T. F. Fairgrieve, Y. A. Kuznetsov, B. Sandstede & X. Wang, *AUTO97: Continuation and Bifurcation Software for Ordinary Differential Equations (with HomCont)*, Concordia University, Montreal, 1997.

[7] K. Yagasaki, Numerical detection of and continuation of homoclinic points and their bifurcations for maps and periodically forced systems, to appear in *Int. J. Bifurcation Chaos*.

An efficient, hybrid frequency-time domain method for the dynamics of large-scale dry-friction damped structural systems.

J. Guillen[1], C. Pierre[2]

Mechanical Engineering and Applied Mechanics
The University of Michigan
Ann Arbor, MI

The steady-state response to periodic excitation of multi-degree of freedom structural systems with several attached dry friction dampers is studied. The general case of elastic/perfectly plastic dampers is considered. One distinguishing feature of the work is that no further approximation of Coulomb's friction law is made in the calculation of the friction force. Namely, the displacement of and the force transmitted by a friction damper are deduced in the time domain from the displacement and velocity of the corresponding degree of freedom to which the friction damper is attached. All other terms in the equations of motion are transformed, following a multi-harmonic balance procedure, into the frequency domain through the use of a Fast Fourier Transform. The resulting solution algorithm is thus hybrid in the frequency and time domains. The convergence of the method is ensured by a modified Broyden's algorithm, which is used to solve iteratively the set of multi-harmonic nonlinear equations in the frequency domain.

The resulting solution procedure is robust and highly performant for all cases considered. It features fast convergence and yields extremely accurate results when compared to direct time integration, in part because no approximation of the friction force is made. For example, in the study, complete frequency responses are obtained for systems with 108 degrees of freedom and 36 dry friction dampers, over the entire range of friction parameters, and where as many as 17 temporal harmonics are taken into account. In the latter case the resulting 1836 frequency-domain equations, of which 612 are nonlinear, are handled effortlessly by the Broyden solver.

The method can handle both friction dampers that are attached to ground and the general case of dampers that connect two degrees of freedom of the structure. As an application, a cyclic assembly of beams coupled by linear elastic elements is studied, with friction dampers located between the beams and the ground or between two beams, or both. This system is a

---

[1]Graduate student research assistant, *guillen@engin.umich.edu*

[2]Professor, *pierre@umich.edu*

simplified model of a dry-friction damped bladed disk used in turbomachinery applications. Assemblies with various number of beams (blades) and of friction dampers are considered. Results are obtained for both tuned and mistuned configurations of these systems subject to various traveling wave "engine order" excitations, for a variety of structural and friction parameters. Interesting, complex features of the nonlinear response are revealed, such as: motions for several stick-slip phases per period; localized motions for mistuned systems, which feature mostly sticking motion at most blades and mostly slipping motion at a few blades; subresonances; effects of higher harmonics.

This work is believed to be the first to develop a robust solution procedure for predicting the complex, multi-harmonic reponse to periodic excitation of large-scale structural systems with many friction dampers. Current efforts include the extension of the method to study the stability of autonomous, dry-friction damped, multi-degree of freedom systems with negative viscous damping. Preliminary results for the latter topic will be presented.

ACCURATE PREDICTION OF THE NONLINEAR DYNAMIC BEHAVIOUR OF AN IMPACT OSCILLATOR

Assistant Professor Annika Stensson
Division of Computer Aided Design
Department of Mechanical Engineering
Lulea University of Technology
SE-971 87 Lulea, Sweden

Impact is an event often occurring in engineering and it is well known that mathematical models of impacting systems can exhibit complex dynamic behaviour. The nonlinearity may cause the system to show phenomena such as multiple attractors, subharmonic response and chaotic motions. This means that different initial conditions can lead to completely different asymptotic behaviour. As a consequence, if a parameter or an initial condition is only changed a small amount, the response can suddenly bifurcate to another type of motion. Most studies on systems with clearances and impacts are theoretical and effects due to small changes in parameter values have been studied. In practice, the parameter values can only be determined within a range of resolution. The parameter values will change during the lifetime of the product, due to wear, variation in temperature, inexact mountings etc. It is also, for most cases, impossible to keep track on the exact initial conditions.

This work focus on to what extent numerical simulation can be used in order to predict the nonlinear behaviour of an impact oscillator. To analyse this problem extensive experiments have been made and the results are compared with numerical simulations.

The mechanical system consists of a harmonically forced impact oscillator with initial clearance, see Figure 1. The system is studied using a systematic variation of the excitation frequency. The chaotic regions are studied carefully. Subharmonic responses of different periodicity are presented and probable coexisting solutions are described.
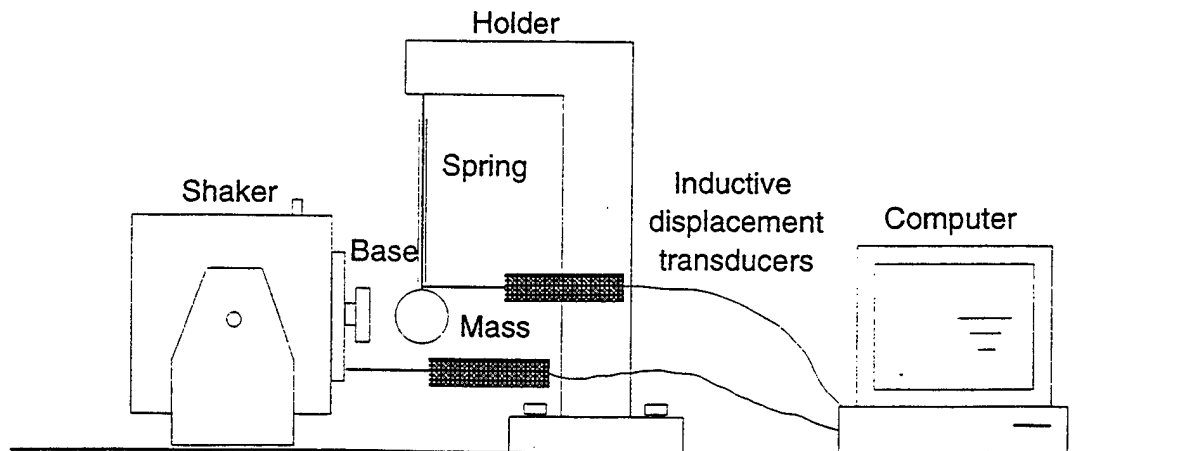

Figure 1. Illustration of the experimental setup.

The investigated region of excitation frequency is shown to include two regions of main chaotic motion which are bounded on both sides by periodic resonance. There are also subharmonic motions within the regions of main chaotic motion. A subharmonic response of type period two/ten and a chaotic motion were obtained in the experiment for the same measured parameter values.

The mass is much heavier than the beam and the deflection is relatively small, which makes it possible to model the system as a single-degree-of-freedom mass/spring system with a linear spring coefficient. The model also includes viscous damping, an instantaneous impact and an initial clearance. The dissipation in the impact event is described by a coefficient of restitution. Within the investigated parameter space, the two main chaotic regions surrounded by large periodic resonances were found by numerical simulations. The experimentally obtained subharmonic motions within the regions of main chaotic motions were shown to be periodic windows in the numerical simulations. The structure of some experimentally obtained chaotic attractors are compared with corresponding attractors from numerical simulations.

It is shown that coexisting solutions are present for some parameter values, but not for others. The periodic two/ten motion and the chaotic motion that were found in the experiment for the same parameter values were studied carefully using numerical simulations. Investigations using the cell-mapping technique showed no coexisting solutions due to sensitivity to initial conditions. However, it is shown that a small variation of the initial gap and/or the excitation amplitude results in these different types of responses. This indicates that the main reason for the two different solutions found in the experiment is due to measuring errors. A measuring error of about 0.4% is inevitable due to the resolution of the inductive displacement transducers and the accuracy of the measuring card.

To conclude, it is shown that the experimentally observed behaviour of the system is closely predicted by numerical simulation of the governing equation of motion. Coexistence of solutions, sensitivity to the parameter values and measuring errors are discussed. By using the information about the dynamical behaviour of the system included in the equations of motion and by using graphical representations such as time histories, phase plane projections, Poincaré sections, bifurcation diagrams and cell-maps, a practising engineer should able to select a good design. For example, the excitation frequency ranges in which stable periodic low amplitude responses can be expected to occur are possible to determine, and the peak amplitudes of such response can be predicted. This can lead to much lower stresses, less noise level and better endurance. However, the designer must be very careful when examining possible variations in parameter values and initial conditions in order to get enough information to be able to make a good choice.

Tuesday, July 28
1330-1500
Session 9.

On Choosing Inputs for System Identification in Nonlinear Systems

T. Doughty, P. Davies and A.K. Bajaj
School of Mechanical Engineering, Purdue University, West Lafayette, IN 47907-1288.

Nonlinear systems can display a wide variety of interesting behavior: from jumps in the response to amplitude-modulated motions and chaos. The conditions under which the system exhibits this behavior depend on the system parameters, the initial conditions and the nature of the excitation. Small changes in any of these may lead to very different response characteristics. Seeking out this interesting behavior in an experimental system may be nearly impossible without analysis of accurate models of the system to guide the experimenter, thus the requirement for system identification to develop accurate models of the system.

Nonlinear system identification requires a deep understanding of the behavior of the system under investigation. Unless the system exhibits behavior that depends on all the terms in an accurate model of the system, some of the model terms will be poorly identified. The experimentalist, therefore, must create excitation conditions that ensure nonlinearities are strongly influencing the response. The problem becomes determining what these desirable excitation conditions might be. This is where analysis of the theoretical model of the system plays a role. Approximations to model coefficients could be used in model analysis to determine the region where the response of interest is likely to be. Experimentally exploring this region, and comparing model predicted response characteristics to measured response characteristics will help identify the regions where the most useful data for system identification might be generated. This data will be used to improve the model estimate and the exploration process can be repeated, fine tuning the model until the theoretical and experimental responses are close.

The research reported in this presentation focused on three different approaches to identification of models of modes in structures. The first identification method uses measured states (displacement, velocity and acceleration) and the continuous time nonlinear differential equation of the system [1]. A matrix relation is constructed wherein time dependent vectors (linear and nonlinear combinations of the states) are known. The model parameters are obtained by solving the matrix equation. The method of Harmonic Balance is the basis of the second approach. Following the work of Yasuda [2] the system's output is assumed, in Fourier Series form, and then substituted into the differential equation generating relationships between the spectral amplitudes of the input and output. As in the first method, a matrix relation is constructed. Knowing the spectral amplitudes, the differential equation's parameters are again obtained by solving a linear matrix equation. The third method is based on the steady state amplitude equation arising from a Multiple Time Scales analysis of the differential equation. When fitted to a collection of input and output data sets, the steady state amplitude equation gives rise to a system of nonlinear, coupled algebraic equations. These are then solved to find the differential equation parameters.

The first two methods both use measured time histories and specifically the information at the excitation frequency and harmonics of the excitation frequency. In an experiment the data will be low-pass filtered to prevent aliasing in data acquisition, and this will remove some of the higher frequency information. The implications of this on the system identification are explored. The higher sampling rates and wider bandwidth

required to retain the significant harmonic data are not necessary for the third method, where only the amplitude at a single frequency is tracked, and compared to the model predictions of the steady state amplitude. However, this approach relies on the smallness of certain terms in the differential equation, and as this assumption is violated the accuracy of the model parameter estimates degrades. The results from both simulations and experiments on cantilevered beams will be discussed.

[1] Young, P., 1996, "Identification, Estimation and Control of Continuous- Time and Delta Operator Systems," Proc. of the International Conference on Identification in Engineering Systems, University of Wales, Swansea, UK, pp. 1-17.

[2] Yasuda, K., Kawamura, S., and Watanabe, K., "Identification of Nonlinear Multi-Degree-of-Freedom Systems (Presentation of an Identification Technique), JSME Int. J., Ser III, Vol. 31, No. 1 (1983), p. 8-14.

An Iterative Approach to Decomposing Harmonics for Nonlinear Systems

Sean O'F. FAHEY

Acoustics Department, Electric Boat Corporation, 75 Eastern Point Road, Groton, CT 06340, USA

Abstract

We present an approach for estimating the discrete Fourier amplitudes for a class of time limited signals encountered in nonlinear systems. Exciting nonlinear systems with periodic deterministic excitation often produce responses that can be described in terms of undamped sinusoids with *phase locked* behavior between spectral components. We describe this approach through the specific application of a combination resonance of the additive type via numerical simulaton. Signals originating from a nonlinear resonance contain harmonics where *a priori* information about the spacing between harmonics is known. In the presented example, we predict the potential for response at *zero* and near ω_1, $2\omega_1$, $\omega_2 - \omega_1$, ω_2, and $\omega_1 + \omega_2$ given an excitation near $\omega_1 + \omega_2$ using the method of multiple scales. We realize significant responses near ω_1 and ω_2 due to an excitation near $\omega_1 + \omega_2$ alone. There are several available tools for decomposing such signals. The discrete Fourier transform offers one route for decomposing spectral components periodic within a sampled window. When response frequency and phase are required and sampling periodicity cannot be assured, other decomposition techniques are more appropriate. Prony techniques can be utilized for uncovering individual frequency components from a time limited signal without such periodicity requirements. We consider the least squares complex exponential. These techniques do not consider *a priori* information about the spacing between spectral components. Hence, we must be able to form global frequency estimates in accordance with our understanding of the spectral spacing. We propose a method for piecing together the spectral estimates from the least squares complex exponential with limited success. As an alternative, we revert to a simultaneous and iterative minimization on a Euclidean norm between measure and model. Such efforts are often avoided because of associated computational costs. An efficient and simple iterative approach for forming and estimating such global estimates is our principal topic.

Recently (Fung Et. Al. 1998; Nayfeh Et Al. 1997; Hajj Et. Al. 1995) provided motivation for examining the phase relations between differing spectra for the purpose of nonlinear structural dynamic identification. They sought and found nonlinear phenomena by exciting structures near twice first mode natural frequencies. Exploiting a principal parametric resonance and a subharmonic resonance of order one-half and examining spectral amplitudes and the *phase difference* between spectral components; they estimated quadratic and cubic stiffness, linear and quadratic damping, modal participation and an effective parametric participation factor. The phrase *phase difference* was coined to distinguish phase relations between spectral components as opposed to *phase* which is a delay measure at some frequency. The structures exhibited strong responses near their first natural frequency, with lesser components at *zero* and at the excitation frequency. The excitation frequency was carefully choosen that all components of practical interest were periodic within sampled windows.

One motive is an interest to examine phase difference relations for other phenomena involving multiple modal effects. This has resulted in some difficulty. Namely, these signal can not be guaranteed to be periodic within a sampled window. Hence, it is not practical or appropriate to use the discrete Fourier transform to estimate multi-modal phase difference. In order to determine phase difference, one must use a techniques without a periodicity requirements. Prony techniques do not require periodicity and are shown to be practical candidates. We will show that although Prony techniques are practical, they have some undesireable characterists.

The modal analysis community has produced several global eigenvalue estimation techniques between signals with common eigenvalues (Leuridan 1982; Vold Et. Al. 1982; Richardson 1986). For a linear systems, one can express all system eigenvalues by examining any transfer function, excluding modal node locations. Since the system eigenvalues are taken as spatially global properties, a common characterist equation can be designated. Each transfer function produces an estimate of this characterist equation. All transfer functions can be compared in forming an global eigenvalue estimate. Harmonics are not expressable within the context of a straightforward global characterist equation; even though we understand from theory how the system response frequencies are over specified. Special procedures are required in collecting this redundancy. Since information is known of the relation between spectra, an auxhillary minimum eigenvalues estimate is required. We demonstrate one method for forming such an minimum eigenvalue estimate. And explain that while the overall measurement quality improves that individual measurement estimates can suffer. Such a technique does not provide a clear mechanism for evaluating errors due to its secondary relationship with respect to the original data.

Eigenvalues are often considered in terms of the solution for the linearized structural dynamic problem. Harmonics are related to the linear system eigenvalues and excitation frequency. Harmonics are not the eigenvalues of the linearized structural dynamic problem. However, harmonics can be discussed as the eigenvalues of a digital delay filter polynomial used in autoregressive moving average (ARMA) signal processing. When we discuss a minimum eigenvalue set we are describing the eigenvalues used by the ARMA community. We do not observe values *at* ω_i rather values *near* ω_i. We want to represent

the spectral components near $a\omega_q \pm b\omega_r$ by the values near ω_q and ω_r alone, incorporating our understanding about what occurs near $a\omega_q \pm b\omega_r$. In this sense we discuss a minimum eigenvalue set.

We desire the difference between measure and model to be minimal. The two common expressions for quantitatively expressing differences between measure and model are the maximin norm and the Euclidean norm (Forsythe 1957). The maximin norm expresses the single largest deviation between measure and model. The Euclidean norm expresses the sum of squared differences. Our interest remains with a distributed measure of error. Hence, we consider the problem in terms of the Euclidean norm. In column matrix form, a real error vector is expressed

$$\{x_{measure}\} - \{x_{model}\} = \{\epsilon\} \tag{1}$$

such the Euclidean norm is

$$\|O\| = \epsilon^T \epsilon \tag{2}$$

where T denotes matrix transpose. We desire to minumize the Euclidean norm with a minimum set of parameters describing the model. This formulation of the problem is ideal. Unfortunately such problem statements are not practical or efficient under many circumstances.

We consider an example in explaining why the Euclidean norm is often sacrified to suboptimal procedures. Given a time limited signal known to be governed by $2M$ constant coefficient complex exponentials

$$E[x] = \sum_{k=0}^{2M-1} A_k \, exp[\lambda_k t] \tag{3}$$

$$x_i - \sum_{k=0}^{2M-1} A_k \, exp[\lambda_k t_i] = \epsilon_i \tag{4}$$

where x_i represents a physical measurement. The signal is evenly sampled and has no spectral content above the Nyquist criterion f_{crit} equal to $1/2\Delta t$, where Δt is the sample rate. The signal is considered in the presense of some added Gaussian noise. In order to minumize the contribution of noise the quantity of data obtained must be strictly greater than that explicitly required for parameter estimation. Hence, x is a data vector choosen with length strictly greater than 2M. Forming the Euclidean norm, one resolves

$$\|O\| = \sum_{i=0}^{N-1} x_i^2 - 2 \sum_{i=0}^{N-1} \sum_{k=0}^{2M-1} A_k x_i \, exp[\lambda_k t_i] + \sum_{i=0}^{N-1} \sum_{k=0}^{2M-1} A_k^2 \, exp[2\lambda_k t_i] \tag{5}$$

This objective function should be a minimum when its first partial derivatives with respect to A_k and λ_k equal zero, expressed

$$0 = -2 \sum_{i=0}^{N-1} x_i \, exp[\lambda_k t_i] + 2A_k \sum_{i=0}^{N-1} exp[2\lambda_k t_i], \quad \forall \quad k \in \{0..2M-1\} \tag{6}$$

$$0 = 2A_k \sum_{i=0}^{N-1} x_i t_i \, exp[\lambda_k t_i] - 2A_k^2 \sum_{i=0}^{N-1} t_i \, exp[2\lambda_k t_i], \quad \forall \quad k \in \{0..2M-1\} \tag{7}$$

The solution of these equation represents the least squares realization for A_k and λ_k. These equations also represent nonlinear expressions in terms of A_k and λ_k for which no closed form solution is available (McDonough and Huggins 1968; Marple 1987). Because of such difficulties suboptimal procedures are often applied in the determination of corresponding parameters.

McBride, Schaefgen, and Steiglitz (1966), McDonough and Huggins (1968), and Evans and Fischl (1973) discuss maintaining the Euclidean norm by simultaneous and iterative minimization by gradient decent procedures or Newton's method. We take their lead; but provide only a minimum set of eigenvalues to explain our model. We evaluate the Euclidean norm and use the conjugate gradient technique to determine optimal eigenvalues, magnitude and phase. This procedure produces estimates that are appropriate for considering the phase difference between spectral components irrelevant of sampling periodicity, when phase locked behavior is known to exist.

Experimental Identification Technique in Time Domain for Nonlinear Rotating Shaft Systems

Kimihiko YASUDA and Keisuke KAMIYA

Department of Electronic-Mechanical Engineering
Nagoya University
Furo-cho, Chikusa-ku, Nagoya, 4640814, Japan

Abstract

For identifying rotating shaft systems, modal testing methods are often used. But the present modal testing methods are not appropriate for rotating shaft systems. The reason is that the methods are unable to determine parameters inherent to the systems such as the unbalance and anisotropy. Furthermore the methods are not applicable to nonlinear rotating shaft systems.

In a previous paper [1], we proposed a new experimental identification technique applicable to nonlinear systems. Then we extended the technique so that it can be applicable to nonlinear rotating shaft systems [2]. These techniques are based on the principle of harmonic balance, and uses data of periodical responses of the systems. To obtain this type of data is not always convenient.

In this study, we attempt to develop other new identification techniques free from inconvenience with respect to the type of data. We consider a rotating shaft system composed of a shaft with a disk mounted on it. The basic procedures of the techniques are to evaluate the error contained in the equations of motion when the experimental data are substituted and to find the parameters which make the error the smallest. To find such parameters, we adopt two techniques, the usual least square method and the Lagrange's multiplier method. In this way, we proposed two identification techniques. The proposed techniques have no limitations as to the type of data.

To check applicability of the proposed techniques, we first conducted numerical simulation. We found that, for data without noises, both techniques yield accurate results. Also we found that, as noises increase, the first method using least square method loses accuracy, but the second

method using the Lagrange's multiplier method does not so much. Thus, the latter usually yields better results. But for applying the latter technique, some iteration technique has to be used, starting from some initial values. To have initial values, the former technique can be used. So both techniques are of value.

Finally we conducted experiments. We compared the maximum amplitudes of deflections obtained in the experiment with those predicted by the identification results. An example of the comparison is shown in the figure below. We found that both techniques yield good identification result.
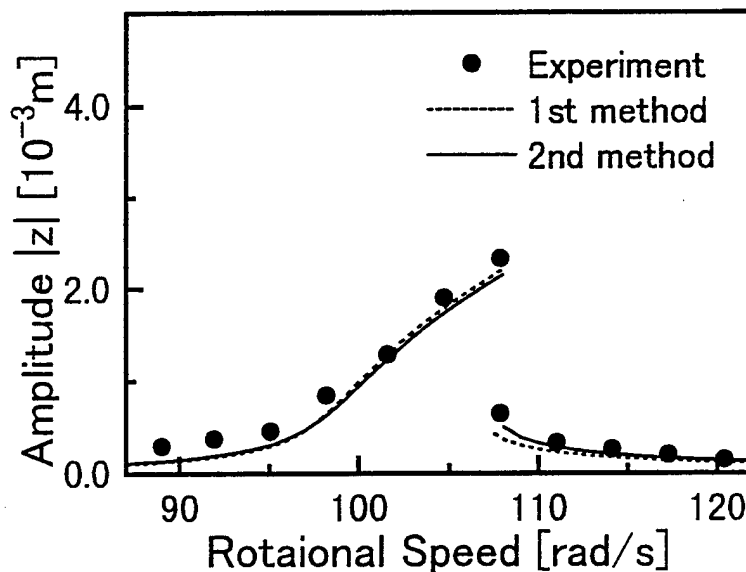
References

[1] K. Yasuda and Kamiya Keisuke, *Experimental Identification Technique of an Elastic Structure with Geometrical Nonlinearity*, Trans. ASME, Journal of Applied Mechanics, 64-2, (1997-6), 275-280.

[2] K. Yasuda, Keisuke Kamiya, and Hiroshi Yamauchi, *An Experimental Identification Technique for a Nonlinear Rotating Shaft System*, Sixth Conference on Nonlinear Vibrations, Stability, and Dynamics of Structures, (1996-6).

Nonparametric Nonlinear System Identification of a Nonlinear Flexible System Using Proper Orthogonal Mode Decomposition

X. Ma, M. A. F. Azeez and A. F. Vakakis
Department of Mechanical and Industrial Engineering
University of Illinois at Urbana-Champaign, Urbana, Illinois -61801, U. S. A.

The method of Proper Orthogonal Decomposition which also known as Karhunen Loeve (KL) method can be used to extract dominant modes of any physical system from time measurement made at several points in the special domain. This has been applied in different fields such as fluid mechanics of acoustical systems. In the current work, we analyze the system of two linearly coupled cantilever beams each grounded by nonlinear springs with cubic nonlinearity (Fig. 1). The dynamics of the system has been studied numerically and experimentally in previous work ([1], [2]). The important parameters of the system are linear coupling stiffness εk and the nonlinear coefficient of the grounded springs $\varepsilon \alpha$. It has been observed that the system possesses two stable modes when the ratio $k / \alpha p^2$ is greater than a critical value, where p is the total energy of the system. When the ratio is smaller than the critical value, the system possesses three stable modes. It is the aim of the current work to find these regions using numerical data and observe the change of the KL mode shapes as the energy in the system is changed.

The KL modes are obtained by exciting each of the beams by means of distributed harmonic forces and recording the displacements along the span of the beams. Then a correlation matrix is created and the dominant mode shapes of energies are obtained from it. Figure 2 gives an example of the first KL mode shapes of a weakly coupled system, the energy percentage of the first KL modes corresponding to two beams are 97.90% and 99.77% respectively.

The energy stored in KL modes gives the measure of the dimensionality of the system. These modes can be used to reconstruct the dynamics of the system using a reduced order dynamical mode. It is numerically verified that the first KL mode can be used to construct the response the system. The energy ratio between the two beams with nonlinearities and without nonlinearities is shown in Figure 3. From it we see that nonlinear localization happens when the two beams are weakly coupled.

Key Words: proper orthogonal decomposition, nonlinear system identification, beams

References:

[1] E. Emaci, T. A. Nayfeh and A. F. Vakakis, Numerical and Experimental Study of Nonlinear Localization in a Flexible Structure with Vibro-Impacts, *ZAMM Z. angew. Math. Mech.* 77(1997) 7, pp527-541, 1997.
[2] A. F. Vakakis, L. I. Manevitch, Y. U. Mikhlin, V. N. Pilipchuk and A. A. Zevin, Normal Modes and Localization in Nonlinear Systems, *John Wiley & Sons, Inc.,* 1996
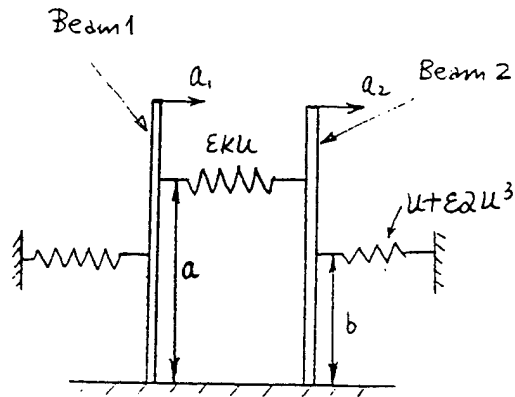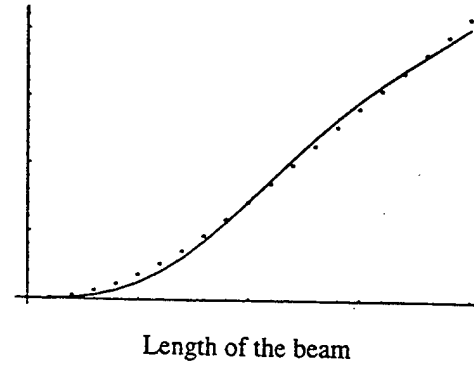
Figure 1: System configuration with
nonlinear springs

Length of the beam

Figure 2: First KL mode shapes of the two
beams with a weakly coupled system
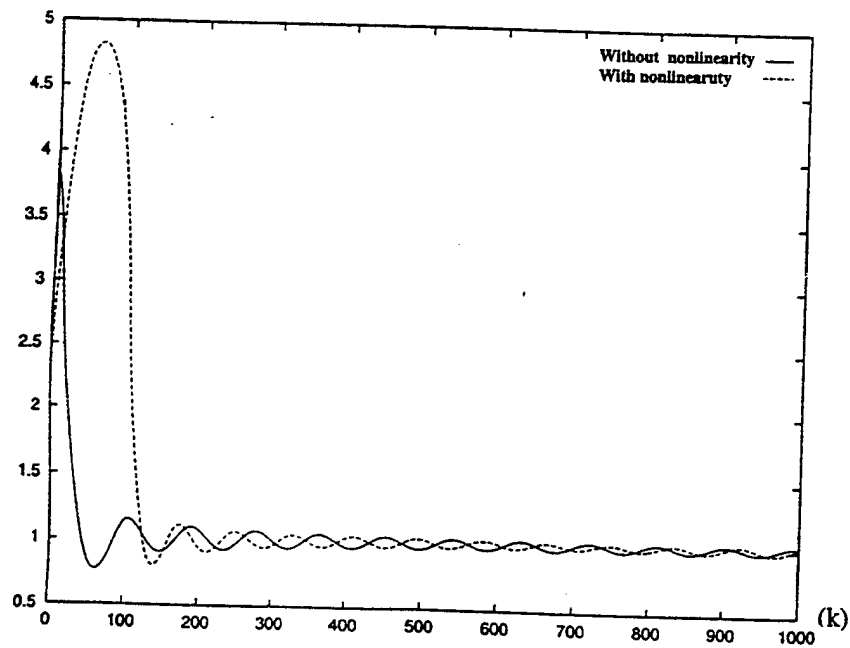$k = 70, \varepsilon = 0.1, \alpha = 10^6$

Figure 3: Ratio of energies of the first two KL modes of the beams
$\varepsilon = 0.1$, without nonlinearity $\alpha = 0$, with nonlinearity $\alpha = 10^6$

IDENTIFICATION OF NON-LINEAR FREE VIBRATION: TIME DOMAIN HILBERT TRANSFORM APPROACH

Dr. Michael Feldman

Faculty of Mechanical Engineering, Technion — Israel Institute of Technology

Haifa, 32000, Israel, email: merbe02@tx.technion.ac.il

This paper summarizes the results of a non-linear free vibration identification that is performed on the base on the Hilbert transform. Some different attempts of applying the HT to frequency domain for non-linear vibration system identification are presented in [7]. The HT of the Frequency Response Function (FRF) of a linear structure reproduces the original FRF, and any departure from this, i.e. distortion, can be attributed to non-linear effects. There exists a possibility to distinguish the common types of weakly non-linearity in mechanical structures from the distortions in the FRF. But the FRF distortion gives no way to quantify the non-linearity which can then be incorporated into the system dynamical model.

Other results of applying the HT to time domains [1, 2] do better: they enable the determination of the non-linear system dynamical model. For this non-parametric identification in the time domain it was proposed that relationships be constructed between the instantaneous frequency and amplitude (system backbone or skeleton curve) plus relationships between the damping coefficient (or decrement) as a function of amplitude [3].

Of course, modern Time-frequency and Time-scale analysis methods (the Wigner-Ville distribution, the Wavelet transform etc.), based on the transient data precessing, could be successfully applied to the non-linear vibration system identification. However the HT in time domain approach has two principal advantages: it leads directly to non-linear parameters of the vibration system model and also it offers the best resolution in the time domain. Really, the obtained instantaneous system modal parameters are functions of time and can be estimated at any point of the transient process. The total number of these points which map the free vibration is much greater than that of the peak points of the signal. It opens the way for averaging and for other statistical processing procedures, making the identification result more precise.

The proposed direct non-parametric time domain method based on the HT allows a direct extraction of the linear and non-linear parameters of the system from the measured time signal of

output. The resulting non-linear algebraic equations are rather simple and do not depend on the type of non-linearity that exists in the structure. When applying this direct method for transient vibration, the instantaneous modal parameters are estimated directly. That enables us to consider an inverse identification problem, namely, the problem of estimation of the initial non-linear elastic and damping force characteristics. The method is robust, uses measurement techniques in current engineering practice and would appear to have considerable practical promise.

References

[1] **Feldman, M.S., 1985:** "Investigation of the natural vibrations of machine elements using the Hilbert transform", Soviet Machine Science, Allerton Press Inc., # 2, pp. 44-47.

[2] **Feldman, M., 1994:** "Non-linear system vibration analysis using Hilbert transform – I. Free vibration analysis method "FREEVIB"", Mechanical Systems and Signal Processing, 8(2), pp. 119-127.

[3] **Feldman, M., 1997:** "Non-Linear Free Vibration Identification via the Hilbert Transform", Journal of Sound and Vibration, v 208, n , pp. - .

[4] **Feldman M., Seibold S., 1998:** "Damage diagnosis of rotors: application of Hilbert-transform and multi-hypothesis testing", Journal of Vibration and Control, , pp. .

[5] **Gottlieb O., Feldman M., 1997:** "Application of a Hilbert Transform-Based Algorithm for Parameter Estimation of a Nonlinear Ocean System Roll Modell", Journal of Offshore Mechanics and Arctic Engineering, ASME, v 119, n , pp .

[6] **Hahn, Stefan L., 1996:** "The Hilbert Transform of the Product $a(t)cos(\omega_0 t + \phi_0)$", Bulletin of the Polish Academy of Sciences, Technical Sciences, V. 44, No 1, pp. 75-80.

[7] **Simon, M., Tomlinson, G.R., 1984:** "Use of the Hilbert transform in modal analysis of linear and non-linear structures", Journal of Sound and Vibration, 96(4), pp. 421-436.

[8] **Spina, D., Valente, C., Tomlinson, G.R., 1996:** "A New Procedure for Detecting Nonlinearity from Transient Data Using the Gabor Transform", Nonlinear Dynamics, 11 , pp. 235-254.

Tuesday, July 28
1530-1700
Session 10A.

Dynamics of a Flexible Cantilever Beam Carrying a Moving Mass

SULTAN A.Q. SIDDIQUI, M. FARID GOLNARAGHI
Department of Mechanical Engineering, University of Waterloo
GLENN R. HEPPLER
Department of Systems Design Engineering, University of Waterloo, Waterloo, Ontario, N2L 3G1 CANADA

Abstract. A number of systems in mechanical and civil engineering can be idealized as a flexible beam carrying a moving mass. Examples include motion of vehicles on bridges, cranes carrying moving loads, robotic arms and space structures. The basic problem in analyzing such systems is that even with a simple model for the beam (e.g., an Euler–Bernouli beam) the coupling between the mass and beam makes the solution of the equations of motion difficult to obtain. The motion of the mass makes the inertial and stiffness properties of the beam time dependent.

Dynamics of the system is described by two coupled nonlinear partial differential equations (PDEs) involving time dependent Dirac-delta functions. Numerically the problem was solved using two approaches both based on Rayleigh-Ritz discretization method. In the first technique the mode shapes of a simple cantilever beam were used as basis functions and the resulting nonlinear ordinary differential equations were solved using an automatic stiff ordinary differential equation (ODE) solver. It should be noted that the mode shapes are not eigen functions as in linear systems but they are used here as basis functions in the Rayleigh-Ritz method. Increasing the number of basis functions would approximate the solution more closely. However it also increases the number ODEs, rendering the system "stiff" and quite impossible to solve using automatic ODE solvers. In the second approach the basis functions were obtained using finite elements. The nonlinear terms in the equations of motion impose high degree of continuity requirements (continuous second derivative) on the finite element formulation. As a result, the finite element basis functions have to interpolate the deflection, slope and curvature at each node. The process leads to a large number of ordinary differential equations (ODEs). Finite differences were used to reduce the ODEs to algebraic equations. The resulting nonlinear algebraic equations are quite difficult to solve using conventional methods, so a new iteration technique was presented. Unlike Newton's method or its variants, this technique does

not require computing the Jacobian which imposes another degree of continuity on the finite element formulation.

The problem was attacked analytically using a perturbation method. For a simplified model (neglecting nonlinearities higher than quadratic) an analytical solution was obtained for the nonlinear equations in terms of elliptic functions. The focus of this analysis was on the behaviour of the system under internal resonance between the mass and the beam. Using the analytical solution, a parametric study was done to investigate the system behaviour in various regions. The frequency interactions between the moving mass and the beam were studied using time-frequency analysis techniques. The results obtained and the techniques developed apply to beams undergoing small oscillations.

This is an extension of an earlier work by Golnaraghi [1, 2] where the beam was modeled rigid and flexibility was incorporated through springs. Later Khalily et. al. [3] used an improved eigen functions method which accounts for the motion of the mass and obtained numerical results. The presentation would be based on a previous publication by the authors [4] and incorporating new results obtained using time-frequency analysis.

References

[1] M. F. Golnaraghi. Vibration suppression of flexible structures using internal resonance. *Mechanics Research Communications Journal*, 18(2/3):135–143, 1991.

[2] M. F. Golnaraghi. Regulation of flexible structures via nonlinear coupling. *Journal of Dynamics and Control*, 1:405–428, 1991.

[3] F. Khalily, M. F. Golnaraghi, and G. R. Heppler. On the dynamic behaviour of a flexible beam carrying a moving mass. *Nonlinear Dynamics*, 5:493–513, 1994.

[4] S. A. Q. Siddiqui, M. F. Golnaraghi, and G. R. Heppler. Dynamics of a flexible cantilever beam carrying a moving mass. *Journal of Nonlinear Dynamics*, accepted for publication 1997.

Nonlinear Oscillations in Coriolis Based Gyroscopes

Dag Kristiansen and Olav Egeland

Department of Engineering Cyberntics
Norwegian University of Science and Technology
N-7034 Trondheim, Norway
e-mail: Dag.Kristiansen@itk.ntnu.no, Olav.Egeland@itk.ntnu.no

Note: This "abstract" only includes the Abstract, Introduction and Conclusion of our paper.

Abstract: In this paper we model and analyze nonlinear oscillations which are known to exist in some Coriolis based Gyroscopes under certain circumstances. A detailed derivation of a nonlinear coupled electro-mechanical model of the gyroscope is given and analyzed using perturbation theory. The model is also simulated and the results are shown to give an accurate description of the experimental results. This work can be used as a starting point of designing nonlinear observers and vibration controllers for the gyroscope in order to increase the performance.

Introduction

Coriolis based gyroscopes, in which vibrating cylindrical shells are used as sensing elements, are gyroscopes which possesses a number of advantages over conventional spinning wheel gyroscopes. Troublesome bearings are totally eliminated, they have low power requirements, short start up time and very low inherent noise [6]. In addition, if the vibrating cylinder is designed to give a dynamically balanced oscillator, it is known that performance is not, at least to a first order, sensitive to linear acceleration [2],[4].

Although this type of gyro has many attractive properties, it also introduces some challenges with respect to modeling and control. One of the most important problem is the existence of unwanted superharmonic resonances [9] in the drive and sense loop of the gyroscope when the excitation amplitude becomes large. This cannot be explained by linear vibration theory. Using nonlinear vibration theory, this phenomena may theoretically be reduced by changing the physical parameters of the gyroscope such as length, radius, height, thickness and material parameters and thereby changing the relative spacing between the linear natural frequencies. However, due to the complex dynamics of the gyroscope and to the fact that one wants to minimize the size, this seems like a very hard task [7] and is of course not applicable to already manufactured gyroscopes.

[5] and [2] analyzed cylinder gyroscopes by representing it as an infinite cylinder. [1] investigated the feasibility of a piezoelectric cylinder gyroscope and derived a electro-mechanical model by using Lagrange's equation. [8],[3] and [10] analyzed the effect of mass imperfections in cylinder gyroscopes. Common for all these references are that they were only analyzing linear models and therefore did not include important nonlinear effects.

In existing industrial gyroscopes, the problem of superharmonic resonances is "solved" by reducing the excitation amplitude, but since the Coriolis acceleration is proportional to this amplitude, this means that the sensitivity of the gyro decreases. However, a more constructive solution may be to introduce vibration damping controllers to reduce the effect of the superharmonic resonances and therefore be able to increase the performance of existing gyros.

In this paper we extend previous proposed models by including geometrical nonlinearities. Based on experimental observations and by using

Lagrange's equation, we derive a nonlinear three-mode model of a cylinder gyroscope. By applying the method of multiple-scales [9], we show analytically the presence of superharmonic resonances. The model is then simulated and the results correspond well to the theoretical analyzis.

Conclusions

In this paper we have proposed a nonlinear 3-mode coupled model of a cylinder gyroscope made of steel with attached piezoelectric transducers. The model was derived based on experimental results and by using the Donnell-Mushtari theory and Lagrange's equation.

We then analyzed the model using the method of multiple-scales. It was shown analytically that the nonlinearities produced perfect tuning for the primary (external) resonance as well as the internal resonances, and that this was a good description of the experimental observations. A simulation of the model supported this conclusion. In the future, we will use this model to design a nonlinear observer and a vibration control law which will enable us to improve the performance of the gyroscope.

References

[1] J.S. Burdess. The dynamics of a thin piezoelectric cylinder gyroscope. *Proc. Inst. Mech. Eng.*, 200:271-280, 1986.

[2] C.H.J. Fox. Vibrating gyroscopic sensors. In *DGON Symposium on Gyro Tecnology*, Stuttgart, FRG, 1984.

[3] C.H.J. Fox. Vibrating Cylinder Rate Gyro, Theory of Operation and Error Analysis. In *DGON Symposium on Gyro Technology*, Stuttgart, FRG, 1988.

[4] B. Kanani and J.S. Burdess. The piezoelectric cylinder gyroscope. *In Proc. of the IMech*, pages 61-66, September 1990, Cambridge.

[5] R.M. Langdon. The vibrating cylinder gyro. *The Marconi Review*, pages 231-249, 1982.

[6] C. Langmaid. Vibrating structure gyroscopes. *Sensor Review*, 16(1):14-17, 1996.

[7] A. Leissa. *Vibration of shells*. Acoustical Society of America, 1993.

[8] P. W. Loveday. A Coupled Electromechanical Model of an Imperfect Piezoelectric Vibrating Cylinder Gyroscope. *Journal of Intelligent Material, Systems and Structures*, 7:44-53, January 1996.

[9] A.H. Nayfeh and D.T. Mook. *Nonlinear Oscillations*, Wiley-Interscience, 1979.

[10] M. Shatalov, J. du Pre Le Roux and F. Koch. Estimation of vibratory gyroscope paramters with data derived from the vibrating element. In *DGON Symposium on Gyro Technology*, Stuttgart, FRG, 1996.

# Measurement of displacements using nonlinear systems

ALMANTAS MOZURAS
Res. Lab. Akustika, Muitines 13-57, 2006 Vilnius, Lithuania, e-mail: alma@ktl.mii.lt

Linear properties of primary information converters are mostly used in conventional measurement devices. However, purely linear converting systems are not available. The use of the linear features in measurement process finally causes the drawbacks, e.g., systematic error due to nonlinear distortions, low information signal-to-noise ratio, the necessity to evaluate a great number of the *a priori* parameters of the transducer in order to receive an absolute result, and low thermal stability because every *a priori* parameter itself has a temperature dependence. To exclude these drawbacks a method has been developed employing nonlinear systems in the base of displacements' measurement.

Suppose we have a contactless converter with nonlinear monotonous characteristic $f(x)$, where x is the distance between the object and the converter head. Let us make the latter to vibrate harmonically in the direction perpendicular to the object surface with the amplitude x_0 and the cyclic frequency ω.
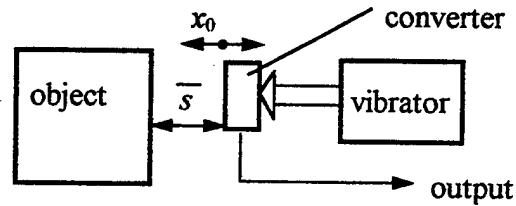
Thus, $x = \bar{s} + x_0 \cos\omega t$, where $\bar{s}$ is the average distance. Our task is to determine $\bar{s}$ and its variation (displacement). During the measurement process the output signal of the transducer is registered. For extracting $\bar{s}$, we differentiate the output signal with respect to time and obtain the coded signal. The information about quantity $\bar{s}$ lies in the characteristic time intervals Δt and T between the extrema of the coded signal ψ.
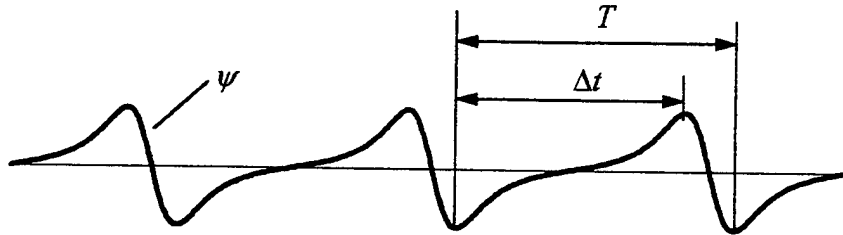
The coded signal may be written as

$$\psi = \frac{df(x)}{dx}\frac{dx}{dt} \, . \tag{1}$$

From the condition $d\psi/dt = 0$ we find the time instants of the signal extrema. After simple transformations, the equation for finding the extrema instants takes the form

$$\frac{d}{dx}\ln\left|df(x)/dx\right| = -\frac{x''}{(x')^2} \quad \text{or} \quad \frac{d}{dx}\ln\left|df(x)/dx\right| = \frac{1}{(x-s)}\cot^2\varphi^* \, , \tag{2}$$

where x' and x'' are the first and the second derivatives with respect to time, respectively, φ^* is the phase of the coded signal ψ extrema. Note that phase φ^* is related to the typical time intervals Δt and T:

$$\varphi^* = \varphi^*(\Delta t, T) . \tag{3}$$

This relation is found by considering the symmetry properties of the signal ψ for each particular $f(x)$. Since Equation (2) relates $\bar{s}$ and φ^*, the coded signal ψ carries the information about quantity $\bar{s}$. During measurement we measure the characteristic time intervals and restore quantity $\bar{s}$ from them applying the Equations (2) and (3).

When using the electrostatic transducer as a converting physical system, the output signal is the charge accumulated on the measuring electrode $Q(x)=E\varepsilon_a S_a/x$, where E, ε_a, and S_a are the electromotive force, absolute dielectric permittivity of the environment, and the area of the electrode, respectively. In the case of the electretic converter the output signal is the charge density induced on the object surface by electret $\sigma_{ind}(x)=-\sigma L_e/\varepsilon /(L_e/\varepsilon + x)$, where σ, L_e, and ε are the surface charge density, thickness, and permittivity of the electret, respectively. In the both cases the coded signal is $\psi = Bx_0^{-1}\sin \omega t(S+\cos \omega t)^{-2}$, where quantities S and B for the electretic transducer are equal to:

$$S = (\bar{s}+L/\varepsilon)/x_0,$$
$$B = -KRLS_e \sigma \omega /\varepsilon, \tag{4}$$

and for the electrostatic transducer:

$$S = \bar{s}/x_0,$$
$$B = KRES_e \omega \varepsilon_a . \tag{5}$$

(K and R are amplification factor and load resistance, $S>1$.) The average distance is calculated using the formula:

$$S = \frac{\cos^2 \varphi^* - 2}{\cos \varphi^*}, \tag{6}$$

where $\cos \varphi^* = \cos(\pi \Delta t / T)$.

The proposed method allows one to exclude the systematic error due to nonlinear distortions and to increase the information signal-to-noise ratio.

The accuracy of the measurement of displacement $\Delta \bar{s}$ is influenced neither by the *a priori* parameters E, ε_a, S_e, L_e, ε, σ, K, and R included in the output signal expressions. Since these parameters are temperature-dependent, absence of their influence contributes to the thermal stability (only the parameter x_0 has an effect).

References

[1] Mozuras, A. and Ragulskis, K., 'A method for measuring displacements', *Certif. of Invent. No. 1634986*, Moscow, 1991.

[2] Mozuras, A., 'Increasing sensitivity and accuracy in measuring amplitudes of mechanical vibrations with velocity sensors', *Vibration Engineering 3*, New York - London, 1989, 309-318.

[3] Mozuras, A., 'Theoretical and experimental research of nonlinear physical systems use in the base of displacements measurement', *IEICE Transactions on Fundamentals of Electronics, Communications and Computer Sciences E76A (8)*, 1993, 1343-1349.

[4] Mozuras, A., 'Inertialess nonlinear systems for information coding', *Nonlinear Dynamics*, 1997 (accepted for publication).

Electromagnetic Levitation Modeling and Control

Bogdan O. Ciocirlan, Dan B. Marghitu, David G. Beale and Ruel A. Overfelt

Department of Mechanical Engineering,
Auburn University, Auburn, Alabama 36849

When a piece of metal is placed above a coil carrying a high frequency current, the induced eddy currents in the metal produce a Lorenz force which can support it against gravity. At the same time the heat produced by Joule dissipation can melt the metal. This is the process of "levitation melting", which is well-establish technique in fundamental work in physical and chemical metallurgy. The great advantage of the electromagnetic levitation melting method is the containerless processing of the melt. This is an important condition when a pure homogenous melt is required.

The greatest difficulty facing levitation melting is the maintenance of stability of the suspended droplet. The possible instabilities are either global or local to the surface. The global instabilities, which cause the metal to move as a whole, must be prevented by a carefully choosing the external current distribution that generates the supporting field so that the droplet is close to a local field minimum. The local instabilities are due to the interaction of the electromagnetic forces with the molten metal producing several effects such as changing of the shape of the surface, surface oscillations or stirring of the material. In most cases a control scheme to assure the stability of the levitated droplet is to be developed. For simulations, a model of electromagnetic levitation is also required.

Our levitation setup was designed by Space Power Institute at Auburn University for purposes such as containerless melting or surface tension measurements in microgravity environment. The instrument is composed of a vacuum chamber enclosing the excitation coil that levitates and heats various small pieces of metal, and several monitoring and measurement systems.

The first step in out work was to reveal the determinism in the underlying dynamics of the molten droplet placed in a high-frequency magnetic field of the levitation coil. We suspended a nickel sample during a parabola performed by the aircraft flowing the levitation instrument, thus simulating

the microgravity conditions. Several nonlinear dynamics tools were employed to analyze the output signal of a top position sensor. The method of delays was first used in order to reconstruct the state space in which the state trajectories can be drawn. The saturation method was then applied in order to determine the attractor dimension and the embedding dimension. The largest Lyapunov exponent was also computed whose sign is a strong criterion to distinguish the chaotic from nonchaotic (periodic and quasiperiodic) motion. Finally, the surrogate data test was performed in order to ascertain the outcomes of the analysis. It was mainly found that the underlying dynamics of the levitated droplet is in fact chaos.

Considering the previous result of the nonlinear dynamics analysis and our observations over the experiments, a control scheme was designed. Since a comprehensive model of the electromagnetic levitation that have to couple the analysis of all phenomena such as the electromagnetic field diffusion, the changing of the shape of the droplet or internal the fluid flow is difficult to be developed or would be computationally very slow comparing to the high speed time varying levitation process, a fuzzy logic control scheme was considered. In order to offer an intuitive image of how such a control scheme works the fuzzy login control of a magnetic particle using DC electromagnets is presented. A pair of horizontal electromagnets were added to the typical magnetic levitation system in order to handle the unexpected horizontal displacements of the particle. To control the vertical motion (i.e. change the vertical equilibrium position), the top electromagnet is commanded so that the net force between the magnetic force generated by the current flowing into the coil of the electromagnet and the gravitational force induce an up and down motion of the particle to the desired position. The pair of horizontal electromagnets are used to bring the particle from its initial horizontal location to a position situated on the vertical symmetry axis of the system. A fuzzy logic control strategy was employed to control the motion of the particle and to keep it stable at the desired position. The mathematical model of the system was also developed and the state-space equations were derived. The behavior of the controller was tested for various initial positions. It was found that for all cases the controlled system behaves in a similar way, the particle being rapidly positioned.

Modal analysis of jointed plates of composites

Michele Lacagnina, Francesco Petrone and Rosario Sinatra

Istituto di Macchine
Facoltà d'Ingegneria, Università di Catania
Viale A. Doria 6, 95125 Catania, Italy

mlacagnina@im.ing.unict.it   fpetrone@im.ing.unict.it   rsinatra@im.ing.unict.it

1. INTRODUCTION

The spread of composites in the various applications draws more and more attention to problems relating to the correct analytical simulation of structural elements which, due to their characteristics, are not classifiable as homogenous and isotropic.

The study of the dynamic behaviour of composites deserves special attention when vibration and noise arise in use. Various studies have been carried out on the subject and software codes using more or less approximate methods provide results which are quite reliable. Yet it still remains difficult to simulate the behaviour of jointed elements, both because of the various building methods and because it is not possible to know the theoretical modelling underpinning the software. While several authors have verified good correspondence between the theoretical and experimental results in flat plates, little is known on the correspondence of the analytical simulation of joints tested under dynamic conditions.

The aim of this paper is to test the correspondence of the results obtainable through modal analysis on joined panels using a widely-spread calculation code together with those experimentally obtained. The simulation of the joint was therefore improved to obtain results as close to reality as possible.

2. EXPERIMENTAL

2.1 Description of the materials used and of the joints.

The experimental tests on plates of composites were carried out using 5 different kinds of composites: two with glass fibre barks and cores respectively 1/2'' and 1'' thick, and one with aluminium barks and a core 1'' thick.

The panels share the characteristics of a similar kind core made of an aluminium hexagonal honeycomb cell. In the panels with aluminium bark, the joints were made using a staff bead system and gluing aluminium angulars (readily available) with an L profile and a 30mm inner edge and angulars with an L profile 30x60mm on the outer edge.

In the glass fibre plates a 50mm wide 'prepreg' bark was glued to both edges using a phenolic glue; the thickness of the glue was checked using a steel wire whose diameter was 0.2mm.

Tests were carried out on plates which were moulded in different ways: L, Z and Omega so as to have a different number of joints (1,2,4 in the various shapes).

Shape and dimensions are identical both in the aluminium bark panels and in the glass fibre bark panels. The L shape is made of 2 panels whose dimensions are 800x600 and 600x400 joined together. The Z shape is made of 3 panels two of which are 800x600 and one is 600x400 with two joints; the omega shape is made of 5 panels, 3 of which are 800x600 and one is 600x400 with 4 joints.

2.2 The measurement chain.

Picture 1 shows the measurement chain used. Excitation on the structure is performed using an 8202 Bruel 8 Kjaer hammer with a dynametric head on various points (j) and the vibration in the reference knots is recorded (I); the signals coming from both the hammer and the accelerometer suitably amplified, filtered by the switchboard and run by D-Tac software; then the modal analysis is carried out using a Cada-PC software.

In order to avoid recording double moding and placing the accelerometer on a nodal point two acce-rometers were used.

The experimental results were confirmed by the CADA PC checking process, in particular by MAC (Modal Assurance Criterion) which evaluates the geometrical correlation between two modal deformations; MPC (Modal Phase Collinearity & Scatter) which shows the relationship between the real and imaginary parts of the modal deformation; another indicator of the complexity of modal deformations is Phase Scatter which represents the statistical variation of the phase angle in each eigenvector of average value. In the real mode shapes it should be close to 0%.

The kind of constraint used in the tests was free-free as it is the easiest to carry out.the suspension system of the structure was built using elastic elements. The dimensions of the panels were chosen so that the rigid mode frequencies are low enough not to interfere with its mode shapes.

In every case the FRF was recorded in a single test discarding the signals that were unclear.

3. NUMERICAL SIMULATION

NASTRAN, a widespread finite element code, was used for the FEM simulation; the material was patterned as 2D ortothrope composite whose core is simulated as a homogenous material with a low mass density. In the finite element code analysis, the core simulation with two different moduli of tangential elasticity was fundamental to obtain the exact correspondence of mode shapes at various frequencies; contrary to what literature shows in studies on static analysis on sandwich panels whose cores are simulated with an average G, in the present study the core anisotropy was not neglected to confirm the analytical mode shapes.

Simulation was carried out taking into consideration the outer banks made of a single layer 0.5mm thick having equal modulus of elasticity in the longitudinal and transverse directions thus avoiding errors in the evaluation of the E-value transversally to the fibres in the single layer. The density of the banks is 1.700kg/m^3. The L-shaped plates are patterned through a mesh 25mm side, the joint was simulated using a composite whose bank thickness was equal to the sum of the real bank and the angular using a 25mm side mesh.

The Z-shaped plates are patterned through a mesh 30mm side, the joint was simulated using a composite whose bank thickness was equal to the sum of the real bank and the angular using a 25x30mm mesh.

The omega-shaped plates are patterned using a 40mm square mesh, the joint was simulated through a composite whose bank thickness was equal to the sum of the actual bank and that of the angular using a 25x40mm mesh.

4. RESULTS

The comparison between the values of natural frequencies obtained with the FEM model and those obtained with experimental analysis for the aluminium bank composite the L-shaped structure the difference is just over 4%; in the z-shaped structure it is just over 5%; in the omega shape the average difference is just over 5%.The comparison between the natural frequency values obtained with the FEM model and those obtained through experimental analysis for the glass fibre composite of 1/2'' thickness in the L shaped structure the difference is just over 1.5%; in the Z shaped one, the average difference is just over 2%; in the omega shaped structure the average difference is just over 3%.

The comparison between the natural frequency values obtained with the FEM model and those obtained through experimental analysis for the glass fibre composite of 1'' thickness in the L shaped structure the difference is just over 2%; in the Z shaped one the difference is just below 2%; in the omega shaped one the results obtained show 2 very close/similar modes (12.2 Hz and 16.3 Hz) with similar vibrating modes. In the same frequency interval, we do not obtain the same experimental results. Moreover, by excluding the 15.2 Hz analytical mode we obtain a good correspondence between analytical and experimental values; therefore it is obvious to think that the 15.2 Hz analytical mode is not real. The average difference is just over 7%.

Tuesday, July 28
1530-1700
Session 10B.

Perturbation Analysis of Bifurcations in a Model of Phase Transitions with Order Parameter

J. P. Cusumano and J. Sikora

Department of Engineering Science & Mechanics

Penn State University

University Park, PA 16802

INTRODUCTION: Spatial distributions of phases have been observed experimentally in materials that undergo stress-induced solid-solid phase transformations. The main feature of the phenomenon is that two or more phases of material may co-exist separated by well defined phase boundaries. Known examples of this kind of material are shape memory alloys. Recently, a theory has been proposed for thermally and stress induced solid-solid phase transitions, (Fried and Gurtin 1993, Fried and Gurtin 1994). In this theory, the material phase is characterized by an order parameter, and phase boundaries are identified with thin layers within which the order parameter suffers large variations. In this paper we investigate a specific one dimensional version of the model of Fried and Gurtin. In the investigations, we limit ourselves to the isothermal process of stress-induced phase transformations. Using a phase plane analysis, we show that such a model is capable of supporting many spatially periodic steady state solutions, each with a multiplicity of phase boundaries. We also perform a bifurcation analysis on the steady states using a perturbation technique, which we use to shed some light on the fundamental continuum-mechanical phenomena involved. The perturbation results are compared to the numerical solutions of the governing partial differential equations.

DESCRIPTION OF THE MODEL: A simple, one-dimensional special case of the theory of Fried and Gurtin (1994) is examined in this paper. Consider an elastic bar, which occupies the interval $[0, 1]$ in the reference configuration. The longitudinal motion of the bar is described by a mapping $y(x, t) = 1 + u(x, t)$, where $u(x, t)$ is the displacement and $y(x, t)$ is the placement. Taking $e(x, t) = u_x(x, t)$ and $s(x, t)$ to be the strain and stress, respectively, and letting the material phase be represented by the order parameter $\phi(x, t)$, the theory can be formulated by fully specified by prescribing a so-called kinetic coefficient and a free energy density. The kinetic coefficient, which in general is a positive-definite function of $(e, \phi, \phi_x, \dot{\phi})$, here is assumed to be a positive constant, and is denoted by β. Writing $p(x, t) = \phi_x(x, t)$, the free energy is postulated in the following form:

$$\Psi(e, \phi, p) = \frac{1}{2}\mu(e - k\phi)^2 + \nu G(\phi) + \frac{1}{2}\gamma^2 p^2 \tag{1}$$

The first term in equation (1) represents the strain energy, which is a convex function with respect to both independent variables. The second term in equation (1) is the exchange energy: we assume that

$$G(\phi) = \frac{1}{2}\phi^2(\phi - 1)^2 \ . \tag{2}$$

The function G has two minima corresponding to the energetically preferred states of $\phi = 0$ and $\phi = 1$, and a local maximum at $\phi = \frac{1}{2}$. The third term in equation (1) represents the energy of an interface.

Based on the above free energy, the displacement u and the order parameter ϕ can be shown to satisfy the following system of equations:

$$
\begin{aligned}
u_{tt} &= \mu\left(u_x - k\phi\right)_x \\
\beta\phi_t &= \gamma^2\phi_{xx} + k\mu\left(u_x - k\phi\right) - \nu g(\phi)
\end{aligned}
\tag{3}
$$

where μ, β, γ, and ν are material parameters, $k = \sqrt{\frac{1}{2}}$ is a constant, and where $g(\phi) = G'(\phi)$. The first of equations (3) is a hyperbolic wave equation representing the balance of linear momentum in the bar. The second equation is a nonlinear reaction-diffusion equation governing the time evolution of the order parameter. The two equations are coupled through the strain energy terms.

REFERENCES

[1] E. Fried and M.E. Gurtin, *Continuum theory of thermally induced phase transitions based on an order parameter*, Physica D, 68 (1993), 326-343.

[2] E. Fried and M.E. Gurtin, *Dynamic solid-solid transitions with phase characterized by an order parameter*, Physica D, 72 (1994), 287-308.

Implementation of Genetic Algorithm and Simulated Annealing in Layout Optimization of Space Trusses

M.H.Kadivar[1], M.R.Pourghassem[2], K.Samani[3] and F.Daneshmand[4]

1 Associate Professor, Shiraz University, Shiraz, Iran
2,3,4 Graduate Student, Shiraz University, Shiraz, Iran

1. Introduction

The topic of global optimization is an area of active research where new algorithms are emerging and old algorithms are constantly being improved[1-3]. A methodical way of dealing with multiple minima for discrete optimization problems is the use of either random search techniques that would sample the design space for the global minimum or to employ enumerative type algorithms. In either case, the efficiency of the solution process deteriorates dramatically as the number of the variables is increased.

Two algorithms, Genetic Algorithm (GA) and Simulated Annealing (SA) have emerged more recently as tools ideally suited for optimization problems where a global minimum is sought. In addition to being able to locate near global solutions, these two algorithms are also powerful tools for problems with discrete-valued design variables. Both algorithms rely on naturally observed phenomena and implementation calls for the use of random selection process which is guided by probabilistic decision. Application of these algorithms to structural design will be demonstrated for optimum topology of a truss in this paper and the results obtained from these algorithms will be compared.

2. Problem Definition

In this paper, shape optimization via GA is applied to a three dimensional structure. Possible node positions are predefined and the objective is to connect the nodes in the way that the weight of the obtained truss becomes minimum, satisfying certain constraints. The structure consists of 19 nodes and 48 elements, hence the design space contains 248 or 2.8E+14 points. The ground structure is such defined that only the elements that are on the surface of the dome are allowed. In other words, each node is restricted to be connected only to its adjacent ones. The ground structure is shown in Fig. 1. To represent the structures in string form, a 48-bit binary string is used. The external load is a concentrated one applied at the top node. The objective function is the weight of the truss. The constraints are corresponding to the stresses in members and the stability conditions. So, we can formulate the optimization problem as follows:

Minimize   W
Subject to

$$\sigma_i - \sigma_{ta} < 0 \quad \text{Element in tension}$$

$$\sigma_i - \sigma_{ca} < 0 \quad \text{Element in compression}$$

Where W is the weight of the structure

3. Results

1. In both algorithms the interfacing of problem-specific design constraints and data is easily carried out involving the writing of an penalized objective function. Constraints violation are considered by changing the cross sectional areas, proportion to violation ratio for kinematically stable structures, and by assigning a low value of fitness for unstable ones.

2. In GA, with different runs, it is seen that larger populations can reach the optimum faster (i.e. with treating fewer strings), although at long runs different runs with various population size may reach the same optimum. The obtained results could be largely affected by the selection of genetic algorithm parameters. So, these parameters should be appropriately selected.

3. SA algorithm is sensitive to cooling schedule.

4. Although both algorithms have reached the same result but the implementation of genetic algorithm seems to be easier with less computational effort.

Finally, genetic algorithm and simulated annealing are efficient and simple optimization methods that are specially suitable for discrete and nonconvex problems.

4. References

1. Hansen, E., "Global optimization using interval analysis, the multidimensional case," Num. Math., 34, pp. 247-270, 1980.

2. Kao, J.J., Brill, E.D., Pfeffer, J.T.,"Generation of alternative optima for nonlinear programming problems," Eng. Opt., pp. 233-251, 1990.

3. Ge., R.,"Finding more and more solutions of a system of nonlinear equations," Appl. Math. Computation, 36, pp. 15-30, 1990. 4. Goldberg, D. E.,"Genetic algorithm in search, optimization & machine learning", New York: Adisson-Wesley Publishing Company, Inc. 1989.

4. Kirkpatrick, S., et al, "Optimization by Simulated Annealing,"science, 220(4598), pp. 671-680, 1983.
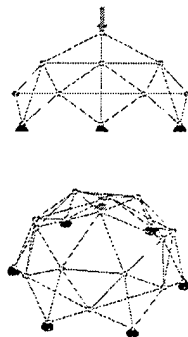
Fig.1- 3-D Space Structure

Modeling and Analysis of Panel Rattle Noise in Automobiles

J. Qiu and Z.C. Feng
Department of Mechanical Engineering
Massachusetts Institute of Technology
77 Massachusetts Avenue
Cambridge, MA 02139

January 13, 1998

Rattles generated by impact of two parts are associated with high peaks of radiated sound pressure waves. The impact process is highly nonlinear and the associated dynamics is extremely complicated. We have conducted experimental study and theoretical analysis of the nonlinear dynamics involving panel impact in order to predict the noise radiation by impact.

Experimental results. Experiments are conducted on a plate which is clamped on two opposite edges and free on the other two edges. The plate is under sinusoidal base excitation at frequencies near the natural frequency of the first mode. A bolt placed beneath the center of the plate serves as the striker. When plate vibration amplitude exceeds the gap between the plate and the striker, impact takes place.

Measurement of the plate vibration is made through accelerometers mounted on the plate. Sound pressure levels are also recorded by a microphone located 50 cm above the plate surface. Tests are conducted for a range of forcing amplitudes. In a typical test, the forcing amplitude is held fixed while the forcing frequency is swept upwards or downwards through the resonance frequency. The plate response show hysteresis for these kinds of frequency sweeps.

For an upward frequency sweep, the impacts occur when the forcing frequency is sufficiently below the natural frequency for the first mode. As the forcing frequency is slowly raised, contact between the plate and the striker takes place. The initial contacts have relatively small velocity hence the radiated sound pressure is low. These contacts are intermittent in nature characterized by repetitive contacts separated by no contact for several forcing cycles. As frequency is further raised, the intermittant impacts gradually changes into more contant impacts. The plate strikes the bolt at a higher velocity and higher

radiated sound pressure is recorded.

Multiple impacts within one forcing cycle have also been recorded. This phenomenon occurs when forcing frequency is above the natural frequency. It seems that the higher vibrational modes of the plate play an essential role for this phenomenon. Hence multiple degree-of-freedom models are needed to model the process.

Modeling. There are existing theoretical models for the impact process. Most models are based on a single degree-of-freedom system. We have carried out analysis of the single degree-of-freedom model to understand the bifurcation sequences observed in the experiments. We partition the space of forcing amplitude and frequency into bifurcation sets; inside each of these sets, a particular dynamic phenomenon is observed. The qualitative partition of the parameter space allows us to obtain analytic predictions of the impact velocity which is most important in noise prediction.

Modeling General, Unsteady, Nonlinear, Aeroelastic Behavior

by
S. Preidikman and D. Mook
Department of Engineering Science and Mechanics
Virginia Polytechnic Institute and State University, Blacksburg, VA 24061

Modeling unsteady aeroelastic behavior is a topic of long-standing interest and importance. The approach followed in this study is to treat the flowing air, the structure, and the devices of the control system as elements of a single dynamical system; and to integrate all of the governing equations numerically, simultaneously, and interactively in the time domain. In contrast with solutions performed in the frequency domain, time-marching schemes can model sub- as well as super-critical nonlinear, aeroelastic behavior as long as the effective angles of attack are not large enough to cause stall. As a consequence, these schemes can be a very effective tool for the design of flutter-suppressing control systems. Because the equations are solved numerically, structural nonlinearities do not present a problem; the present aerodynamic model is inherently nonlinear.

There is a fundamental complication with the time-domain approach: *to predict the aerodynamic loads one must know the motion of the structure, and to predict the motion of the structure one must know the aerodynamic loads.* To overcome this complication, an iterative scheme was developed. The procedure is based on Hamming's fourth-order predictor-corrector method. Hamming's method was extended and adapted to the present problem to avoid evaluating the aerodynamic loads at fractional time steps and to accommodate aerodynamic loads that are proportional to the acceleration (the so called added-mass effect in hydrodynamics). It turns out that the present numerical scheme, with some further adaptations and innovations, is also ideally suited for ship dynamics problems.

The general unsteady vortex-lattice method, a generalization of the familiar vortex-lattice method for steady, incompressible flows, is used to predict the aerodynamic loads. The technique accounts for the aerodynamic nonlinearities associated with angles of attack, static deformation, vorticity-dominated flow, and unsteady behavior; and is valid for arbitrary angles of attack, planforms, and motions as long as stall and vortex-bursting do not occur. The distribution of vorticity in and the shape of the wakes are determined as part of the solution so the history of the motion is stored in the wakes.

As an example, we consider the flutter of a wing. The entire wing is modeled as a cantilever beam with an elastic support to capture the influence of the fuselage. The elastic, linear, and structurally undamped wing is free to bend about two axes and twist. The mass center of each section does not coincide with the elastic axis; thus, there is dynamic coupling between flexural and torsional motions. The equations of motion are discretized by the finite element method.

The deformation of the wing is represented as an expansion in terms of the mode shapes. The time-dependent coefficients are the generalized coordinates of the motion. The modes may be found by experiments, analysis, energy methods, and finite-element techniques. For complicated geometries and/or anisotropic materials, it is advantageous to use a finite-element element method. The use of composite materials has created numerous opportunities in the field of aeroelastic tailoring. To transfer the aerodynamic loads from the aerodynamic grid to the finite-element mesh, we have developed a method based on the concept that the virtual work done by the elastic and aerodynamic loads be equal

In the presentation, we discuss some calculated responses to initial conditions at various subsonic airspeeds and angles of attack. The examples include sub- and super-critical responses as well as true limit cycles (i.e., motions that are independent of the initial conditions) in between. The calculated results show the frequencies of the first and fourth modes merging near the onset of unstable behavior.

Control of Rolling in Ships by Means of Active Fins Governed by a Neural-Network Controller

D. Liut, D. Mook, H. VanLandingham and A. Nayfeh
Department of Engineering Science and Mechanics
Virginia Polytechnic Institute and State University
Blacksburg, VA 24061 USA

A method to reduce the rolling motion of a ship in a seaway by means of actively controlled fins is described. The method is based on a multidisciplinary simulation: 1) the motion of the ship in a seaway is simulated by a numerical model called *LAMP* (Large-Amplitude-Motion Program), which is based on a source-panel method to model the flowfield around the ship, 2) the forces on the fins are simulated by a general unsteady vortex-lattice method, and 3) the commands to the fins are generated by a neural network. The ship is considered to be a rigid body and the complete equations of motion are integrated numerically in the time domain so that the motion of the ship and the complete flowfield are calculated simultaneously and interactively. The program to predict the forces generated by the sea on the ship and the one to predict forces on the fins, originally quite different, have been efficiently implemented together. The motion of the ship is taken into account when the flowfield around, and the loads on, the fins are calculated. But the disturbance in the flowfield around the ship generated by the fins is ignored when the loads generated on the ship by the sea are calculated. The neural network controlling the fins is progressively trained, by means of a new moment-matching strategy. The results show substantial reductions in roll.

Wednesday, July 29
0800-0930
Session 11.

Parametric Identification of an Experimental Magneto-Elastic Oscillator

B. F. FEENY

Michigan State University
Department of Mechanical Engineering
East Lansing, MI 48824 USA

C.-M. YUAN

Taoyuan Institute
Department of Mechanical Engineering
Taoyuan, Taiwan R. O. C.

J. P. CUSUMANO

Pennsylvania State University
Department of Engineering Science and Mechanics
State College, PA 16801 USA

We applied the harmonic-balance parametric-identification scheme (Yasuda *et al.* 1988) to unstable periodic orbits extracted from chaotic data of an experimental periodically driven magneto-mechanical oscillator with a two-well potential.

Unstable periodic orbits can be extracted from chaotic data from either discrete or continuous-time systems. These orbits have been used in system identification, usually in the Poincaré section (Hammel and Heagy, 1992; Kesaraju and Noah, 1994; Van de Wouw *et al.*,1995). The harmonic balance method has been used with the unstable periodic orbits in a variety of numerical test cases, including autonomous and non-autonomous oscillators (Yuan and Feeny, 1998).

The experiment consisted of a stiffened beam buckled by two magnets. Additional rigidity was included to make the system behave as a single degree of freedom (Cusumano and Kimble, 1994). The uncovered portion of the beam near the clamped end acted as an elastic hinge from which the position of the beam was measured by strain gauges. Two rare-earth permanent magnets were placed on the base of the frame holding the beam to create the two-well potential. The frame was then fixed through a rigid mount to an electromagnetic shaker. A periodic driving signal was fed through a power amplifier to the shaker to provide the external forcing function, by which the chaotic data were generated. The experimental chaotic set was reconstructed by the method of delays, and the unstable periodic orbits were extracted.

The identification process involves the choice of a mathematical model of the form

$$\ddot{x} + \alpha \dot{x} + \sum_{i=1}^{p} \beta_i f_i(x) = a \cos \Omega t,$$

where the parameters are unknown. We chose two models for the nonlinear stiffness in the differential equation of motion. We first chose a polynomial to fit the characteristics of the nonlinear function, since we know that the magnetic and elastic forces are smooth. The second model we implemented was an interpolation model (Yasuda and Kawamura, 1989).

The identification results for the polynomial model were evaluated by consistency from various combinations of periodic-orbit data. The interpolation-model force characteristic is consistent for a

range of about 10 to 18 interpolation functions. A visual comparison between the polynomial and interpolation models suggest a qualitative fit of the actual physical force characteristic.

We also evaluated the identified model by comparing numerical simulations with the experiment, and also by comparing the properties of the models linearized about the stable equilibria with small-motion properties of the experiment. The interpolation model seemed to accomodate finer qualitative details in the phase portraits, an also produced better estimations of the equilibrium locations and natural frequencies near each equilibrium.

References

Cusumano, J. P., and Kimble, B. W., 1994, "Experimental observation of basins of attraction and homoclinic bifurcation in a magneto-mechanical oscillator," *Nonlinearity and Chaos in Engineering Dynamics*, Thompson, J. M. T., and Bishop, S. R., eds., Wiley, Chichester, 71-84.

Hammel, S., and Heagy, J., 1992, "Chaotic system identification using linked periodic orbits," presented at the *SIAM Conference on Applications of Dynamics Systems*, Snowbird, Utah, October 15-19.

Kesaraju, R. V., and Noah, S. T., 1994, "Characterization and detection of parameter variations of nonlinear mechanical systems," *Nonlinear Dynamics* 6, 433-457.

Van de Wouw, N., Verbeek, G., and Van Campen, D. H., 1995, "Nonlinear parametric identification using chaotic data," *Journal of Vibration and Control* 1, 291-305.

Yasuda, K., Kawamura, S., and Watanabe, K., 1988, "Identification of nonlinear multi-degree-of-freedom systems (presentation of an identification technique)," *JSME International Journal, Series III*, **31**, 8-14.

Yasuda, K., and Kawamura, S., 1989, "A nonparametric identification technique for nonlinear vibratory systems," *JSME International Journal, Series III*, **32** (3) 365-372.

Yuan, C.-M., and Feeny, B. F., 1998, "Parametric identification of chaotic systems," accepted by the *Journal of Vibration and Control*.

Identification of Viscoelastic Properties of Foam Used in Car Seats

S. White, S.K.Kim, A. K. Bajaj, P. Davies
School of Mechanical Engineering, Purdue University, West Lafayette, IN 47907-1288.
and D.K. Showers
Johnson Controls, Corporate Research, Milwaukee, Wisconsin.

Quantifying vibration comfort of passengers in car seats is a complex problem, involving understanding how people respond both physically and subjectively to vibration. The investigations described in the presentation focus on a component of the physical modeling, the modeling of the seat foam behavior. The person in the seat is a complicated dynamical system involving nonlinearities due to geometry (posture) and material properties of both the human and the seat. Two approaches to modeling the system are finite element modeling and simplified multiple mass, spring and damper modeling [1]. The large computational time required to run full finite element model simulations of the system makes it attractive to investigate the simplified modeling approach. Both modeling approaches require estimates of material properties. This presention will be focused on an investigation into the seat foam properties and its modeling by using spring-mass-damper type models.

Four inch foam blocks cut from car seats were used in the investigation. A fixture was fabricated so that the foam was sandwiched between a base plate and a mass that could be varied to induce different compression ratios. Both the static and dynamic stiffnesses of the foam vary nonlinearly as the foam passes through different behavior regimes at different levels of compression. Under the assumptions of unidirectional strain and negligible inertia for the viscoelastic foam material, the behavior of the foam block plus mass may be described by a second order integro differential equation with a nonlinear (polynomial type) stiffness and a linear relaxation term which is the convolution of the response with a relaxation kernal. Different models of the relaxation kernel appear in the literature, but one commonly used is a model in the form of a sum of exponentials [2]; this was used in the investigations described here. The model also includes a linear viscous dissipation term. Both this term and the relaxation term contribute to energy dissipation in the system. Three issues were investigated: does the relaxation term improve the model, what is the appropriate form of the nonlinear stiffness term, and how do these terms change at different compression ratios?

The method of harmonic balance was used to predict the response of the model to harmonic base excitation and these predictions were compared with measured responses. System identification was performed in two stages. The parameters in the linear relaxation term in the analytical model were estimated by fitting a complex exponential model to the measured response at low excitation levels. The nonlinear terms were estimated from responses at higher excitation levels using a system identification method based on harmonic balance.

The results indicate that nonlinear behavior is of high order with both softening and hardening characteristics becoming apparent as the excitation level changes. The stiffness characteristics change as a function of compression ratio, becoming larger as the compression ratio increases. The role of the relaxation terms is difficult to quantify,

though this may be, in part, due to the difficulties of accurately identifying these terms. The benefits and limitations of this approach to modeling foam will be discussed in the context of occupant in car seat vibration modeling.

[1] Nishiyama, Shuji, "Development of simulation system on vehicle-occupant dynamic interaction (1st Report, Theoretical analysis and system verification)", Transactions of the Japan Society of Mechanical Engineers, Part C v 59 n 568, Dec 1993. p 3613-3621.

[2] Enelund, M., Fenander, A., and Olsson, P. "Fractional integral formulation of Constitutive equations of viscoelasticity". AIAA Journal, Vol 35, No.8, August 1997, pp.1356-1362.

Tracking Slowly-Varying Hidden Variables Using Phase Space Reconstruction

J. P. Cusumano, D. Chelidze, and A. Chatterjee
Department of Engineering Science & Mechanics
Penn State University
University Park, PA 16802

INTRODUCTION: Current efforts to develop machinery condition monitoring and failure prediction technology are hampered by the fact that most damage processes are hidden from the observer, especially during the early stages. In this paper, a model based method that can be used to experimentally track damage evolution is described. Our approach treats damage as evolving in a hierarchical dynamical system consisting of a "fast time" directly observable subsystem coupled to a "slow time" subsystem which can be thought of as a hidden rate law governing the damage evolution. The method exploits the time scale separation between fast dynamic variables and slowly drifting parameters. Locally linear tracking models are constructed using data sampled on a fast time scale, employing delay coordinate embedding. The short time prediction error of the reference tracking models are used as the parameter drift observer. The method is successfully applied to a forced mechanical oscillator with a two-well potential. A small perturbation in one of the potential energy wells is provided by a battery-powered electromagnet. In this context, the battery state is taken to be "hidden," and the system "fails" as the battery runs down. We demonstrate that the slow-time battery discharge curve can be tracked quite well using only scalar strain time series from the fast-time mechanical subsystem.

TRACKING ALGORITHM: Multiple records of scalar time series are collected, with the time between records being long. Each record consists of data collected in fast time. The scalar time series is used to reconstruct the state space with an appropriate dimension (say n) for the system. The reconstructed vectors $\mathbf{x} \in \mathbb{R}^n$ are modeled by an as yet undetermined k-step map of the form

$$\mathbf{x}_{l+k} = \mathbf{P}^k(\mathbf{x}_l; \boldsymbol{\phi}). \tag{1}$$

It is assumed that the "parameter" $\boldsymbol{\phi}$ is approximately constant over the time needed to collect one fast time data record, and hence the fast subsystem as modeled by Eq. (1), can be considered approximately stationary. Local linear maps are used to estimate Eq. (1) from the initial data record. This *reference system* is then used as a predictor for subsequent data records collected at later times.
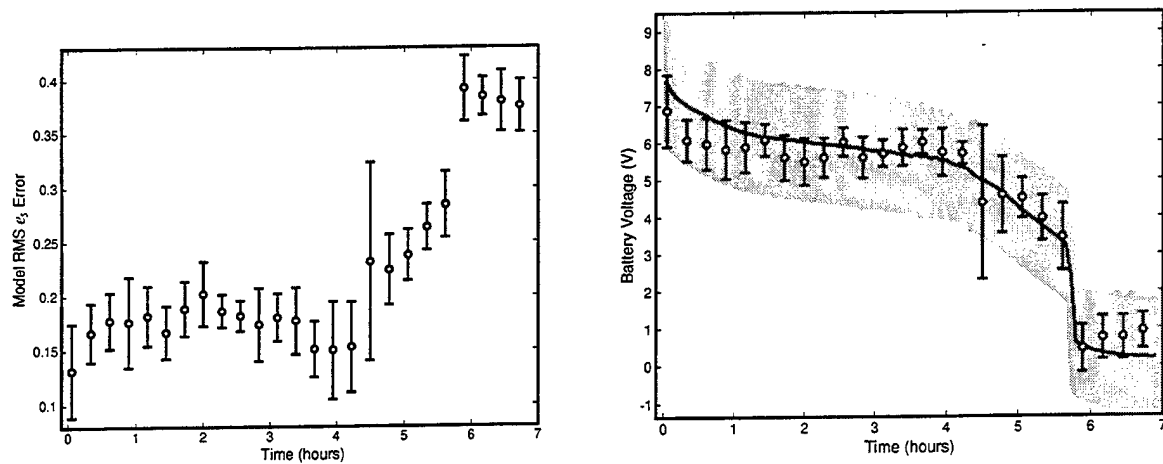
Fig. 1: Tracking results using fast-time model prediction errors: (left) plot of RMS 5-step predictor error, e_5, vs. time; (right) adjusted value of e_5 plotted over the actual battery data. The light grey gives the envelope of the battery voltage, and the solid medium grey line is its time local average in each of 100 equal time intervals.

EXPERIMENTAL RESULTS: The method was applied to a forced single degree of freedom oscillator with a two-well potential. The pendulum-type oscillator consists of a flexible steel beam with additional stiffening elements added to constrain the system to one degree of freedom over the frequency range of interest (< 50 Hz). The nonlinear potential at the beam tip is realized using a permanent magnet for one well and permanent/electromagnet stack for the other. Electric power for the electromagnet is supplied using a 9 V battery which discharges during the experiment until it fails. As the battery drains, the stiffness in the potential well with the electromagnet decreases by a few percent. The uniformity of power spectra taken during the experiment shows that the system was chaotic throughout most of the experiment, and that the chaotic motions did not undergo any drastic changes in character.

The results of applying the procedure are shown in Fig. 1. The raw 5-step predictor error e_5 is shown on the left, and exhibits a clear change over the time of the experiment. The model residual, μ_5, is a measure of the mean norm of the modeling error vector, whereas the predictor error e_5 is a measure of the mean norm of the estimated error vector. However, what is needed to observe the nonstationarity of the system is a measure of the true drift error vector. It is therefore reasonable to assume that a "calibration" of the drift observable can be obtained by a suitable function of μ_5 and e_5. In particular, we looked for a least squares fit to the battery data of a linear combination of e_5 and μ_5 by minimizing the following expression The result of carrying out this fit is shown on the right of Fig. 1.

The results show that the local linear model's short time prediction error performs reasonably well as an observer for the evolution of the hidden state of the the slow-time system.

Robust Control of Adaptive Structures with Embedded Sensors and Actuators

D. G. Wilson *   C. T. Abdallah †   G. P. Starr ‡   R.D. Robinett §

The development of lightweight flexible structures involving both advanced control and material system research will impact several application areas. Future Space applications will require lightweight robotic arms capable of accurately positioning larger payloads, performing tasks at high bandwidths, while exerting large external forces, and satisfying challenging slew requirements. Underground storage tank remediation, a Department of Energy application, requires long reach slender manipulators to fit through small openings, yet once inside they must perform in a large workspace. These operations in hazardous environments will increase structural bending of the members and suggest the need for vibration suppression capabilities. Industrial robots have used massive stiff structures to suppress deflection, resulting in relatively slow motion and high power consumption. In the development of Large Space Structures slewing and repositioning of spacecraft with flexible appendages while suppressing vibrations is of much interest.

The application of composite material technology for fabricating lightweight structures has the potential to reduce weight and improve performance at the cost of increased deflection and vibration. One way to reduce vibration is the application of robust controller designs that utilize *smart* structure technology. Smart and/or adaptive structures with both sensors and actuators, strategically embedded along the structure, can actively suppress vibrations and perform optimal slewing.

Two major approaches to controller design for slewing flexible structures are 1) model-based controllers which utilize state estimators based on plant information and 2) dissipative controllers which use knowledge of plant information to optimize performance but not for closed-loop stability. Typically the controller design is combined with a near-minimum time input trajectory optimal rotational maneuver. Examples of these methods are highlighted in the following references. In Liu and Yang [1] three simple and efficient methods are presented for the vibration control of slewing flexible structures. They investigated efficient rigid-body slewing using a constrained motion method and applied optimal control at the terminal state to minimize the flexible body vibration. This method produced the minimum residual vibration or settling time of the structure. The second method uses a combination of constrained motion with active damping which utilizes piezoceramic actuators with velocity feedback for active damping control. This method improved the transient vibration characteristics. The third method combines both the first and second methods to produce optimal torque control for vibration suppression during and after the slewing motion. Joshi, Maghami, and Kelkar [2] propose a class of dynamic dissipative compensators which robustly stabilize the plant in the presence of unmodeled dynamics and parametric uncertainties. They develop both robust stability criteria and a method for implementing the controller as a strictly proper

*Graduate Student, ME Dept., University of New Mexico
†Professor, EECE Dept., University of New Mexico
‡Professor, ME Dept., University of New Mexico
§Manager, Intelligent Systems Sensors & Control Dept., Sandia National Laboratories

compensator. Results are shown for a large space antenna and a laboratory model of a flexible spacecraft. The results demonstrated that dynamic dissipative compensators can ensure robust stability and performance.

The authors have designed and analyzed a robust controller based on the dynamic dissipative compensator methodology [2] utilizing a prototype single-axis adaptive structure. The results of this study include both analytical and numerical verification. The dynamic dissipative controller has been applied to an adaptive structure. The testbed includes; 1) an adaptive structure designed and constructed from graphite/epoxy composites with embedded structural actuation and sensing capability, and 2) a single-axis servo motor and encoder for rigid motion slewing. Using the dynamic dissipative compensator methodology, only the positional information from both the rigid-body and beam strain deflection sensors are used. The controller is considered to be marginally strictly positive real. Each controller channel is based on second order transfer functions. Criteria is also given for the selection of each of the transfer function coefficients. The compensator is diagonal or decoupled from each individual sensor/actuator pair.

Near-minimum time maneuvers based on an equivalent *rigid* structure are used to slew the flexible adaptive structure. The set of input trajectories used are adapted from a near-minimum time maneuver of a rigid body for a flexible slewing structure and are discussed in reference [3]. Tests were performed to compare the benefits of using adaptive rather than passive structures. The adaptive structure was developed using graphite/epoxy woven fabric prepreg material with embedded piezoceramic patches for actuation and embedded strain gauges for sensing. Dynamic characteristics of the adaptive structure are reported in reference [4]. The geometry of the adaptive structure is such that the first two cantilever bending modes are in the neighborhood of 8 and 40 Hz, respectively. A dynamic model was developed, which included the derivation of the equations of motion, based on the quadratic modes technique. This technique automatically captures the centrifugal stiffening term. A nonlinear optimization algorithm was used to determine controller coefficients to produce a rest-to-rest, residual vibration-free, 90° near-minimum time maneuver. Comparisons are made with a conventionally designed LQG controller. By using different varying tip masses, the controllers were tested in relationship to parametric uncertainty. The results from slewing the adaptive structure showed a reduction in residual vibration, improvement in slewing near-minimum time maneuvers, and robustness to parameter variations.

[1] Y.C. Liu ad S.M Yang, "Three Simple and Efficient Methods for Vibration Control of Slewing Flexible Structures", *J. of Dynamic Systems, Measurement, and Control*, Trans. ASME, **Vol. 115**, pp. 725-730, Dec., 1993.

[2] S.M. Joshi, P.G. Maghami, A.G. Kelkar, "Design of Dynamic Dissipative Compensators for Flexible Space Structures", *IEEE Trans. on Aerospace and Electronic Systems*, **Vol. 31, No. 4**, pp. 1314-1323, Oct. 1995.

[3] J.L. Junkins, Z.H. Rahman, and H. Bang, "Near-Minimum-Time Control of Distributed Parameter Systems: Analytical and Experimental Results," *J. of Guid., Control, and Dyn.*, **Vol. 14(2)**, pp. 406-415, 1991.

[4] D.G. Wilson, I.R. Searle, R. Ikegami, G.P. Starr, "Dynamic Characterization of Smart Structures for Active Vibration Control Applications", *ASME Winter Annual Meeting, Symposium on Vibro-Acoustic Applications*, Atlanta, GA, Nov. 17-22, 1996.

Abstract

Simulation of structure control and controller design for smart structures within a Finite Element code

Manfred W.Zehn[1]
Institute of Mechanics
Marc Enzmann
Institute for Automation and Control
Otto-von-Guericke-Universität Magdeburg, Germany

This paper investigates some aspects of control of smart structures for suppression of vibration (active damping), in terms of both controller simulation and design. It is fundamental for understanding of interaction in an actively controlled structure to have an accurate model. The basis structure as well as the active elements the piezo sensors and actuators can be modelled with appropriate piezo-elements. In the examples shown in the paper PZT patches mounted on the surface are modelled for sensing and control actuators. The leads to rather complex FE-models in particular if 3D modelling are applied. Sensor and actuator location and collocation are not topic of the current paper. However complex the FE model might be it always lacks to reality. And moreover model reduction techniques are necessary to make a controller design feasible. To close the gap between the FE model and reality experimental model identification is used to correct the model with an updating procedure before put to use to controller design and simulation. In order to integrate controller design methods and the simulation of control action into a Finite Element package, appropriate interfaces between structure and controller have to be designed. From the control-system designer's point of view the definition of these interfaces must absolutely take the nature of the plant and the possible control-design methods into consideration.

The control of mechanical structures will in most cases be a MIMO (Multiple Input - Multiple Output) problem. The complexity of these problems (controllability and observability of structures with spatial distributed parameters) renders the application of time-continuous controllers extremely difficult and thus enforces the use of digital controllers.

Actuator nonlinearities, uncertain parameters and boundary conditions, neglected plant dynamics and measurement noise are -among others- potentially destabilizing factors, that any controller will have to cope with. This makes robustness a stringent requirement for the controller. In recent years a number of new control design methods have emerged, which incorporate robustness issues in the design process. Most of these techniques make use of state-space descriptions of plant and controller.

Due to the large order of Finite-Element models it is not possible to transform the FE description into a state-space description directly and use the resulting plant model. For disturbance-attenuation and damping-augmentation problems modal reduction techniques have been applied rather successfully. The modal control philosophy is that controlling vibration is

---

[1] presenter

tantamount to controlling the structure's normal modes of vibration. Nevertheless, depending on the measurement signals a simple modal truncation can lead to an incorrect dynamical model with respect to input/output properties of the plant. At the University of Magdeburg's Innovative Research Group ADAMES we have developed, implemented and tested a model reduction technique that takes the control-designer's needs into consideration, can be implemented in or interfaced to any FE package rather effortlessly and requires only a small number of additional computations. For modal control the FE model (provided that we have a proper model) gives us much better quality eigenvektors with more co-ordinates distributed over the structure as experimental modal analysis is capable.

A reduced state-space description of the mechanical structure can very easily be transferred to Matlab, if it is desired to use the wealth of control-system related toolboxes that this package offers. If on the other hand control design algorithms are to be implemented in the Finite-Elements package, it might be necessary to include algorithms that dicretise the plant model in time as a last component of the structure-control interface.

The control-structure interface requires a number of additional calculations. Assuming a zero-order-hold at the controller input, the controller output must be calculated for every time step, using controller states and plant outputs. The resulting signal is assumed to be constant over a sample period, thus the integration in time will process from one sampling instant to the next.

To do all that preliminary work before testing and final tuning on real structure within the FE-system is a challenging undertaking, but it can reduce the number of experiments necessary for final design of controller. On the other hand influences of changing in the structure on the controller can be examined.

The paper concluded with few examples to illustrate methods and tools proposed can be very helpful in design of structural controllers.

Wednesday, July 29
1000-1130
Session 12.

ON A PARTICLES-SYSTEM-MODEL REPRESENTING THE MOTION OF THE GENERATED WAVE
- A SUITABLE MODEL FOR CONTROL SYSTEM DESIGN -

Tuneo KOBAYASHI*, Koichi OSUKA*, Ben T. NOHARA†, and Toshiro ONO*

*Osaka Prefecture University, †Mitsubishi Heavy Industries

1 INTRODUCTION

The motion of the generated wave is usually represented using the potential theory[1]. In the potential theory, however, it is difficult to obtain the equation of state or the transfer function, which is a presentation of the characteristics of the control object as well as a design tool for control system. Therefore, it is important to obtain a suitable model for the control system design of the generated wave.

The authors show a particles-system-model to be appropriate in order to obtain the equation of state or the transfer function for the generated wave. The effectiveness of the model is confirmed by some computer simulations as well as experiments using a one-dimensional test tank. The feature of the obtained model is equivalent to the induced results from the potential theory.

2 A PARTICLES-SYSTEM-MODEL REPRESENTING THE MOTION OF THE GENERATED WAVE

2.1 WAVE GENERATION THEORY

Fig.1 shows the wave generation by the piston type paddle, where (x, y), h, $\eta(x, t)$ indicate the coordinate system, water depth and the surface elevation at the position x and the time t, respectively.

Let the motion of the paddle $X(t)$ be $a\sin(\omega t)$ as shown in Fig.1. Then $\eta(x, t)$ is written by the following equation in the potential theory.

$$\eta(x,t) = Aa\cos(\omega t - kx) + \sum_{j=1}^{\infty} C_j e^{-k_j x} a\sin(\omega t) \tag{1}$$

Here, ω, k and k_j indicate angular frequency, the wave number of the progressing wave and the wave number of the local wave, respectively. k and k_j satisfy the following dispersion relations.

$$\omega^2 = gk\tanh(kh), \qquad \omega^2 = -gk_j\tan(k_j h) \tag{2}$$

where g denotes the acceleration due to gravity. Moreover A and C_j are written by

$$A = \frac{2\sinh^2(kh)}{kh + \sinh(kh)\cosh(kh)}, \qquad C_j = \frac{2\sin^2(k_j h)}{k_j h + \sin(k_j h)\cos(k_j h)} \tag{3}$$

In Eq.(1), the first and second terms of the right hand side correspond to the progressive wave to the right direction and the local wave, respectively. The local wave vanishes exponentially as x increases.

2.2 A PARTICLES-SYSTEM-MODEL

Fig.2 shows a particles-system-model which presents the motion of the generated wave. Here, M, K_0, d, and $x_n(t)$ indicate the mass of a particle, the constant of spring, the distance between two particles and the displacement of each particle, respectively. We assume that the number of particles is sufficiently large.

The following equation must stand up in order to satisfy the condition: the displacement of a particle $x_n(t)$ equals the surface elevation $x=n_d$.

$$M = 1, \qquad K_0 = \frac{\omega^2}{2(1 - \cos(kd))} \tag{4}$$

Here, M and K_0 mean the mass of a particle and the spring constant, respectively.

3 COMPARISON WITH THE THEORETICAL SURFACE ELEVATION

The obtained model is compared with the theoretical surface elevation of Eq.(1) by the computer simulation.

Fig.3 shows the simulation result and the theoretical surface elevation, which are represented by the solid line and the dashed line, respectively. The simulation result gives good agreement with the value of the theoretical surface elevation without the transient region.

4 COMPARISON WITH THE MEASURED SURFACE ELEVATION

Here, the obtained model is compared with the measured surface elevation by experiments using a one-dimensional test tank[2]. Photograph 1 shows an experimental apparatus of a test tank. Fig.5 presents the outline of an experimental apparatus.

The result is shown in Fig.4, where the dashed line and the solid line represent the calculation result of the model and the measured surface elevation, respectively. The simulation result is in beautiful agreement with the measured surface elevation.

5 CONCLUDING REMARK

The authors proposed a suitable model for the control system design of the generated wave. The followings were confirmed.

(1)The feature of the obtained model is equivalent to the induced results from the potential theory.
(2)The obtained model simulates the real motion very well.

REFERENCES
(1)for example, Crapper, G.D.: Introduction to Water Waves, Ellis Horwood Ltd(1984)
(2)Nohara, B.T.: An Absorption Algorithm and Its Implementation for Irregular Ocean Waves in a Tests Tank, J. of the Braz. Soc. Mechanical Sciences, (1998)(in printing)
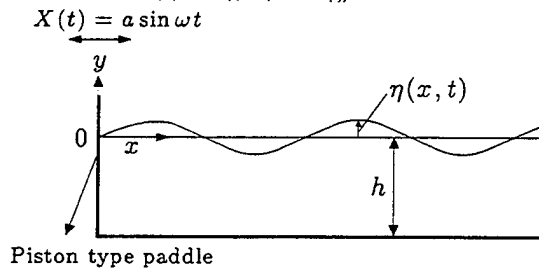
Fig.1 Wave generation by the piston type paddle
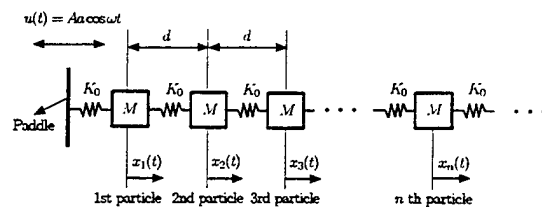
Fig.2 A particles-system-model
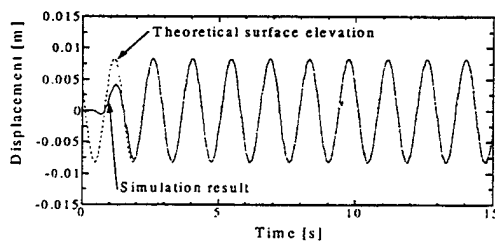
Fig.3 Simulation result and theoretical surface elevation
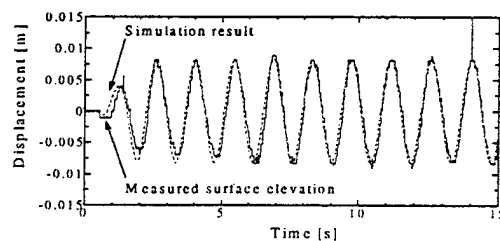
Fig.4 Simulation result and measured surface elevation
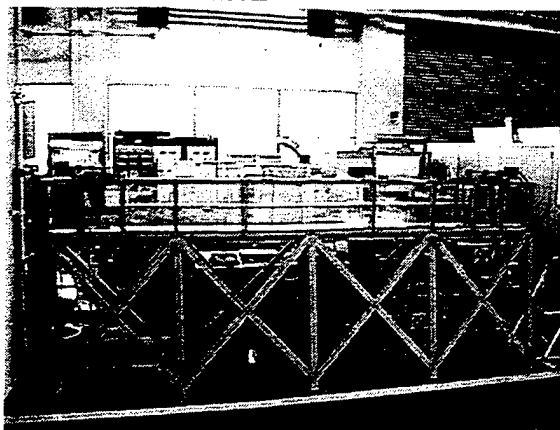
Photograph 1 A One-dimensional test tank
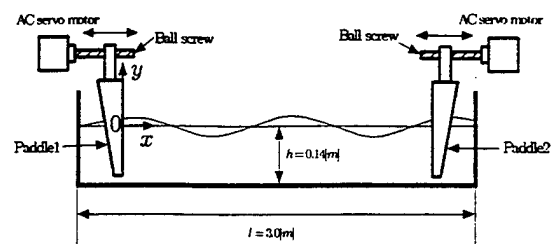
Fig. 5 Outline of an experimental apparatus

Neural networks used for dynamic systems simulation and neurocontrollers design

T. Březina, J. Krejsa

Faculty of Mechanical Engineering
Technical University of Brno
Technická 2,616 69, Brno, Czech Republic
Email: jkrejsa@fme.vutbr.cz

The contribution summarises our experiences with the usage of artificial neural networks, particularly in design of neurocontrollers and simulation of non-linear dynamic systems. Neural networks as part of artificial intelligence methods become widely used tools in various engineering tasks. Well trained network is robust, noise nonsensitive, it has short time response time and creation of solved problem's mathematical model is not necessary. But several limiting problems occur while working with neural networks:

a) difficult verification of neural networks responses (network always produce output even for invalid inputs)
b) time consuming training phase (which increases dramatically for real tasks = big networks)
c) design of network's optimum topology (the way neurons are connected to each other)

The topology essentially changes behaviour of the network (responses precision) together with training times. So far there is no general method for optimum topology determination. This is a big limitation for usage of neural networks in real tasks, because usually neural network expert is needed to set network's properties. Therefore several methods for automatized topology design were presented. Methods based on use of evolutionary algorithms (such a genetic algorithm) are the most advanced.

In the paper we discuss the practical experiments with optimum topology design, coming from genetic programming. Topologies of neural networks, types of nodes transfer functions non-linearities and weights values are described via certain modifications of the cellular encoding. . Encoding is chosen in such a way, that the consistency of the network described by the code, same as required number of its inputs and outputs is ensured for the arbitrary chromosome. The code also contains types of nodes transfer functions and synaptic weights values. The code is further understood as the chromosome manipulated by genetic algorithm (selection, cross-over and mutation operators are defined on the chromosome). Neural networks described by cellular code represent the individuals with corresponding chromosomes.

The concept of neurocontroll is based on the design of neural network, which simulates the behaviour of controlled system, with exchanged inputs and outputs of the system.

Serial connection of control unit with controlled system then represents the unit with the transition of input to output with transport delay. Such unit can be used in more complex controller. The unit which provides the inverse behaviour of the system is realised by artificial neural network – neurocontroller. Realisation of such controller therefore becomes the simulation task (the simulation of dynamic system behaviour using neural networks)

The data describing the behaviour of modelled dynamic systems were found by numerical simulation. Following tasks were solved using evolution neural networks:

Simulation of non-linear dynamic system
- DC motor with non-linear load
- 1DOF system with attached pendulum

Control
- Reluctance motor
- DC motor with non-linear load
- Polymerization unit

Obtained simulators and neurocontrollers of dynamic systems are made of neural networks with generally non-standard topologies. Those topologies can have surprisingly small structure while keeping reasonable properties of the network. So far it seems that evolutionary evolved networks can save about 30 % of neurons and up to 60 % of network's connections compare to the classical networks with the same quality of response. This is important mainly for purposes of real time control, when fast responses of the controller are required. Other nice feature of this approach is that neural network expert is no longer needed, the network is designed automatically.

Numerical precision of evolved networks was compared with traditional multilayer perceptron networks trained by back-propagation algorithm. Evolved networks reached significantly better results mainly in the simulation tasks, for the control tasks the evolved networks had only slightly better results (in term of global test error).

Main disadvantage of this approach is very high computational cost in the evolution part – training, but genetic algorithm used for evolution of topologies is ideal for hardware implementation, which could increase the speed of learning process dramatically.

We have found evolutionary neural networks useful and promising as the tools for both the simulation and control of dynamic systems. So far this method was tested only on simulation data but at the present time real control tasks are being proceeded.

Control of Large-Scale Linear Time-Periodic Dynamical Systems

S. C. Sinha and Venkatesh Deshmukh
Nonlinear Systems Research Laboratory
Department of Mechanical Engineering
Auburn University, Auburn, AL 36849
E-mail: ssinha@eng.auburn.edu

Abstract

This study is intended to provide a general methodology for developing reduced order controllers for linear, time periodic large-scale dynamical systems which arise in modeling of numerous engineering structures. A vast amount of research has been done to study the dynamics and control of large-scale time invariant systems, however, very little has been accomplished in case of time varying large-scale systems.

First, the linear time periodic dynamical system is converted into a time invariant one by application of the Lyapunov-Floquet transformation. An efficient computational scheme is used for computing the state transition matrix which can be subsequently factored to yield the Lyapunov-Floquet transformation matrix. The dimension of the time invariant large-scale dynamical system is then reduced on the basis of number of modes to be controlled. The order reduction is achieved using methods such as modal decoupling or aggregation and the controller gains are calculated by classical control techniques. The time periodic control gains are then transformed back to the original coordinates to guarantee the asymptotic stability of the large-scale time periodic system. The computational procedures discussed above are highly time efficient and suitable for real time implementation. Robustness of the controller is tested by perturbing the asymptotically stable dynamical system with linear, non-linear (in terms of state) and stochastic disturbances. The strength of disturbances influence the controller gains of the order reduced systems. The proposed scheme is illustrated by examples.

SUPPRESS CHAOS IN MATHIEU'S EQUATION BY THE SYSTEM VARIABLE SUBSTITUTION

Wu   Fengmin   Li   Qiaowen

(Department of Physics, Zhejiang University of Technology, Hangzhou

310014, P.R.C.)

ABSTRACT

Based on Pecora-Carroll's idea of synchronization of chaotic system[1], we present a method to suppress chaos through the system variable substitution , i.e. using some external signals to take the place of the variables of chaotic system. The signal can be either periodic one or quasi-periodic, or chaotic which is produced by another system. The chaotic system is a special form of Mathieu's equation[2-4] described as follows:

$$\ddot{X} + X + \delta(\dot{X} + n_1 X^2 \dot{X}) + \mu X + \beta_{10} X^3 + 2\varepsilon \cos 2t(-X + X^3/6) = 0. \tag{1}$$

Many bifurcations and chaotic phenomena have been shown in this system[5].

With certain set of parameters and initial condition, system (1) shows chaotic behavior. If we replace the X term in system (1) with $X^*(t)$, system (1) with control can be described as:

$$\dot{X} = Y$$
$$\dot{Y} = -\underline{X^*(t)} - \delta(Y + n_1 X^2 Y) - \mu X - \beta_{10} X^3 - 2\varepsilon \cos 2t(-X + X^3/6), \tag{2}$$

$X^*(t)$ are the external signals. We got them from a system which is described by the same evolution equations, but with a set of parameters such that the system are in the periodic, quasi-periodic or chaotic regimes.

By using these signals, we have achieved the goal of suppressing chaos numerically through substituting for the X term.

If we use these signal to replace the variable X of $\beta_{10} X^3$ term in system (1), we can also achieve the chaos suppression and get regular orbits. theoretically all the terms

about X in system (1) can be substituted.

With the same signal, the behavior of controlled system can be changed by varying the moments of control switching on or off. It is obvious that the cause of this phenomena is the sensitivity to initial condition of chaotic system.

On the other hand, system (1) can also be switched its behavior from the periodic to the chaotic by the same method. This possibility may be of interest to many biological systems showing that chaos can be healthier than order under some circumstances.

In conclusion, the numerical results indicate that the proposed method is capable of suppressing chaos of chaotic system and switching the behavior of a nonlinear system from periodic to chaotic. These results may be applied to other chaotic systems including multi-degree-of-freedom systems described by a set of differential equations.

1   Pecoea L M and Carroll T L, Synchronization of chaotic system. *Phys Rev Lett*, 1990,**64**:821~828

2. T.Paston and I.Stewart, *Catastrophe Theory and Its Applications*,(Pitman,San Francisco,1978)

3. A.H.Nayfeh and D.T.Mook,*Nonlinear Oscillations*,John Wiley and Sons,New York,(1979)

4.   M.Golubitsky and D.G.Schaeffer, *Singularities and Groups in Bifurcation Theory*,Springer-Verlag,   New York,(1985)

5. F.M.Wu , Chaos and Bifurcation in Euler's dynamically buckling problems. *J.of Nonlinear Dynamics in Science and Technology*,3,267(1994)

Non-Linear Vibration of an Elasto-Plastic Beam with Damage

Luiz Fernando Penna Franca
Marcelo Amorim Savi
Instituto Militar de Engenharia, Department of Mechanical and Materials Engineering
22.290.270 - Rio de Janeiro - RJ - Brasil

Pedro Manuel Calas Lopes Pacheco
CEFET/RJ, Department of Mechanical Engineering
20.271.110 - Rio de Janeiro - RJ - Brasil

Vibration analysis of elasto-plastic structures is important in many engineering problems. Damage phenomenon, observed in situations like low-cycle fatigue, introduces non-linear effects that can promote alterations on the structure behavior.

The present contribution considers a pin-ended beam submitted to cyclic loading by employing an idealization, known as Symonds' model (Symonds and Yu, 1985). The considered idealization proposes a model where a pin-ended beam with length $2L$, and uniform rectangular cross section, is represented by two rigid links, each of length L, which are joined by an elasto-plastic element. The two rigid bars are assumed to have mass per unit length ρ, the same as for the uniform beam. A constitutive model with internal variables is introduced to describe the inelastic deformations and the damage processes of the elasto-plastic element. Both kinematic and isotropic hardening are considered.

By geometric and equilibrium considerations, it is possible to establish the following governing equations to describe the pin-ended beam motion (Symonds and Yu, 1985),

$$
\begin{aligned}
y_1' &= y_2 \\
y_2' &= -c_0 y_2 - n \sin y_1 + \mu_0 m + \delta \sin(\Omega \tau)
\end{aligned}
\tag{1}
$$

where n and m are forces and moments, respectively, acting on the elasto-plastic element. c_0 is the dissipation parameter, μ_0 is a constant. δ and Ω are forcing parameters. The constitutive equation is given by (Savi and Pacheco, 1997),

$$
\sigma = (1-D)E(\varepsilon - \varepsilon^P)
$$

$$
\dot\varepsilon^P = \gamma \operatorname{sign}[\sigma - (1-D)\beta], \quad \dot\alpha = \left|\dot\varepsilon^P\right|, \quad \dot\beta = H\dot\varepsilon^P
$$

$$
\dot D = \frac{\gamma}{S_0}\left[\frac{1}{2}E\left(\varepsilon - \varepsilon^P\right)^2 + \frac{K\alpha^2}{2} + \frac{1}{2H}\beta^2\right]
\tag{2}
$$

where $\operatorname{sign}(x) = x / |x|$. σ is the one-dimensional stress, ε and ε^p are the total and plastic one-dimensional strain, respectively. β is the back stress and α is the internal hardening variable. β and α are associated with kinematic and isotropic hardening, respectively. D is the damage variable. γ represents the rate at which plastic deformations take place. E is the Young modulus. K and H are the isotropic and kinematic hardening parameters, respectively. S_0 is the damage parameter. The yield function, $h(\sigma, \alpha, \beta, D)$, the *Kuhn-Tucker conditions* and the *consistency condition* are given by:

$$h(\sigma,\alpha,\beta,D) = |\sigma - (1-D)\beta| - [\sigma_y - (1-D)K\alpha]$$

$$\gamma \geq 0, \quad \gamma h(\sigma,\alpha,\beta)=0, \quad \gamma \dot{h}(\sigma,\alpha,\beta)=0 \quad \text{if} \quad h(\sigma,\alpha,\beta)=0. \tag{3}$$

A numerical procedure is developed using operator split scheme to promote the separation of the variables space in a phase space and a plastic-damage space. First, equation of motion (1) is integrated using any classical scheme, like fourth order Runge-Kutta, assuming that the variables n and m are known parameters. n and m are evaluated by considering an elastic predictor step (trial state), where plastic variables $(\varepsilon^p,\alpha,\beta,D)$ remain constant from the previous time instant. The next step of solution procedure consists on a plastic corrector step where the feasibility of trial state is evaluated using the *return mapping algorithm* (Simo and Taylor, 1985). An iterative process is used to determine damage variable, D. After this step, it is possible to recalculate variables n and m, and a new iterative process takes place until the convergence is achieved (Savi and Pacheco, 1997).

Qualitative changes on the beam response, predicted by the models with and without damage, may occur. Figure 1 shows phase plane orbits predicted by these two models. Damage effect promotes the material softening which causes changes on the motion. The beam may oscillate around different equilibrium points. Figure 1a shows steady state response for both models when $\Omega = 0.75$ and $\delta = 0.3$. Figure 1b shows the response for $\Omega = 1$ and $\delta = 0.5$. In this situation, the model without damage presents a periodic steady state response while the model with damage presents no steady state since a critical damage, $D_{cr} = 0.8$, is reached after 254 cycles.
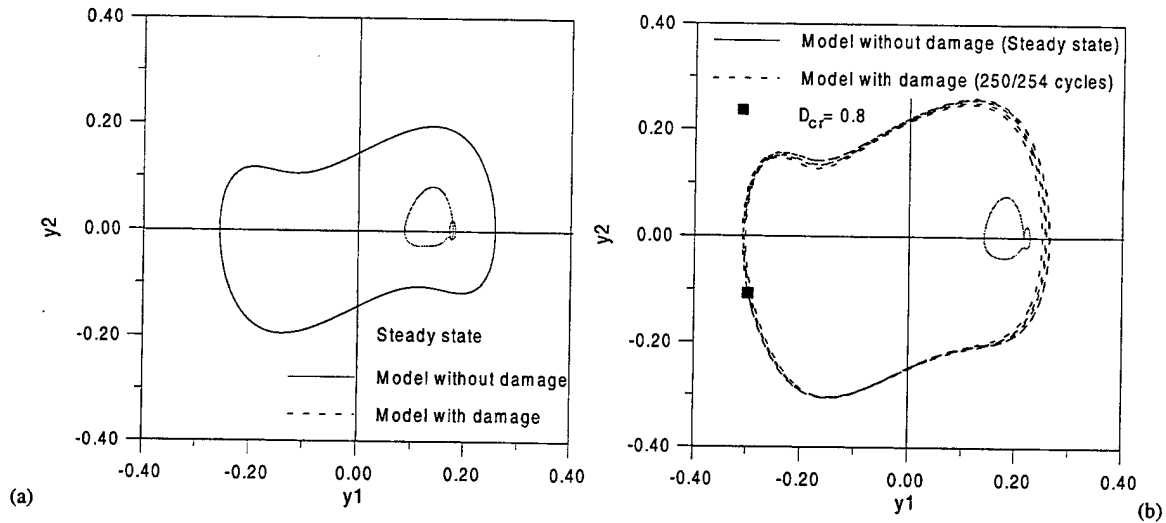
Figure 1: Phase plane orbits predicted by the models with and without damage.
(a) $\Omega = 0.75$ and $\delta = 0.3$; (b) $\Omega = 1$ and $\delta = 0.5$.

REFERENCES

• Savi, M.A., and Pacheco, P.M.C.L., 1997, "Non-Linear Dynamics of an Elasto-Plastic Oscillator with Kinematic and Isotropic Hardening", *Journal of Sound and Vibration*, Vol.207, n.2, pp.207-226.

• Simo, J.C., and Taylor, R.L., 1985, "Consistent Tangent Operators for Rate-Independent Elastoplasticity", *Computer Methods in Applied Mechanics and Eng.*, Vol. 48, pp. 101-118.

• Symonds, P.S., and Yu, T.X., 1985, "Counterintuitive Behavior in a Problem of Elastic-Plastic Beam Dynamics", *ASME Journal of Applied Mechanics*, Vol. 52, pp. 517-522.

Wednesday, July 29
1330-1500
Session 13.

Synchronization by Linear Feedback in Chaotic Systems and Lyapunov Exponent

Mikio Nakai* and Nobuyuki Tsukamoto**

*Department of Precision Engineering, Kyoto University,
Yoshidahonmachi Sakyo-ku Kyoto-shi, 606-01 JAPAN
E-mail: nakaim@prec.kyoto-u.ac.jp, Fax : +81-75-771-7286
**Canon Co. Ltd.

This paper describes gain constant in synchronization of chaotic systems by linear feedback and the maximum Lyapunov exponent. As the subsystems A and B of chaotic systems, the following Duffing oscillator systems are considered.

$$A : \quad \frac{dx_1}{dt} = x_2 + u_1$$
$$\frac{dx_2}{dt} = -kx_2 - x_1^3 + \bar{B}\cos(t) + u_2 \quad (1)$$

$$B : \quad \frac{dy_1}{dt} = y_2$$
$$\frac{dy_2}{dt} = -ky_2 - y_1^3 + \bar{B}\cos(t) \quad (2)$$

where parameters k and $\bar{B}$ have the same values in the subsystems A and B.

The following negative feedback was introduced into the A subsystem so that the subsystems A and B can synchronize.

$$u_1 = -K_1(x_1 - y_1)$$
$$u_2 = -K_2(x_2 - y_2)$$

where K_1 and K_2 are gain constants.

Figure 1 shows birfurcation diagram of the A subsystem for $k = 0.1$, $\bar{B} = 5.0 \sim 9.0$ when no feedback is performed, $K_1 = K_2 = 0$. In two cases gain constants are $K = K_1 > 0$, $K_2 = 0$ and $K = K_1 = K_2 > 0$ for $k = 0.1$, $\bar{B} = 5.8$ where chaotic motion occurs, we investigated the relationship between the gain constant K and periods n_s, when the synchronization can be achieved. Those results are presented in Fig.2. When $K = K_1 > 0, K_2 = 0$, two subsystems does not synchronize for $K < 0.2$. For $K > 0.2$, n_s decreases exponentially as the value of K increases. Here, denote the minimum value of K in the synchronization by K_{amin}.

On the other hand, when $K = K_1 = K_2 > 0$, the minimum value K_{bmin} of K is $K_{bmin} = 0.1$ in the synchronization, and this value is a half of K_{amin}.

Also, it nearly equals to the maximum Lyapunov exponent $\lambda_{max} = 0.10079$. As K increases, the period n_s exhibits more remarkable decrease than that for $K = K_1 > 0$, $K_2 = 0$.
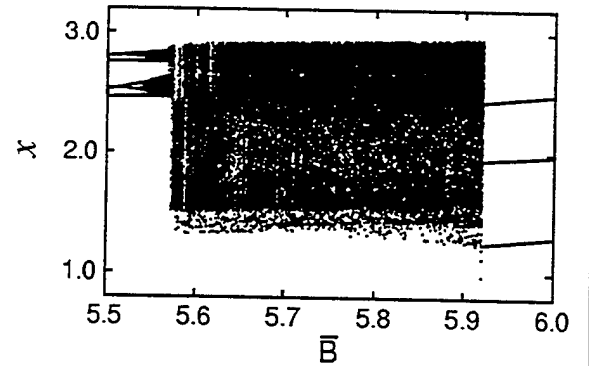
Figure 1: Bifurcation diagram in the Duffing oscillator system for $k = 0.1$
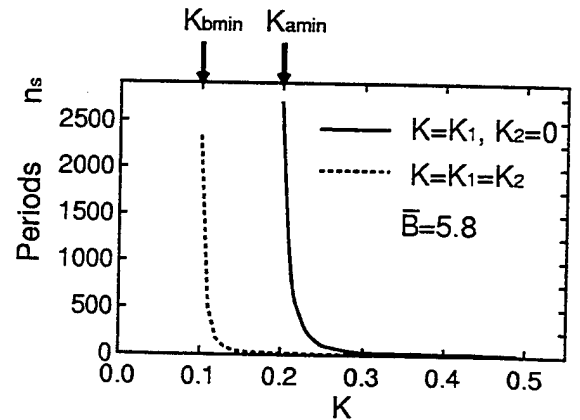
Figure 2: n_s versus different values of K in the synchronization of the two Duffing oscillator subsystems for $k = 0.1$, $\bar{B} = 5.8$
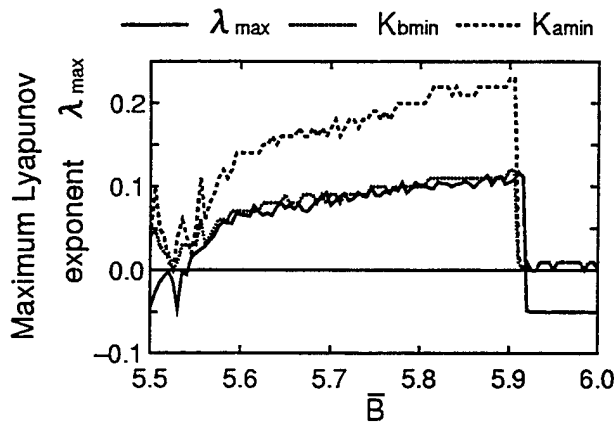
Figure 3: K_{amin}, K_{bmin} and λ_{max} in the synchronization of the two Duffing oscillator subsystems ($\bar{B} = 5.5 \sim 6.0$) when there is a phase difference of one or two periods between periodic orbits of the A and B subsystems
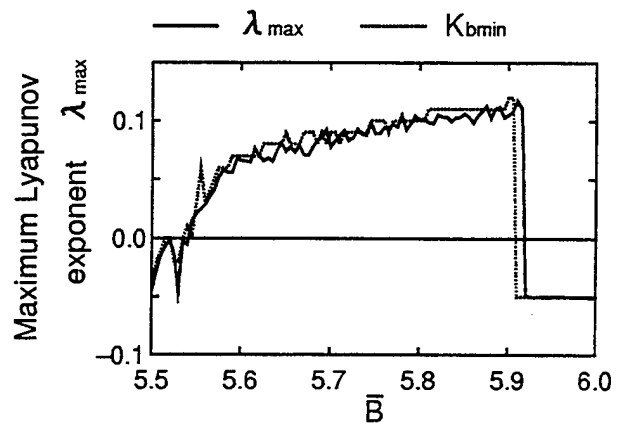
Figure 4: K_{bmin} and λ_{max} in the synchronization of the two Duffing oscillator subsystems ($\bar{B} = 5.5 \sim 6.0$) when the response of the A subsystem converges to a periodic orbit in phase with that of the B subsystem

Next, we examine the relation among K_{amin}, K_{bmin} and λ_{max}. For the initial value of $x_1(0) = x_2(0) = -1.0$ and $y_1(0) = y_2(0) = -1.01$, Fig.3 shows the values of K_{amin}, K_{bmin} and λ_{max} versus $\bar{B}$, when $\bar{B}$ is changed from 5.5 to 6.0. From this figure it is found that the relation of $K_{bmin} \approx \lambda_{max}$ is applicable to the region of $5.54 < \bar{B} < 5.92$ where chaotic motions occur and then $\lambda_{max} > 0$. Furthermore, in this region, the relation of $K_{amin}/K_{bmin} \approx 2$ is valid. However, in the region where the two subsystems converge to a periodic orbit, $\lambda_{max} < 0$, both K_{amin} and K_{bmin} are smaller than those in chaotic motions, but K_{bmin} does not coincide with λ_{mqx}. For an example, over the range of $\bar{B} > 5.92$, the subsystems A and B converge to the period-3 orbit as shown in Fig.1. However, since there is a phase difference of one or two periods between two subsystems for this region, $K_{amin} = K_{bmin} = 0.01$. Figure 4 shows K_{bmin} obtained by taking the initial value in order to converge to a periodic orbit with the same phase in two subsystems and the maximum Lyapunov exponent λ_{max}. This figure reveals that $K_{bmin} \approx \lambda_{max}$ is applicable to all regions of period orbits and chaotic motions.

In addition, for the piecewise linear, the Lorenz and the Rössler systems, we also examined the relation among K_{amin}, K_{bmin} and λ_{max}. The results suggest that the following relation can establish if the two subsystems are the same chaotic systems.

$$K_{bmin} \approx \lambda_{max}, \quad \frac{K_{amin}}{K_{bmin}} > 1$$

If two subsystems converge to a periodic orbit with

the phase difference of several periods, $K_{bmin} \approx \lambda_{max} > 0$. It could be further proved that the relation of $K_{bmin} \approx \lambda_{max}$ holds.

These above results therefore lead to the conclusion that the maximum Lyapunov exponent of the system can be determined by calculating gain constant K_{bmin} in the synchronization of the same two systems.

Furthermore, if the linear feedback gain K can be increased sufficiently, mean error ε between x_1 and y_1 in the synchronization of two different subsystems becomes constant. The value of ε can be allowed to measure similarity in two different subsystems.

Reference

Pecora, L. M. and Carrol, T.L., " Synchronization in chaotic systems", *Physical Review Letters*, Vol.64, No.8, 1990, pp.821-824.

Stabilization of the Parametric Resonance of a Cantilever Beam by Boundary and Bifurcation Control

Jun KAWAZOE, Hiroshi YABUNO, Nobuharu AOSHIMA

Institute of Applied Physics

University of Tsukuba

Tsukuba-City 305 Japan

Abstract

There are many studies on oscillations of the column subjected to a base excitation. For instance, there are the analysis of the response of a beam-mass oscillator under combined harmonic and random excitation[1], and the investigation of a method of active control for suppressing the vibration of a mechanically flexible cantilever beam which is subject to a distributed random disturbance and also a seismic input at the clamped end [2]. However, these studies are investigated with respect to the response in the case when the base is laterally excited.

On the other hand, the analysis of the response in the case when the base is vertically excited receive much attention in recent years. The vertical excitation produces the parametric resonance in the case when the excitation frequency is in the neighborhood of twice the natural frequency of the beam . Anderson et al theoretically and experimentally show that the inertia and curvature nonlinearities and quadratic damping term have significant influence on the nonlinear characteristics of the frequency-response [3]. By the way, there are some studies on the control of the oscillation for the parametric resonance in the single-degree-freedom model. Yabuno theoretically proposes the bifurcation control method in order to stabilize a parametric resonance [4]. But, there is no study on the control of the oscillation of the parametrically excited beam in the continuum system.

In this research, an experimental and theoretical investigation into the passive control method for stabilization of a parametrically excited slender cantilever beam is presented. As mentioned above, the beam subjected to the sinusoidal and vertical excitation is parametrically excited in the case when the excitation frequency is in the neighborhood of twice the natural frequency of the beam. The cantilever beam is treated as continua, and a simple pendulum mounted to a tip mass of the

beam is used as a passive vibration absorber for the parametric resonance. The equation governing the motion of the system is formulated by Hamilton's principle, taking into account the coupling effect between the beam and the pendulum mounted to the tip mass of the beam. Using the method of multiple scales, the modulation equations of the system are derived. By theoretically analyzing the modulation equations, we show that the beam is stabilized, even in the case when the excitation frequency is in the neighborhood of twice the natural frequency of the beam, by shifting the unstable region due to the coupling effect between the beam and pendulum. In addition, the experimental results verify that the theoretically proposed method makes it possible to stabilize the parametric resonance of the beam.

References

[1] Stephen Ekwaro-Osire and Atila Ertas, *Response Statistics of a Beam-Mass Oscillator Under Combined Harmonic and Random Excitation*, Journal of Vibration and Control 1(1995), 225-245.

[2] Akira Ohsumi and Yuichi Sawada, *Active Control of Flexible Structures Subject to Distributed and Seismic Disturbances*, Trans. ASME, Journal of Dynamic Systems, Measurement, and Control **115**(1993),649-650.

[3] T. J. Anderson et al, *Experimental Verification of the Importance of the Nonlinear Curvature in the Response of a Cantilever Beam*, Trans. ASME, J. Vib. Acoust. **118**(1996), 21-27.

[4] Hiroshi Yabuno, *Bifurcation Control of Parametrically Excited Duffing System by a Combined Linear-Plus-Nonlinear Feedback Control*, Nonlinear Dynamics **12**(1997), 263-274.

Stabilization of the Parametric Resonance
in a Magnetically Levitated Body by a Bifurcation Control

Hiroshi SAKAI

Graduate student, Master's Program in Science and Engineering, University of Tsukuba

Hiroshi YABUNO

Assistant Professor, Institute of Applied Physics, University of Tsukuba

Nobuharu AOSHIMA

Professor, Institute of Applied Physics, University of Tsukuba

Tsukuba-City 305-0006 Japan

Parametric resonance occurring in a magnetically levitated body subjected to periodically varying magnetic force is stabilized by a bifurcation control. A pendulum mounted to the body is used as a vibration absorber under the bifurcation control method. [The analysis using the method of multiple scales] The appropriate feedback gain of the bifurcation control method is obtained by (Yabuno, H. 1997). We consider the system as shown in Fig. 1. The magnetically levitated body can be moved freely only in the vertical
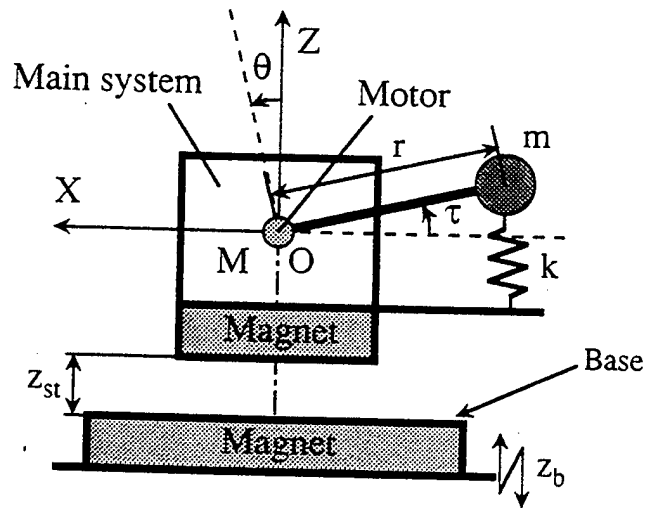
Fig. 1 The analytical model.

direction. The magnetic force acting on the body is regardes as a asymmetric nonlinear restoring force. The base with the magnet which repulses the magnet on the body is sinusoidary excited in the vertical direction, and then the magnetic force acting on the body is periodically changed. Due to the asymmetry and the periodically change of the magnetic force, the govering equation is simillar to parametric exciting Duffing system. A parametric resonance therefor occurs in the case when the frequency of the base excitation is in the neihborhood of twice the natural frequency.

The dimensionless equations governing the motion of the system under the feedback torque, τ, constructed with the linear combination of the displacement and velocity in the vertical direction are expressed as follows

$$\ddot{z} + (1 + \frac{\tau_1^*}{r^*} - 2\epsilon\alpha_{zz}\cos\nu t)z - k^*r^*\theta = \epsilon\cos\nu t - \mu_z\dot{z} - \frac{\tau_2^*}{r^*}\dot{z} \tag{1}$$

$$\ddot{\theta} + k^*(1 + \frac{1}{m^*})\theta + \frac{1}{r^*}\{1 - \frac{1}{r^*}(1 + \frac{1}{m^*})\tau_1^* - 2\epsilon\alpha_{zz}\cos\nu t\}z$$

$$= -\frac{1}{r^*}\epsilon\cos\nu t - \mu_\theta\dot{\theta} + \frac{1}{r^{*2}}(1 + \frac{1}{m^*})\tau_2^*\dot{z}. \tag{2}$$

Here z is a dimemsionless vertical displacement in the Z-direction, α_{zz} is a dimensionless coefficient with respect to the quadratic nonlinear component of magnetic force and this coefficient the causes parametric resonance, ϵ is the amplitude of the excitation, and ν is the frequency of the excitation. The symboles with $*$ express dimensionless constant values; $\tau_1^*(\dot{\iota}0)$ and $\tau_2^*(\dot{\iota}0)$ are the dimensionless feedback gains with respect to z and $\dot{z}$, respectively. The dot denotes the derivative with respect to the dimensionless time.

Analyzing Eqs.(1) and (2) by the method of multiple scales, we obtain the boundary between the stable and unstable regions, i.e., the bifurcation set, for the trivial solution as follows:

$$\epsilon = \sqrt{a(\nu - b)^2 + (c + d\tau_2^*)^2}, \tag{3}$$

where a, b, c and d are the functions of τ_1^*. Figures 2 and 3 illustrate the bifurcation sets for several values of τ_2^* and τ_1^*, respectively.
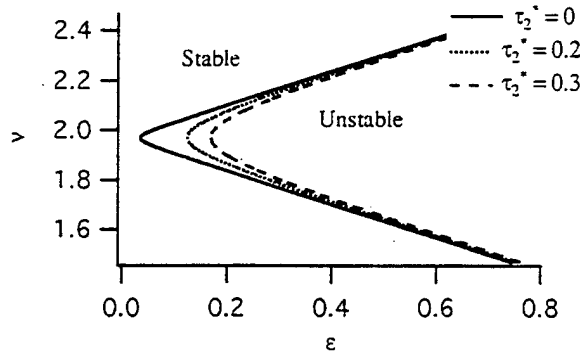
Fig. 2 Bifurcation set ($\tau_1^* = 0$).
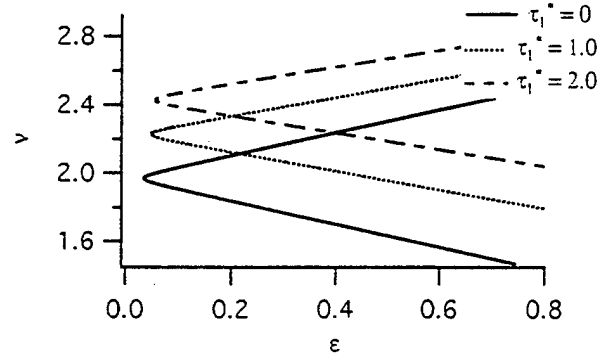
Fig. 3 Bifurcation set ($\tau_2^* = 0$).

As a results, the influence of τ_1^* and τ_2^* on the stabilization for the parametric resonance is summarized as follows:

- Increasing the dimensionless feedback gain with respect to the dimensionless vertical velocity, τ_2^*, corresponds to increasing the viscous damping force in the vertical direction. The boundaries are shifted to the positive direction of the dimensionless amplitude of the excitation, ϵ, as shown in Fig. 2 and the stable region becomes wider.

- Increasing the dimensionless feedback gain with respect to the dimensionless vertical displacement, τ_1^*, corresponds to increasing the natural frequency. The boundaries are shifted to the positive direction of the dimensionless frequency of the excitation, ν, as shown in Fig. 3 and the stable region is not changed.

Vibration and Control by Parametric Excitation for Driving Belt

Hiroki OKUBO, Kouetsu TAKANO, Osami MATSUSHITA, Keiji WATANABE
and Yoshi HIRASE

Abstract

Belt systems are applied to driving equipments for power transmission in industrial machinery, as in a tank, snow mobile, automated teller machine, etc. A part of the driving unit installed with the crawler driven vehicle by a DC motor is operated in the running performance test. This is similar to the running performance test of a vehicle tire. In certain conditions of high speed, called critical speeds, the upper part of the belt between the driving and idler wheels vibrates in the vibration shape of the first bending mode. The high speed operation of these axially moving belt systems encounters the belt resonance vibration problem. These vibration resonances at critical speeds are a barrier for the trend to design the high speed operating machines.

In this paper, the simplest belt system(Fig.1) as a bridge structure connecting driving and driven pulleys located at both ends is selected for proposal as a basic idea for vibration reduction control methods.
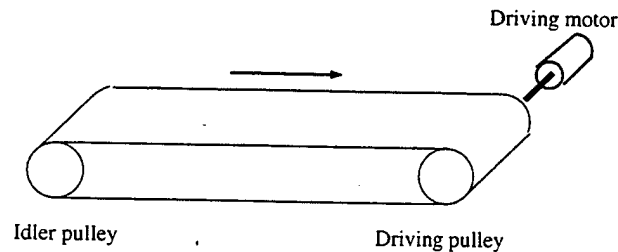
Figure 1: Driving Belt model.

The belt vibrating system can be thus described by the equation of motion of the string. In this system, the eccentricity of a pulley causes the forced vibrations of the belt in relation to the pulley revolution, as well as rotor vibration caused by unbalance.

In order to combat these forced vibrations, many ideas are presented which includes the addition of external damping devices and roller bearings in the middle of the belt span. Some of the references propose a vibration control method using the feedback control theory which implies the closed loop electric device. The result is not practical for industrial uses. All of these ideas imply relevant additions of equipment to machines.

Our idea allows for no additional mechanical parts and incorporates with the open loop control technique. Usually, motor input torque to drive the pulley employs DC voltage fed to the motor. However, if a harmonic wave is superimposed using modified DC voltage, the pulley rotation speed fluctuates with the changing tension, i.e., the parametric excitation. This nonlinear parametric excitation can be adjusted to reduce the vibration by directing the magnitude and phase of the additional harmonic wave to the opposite vibration source of

the linear system. The parametric excitation cancel the vibration source so that the resultant vibrations disappear. This method is realized through only electronic modification of the motor driving circuits.

In this paper, the resonance vibration characteristics are analysed. The causes of vibration are identified from the results of forced vibrations of the linear system.

The mathematical models are introduced by using the equation of motion of the forced vibration including the parametric excitation.

$$\ddot{x} + \omega_n^2 \{1 + h\cos(\nu t + \alpha)\}x + 2\zeta\omega_n\dot{x} = e\omega^2\cos\omega t + g$$

where x = the displacement of the belt vibration
ω_n = the natural angular velocity of the belt vibration
ζ = damping ratio of the belt
ω = pulley ratational speed
e = ecdentricity
ν = fluctuation angular velocity of tension
h = gain to be selected
α = phase to be selected
g = gravity

The control method by parametric excitation can be discussed in order to combat these forced vibrations. The harmonic fluctuation frequency can be selected in two case; $\nu = \omega$ or $\nu = 2\omega$ in case of resonace of $\omega = \omega_n$. According to this mathematical analysis on the forced nonlinear vibration, the strategy of vibration reduction control is clarified.

The vibration amplitude a of x is shown in Figure.2 and 3.
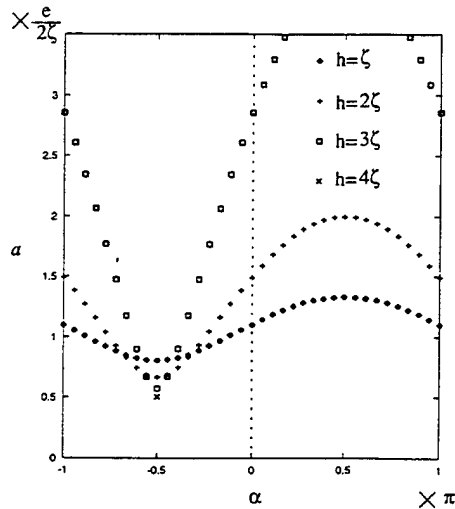
Figure 2: Amplitude at vibration resonance by parametric excitation ($\nu = 2\omega$).
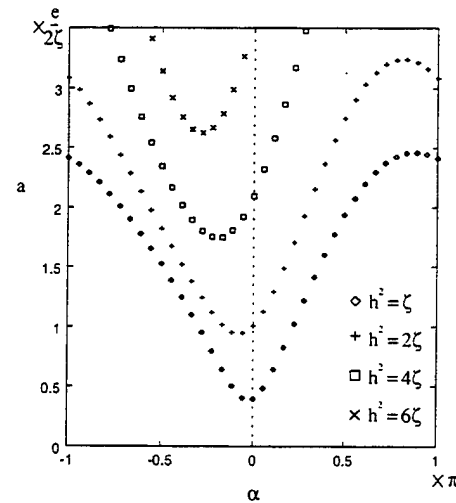
Figure 3: Amplitude at vibration resonance by parametric excitation ($\nu = \omega$) in case of $\zeta = 1.93e^2\omega_n^4/g^2$.

As the result, the follows are obtained.

- This system is subject to the limitation of stability in case of $\nu = \omega$ and $\nu = 2\omega$.

- Control good parameters (h, α) for the vibration reduction are proposed.

- The effectiveness of parametric excitation control is proven numerically.

Seismic Response Mitigation by a Nonlinear Sliding Mode Controller

Mahendra P. Singh, Enrique E. Matheu and Luis M. Moreschi
Department of Engineering Science and Mechanics
Virginia Polytechnic Institute and State University
Blacksburg, Virginia 24061

ABSTRACT

The sliding mode control approach is gaining increasing attention in the structural dynamics community for the control of structural motions caused by earthquakes and wind, primarily for the reason of its robustness under parametric uncertainty. The approach consists of enforcing constraints that satisfy certain stability and optimality conditions by means of appropriate control actions. In the classical approach, the control actions are usually defined as linear functions of the measured system states. However, to reduce the required control effort and also to reduce the peak response more effectively, one can also utilize a nonlinear controller with certain advantages.

In the sliding mode approach, it is common to define the control actions consisting of two parts: (1) equivalent control that depends on the available states and compensates for the system's response and, (2) and the second term that compensates for the unmeasured disturbance and keeps the sliding motion in an acceptable regime. The second terms is usually defined as linear function of the sliding motion variables. For seismically excited buildings, the first term is more dominant than the other. One can, however, choose to reduce the dominance of the equivalent control term. This can be accomplished by using a nonlinear controller where the second term is expressed as a nonlinear function of the sliding state variables. The paper will present the numerical example of a multistory building structure subjected to earthquake induced ground motions to demonstrate the relative effectiveness of these two control action terms in reducing the peak structural response and their respective contributions to the magnitude of the overall control effort.

Wednesday, July 29
1530-1700
Session 14.

INFLUENCE OF STATIC NONLINEARITY TO RESONANCES DUE TO A CRACK
(SUPERHARMONIC RESONANCE)

Yukio ISHIDA and Feng LU
Dept. of Electronic-Mechanical Engineering, Nagoya University
Furo-cho, Chikusa-ku, Nagoya, 464-8603, Japan

Introduction

There are many studies on vibrations of cracked rotors. However, most of them investigated changes which appeared in vibrations when cracks occurred in linear rotor systems. Cracked rotors have rotating nonlinear characteristics of a piecewise linear type due to open-closed mechanisms. Previous researchers proposed to utilize resonance caused by this rotating nonlinearity as a signal of the occurrence of a crack.If a rotor system has mechanical elements, such as ball bearings and journal bearings, static nonlinearity appears and, as a result, nonlinear resonances similar to those due to cracks appear. Therefore, it is difficult to detect cracks in such nonlinear systems using existing diagnoses. In this paper, we investigate vibrational changes which appear when cracks occur in rotor systems with static nonlinearity. Especially, we focus on the effect of the static nonlinearity to the 2nd and 3rd order superharmonic resonances due to crack. Nonlinear equations of motion with both static and rotating nonlinear spring characteristics are derived. Changes in the shapes of resonance curves are investigated by theoretical analyses and numerical simulations.

Equations of Motion

The equations of motion of a cracked rotor with static nonlinear spring characteristics(Fig.1) are given as follows.

$$\ddot{\theta}_x + i_p \omega \dot{\theta}_y + c\dot{\theta}_x + (1 \mp \Delta_2)\theta_x + (\Delta_1 \pm \Delta_2)(\theta_x C_2 + \theta_y S_2) + n_{\theta x} = M\cos(\omega t + \alpha)$$

$$\ddot{\theta}_y - i_p \omega \dot{\theta}_x + c\dot{\theta}_y + (1 \mp \Delta_2)\theta_y + (\Delta_1 \pm \Delta_2)(\theta_x S_2 - \theta_y C_2) + n_{\theta y} = M\sin(\omega t + \alpha) + M_0 \quad (1)$$

If the restoring forces are approximated by power series, these equations become

$$\ddot{\theta}_x + i_p \omega \dot{\theta}_y + c\dot{\theta}_x + \theta_x + \Delta(\theta_x C_2 + \theta_y S_2) + N_{\theta x} + n_{\theta x} = M\cos(\omega t + \alpha)$$

$$\ddot{\theta}_y - i_p \omega \dot{\theta}_x + c\dot{\theta}_y + \theta_y + \Delta(\theta_x S_2 - \theta_y C_2) + N_{\theta y} + n_{\theta y} = M\sin(\omega t + \alpha) + M_0 \quad (2)$$

where $S_n = \sin n\omega t$ and $C_n = \cos n\omega t$. We call Eq.(1) a piecewise linear model, and Eq.(2) a power series model. The rotating nonlinear terms $N_{\theta x}$ and $N_{\theta y}$ are given by[1]

$$N_{\theta x} = (\varepsilon_2/4)\left[(-3S_1 + S_3)\theta_x^2 + 2(C_1 - C_3)\theta_x\theta_y - (S_1 + S_3)\theta_y^2 \right]$$

$$N_{\theta y} = (\varepsilon_2/4)\left[(C_1 - C_3)\theta_x^2 - 2(S_1 + S_3)\theta_x\theta_y + (3C_1 + C_3)\theta_y^2 \right] \quad (3)$$

and the static nonlinear terms $n_{\theta x}$ and $n_{\theta y}$ are given by

$$n_{\theta x} = \partial V_n / \partial \theta_x, \quad n_{\theta y} = \partial V_n / \partial \theta_y, \quad V = V_0 + V_n = V_0 + \sum_{(i+j=3)} \varepsilon_{ij}\theta_x^i\theta_y^j + \sum_{(i+j=4)} \beta_{ij}\theta_x^i\theta_y^j \quad (4)$$

where V is the corresponding potential energy, ε_{ij} is the static unsymmetrical nonlinear coefficients ,and β_{ij} is the static symmetrical nonlinear coefficients . By the transformation $\theta_x = \theta\cos\varphi$, $\theta_y = \theta\sin\varphi$, we can transform Eq.(4) into the polar coordinate expression[2].

$$V = V_0 + (\varepsilon_c^{(1)}\cos\varphi + \varepsilon_s^{(1)}\sin\varphi + \varepsilon_c^{(3)}\cos3\varphi$$
$$+ \varepsilon_s^{(3)}\sin3\varphi)\theta^3 + (\beta^{(0)} + \beta_c^{(2)}\cos2\varphi \quad (5)$$
$$+ \beta_s^{(2)}\sin2\varphi + \beta_c^{(4)}\cos4\varphi + \beta_s^{(4)}\sin4\varphi)\theta^4$$

2nd Order Superharmonic Resonance

In order to investigate the effect of the static nonlinearity , we carry out numerical simulations by Eq.(1) and theoretical analyses by Eq.(2) for the cases with only the rotating nonlinearity,and with both static and rotating nonlinearities. In theoretical
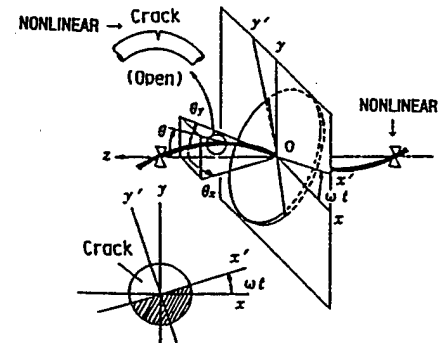

Fig.1 Model of a cracked rotor

analyses, we assume the approximate solution in the accuracy of order $O(\varepsilon)$ as follows:

$$\theta_x = R\cos\theta_f + P\cos(\omega t + \beta) + \varepsilon(a\cos\theta_f + b\sin\theta_f) + A_x$$
$$\theta_y = R\sin\theta_f + P\sin(\omega t + \beta) + \varepsilon(a'\sin\theta_f + b'\cos\theta_f) + A_y$$

(6)

where $\theta_f = \omega_f t + \delta$ and $\omega_f = 2\omega$. The terms with the small parameter ε represent deviations. Substituting Eq.(6) into Eq.(2) and using the harmonic balance method, we can obtain the expression for the resonance curves. The results of numerical simulations and theoretical analyses are shown in Fig.2~Fig.4. Figure 2 and Fig.3 show the influence of the static unsymmetrical nonlinearity. The resonance curves for $\varepsilon_S^{(1)} = 0$ show the resonance due to only crack. As $\varepsilon_S^{(1)}$ increases in the positive side, the magnitude of the resonance increases. On the contrary, as $\varepsilon_S^{(1)}$ increases in the negative side, the resonance decreases and finally disappears. Figure 4 shows the influence of the static symmetrical nonlinearity. The resonance curves become a hard spring type for $\beta^{(0)} > 0$, and a soft spring type for $\beta^{(0)} < 0$.

3rd Order Superharmonic Resonance
The influence of the static symmetrical nonlinearity are shown in Fig.5.

Conclusions
Concerning the resonance of superharmonic resonances $[2\omega]$ and $[3\omega]$ in cracked rotors, we obtained the following results:
(1) The static nonlinearity has an influence on the resonances due to a crack. (2) The static unsymmetrical nonlinearity has an influence on the magnitude of the resonance. (3) The static symmetrical nonlinearity has an influence on the inclination of the resonance. It becomes a hard spring type or a soft spring type depending on the sign of the nonlinear coefficient. (4) The results of the theoretical analysis by a power series model agree well with the results of the numerical simulation by a piecewise linear model.

References
(1) Yukio ISHIDA and Toshio YAMAMOTO, Proc.4th International Symposium on Transport Phenomena and Dynamics of Rotating Machinery. vol.B. pp341-350. April 1992
(2) Yukio ISHIDA and Feng LU, Proc. Asia-Pacific Vibration Conference'97. pp714-719.Nov.1997
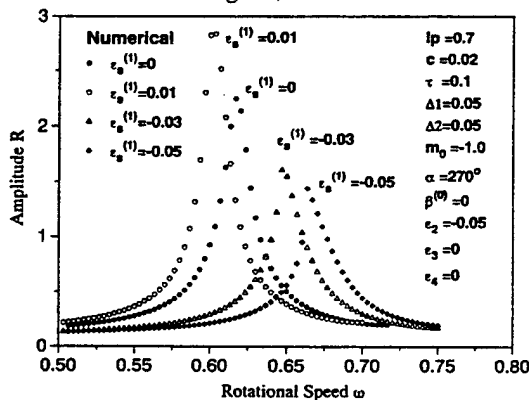
Fig.2 Influence of the static unsymmetrical nonlinearity on 2nd order superharmonic resonance by numerical simulations
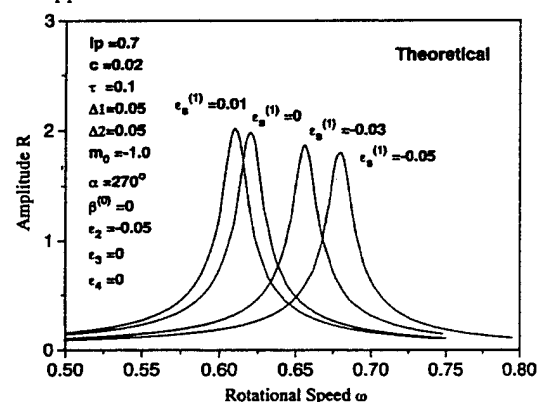
Fig.3 Influence of the static unsymmetrical nonlinearity on 2nd order superharmonic resonance by theoretical analyses
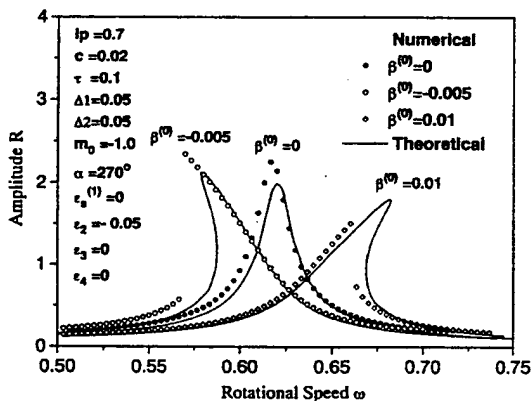

Fig.4 Resonance curve of 2nd order superharmonic resonance with static symmetrical nonlinearity
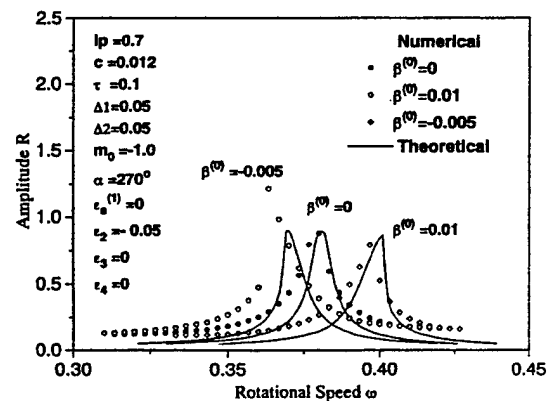
Fig.5 Resonance curve of 3rd order superharmonic resonance with static symmetrical nonlinearity

Simulation study of orbits
with impacts between a rotor and a backup bearing

Horst Ecker

Vienna University of Technology
Wiedner Hauptstr. 8-10/E303, A-1040 Vienna, Austria
Email: hecker@email.tuwien.ac.at

Summary

This paper investigates the steady-state response of a rigid, single mass rotor with imbalance eccentricity supported by an active magnetic bearing with nonlinear characteristic. The rotor may have intermittent contact with a fixed, rigid and circular backup bearing. An offset position of the the backup bearing is assumed.

Backup bearings are necessary to prevent the non-rotating parts of an Active Magnetic Bearing (AMB) from solid contact with the rotor. They are in regular use during the transient behavior of a rotor when a magnetic bearing starts or stops operating and a transfer of support from the backup bearing to the AMB (or vice versa) takes place. However, a rotor might also have intermittent or permanent contact with the backup bearing during steady-state operation due to abnormal operating conditions. This can occur, for instance, due to a bearing overload resulting in an off-center orbit of the rotor which cannot be compensated by the magnetic bearing controller, or a high rotor unbalance leading to a steady-state orbit exceeding the backup bearing clearance. Misalignement of the effective centers of an AMB and the backup bearing in combination with a small clearance between rotor and backup bearing may also cause contact and rub between a rotor and a backup bearing.

This investigation is based on a magnetic bearing actuator that consists of two pairs of opposed electromagnets arranged symmetrically about x-axis and y-axis. Each pair of magnets is independently controlled by an idealized PD-controller based on the magnetic flux in the airgap. However, control is nonlinear since geometric coordinate coupling is taken into account. The magnetic bearing model employed in this investigation was developed in [1] and used in several investigations [2] and [3].

A rather simple model for the backup bearing is used in this investigation. It is assumed that the sleeve bearing is a fixed and rigid ring. This assumption is valid only if the mass and stiffness ratios between the backup bearing housing and the AMB-suspended rotor are sufficiently high As this investigation is mainly focused on the effect of impact friction and bearing offset, the model is kept as simple as possible.

The contact between the rotor and the backup bearing is modeled as an impact of infinitesimally short period of time, occuring between two rigid surfaces with Coulomb friction coefficient μ. Energy dissipation during the impact is accounted for by introducing a coefficient of restitution ε. Different kinds of impact are possible when friction is taken into account. "Sticking impact" occurs when the contact points on both bodies do not move relative to each other within a tangential plane to the contact surfaces. However, for low values of the friction coefficient and/or for a large tangential velocity at the contact point, compared to the radial velocity of the rotor "sliding contact" occurs. Since, in general, the radius of the rotor at the bearing station is much larger than the clearance of the backup bearing, and since the rotational frequency of the rotor is constant, only sliding contact is considered in this investigation.

The nonlinear equations of motion of the rotor were solved by numerical simulation with a state-of-the-art Runge-Kutta algorithm. A state vector was picked from a sufficiently large steady-state orbit without rotor-bearing contact and chosen as initial condition for a single simulation run. In the presented parameter studies the excitation frequency Ω was increased step-by-step. The state vector at the end of the previous simulation run was used as an initial vector for a subsequent run. Usually, the simulation was stopped after 300 revolutions (periods) of the rotor.

Numerically, the most crucial point in this investigation is the precise calculation of the time instant at which a contact occurs. Since the domains of attraction for certain periodic solutions are rather narrow, results can change qualitatively if numerical errors introduced at the instant of contact are not sufficiently small. Therefore, a root finding procedure was started each time when a contact event was detected after an integration step. After calculating

the exact contact time, impact equations were evaluated and integration was restarted with new initial conditions after the impact.

Figure 1 shows bifurcation diagrams for the Y-amplitude of a rotor in a backup bearing with offset values as used in [3]. Note the different frequency ranges and the different scales on the vertical axes of the left and the right figures. The diagrams at the bottom of Fig.1 show the corresponding angular position of the rotor at the contact. In the case of a periodic solution it is shown primarily how many contacts occur during a single period of a periodic orbit. The one-periodic solution for excitation frequencies $\Omega < 0.795$ corresponds to an orbit of the rotor without backup bearing contact. After a bifurcation at $\Omega \cong 0.795$ a stable two-periodic orbit develops. However, above $\Omega \cong 0.805$ this periodic solution was not attracted anymore within 300 periods. A small window with multiperiodic solutions is observed in the frequency range of $0.807 < \Omega < 0.809$. A rather large window with a number of different multi-periodic solutions occurs in the vicinity of $\Omega \cong 0.82$. Above $\Omega \cong 0.823$ quasi-periodic solutions were found.

Figure 2 shows various orbits for selected frequencies, corresponding to the bifurcation map in Fig.1. Note the difference between the two-periodic orbit (a) with one contact at $\Omega = 0.80$ and the complicated twelve-periodic orbit with eighteen contacts at $\Omega =0.822$. Orbit (c) at $\Omega =0.83$ is a quasi-periodic orbit with three contacts.
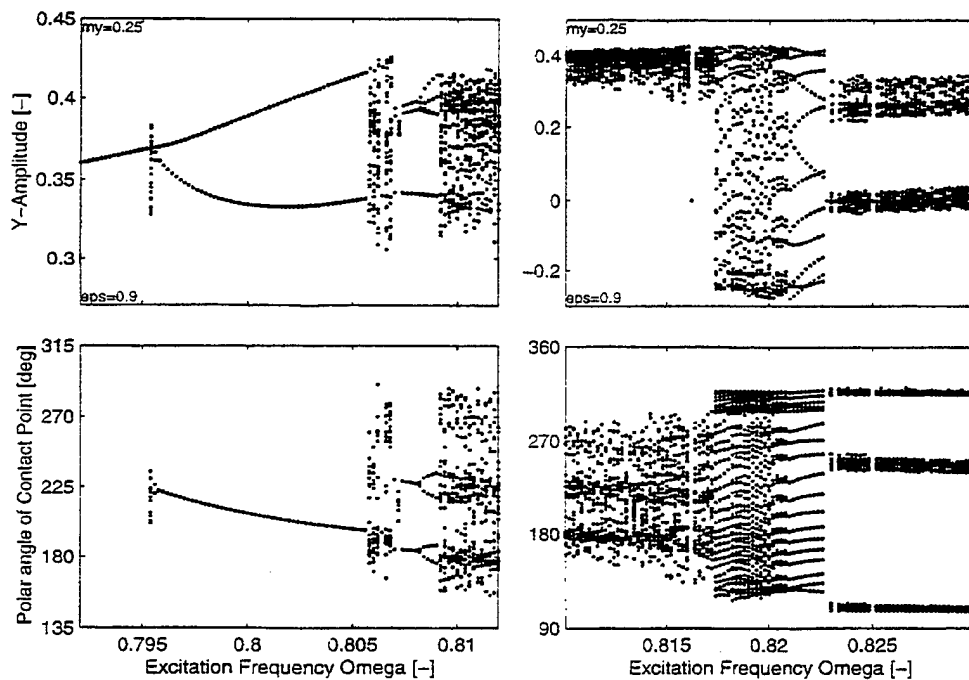
Figure 1: Bifurcation diagram for friction coefficient $\mu=0.25$ and restitution coefficient $\varepsilon=0.9$. Backup bearing offset is approx. 10% of AMB-clearance.
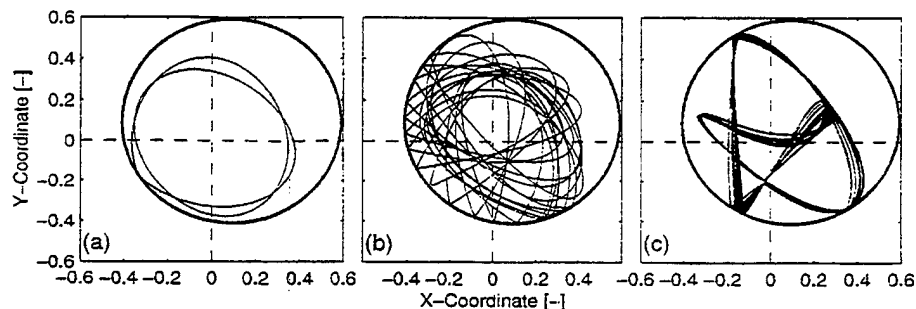
Figure 2: Orbits of the rotor axis within backup bearing clearance corresponding to Fig.1:
(a) $\Omega = 0.80$, (b) $\Omega =0.822$ and (c) $\Omega =0.83$

References

[1] Knight, J.D., Walsh, T.F., Virgin, L.N.: Dynamic analysis of a magnetic bearing system with flux control.

2nd Int. Symposium on Magnetic Suspension Technology (Seattle, WA, July), 359-366, 1993.

[2] Ecker, H., Knight, J.D., Wu, L.: Nonlinear dynamic simulation of an active magnetic bearing with non-symmetric coordinate coupling forces. ASME IGTI Congress, (Orlando, FL, June), 1997.

[3] Ecker, H.: Nonlinear stability analysis of a single mass rotor contacting a rigid backup bearing. Euromech Colloquium 386 „Dynamics of Vibro-Impact Systems", (Loughborough,UK, Sept.), 1998.

Perturbed rotations of a rigid body, close to the Lagrange case

Leonid D. Akulenko and Dmitrii D. Leshchenko

The authors investigated some new problems of the motion of a rigid body about a fixed point under the action of perturbing torque of forces of different physical nature. The motion with the moment of external forces in Lagrange's case is considered as a nonperturbed motion. The influence of the perturbations is determined by the averaging method for the Lagrange-Poisson motion.

We have established the conditions of the feasibility to average (with respect to the nutation angle) the equations of the rigid body motion related to the Lagrange case. The averaged system of equations is obtained and qualitative analysis of motion is conducted. In the case of the rotational motion of the body in the linear-dissipative medium, the numerical integration of the averaged system of equations is conducted.

The authors investigated perturbed rotational motions of a rigid body that are close to regular precession in the Lagrange case. The averaged systems of equations of motion is obtained in the first and second approximations. We considered mechanical models of perturbations related to the rigid body motion in the following cases: a) the linear-dissipative medium; b) under the action of a torque that is constant in the attached axes; c) with the cavity containing viscous fluid; d) with the distribution of mass that is close to Lagrange's case. The qualitative distinctions of the motion in these cases are noted.

The authors investigated perturbed rotational motions of a rigid body that are close to regular precession in the Lagrange case when the restoring torque depends on the nutation angle. Analogously to the case of constant restoring torque, the averaged systems of equations of motion is obtained and investigated in the first and second approximations. For the motion under the action of the resistance torque, applied by the medium, and the torque that is constant in the body-connected axes, we have found out the evolution of the precession and nutation angles.

Dimensionality and spatial coherence in the complex finite dynamics of an experimental continuous elastic system

R. Alaggio (°), G. Rega ("), and F. Benedettini (°)

(") Dipartimento di Ingegneria delle Strutture, Acque e Terreno, Università dell'Aquila, L'Aquila, Italy
(") Dipartimento di Ingegneria Strutturale e Geotecnica, Università di Roma La Sapienza, Roma, Italy

The in-depth characterization of the nonregular finite dynamics of an experimental flexible continuous system on the basis of measures of its nonregular response involves some main steps: (i) quantitatively characterizing complex attractors as to strangeness and chaoticity; (ii) describing bifurcation paths in parameter space, with main attention devoted to transition from regular to nonregular dynamics; (iii) locally and globally characterizing the flow structure in phase space; (iv) identifying the configuration variables that mostly contribute to nonregular motions. The analysis of the asymptotic response has to be performed on attractors reconstructed by means of the delay-embedding technique. The topic of the system dimensionality has to be tackled by performing an analysis of the spatial coherence of the nonregular flow, too. The consistency between attractor dimension calculations and spatial coherence calculations has to be verified. All previous topics, besides being of interest in themselves, are necessary steps for building and verifying proper mathematical models of the experimental system.

In this work, the relevant analyses are made with reference to an experimental elastic cable/mass model hanging at two supports which can move sinusoidally either in phase or out-of-phase in the vertical plane. The system parameters realize a condition of 2:2:1 multiple internal resonance involving the first antisymmetric in-plane (V2) and out-of-plane (H2) modes, and the first symmetric out-of-plane (H1) mode. In previous works (Rega et al., 1997), the regular response of the system over wide ranges of excitation frequency was studied. Very rich regular dynamics, as well as some zones of nonregular motion, were observed. The transition to nonregular dynamics is herein investigated in-depth in various external resonance zones, characterizing the bifurcation paths and identifying the involved configuration variables.

Though being the non-regular behaviour quite varied, the bifurcation paths exhibited near primary and ½-subharmonic resonance conditions can be traced back to two canonical scenarios of dynamical systems, which are here seen to compete sometimes with each other: (i) the quasiperiodic scenario and (ii) a scenario in which is involved the global bifurcation of an homoclinic invariant set of the symmetric flow. The nonregular dynamics exhibited by the continuous system in each of the two resonance zones has low correlation dimension $(2 < Dc < 4)$, and the first scenario generally results in higher correlation and linear phase space dimensions.

Attention is mostly focused on the quasiperiodic scenario, which is recognized responsible for transition to chaos in primary and ½- subharmonic resonance zone with in-phase and out-of-phase support motion, respectively. The results we deal with refer to the former condition. The system exhibits a strongly varied behaviour due to the involvement in the dynamics of a third harmonic of frequency incommensurable compared to the two harmonics formerly responsible for a two-frequency quasiperiodic motion, namely the first in-plane (V1) and out-of-plane (H1) modes of the cable (motion on a 2-Torus). The spatial coherence analysis shows that the first antisymmetric out-of-plane mode (H2) is the one responsible for the further incommensurability. In the overall transition region the model shows a close sequence of regular and nonregular response classes: (i) two-frequency quasiperiodic motions on two-dimensional manifolds; (ii) two-frequency phase-locked quasiperiodic motions on three-dimensional manifolds; (iii) stable three-frequency quasiperiodic motions; (iv) chaotic motions ensuing from evolution of unstable three-frequency quasiperiodic motions; (v) phase-locked periodic solutions which are invariant sets of dimension 1 on three-dimensional manifolds. Various types of bifurcation are documented: (i) transition from 2T-quasiperiodic (on a 2-Torus, as well as phase-locked on a 3-Torus) to stable 3T-quasiperiodic; (ii) transition from stable to unstable 3T-quasiperiodic, with evolution of the latter towards a chaotic attractor; (iii) phase-locking of chaotic motion on a 2T-quasiperiodic attractor and of stable 3T-quasiperiodic motion on high periodicity solutions. Due to subsequent Hopf bifurcations, the number of configuration variables (experimental eigenfunctions) involved in the motion grows - from 1 (periodic motion: V1) to 2 (2T-quasiperiodic: V1, H1) to 3 (3T-quasiperiodic, phase locked 2T-quasiperiodic, phase locked periodic motions: V1, H1, H2). Almost the whole power of the chaotic response can be decomposed on a three-modal (V1, H1, H2) basis, thus showing that the dynamics of the continuous system – which are governed by relatively few modes in the regular response regions - remain substantially low-dimensional in nonregular regions, too. In any case, the importance of the first antisymmetric out-of-plane mode (H2) in the transition to nonregular motion is recognized.

Some results relevant to the second recognized scenario, which involves the bifurcation of an homoclinic invariant set in a symmetric flow, are also presented.

The second recognized scenario manifests itself at one edge of the stability zone of the antisymmetric ballooning regular motions characterized by the coupling VnHn (n = even, antisymmetric modes, respectively in-plane and out-of-plane). Due to the nature of the phenomenon (herein illustrated for the case of ½-subharmonic resonance and out-of-phase motion), the experimental analysis regards not only attractor global properties (as dimension or strangeness) but also the flow structure, in particular the presence and the features (dimension and stability) of associated invariant sets. When the cable model follows the aforementioned scenario, the attractors exhibited in chaotic zones show the lowest observed dimensionality: indeed, the transition from regular to nonregular behaviour happens without increasing the number of involved modes over the two (Vn, Hn) already present in the neighboring regular zones.

Modeling and Analysis

of Switching-Mode DC-DC Regulators

M. Alfayyoumi   A. H. Nayfeh   D. Borojevic

Virginia Polytechnic Institute and State University

Blacksburg, Virginia 24061

Abstract

The nonlinear dynamics of PWM DC-DC switching regulators operating in the continuous conduction mode are investigated. A quick review of the existing analysis techniques of DC-DC PWM switching converters and their limitations are first presented. A discrete nonlinear time-domain model is developed for open-loop DC-DC converters. This model is then extended to closed-loop regulator systems implementing any type of compensation scheme. The equilibrium solutions of the closed-loop regulator system are then identified. The eigenvalues of the Jacobian matrix evaluated at the equilibrium solution of the discrete nonlinear system are used to asses its stability. The methods developed are used to study the dynamic behavior of a buck DC-DC regulator implementing different types of compensation design: proportional, integral, proportional-integral, and proportional-integral-derivative feedback control. A detailed bifurcation analysis of the dynamic solutions as a design or a control parameter is changed is presented. An interesting period-doubling route to chaos is shown to be inherent in voltage-mode regulators, depending on the parameter values of the compensator. A comparison with the expected behavior of the system using averaged techniques is also presented. The equilibrium solutions and their stability were also found to be in agreement with the results obtained using iterative mapping. Further investigations were carried out to identify the chaotic behavior and improve the understanding of DC-DC converters operating in chaotic regions.

Thursday, July 30
0800-0930
Session 15.

The Characterization of Stochastic Layers in Duffing Oscillators

Albert C.J. Luo, NSERC Post-Doctoral Fellow
Department of Mechanical Engineering
University of California, Berkeley, CA 94720

Ray P.S. Han, Professor
Department of Mechanical Engineering
University of Iowa, Iowa City, Iowa 52242-1527

Extended Abstract

A new analytical approach to study stochastic layers in the vicinity of a separatrix is proposed in this work, so as to gain a better understanding of the chaotic motion caused by the interaction of nonlinear resonance in Hamiltonian systems. It is based on an accurate whisker map formed by energy increments and resonant conditions. Noting that their resonant conditions are different, it is proposed that the stochastic layer be divided by the separatrix into 2 subdomains termed the α and β-layers. For the twin-well potential Duffing oscillator, they correspond respectively, to the inner and outer layers with the following characteristics; for the former, the resonant order is based on the $(m{:}1)$ resonant orbit and for the latter, the $\left((2n-1){:}1\right)$ resonant orbit. This is contrary to existing approaches where the resonant order is selected arbitrarily. We called our approach the incremental energy (IE) method.

Consider a 2-D time-periodic system:

$$\dot{x} = f(x) + g(x,t); \quad x = \begin{pmatrix} x \\ y \end{pmatrix} \in \Re^2, \tag{1}$$

in which $f(x)$ is an unperturbed Hamiltonian vector field on $\Re^2$ and $g(x,t)$ is a T-periodic, time-dependent Hamiltonian. They are of the form given by,

$$f(x) = \begin{pmatrix} f_1(x) \\ f_2(x) \end{pmatrix}, \text{ and } g(x,t) = \begin{pmatrix} g_1(x,t) \\ g_2(x,t) \end{pmatrix}, \tag{2}$$

and assumed to be sufficiently smooth (C^r, $r \geq 2$) and bounded on bounded sets $D \subset \Re^2$ in

the phase space. The total Hamiltonian of *Eq.* (1) comprises an unperturbed and a perturbed Hamiltonian, $H_0(x,y)$ and $H_1(x,y,t)$ respectively. That is

$$H(x,y,t) = H_0(x,y) + H_1(x,y,t).$$ (3)

In view of *Eq.* (3), the terms in *Eq.* (2) can be expressed by,

$$\left. \begin{aligned} f_1 &= \frac{\partial H_0}{\partial y}, f_2 = -\frac{\partial H_0}{\partial x}, \\ g_1 &= \frac{\partial H_1}{\partial y}, \ g_2 = -\frac{\partial H_1}{\partial x}. \end{aligned} \right\}$$ (4)

In transiting from t_i to $t_i + T_\alpha$ in *Eq.* (3), the map that describes the change of $H_0(x,y)$ and the phase angle in $supp\Gamma^\alpha$ is given by

$$\left. \begin{aligned} E_{i+1} &= E_i + \Delta H_0^\alpha(\varphi_i), \\ \varphi_{i+1} &= \varphi_i + \Delta\varphi^\alpha(E_{i+1}); \end{aligned} \right\}$$ (5)

where $E_i = H_0(q(t_i))$, $\varphi_i = \varphi(q(t_i))$. Also, in *Eq.* (5), $\Delta H_0^\alpha(\varphi_i)$ denotes the energy increment of *Eq.* (1) based on the α-orbit of E_i for the initial phase angle φ_i, and $\Delta\varphi^\alpha(E_{i+1})$ denotes the change of phase angle related to the α-orbit. The map of $supp\Gamma^\beta$ can be obtained in a same manner. If $E_i = E_0$ is the energy of the separatrix, *Eq.* (5) becomes the generalized separatrix map (or the generalized whisker map).

In *Eq.* (1), if $\forall \varepsilon > 0$, $\exists \delta > 0$ and the resonance number set at $(m_\alpha : n_\alpha) \in R_\alpha^\varepsilon$ (or $(m_\beta : n_\beta) \in R_\beta^\varepsilon$), the strength of excitation can be determined from,

$$\left| \Delta H_0^\alpha(\varphi_0) \right| = \left| E_\alpha^{m_\alpha/n_\alpha} - E_0 \right| \leq \delta \ \text{ or } \ \left| \Delta H_0^\beta(\varphi_0) \right| = \left| E_\beta^{m_\beta/n_\beta} - E_0 \right| \leq \delta .$$ (6)

This provides for an analytic prediction (instead of numerical) when the specific resonance $(m_\alpha : n_\alpha) \in R_\alpha^\varepsilon$ is absorbed into the stochastic layer. Note that the resonant number sets in the stochastic layer are defined as

$$R_\alpha^\varepsilon = \left\{ (m_\alpha : n_\alpha) \,\middle|\, m_\alpha \omega_\alpha = n_\alpha \Omega, \; m_\alpha, n_\alpha \in \aleph \text{ are irreducible, and } |q_\alpha(t) - q_0(t)| < \varepsilon \right\},$$
$$R_\beta^\varepsilon = \left\{ (m_\beta : n_\beta) \,\middle|\, m_\beta \omega_\beta = n_\beta \Omega, \; m_\beta, n_\beta \in \aleph \text{ are irreducible, and } |q_\beta(t) - q_0(t)| < \varepsilon \right\}. \tag{7}$$

The condition given by *Eq.* (6) implies that the current practice of restricting the excitation strength Q_0 to small values in order to preserve computational accuracy of the energy increments becomes unnecessary. We find that it is more meaningful to apply this limitation on a parameter γ pertaining to the elliptic modulus of the unperturbed orbit. Since this parameter is independent of Q_0, we showed from its usage that good accuracy is maintained even for very strong excitations. Additionally, it is found that if the energy of the resonant orbits is employed in evaluating the IE-based Q_0, the result will remain bounded for all magnitudes of Q_0.

As a illustration of the proposed method, the twin-well potential Duffing oscillator is investigated. Using the IE approach, the excitation strength based on the energy of the resonant orbit, as well as that from the homoclinic orbit are determined. Also, similar results based on approximate and accurate standard mapping methods, the Chirikov overlap criterion and the renormalization group technique are computed. These and the IE-computed results are then compared against numerically generated solutions obtained via a symplectic scheme. Good agreement is observed in all cases. Finally, Poincare mapping sections are provided to illustrate these stochastic layers and to demonstrate the good agreement between the analytical and the numerical predictions of the number of resonance observed in the computer simulations.

Title: Instant chaos and hysteresis in beam-pendulum systems

Authors: Ira B. Schwartz[1] and Ioannis T. Georgiou[2]

Mailing Address: US Naval Research Laboratory, Special Project for Nonlinear Science, Code 6700.3, Plasma Physics Division, Washington, DC 20375-5320

Electronic Mail: schwartz@nls4.nrl.navy.mil

FAX: 202 767 8357   **Phone: 202 404 8359**

Abstract: A novel bifurcation to high-dimensional hyperchaos is observed in a driven coupled pendulum-flexible rod system. When the rod is in resonance with the pendulum, the system changes from a low dimensional periodic attractor to a high dimensional chaotic attractor abruptly. The bifurcation, which is hysteretic, is conjectured to stem from an unstable global invariant manifold of slow frequency motions.

One of the prime problems studied in physics is that of the forced, damped pendulum [1,2]. Studied extensively in isolation, the pendulum is always attached to some support. If the rod is sufficiently stiff, one expects the pendulum dynamics to be slightly perturbed from the ideal infinitely stiff case. However, if the rod itself is sufficiently flexible, the overall picture may be changed dramatically. In this letter we report on some new dynamical behavior in the numerical simulations of a forced, damped pendulum coupled to a linear rod which is flexible. In particular, we examine the system when it is operating in a resonant mode, where the pendulum frequency is half that of the fundamental frequency of the rod. It is known that when the rod is sufficiently stiff, the dynamics resides on a global slow invariant manifold; i.e., the rod is slaved to the motion of the pendulum [3]. As a result of this slaving motion, the dynamics is a perturbation of a parametrically driven pendulum. However, when operating at resonance, the dynamics changes dramatically in that there exists some critical amplitude of the driving force that causes an abrupt change from periodic behavior to high dimensional hyper-chaotic behavior, where there are two or more positive Lyapunov exponents. That is, there is no bifurcation sequence to chaotic behavior since the chaos appears discontinuously. In contrast, low dimensional systems which either possess certain symmetries [4] or have piecewise linear vector fields [5], have also produced what is termed "instant chaos". When chaos appears, it is small amplitude in nature, implying it bifurcates as a supercritical bifurcation [5]. In our model, we have smooth vector fields, and the chaos appears as high dimensional dynamics. Furthermore, it appears as a subcritical bifurcation point since it exhibits hysteretic behavior as a function of amplitude forcing.

{1} F. C. Moon, CHAOS 1,31 (1991); P. V. Bayly and L. N. Virgin, Inter. J. Bifur-

1. Presenter
2. Currently a Science and Research Associate with SAIC, McClean, VA

cation and Chaos in Appl. Sci. and Eng. s, 983 (1992); G. L. Baker, J. P. Gollub and J. A. Blackburn, CHAOS 6, 528 (1996), P. M. Battelino, C. Grebogi, E. Ott, and J. A. Yorke, Physica D 32, 296 (1988)J. W. Miles and Q. -P. Zou, J Sound and Vibration 164, 237 (1993).

{2} D'Humieres, D.; Beasley, M.; Huberman, B.A.; Libchaber, A., Phys. Rev. A. 26, 3483 (1982).

{3} Ioannis T. Georgiou and Ira B. Schwartz, International Journal of Bifurcation and Chaos, 6 673-692, (1996); Ioannis T. Georgiou and Ira B. Schwartz, Dynamics of Large Scale Coupled Structural-Mechanical Systems: A Singular Perturbation-Proper Orthogonal Decomposition Approach, Siam J. Appl. Math. submitted [1997].

{4} Guckenheimer, J. and Worfolk, P. Instant chaos, Nonlinearity 5, 1211-1222 (1992)

{5} Ohnishi, M. and Inaba, N., A singular bifurcation into instant chaos in a piecewise-linear circuit, IEEE Trans. Cir. Systems, vol. 41, pp. 433-442 (1994).

SYNCHRONISATION AND CHAOS IN A PARAMETRICALLY AND SELF-EXCITED SYSTEM WITH TWO DEGREES OF FREEDOM

Jerzy Warmiński, Grzegorz Litak, Kazimierz Szabelski

Department of Applied Mechanics, Technical University of Lublin, Nadbystrzycka 36 str., 20-618 Lublin, Poland

1. Introduction

Vibrations described by differential equations with self-excited as well as parametric excitation terms occur in some dynamic systems [1,2,4]. Systems with one degree of freedom have been studied deeply by Tondl [1] and Yano [2]. Recently systems wth many degrees of freedom attract the interest in context of chaotic vibrations and synchronization phenomena [3]. Such type of differential equations one can also meet while describing some mechanisms of vibrations generation in case of manufacture processes [6].

2. Vibrating system model

Dimensionless equations of motion can be written as:

$$\ddot{X}_1 + (-\alpha_1 + \beta_1 X_1^2)\dot{X}_1 + \delta_1 X_1 + \gamma_1 X_1^3 + (\delta_2 - \mu\cos 2\vartheta\tau)(X_1 - X_2) = 0$$

$$\ddot{X}_2 + M(-\alpha_1 + \beta_1 X_2^2)\dot{X}_2 + M\delta_1 X_2 + M\gamma_1 X_2^3 - M(\delta_2 - \mu\cos 2\vartheta\tau)(X_1 - X_2) = 0$$

The mathematical model consists of two Van der Pol oscillators with Duffing, coupled by linear spring with periodically changing elasticity. The physical model of this system is presented in Fig.1.
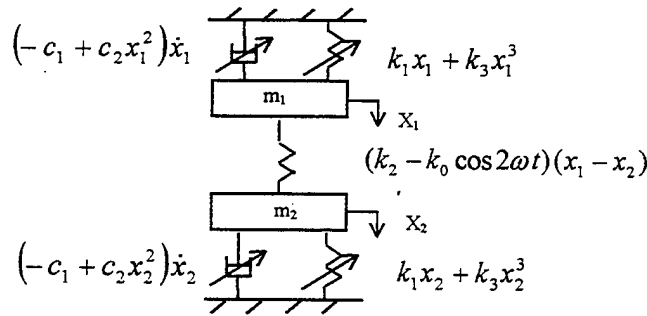
Fig.1 Physical model of the parametric self-excited system

3. Regular and Chaotic Vibrations

We have made the simulations of the examined system for various sets of parameters. For small value of parameter μ the system has periodic and quasi-periodic solutions. In Fig. 2a we present the bifurcation diagram versus excitation frequency $\vartheta=[0.5,1.5]$ and $\alpha_1=0.01$, $\beta_1=0.05$, $\gamma_1=0.3$, $\mu=1.6$, $M=1.0$, $\delta_1=0.1$, $\delta_2=0.3$. The picture shows a number of interesting details of bifurcations. In the major part of this plot periodic oscillations, represented by singular points for given value of ϑ, are visible however the region of vibrations near $\vartheta=1.0$ exhibits chaotic vibrations represented by a dark interval. Examples of phase diagrams for co-ordinates x_1, x'_1 for chaotic solutions are presented in Fig 2b.
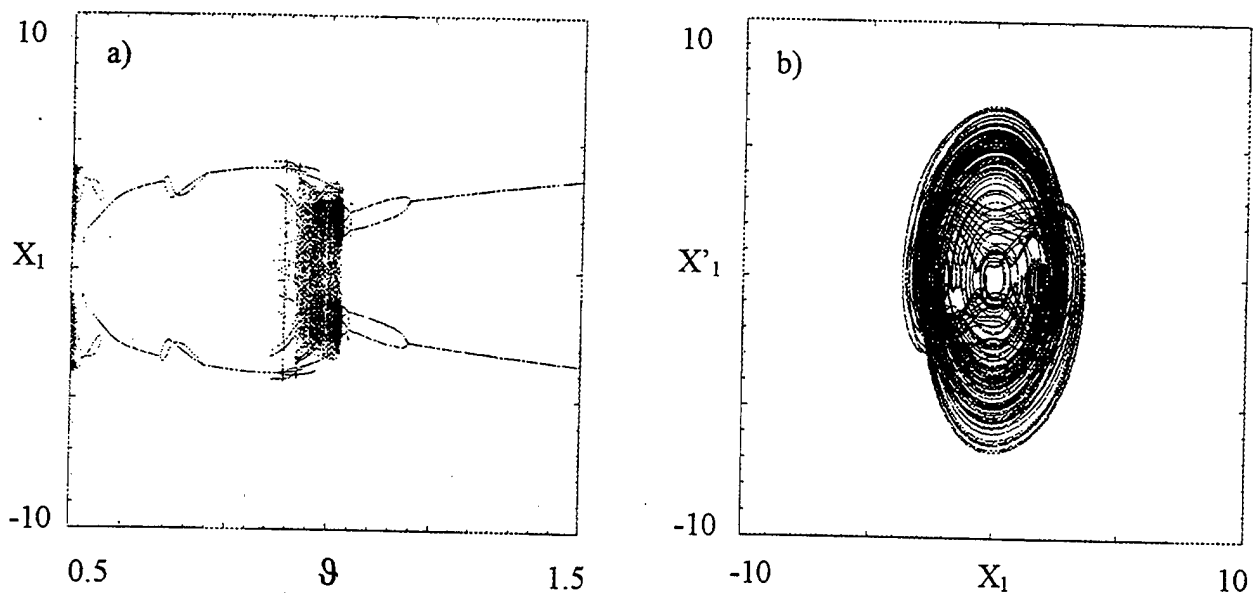
Fig.2 Bifurcations diagram versus θ parameter (a); phase diagram chaotic vibration for θ=1.0 (b)

4 Remarks and Conclusions

In this note we have investigated the complex system of coupled non-linear oscillators excited parametrically. As usual the interaction between self-excited and parametric excitation leaded to a number of interesting results like entrainment of frequency and synchronisation phenomena. The transition from regular to chaotic solutions was discussed. The paper is the continuation of [5] where authors carried out a detailed analysis of one parametrically excited van der Pol oscillator.

References

1. A.Tondl, 'On the interaction between self-excited and parametric vibrations', *National Research Institute for Machine Design, Monographs and Memoranda* No.25 Prague 1978
2. S.Yano, 'Considerations on self-and parametrically excited vibrational systems' Ingenieur-Archiv 59, 285-295, 1989
3. T.Kapitaniak , O.Chua Leon 'Locally-Intemingled Basins of Attraction in Coupled Chua's Circuits' *Int. Journal of Bifurcations and Chaos*, Vol.6,No2, 357-366,1996
4. K.Szabelski, J.Warmiński, The non-linear vibrations of parametrically self - excited system with two degrees of freedom under external excitation. *Int. Journal of Nonlinear Dynamics* 14:23-36,1997
5. G.Litak, K.Szabelski, J.Warmiński, G.Spuz-Szpos, Vibration Analysis of Self-Excited System with Parametric Forcing and Nonlinear Stiffnes, *International Journal of Bifurkation and Chaos* ,1998, in press
6. M. Wiercigroch, Chaotic vibrations of a simple model of the machine tool - cutting process system, *Transactions of ASME, Journal of Vibration and Acoustics*, Vol. 119, 468-475,1997

Experiments on the Chaotic Vibrations of a Cylindrical Shell-Panel: Influence of Boundary Condition on Chaotic Responses

Ken-ichi NAGAI
Department of Mechanical Engineering
Gunma University, 1-5-1 Tenjincho, Kiryu, Gunma 376-0052, Japan
E-mail: nagai@cc.gunma-u.ac.jp
Takayuki HATA
ANEST IWATA Co, Ltd., Yokohama 223-0056, Japan
Takao YAMAGUCHI
SUBARU Research Center Co, Ltd., Ota, Gunma 373-0026, Japan

Experimental results are presented for chaotic vibrations of shallow cylindrical shell-panels with square boundary under periodic lateral excitations. The chaotic responses of the shells are tested under two different boundary conditions. Both curved sides of the shell boundary are simply supported and other straight sides include a pair of free edges or a pair of simply supported edges. Two boundary conditions are distinguished by a symbol (SF) of the shell having the free edges and the symbol (SS) with all edges simply supported. As shown in Figure 1, the simply supported edge of the shell is formed to be a rounded edge to swing on a flat wall of boundary. Adhesive films connect the edge to the shell frame. Static deflections due to concentrated static force and natural frequencies with small amplitude are measured. Changing the exciting frequency, chaotic regions are examined carefully in the frequency response test. The chaotic responses of the shell are confirmed by the Fourier spectrum analysis, the Poincaré projection and the maximum Lyapunov exponent. Frequency regions of the chaos are plotted in various excitation amplitudes. The vibrator shakes both the shell and the shell frame. The relative displacement of the shell to the supporting frame is measured by two laser displacement sensors and the chaotic responses are recorded. The representative non-dimensional notations are introduced as follows;

$$\xi = x/a, \ \eta = y/b, \ \alpha = a^2/Rh, \ \beta = a/b, \ w = W/h, \ p_d = a_d \rho a^4/D, \ q_s = Q_s a^2 \beta/Dh, \ \tau = \Omega_0 t, \ \omega = 2\pi f/\Omega_0 \quad (1)$$

$$D = Eh^3/12(1 - v^2), \ \Omega_0 = (1/a^2)\sqrt{D/\rho h}, \quad (2)$$

where, α is the non-dimensional shell curvature. β is the aspect ratio of the side length of the rectangular boundary. p_d is the non-dimensional intensity of distributed load due to the periodic acceleration a_d. q_s is the non-dimensional static load by the concentrated load Q_s. D is the bending rigidity of the shell. ω and τ are the non-dimensional exciting frequency and the non-dimensional time, respectively. f is the exciting frequency.
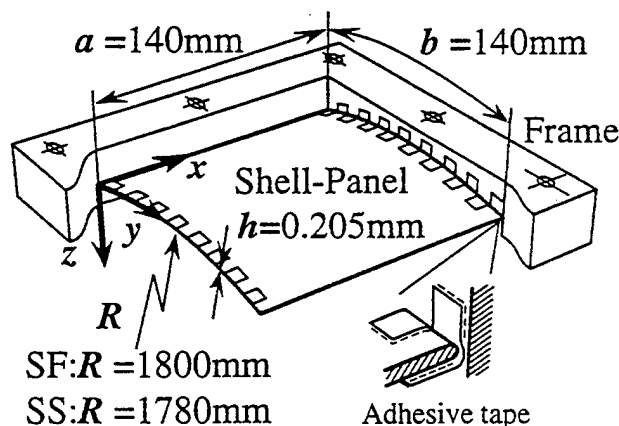
Figure. 1 Cylindrical shell-panel and frame
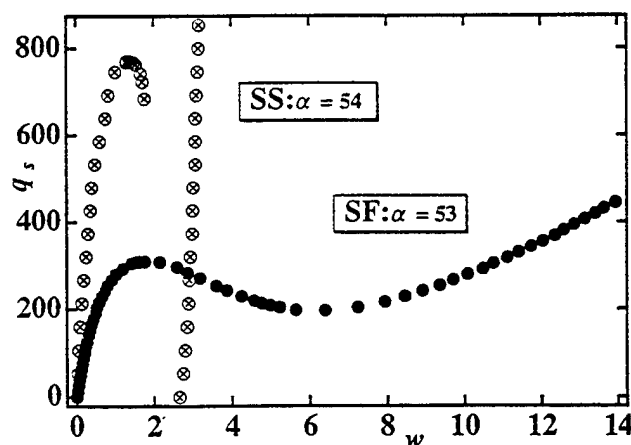
Figure.2 Deflection of the shells under concentrated load acting on the center and measured at $\xi=0.6$, $\eta=0.4$

The shell curvatures $\alpha = 53$ of the (SF) and $\alpha = 54$ of the (SS) are tested. Figure 2 shows the static deflection w under the concentrated static force q_s. Both of shells show the soft-hardening spring included negative slope. Figure 3 shows the frequency response curves. w_{rms} is the root mean square value of the periodic response. ω is the non-dimensional exciting frequency. In the figure, chaotic responses are assigned by name of chaos. A sign (m,n) denotes the mode of vibration with small amplitude, while the integer m and n imply predominant half wave number of the deflection in the x-direction and y-direction, respectively. Figure 4 shows the Poincaré maps of the chaos at the phase delay θ measured from the maximum amplitude of the exciting force.

It is found that following results: the typical chaos attractors of the shells are focused onto the Poincaré section. The chaotic responses of the shells are generated mainly close to the principal resonance response. The chaos of the shell is emerged mainly due to the characteristics of dynamic snap-through. In a higher frequency range, the chaos is excited accompanied with an internal resonance condition of multiple modes of vibration. The maximum Lyapunov exponents for individual chaotic responses of the shell including the free edges are ranging from 0.03 to 0.15, while the values of the shell of all edges simply supported are taken within 0.1 to 0.4.

References

1. Nagai, K., 'Experimental study of chaotic vibration of a clamped beam subjected to periodic lateral forces', *Trans. of Japan Soci. of Mech. Engrs* 56-525, 1990, 1171-1177 (in Japanese).
2. Nagai, K. and Yamaguchi, T., 'Chaotic vibrations of a post-buckled beam carrying a concentrated mass (1st Report, Experiment)', *Trans. of Japan Soci. of Mech. Engrs* 60-579, 1994, 3733-3740 (in Japanese).
3. Yamaguchi, T. and Nagai, K., 'Chaotic vibrations of a post- buckled beam carrying a concentrated mass (2nd Report, Theoretical Analysis)', *Trans.of Japan Soci. of Mech. Engrs* 60-579, 1994, 3741-3748 (in Japanese).
4. Nayfeh, A.H., Raouf, R.A. and Nayfeh, J.F.,'Nonlinear response of infinitely long circular cylindrical shells to subharmonic radical loads', *J. of Applied Mech.*, 58, 1991, 1033-1041.
5. Maestrello, L., Frendi, A. and Brown,D.E., 'Nonlinear vibration and radiation from a panel with transition to chaos', *AIAA J.*, 30-11, 1992, 2632-2638.
6. Nagai, K. and Yamaguchi, T.,'Chaotic oscillations of a shallow cylindrical shell with rectangular boundary under cyclic excitaion', *High Pressure Technology*, PVP- Vol. 297, 1995, ASME, 107-115.
7. Yamaguchi, T. and Nagai, K. , 'Chaotic Vibrations of a Cylindrical Shell-Panel with an In-plane Elastic-Support at Boundary', *Nonlinear Dynamics*, 13-3, 1997, 259-277.
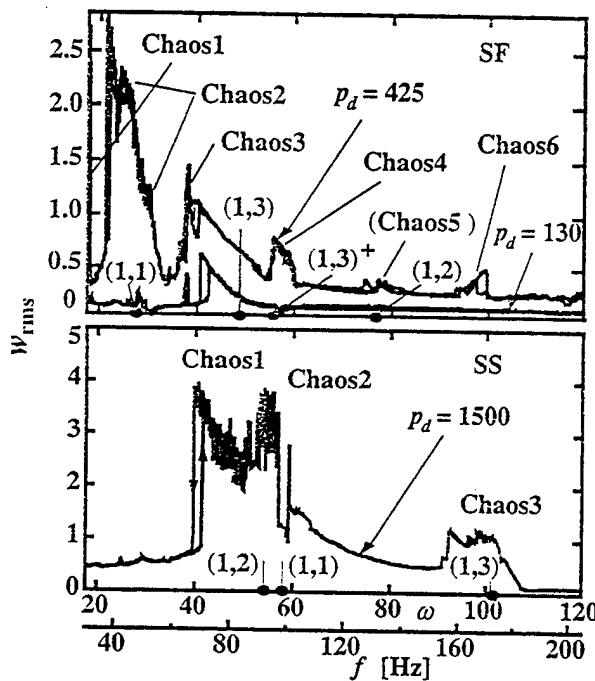8. Wolf, A., et al., 'Determining Lyapunov exponents from a time series', *Physica* 16D ,1985, 285-317.

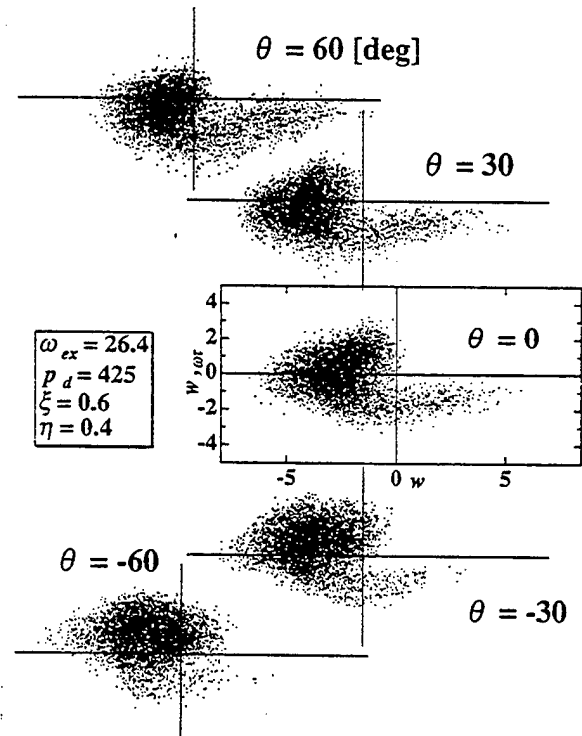*Figure.3* Frequency responses curves of the shell

Figure.4 Poincaré map of the shells (SF) boundary

On the Appearance of Chaos in a Nonideal System

D. Belato[1], J.M. Balthazar[2], H.I. Weber[3], and D.T. Mook[4]

[1] Faculdade de Engenharia Mecânica, UNICAMP, CP 6122.CEP 13083-970 Campinas-SP-Brazil
[2] Instituto de Geociências e Ciências, UNESP, CP 178.CEP 13500-230, Rio Claro-SP-Brazil
[3] Pontifica Univesidade Católica-PUC, CEP 22453-900, Rio de Janeiro-RJ-Brasil
[4] Engineering Science and Mechanics Department, VPISU, Blacksburg, VA 24061 USA

Abstract. *A nonlinear dynamic system consisting of a simple pendulum with a moving pivot is investigated. A nonideal DC motor produces an oscillatory motion of the pivot. Near resonance the response of the system can exhibit intermittent chaos.*

Introduction. Generally, in modeling vibrating mechanical systems, one assumes that the external driving force is not influenced by the response of the system; such systems are said to be ideal. In many practical situations, however, a small force excites a relatively large mechanical system, and the excitation can no longer be considered ideal; one must account for the influence of the response on the excitation. One must include governing equations for the excitation, which gives the system an additional degree of freedom, and determine the vibrations and the excitation simultaneously. Nonideal systems were exhaustively studied by Kononenko (1969), and a complete overview of different approaches and bibliographic references was presented by Balthazar et al. (1998).

The particular mechansim considered here consists of a simple pendulum whose pivot is forced to oscillate along a horizontal axis by a nonideal DC motor as shown in Figure 1. We investigated this system by numerically integrating the equations of motion and found that it displays complex behavior as the control parameter (voltage supplied to the motor) is varied. Near the fundamental resonance, there is a transition from periodic to aperiodic motion through an intermittent phenomenon. Krasnopol'skaya and Shvets (1990,1993) studied a similar system using an averaging method. They also found that the system exhibited periodic as well as chaotic responses.

Equations of Motion. The equations of motion are given by the following [see Belato (1998) for the details]:
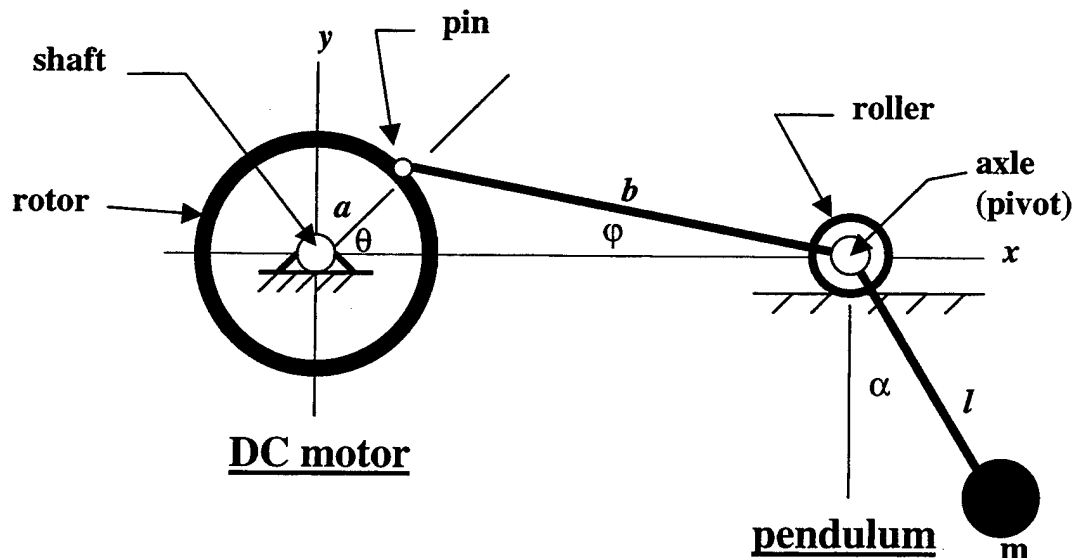
Figure 1. Schematic of the electromotor-pendulum system

$$(J + \beta_4 F^2 \sin^2 \alpha)\ddot{\theta} = \beta_1 - (\beta_2 + \beta_3 F^2)\dot{\theta} - \beta_4(\sin^2 \alpha)F\dot{F}\theta - \beta_5 F(\cos\alpha + \dot{\alpha}^2)\sin\alpha$$

$$\ddot{\alpha} + \sin\alpha = \varepsilon_2(F\ddot{\theta} + \dot{F}\dot{\theta})\cos\alpha - \beta_6\dot{\alpha}$$

where

$$F = \left[1 + \frac{\varepsilon_1 \cos\theta}{\sqrt{1 - \varepsilon_1^2 \sin^2\theta}}\right]\sin\theta, \quad t^* = \omega t, \quad \beta_1 \text{ is the control parameter}, \quad \beta_2 = \frac{K_T K_E}{R\omega} + \frac{c_m}{\omega},$$

$$\beta_3 = \frac{c_3 a^2}{\omega}, \quad \beta_4 = ma^2, \quad \beta_5 = mal, \quad \beta_6 = \frac{\mu}{\omega ml^2}, \quad \varepsilon_1 = \frac{a}{b}, \quad \varepsilon_2 = \frac{a}{l}$$

and the overdot indicates the derivative with respect to t^*; c3 is the damping coefficient for the friction at the axle (pivot); μ is the damping coefficient and ω is the natural frequency for the pendulum; and J is the moment of inertia of the rotor, R is the electrical resistance, K_T is the torque constant, K_E is the back EMF constant, and c_m is the internal-loss constant for the motor.

Numerical Simulations and Concluding remarks. SIMULINK™ was used to numerically integrate these equations for the following parameters and initial conditions: $\beta_2 = 0.02448$, $\beta_3 = 0$, $\beta_4 = 0.002$, $\beta_5 = 0.0084$, $\beta_6 = 0.01$, and $\varepsilon_1 = \varepsilon_2 = 0.233$ and $\theta(0) = \alpha(0) = 0$ and $\dot{\theta}(0) = \dot{\alpha}(0) = 0$. In Figure 2 α is plotted as a function of time for two values of the control parameter: (a) $\beta_1 = 0.02253$ and (b) $\beta_1 = 0.02254$. For the former the motion is periodic, and for the latter it is aperiodic with random bursts in the regular regime.
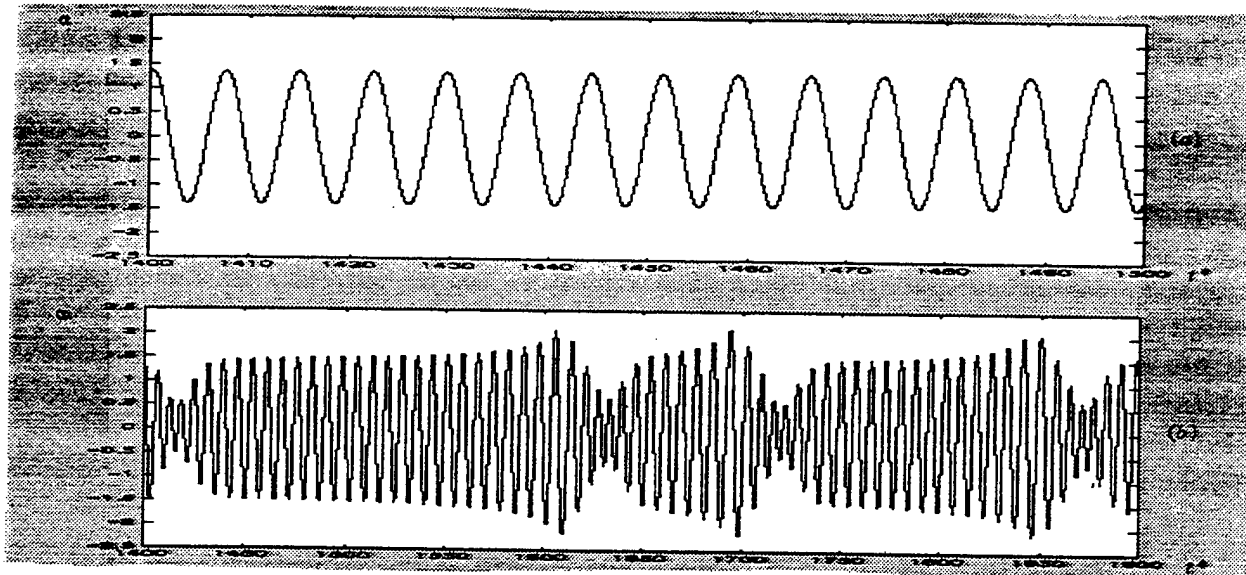
Figure 2. α **as a function of time:** (a) $\beta_1 = 0.02253$ and (b) $\beta_1 = 0.02254$

Balthazar JM, Mook DT, Weber HI, Mattos MC, and Weiczorec S, *The State of the Art on Nonideal Vibrations*, J. Brazilian Society of Mechanical Sciences, to appear in 1998.

Belato D, Balthazar JM, Weber HI, and Mook DT, *On the Nonlinear Vibrations of a Nonideal Electromotor-Pendulum*, Proceedings of the 14th Brazilian Congress of Mechanical Engineering, 1997.

Belato D, *Não Linearidades do Eletro-Pêndulo*, Master's Thesis (in Portuguese), Faculdade de Engenharia Mecânica da Universidade Estadual de Campinas, Campinas-SP-Brazil, 1998.

Krasnopol'skaya TS and Shvets AYu, *Chaotic Interactions in a Pendulum-Energy Source System*, Prikladnaya Mekhanika, 26, 5, 1990, and *Chaos in Systems with a Limited Power Supply*, 29, 3, 1993.

Kononenko VO, *Vibrating Systems with a Limited Power Supply*, Iliffe Books, London, 1969.

Pomeau Y and Manneville P, *Intermittent Transition to Turbulence in Dissapative Dynamical Systems*, Communications in Mathematical Physics, 74, 1980.

Thursday, July 30
1000-1130
Session 16.

Title:Sweep tests on Non-linearly Damped Vibrating Systems

Authors:B. Ravindra and P. Hagedorn

 Institut fur Mechanik II,
 Darmstadt University of Technology, Darmstadt, D-64289, Germany

Abstract:

Non-stationary responses occur when vibrating systems are subjected to
sweep tests. A common industrial practice is to mount the vibrating
system on a vibrating shaker and subject it to a specified frequency sweep.
These sweep tests occupy an important place in the quality control of
many products and in the design of robust packaging for transporting
sensitive electronic equipments. Another context of applications
is vibration isolation. The objective in this work is to explore
the role of nonlinear damping in the analysis of non-stationary responses
of vibrating systems. It is known that, orifice type dampers, pneumatic
dampers, Rubber isolators etc., exhibit nonlinear damping characteristics.
Apart from these, it has been observed in the experiments that damping phenomena
in steel beams also follows a power-law type description.
The aim of this paper is to provide a framework for analysing
these diverse systems when subjected to a non-stationary excitation.
The change in bifurcation structure due to the non-stationarity
of excitation is also examined.

Stick-Slip Vibrations Induced by Alternate Friction Models

†R. I. Leine,   †D. H. van Campen,   †A. de Kraker,
and ‡L. van den Steen

†*Department of Mechanical Engineering,*
Eindhoven University of Technology,
P. O. Box 513, 5600 MB Eindhoven, The Netherlands
E-mail : remco@wfw.wtb.tue.nl

‡*Shell International Exploration and Production B.V.,*
P.O. Box 60, 2280 AB Rijswijk, The Netherlands

Abstract

The presence of stick-slip vibrations can be highly detrimental to the performance of mechanical systems.

The first step to reduce or avoid these vibrations is to create a representative numerical model that can be used to evaluate all possible phenomena and can be incorporated in a control system. The study of stick-slip vibrations is faced with difficulties, as during the stick-slip motion two different mechanisms take place. The modeling of the static friction mechanism and that of the kinetic friction mechanism yield a set of differential equations with discontinuous right-hand side.

A standard method to solve discontinuous differential equations consists of applying a smoothing method (also called normalization method). The smoothing method replaces the discontinuous system by a smooth adjoint system. The smoothing method yields a system of ordinary but stiff differential equations and consequently leads to large computational times.

The problems of the smoothing method led to the development of models which switch between different sets of equations, the so-called "alternate friction models" or "switch models". The classical approach to integrate the switch model starts from an initial state with a set of differential equations.

After each timestep the state vector is inspected on a possible event within this timestep (e.g. slip to stick transition). If an event happened, the integration process is halted and an iteration procedure is started to find the switching point (within a certain range of accuracy). Having thus evaluated the switching point, a new integration process is started with a modified set of differential equations and initial conditions identical to the state at the switching point.

The need to halt the integration process, determine the discontinuity with an iteration process and restart the integration again is undesirable from a numerical point of view. Standard integration methods integrate a set of differential equations over a specified time interval. So, if the integration needs to be halted at the discontinuity, standard integration methods cannot be applied.

In the present paper a simple and efficient switch model is presented to simulate stick-slip vibrations. The specific switch model presented here consists of a set of ordinary non-stiff differential equations. This has the advantage that the system can be integrated with any standard ODE-solver available in mathematical packages (MATLAB, MATHEMATICA, MAPLE) or ODE-solvers of existing software libraries (NAG). The system is thus integrated without the need to halt which minimizes start-up costs.

Shooting methods as periodic solution solvers in combination with switch models have not been addressed in the past. A method to combine shooting with the proposed switch model, without the use of normalization, is presented. The fundamental solution matrices, necessary for the application of the shooting method, are obtained with a sensitivity method where initial disturbances are tracked in orthogonal directions.

A single-degree-of-freedom model is used to introduce and evaluate the numerical methods. An important advantage of the switch model is the possibility of incorporating tribological enhancements of the classical friction model. It is shown how time-dependent static friction can be incorporated in the switch model.

The switch model can also be used for systems with greater complexities. A single violin string with a bow that is moving at a constant velocity over the string is considered. The friction force between bow and string induces lateral displacement and rotation of the string (2–DOF system). This two-degree-of-freedom system can efficiently be modeled with the switch model.

Harmonic balancing approach
for hysteretic multidegree of freedom oscillators of Masing type

Danilo Capecchi[1] Renato Masiani[2] and Fabrizio Vestroni[2]

1-Dip. di Scienza delle Costruzioni Università, di Napoli "Federico II"
Piazzale Tecchio 80, 80125 Napoli.
2-Dip. di Ingegneria Strutturale e Geotecnica, Universita' di Roma "La Sapienza"
Via Eudossiana 18, 00184 Roma, Email : vestroni@scilla.ing.uniroma1.it

A of growing interest has been registered for the dynamical behaviour of hysteretic systems and the appearance theoretical and experimental papers became more frequent in recent years. Theoretical interest arised from the circumstance that hysteretic restoring forces are non-monodromic when described, as usually, in terms of force and displacement. This does not allow modern methods from nonlinear dynamics to be used for the investigation of these systems. Consequently, most of published papers in the past employed heuristic methods which do not require the explicit formulation of the vector field, such as the methods of harmonic balance and slowly varying parameters [1].

It has been shown that for the elastoplastic [2], and for a general class of hysteretic models [3-5], the restoring force, when formulated in a differential form, can be described as a single-valued function, with a low continuity order, by enlarging the dimension of the space of the state variables. This formulation facilitates the investigation of the dynamic response.

According to this formulation, the present work deals with the study of the dynamic response of a simple discrete system to a harmonic excitation and can be considered as the complementary continuation of [5]. The complementarity consists in the fact that the stationary response is studied by means of harmonic balancing with many components [3], that is a modal domain instead of a time domain approach is used. The motivation is due to the difficulty over convergency encountered in some parameter values range with the time domain approach. Indeed the harmonic balancing, because of its integral nature, reduces the effects of the singularity in the vector field and it is potentially more effective from a numerical point of view.

The hysteretic model referred to is composed of a nonlinear elastic model and a pure hysteretic *Masing* model; the two contributions are joined together in such a way that the degree of hysteresis, the yielding force value and the initial stiffness can be varied independently. The peculiar characteristic of the Masing models allows for an efficient procedure to find periodic motions. The only unknowns are the Fourier coefficients of the displacement history; no explicit use is necessary of the Fourier coefficients for the state variables. In practice, for a chain model with n masses, the algebraic system resulting from the application of the harmonic balancing to the motion equations is $2nm$, where m is the number of harmonic used, and the factor 2 accounts for the sine and cosine coefficients. For $m=1$ the classic harmonic balancing method is recovered.

The results obtained refer to the two degree-of-freedom structure already considered in [5], which is in internal resonance condition of the type 1:3. The results previously obtained are confirmed and because of the efficiency of the algorithm a larger set of parameters are considered which make it possible to have a better view of the various phenomena. When the hysteretic model used has full hysteresis, the behaviour is similar to that obtained with elastoplastic model [2]: the response is mainly 1T periodic solution, strong coupling is present around first resonance, while it is negligible around the second resonance. Where two modes are involved in the response by the internal resonance phenomenon, each mode oscillates with its own frequency and even though the motion is periodic the deformed shape configuration changes during a period. Since the hysteretic model can be seen as a nonlinear elastic model with numerous odd nonlinearities, the second mode resonance is involved at various frequency values.

The reduced hysteresis model exhibits multivaluedness in the frequency response curves, both around the first and second resonance; the behavior becomes very complex and difficult to explain around the first resonance. For increasing level of excitation, a new important resonance arises in the region of combination resonance; the inspection of the eigenvalues of the Poincaré map reveals that the resonance in this frequency range, still due to the second mode, consists of unstable 1T periodic oscillations: here stable quasi-periodic motion occurs. According to the level of hysteresis and of the excitation, this zone shows windows of apparently 2T periodic motion. Though the quasi-periodic motion cannot be studied with the harmonic balancing, it is shown however that some approximate conclusions can be drawn also in this situation.

It is worth noticing that resonance phenomena are very important not only for systems in 1:3 internal resonance conditions, but in a large range of the ratio between the two frequencies, as a consequence of the wide resonance around the first natural frequency. This is one of notable differences from the nonlinear elastic systems, which exhibit internal resonance phenomena in a very small region of frequency ratio.

1 D. Capecchi, F. Vestroni, "Periodic response of a class of hysteretic oscillators", *Int. J. of Non-Linear Mechanics*, **25**, 309-317, 1990.

2 D. Capecchi, F. Vestroni, "Asymptotic response of two degree-of-freedom elastoplastic systems under harmonic excitation", *Nonlinear Dynamics*, **7**, 1995, 317-333

3 D. Capecchi, "Periodic response and stability of hysteretic oscillators", *Dynamics and Stability of Systems*, **6**, 1991, 89-106.

4 D. Capecchi, R. Masiani, "Reduced phase space analysis for hysteretic oscillators of Masing type", *Chaos, Solitons & Fractals*, 1996.

5 D. Capecchi, R. Masiani, F. Vestroni, "Periodic and non-periodic oscillations of a class of hysteretic two degree of freedom", *Nonlinear Dynamics*, **13**, 1997, 309-325.

Approximate Model for the Dynamics of Belt/Pulley Frictional Contact

M. J. Leamy   J. R. Barber   N. C. Perkins
Graduate Student Research Assistant   Professor   Associate Professor

Mechanical Engineering and Applied Mechanics

2250 G. G. Brown

The University of Michigan

Ann Arbor, MI 48109-2125

fax: (734) 647-3170

1   Abstract

This study is motivated by the need to develop belt drive models which predict the drive's dynamic response to harmonic excitation. Particular attention focuses on modeling nonlinear belt response in frictional contact at the belt/pulley interface. To this end, a first model is proposed appropriate for accessory drives with "small convection," that is, belts with small translational speed. Figure 1 depicts a simple model of a belt in frictional contact with a pulley, which is utilized to study the belt's elastodynamic response to a train of incoming harmonic tension waves. Convective effects are ignored and the frictional surface is assumed to obey Coulomb's friction law, where μ is the coefficient of friction. The belt is treated as a one-dimensional rod. Through a non-dimensionalization, a single dimensionless parameter

$$\Omega = \frac{\omega^* P^*}{\mu N^* c^*} \tag{1}$$

is identified which governs the dynamic response. Here, ω^* denotes the frequency of tension waves, P^* denotes their amplitude, μ represents the coefficient of friction, N^* the normal force, and c^* denotes the elastic wave speed.

A numerical solution is developed and exercised over a wide range of values of Ω. An approximate closed form solution is derived assuming the belt stretches quasi-statically, and is shown to yield accurate results for small values of Ω. Reported results include the distortion of an initially harmonic tension wave, the energy reflected from the frictional support (Figure 2), and the distance harmonic waves penetrate into the support. The results suggest that the quasi-static stretching assumption may be further utilized as a modeling simplification for belt drives characterized by values of $\Omega < 1/3$.

2 Figures
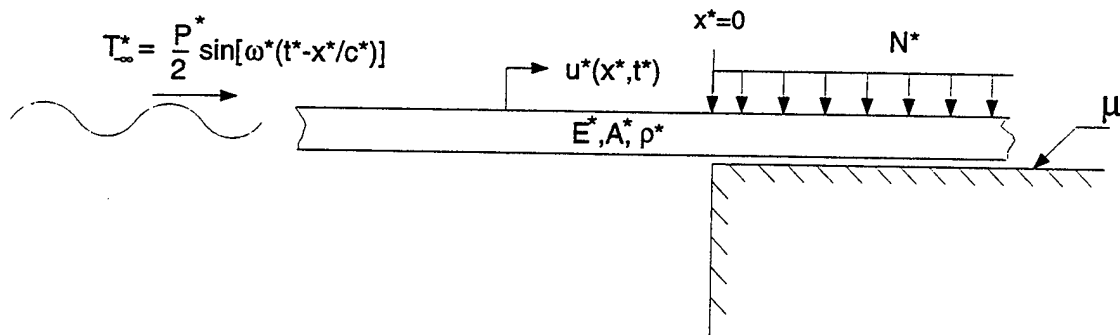
Figure 1: Small convection model. E^*, A^*, and ρ^* represent material properties of the belt, μ denotes the coefficient of friction, N^* the normal force, and u^* the displacement field as a function of space x^* and time t^*. Incoming tension waves travel at wave speed c^*, have amplitude $P^*/2$, and frequency ω^*.
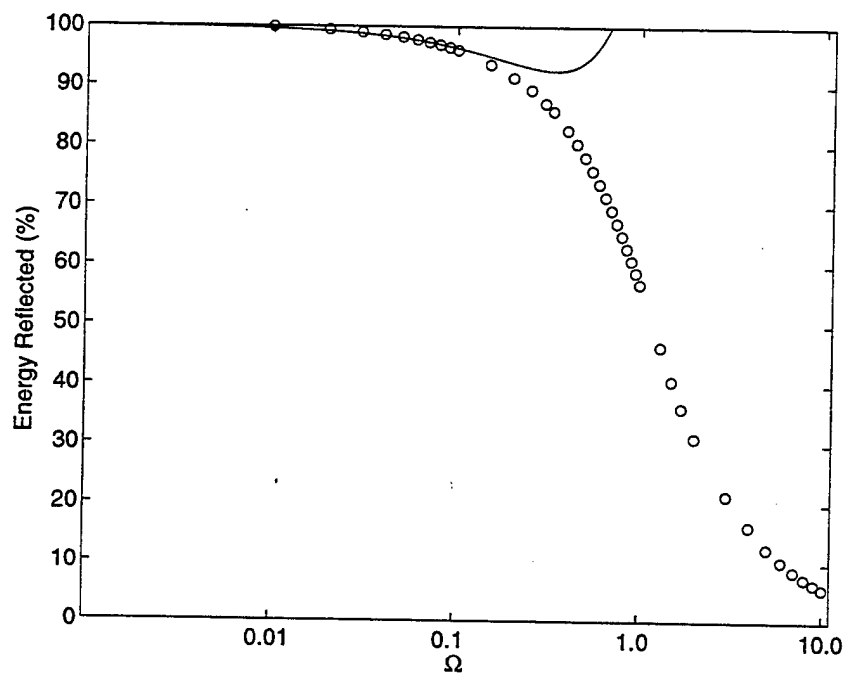
Figure 2: Percent energy reflected as a function of Ω for small convection model. Numerical Solution o, closed-form solution —.

3 References

[1] Grashof, B. G., 1883, Theoretische Maschinenlehre, Bd 2. Leopold Voss. Hamburg. .

[2] Gerbert, G. G., 1991, "On Flat Belt Slip," *Vehicle Tribology*, Tribology Series 16, pp. 333-339, Elsevier, Amsterdam.

[3] Gerbert, G. G., 1996, "Belt Slip – A Unified Approach," *ASME Journal of Mechanical Design*, Vol. 118, September, pp. 432-438.

[4] Johnson, K. L., 1985, *Contact Mechanics*, London, Cambridge University Press, Chapter 8.

Dynamics of Rotating Piezoelectric Rings Subjected to Radial Pressure Load

Jörg WAUER

Institut für Technische Mechanik, Universität Karlsruhe
Kaiserstraße 12, D–76128 Karlsruhe, Germany
E-mail: wauer@itm.uni-kalrsruhe.de

The dynamics of elastic rings, disks and cylinders is well–understood. If the effect of a stationary rotational speed is incorporated, modeling and analysis of the dynamic behavior are more difficult but also for that case, the essential problems are completely discussed. As well for rings, but also for disks and cylinders, eigenfrequencies, critical speeds and the stability of the steady–state response were recently dealt with by several authors. It was shown that former results obtained by neglecting the pre–deformation owing to centrifugal forces completely, were corrected significantly. Meanwhile it is well–established that the so–called stiffening effect is fundamental to explain all the appearing dynamic phenomena.

In recent years, considerable attention has been given to the study of vibrations of piezoelectric and pyroelectric solids. But in all related papers, structural members at rest were examined. The main objective of the present contribution is to focus attention on rotating media for which only some limited results exist not applicable for higher speed rates for which the stiffening effect becomes significant. Such high angular speeds together with an external pressure will now be taken into consideration. Discussing the stability of the resulting stationary deformation state is of special interest, here for the most basic case of one–parametric thin rings (with one characteristic space coordinate).

To formulate the governing eigenvalue problem, the conventional electrically quasistatic theory and the classical linear constitutive equations for a piezoelectric material (of hexagonal 6mm class) are used. To calculate not only the stationary deformation due to the steady centrifugal forces and the radial pressure but also the superimposed vibrations characterizing the stability behaviour, a geometrically nonlinear deformation theory has to be applied. It can be taken for elastic rings from a former work of the author [2] to be generalized to piezoelectric material or from a recent paper by Tzou and Bao [1] presenting a general theory of piezothermoelastic shell laminates at rest to be spezified to the rotating ring problem. Anyway, a nonlinear boundary value problem for the deformation varibles and the electric field variable is the starting point.

For convenience, the crystal axes are chosen to be coinciding with the rotational axis and two perpendicular other ones located in the plane of the ring. The deformation of the ring will be described in a body–fixed reference frame. Based on Bernoulli–Euler theory, it is expressed by the radial and circumferential displacements of the middle fibre. As the

electric field variable, the electrostatic potential is introduced. As mechanical body force, a radial pressure load is assumed (but electrical source terms could also be taken into consideration).

In a first solution step, the stationary electromechanical state is determined (in a linear approximation). After that, the linearized variational equations characterizing the superimposed coupled small piezoelectric oscillations are deduced. They form a multi-field eigenvalue problem to be solved finally. The quantitative influence of the rotational speed and the pressure load on the eigenfrequencies is presented where for uniform ring properties, semi–analytical results can be obtained. Also the effect of the piezoelectric moduli is shown; the limiting case of a purely elastic ring is deduced. The eigenvalue-speed diagram with the varied load parameter yields a clear stability proof to summarize the present work. By a slight modification, it can also be used to identify possible critical speeds.

References

1. Tzou, H.S., Bao, Y. 1997. Nonlinear Piezothermoelasticity and Multi–Field Actuations, Part 1: Nonlinear Anisothropic Piezothermoelastic Shell Laminates. *J. Vibr. Acoust.* **119**, 374–381.

2. Wauer, J. 1987. Stabilität dünner rotierender Kreisringe under radialem Druck, *Z. Angew. Math. Mech.* **67**, T159–161.

Thursday, July 30
1330-1500
Session 17.

ROTOR DROP NONLINEAR TRANSIENT ANALYSIS
OF MAGNETIC BEARING ROTORS ON AUXILIARY BEARINGS

P. E. Allaire, Wade Professor
W. C. Foiles, Research Associate
804-924-6233 (Presenting Author)

Mechanical, Aerospace, and Nuclear Engineering
University of Virginia, Charlottesville, VA 22901

ABSTRACT

The drop of a magnetic bearing supported rotor on auxiliary bearings is a matter of significant importance. The rotor may be operating at full rotational speed when the magnetic bearings may be shut off, for one reason or another, and drop on the auxiliary bearings. If large amplitude whirling motions of the rotor in the auxilary bearings result, contact or other effects may result in significant damage to the machine. If the rotor simply drops onto the bottom of the auxiliary bearing clearance and oscillates back and forth a few times, little or no damage may result in the machine.

Previous literature has discussed rotor drops [Kirk et al., 1994, 1997], as well as others [Raju et al., 1995, Ramesh et al., 1994, and Swanson et al., 1995] for a drum type rotor to simulate an aircraft gas turbine compressor. The results included experimental rotor drops and theoretical modeling. Tessier [1997] reported on the mathematical modeling and experimental rotor drop for an industrial compressor. Foiles and Allaire [1997] discussed nonlinear transient modeling of two rotors as they drop on auxiliary bearings. This work extends the results of the previous paper by the same two authors.

This paper investigates rotor drops for two rotors with somewhat different physical characteristics but mounted on the same auxiliary bearing sytems. Rotor No. 1, which may simulate a generator or turbine rotor, has the rotor mass distributed along the rotor for a relatively long distance in the axial direction. It has rotor of length 2.36 m (92.9 in), magnetic bearing span of 1.36 m(53.4 in) auxiliary bearing span of 1.75 m (69.0 in), center of mass diameter 1.03 m (40.5 in) from the left end, weight 13,450 N (3,024 lbf). The magnetic bearings are located at stations 7 and 23 while the auxiliary bearings are located at stations 4 and 26.

Rotor No. 2, which may simulate a centrifugal compressor with a few stages in the center, has a large central mass on a nearly uniform rotor. Rotor No. 2 has a total length of 2.32 m (91.4 in), magnetic bearing span of 1.55 m (61 in), auxiliary bearing span of 2.08 m (82.0 in), center of mass of 1.40 m (55.0 in) from the left, diameter of 356 mm (14 in), shaft diameter at the magnetic bearings of 146 mm (5.75 in), catcher bearing diameter of 4.35 in at station 2, shaft diameter at the right catcher bearing of 5.1 in at station 23, and weight of 13,400 N (3,000 lbf). Magnetic bearings are located at stations 7 and 20. Each rotor is assumed to have an operating speed of 7,000 rpm.

Two rotors similar to typical industrial rotors supported on magnetic bearings were subject to rotor drops on auxiliary bearings with various levels of Coulomb friction and unbalance on auxiliary bearings with relatively low support stiffness and damping properties. The rotors had relatively similar properties with the first free-free mode of Rotor No. 1 at 6,947, just below the operating speed of 7,000 rpm and the first free-free mode of Rotor No. 2 at 7,974 rpm is just above operating speed.

Rotor No. 1 almost never went into full clearance whirl while Rotor No. 2 nearly always did. The rotors have rather similar characteristics so it is

not clear why one rotor consistently went into full clearance whirl while the other did not.

When Rotor No. 1 oscillated in the bottom of the bearing clearance, the whirl pattern was neither forward or backward in character. However, in full clearance whirl for Rotor No. 2, the whirl precesses in the backward direction, similar to the results obtained by Kirk and Ishi [1993] and Maslen and Barrett [1995]. In each case, a critical coefficient of friction exists where the rotor will go from not whirling to whirling under similar conditions of imbalance and support characteristics.

For Rotor No. 1, the higher the level of imbalance, the higher the level of vibration in the bottom of the clearance circle. The phase angle of imbalance at the time of rotor drop for Rotor No. 2 did have an influence on initiation of full clearance whirl at 30 oz-in, no whirl at 0 degrees and full whirl at 180 degrees. In a number of cases, the initiation of full clearance whirl was delayed well past the first bounce after striking the bottom of the auxiliary bearing surface, as also noted by Fumigali and Schweitzer [1995].

There seem to be quite a few factors affecting the initiation of full clearance whirl in industrial rotating machines supported in magnetic bearings. These include the rotor mechanical characteristics such as free-free modes, distribution of mass as well as auxiliary bearing properties such as mass, friction coefficient, stiffness and damping coefficients. The influence of specific rotor or auxiliary bearing properties on full clearance whirl is not very well understood at this time.

REFERENCES

Foiles, W. C., and Allaire, P. E., 1997, "Nonlinear Transient Analysis of Active Magnetic Bearing Rotors During Rotor Drop on Auxiliary Bearings," Proceedings of MAG '97, P. Allaire, Ed., Technomics Publishers, pp. 154-166.

Kirk, R. G., Swanson, E. E., Kavarana, F. H., Wang, X., and Keese, J., 1994, "Rotor Drop Test Stand for AMB Rotating Machinery Part I: Description of Test Stand and Initial Results," Proceedings of Fourth International Symposium on Magnetic Bearings, G. Schweitzer, Ed., Hochschulverlag AG an der ETH, Zurich, pp. 207-212.

Kirk, R. G., Raju, K. V. S., Ramesh, K., 1997, "Modeling of AMB Turbomachinery for Transient Analysis," Proceedings of MAG '97, P. Allaire, Ed., Technomics Publishers, pp. 139-153.

Maslen, E. H., and Barrett, L. E., 1995, "Feasible Whirl of Rotors in Auxiliary Bearings," Proceedings of MAG '95, P. Allaire, Ed., Technomics Publishers, pp. 217-226.

Raju, K. V. S., Ramesh, K., Swanson, E. E., and Kirk, R. G., 1995, "AMB Rotor Drop Initial Transient on Ball and Solid Bearings," Proceedings of MAG '95, P. Allaire, Ed., Technomics Publishers, pp. 227-235.

Ramesh, K., and Kirk, R. G. "Rotor Drop Test Stand for AMB Rotating Machinery Part II: Steady State Analysis and Comparison to Experimental Results," Proceedings of Fourth International Symposium on Magnetic Bearings, G. Schweitzer, Ed., Hochschulverlag AG an der ETH, Zurich, pp. 213-218.

Swanson, E. E., Kirk, R. G., and Wang, J., 1995, "AMB Rotor Drop Initial Transient on Ball and Solid Bearings," Proceedings of MAG '95, P. Allaire, Ed., Technomics Publishers, pp. 207-216.

Tessier, L. P., 1997, "The Development of an Auxiliary Bearing Landing System for a Flexible AMB-Supported Hydrogen Process Compressor," Proceedings of MAG '95, P. Allaire, Ed., Technomics Publishers, pp. 120-128.

Modeling and Analysis of a Self-Centering Auxiliary Bearing

George T. Flowers and Abraham George
Auburn University
Auburn, AL 36849

Active magnetic bearings are one of the most innovative recent developments in the field of rotating machinery. This technology provides the potential for significant improvements over other types of rotor support, including elimination of wear and bearing friction-related energy losses as well as a means of actively suppressing rotor vibration.

A critical component of any magnetic bearing design is the auxiliary bearing, which protects the soft iron core of the magnetic bearing and provides rotor support in case of overload or failure of the primary (magnetic) bearing. Magnetic bearing systems appear to provide particularly great promise for use in aeronautical applications. In this regard, current effort is directed toward developing jet engines and flywheel energy storage systems for satellites with rotors supported by magnetic bearings. For such applications, the rotor will be subjected to much higher than nominal loads for brief periods (during a rocket launch for satellites or during a high g-force maneuver for an aircraft). Since the weight of the bearing system is an important consideration, a sensible strategy is to design the magnetic bearings to handle nominal loads (with an appropriate safety factor) and have auxiliary bearings to provide support during critical loading periods.

A number of different bearing types have been suggested as auxiliary bearings. These include bushings, rolling element bearings, and various types of journal bearings. The most commonly considered are rolling element bearings. For extended periods of operation, methods for providing adequate lubrication (for removal of friction produced heat) and damping (for acceptable rotordynamic performance) must be found. In addition, a major disadvantage associated with using rolling element bearings (or bushings) is the requirement of a clearance between the rotor and the inner race of the bearing, without which many of the advantages associated with using magnetic bearings would be reduced or eliminated. This clearance introduces a nonlinear dynamical feature, which may significantly impact the behavior of the rotor. The present work is specifically concerned with addressing the dynamical problems associated with this nonlinear effect.

There are quite a number of studies in the literature concerned with nonlinear rotordynamics. Groundbreaking work includes that of Yamamoto (1954), who conducted a systematic study of rotor responses involving bearing clearance effects. Also, Black (1968) studied the rotor/stator interaction with a clearance. Ehrich (1966, 1988 and 1991), Bently (1974), and Childs (1979 and 1982) observed and studied subharmonic responses associated with clearance effects. Gelin, et al, (1990) was one of the first to consider the dynamics of a magnetic bearing supported rotor interacting with an auxiliary bearing. Additionally, Lawen and Flowers (1996) provides a good background review of other work specifically related to auxiliary clearance bearings.

A potential solution to the clearance problem is the use of a bearing configuration that will be non-contacting when auxiliary support is not needed and will automatically close the clearance when auxiliary support is needed. A conceptual diagram for one such auxiliary bearing configuration is shown in Figure 1. It consists of a series of rollers that are constrained to move along slotted paths. Under normal operating conditions (non-contacting), there is a clearance between the rollers and the shaft. During contacting, the friction force between the spinning rotor and the rollers drives the rollers along their slotted paths, forcing the shaft toward a centered configuration.

This concept is quite new and the dynamics are (of course) very nonlinear. There are many design issues that must be addressed with regard to the best choice of bearing parametric configuration. With this need in mind, the present study examines the dynamical

ROTOR

STATOR

ROLLER
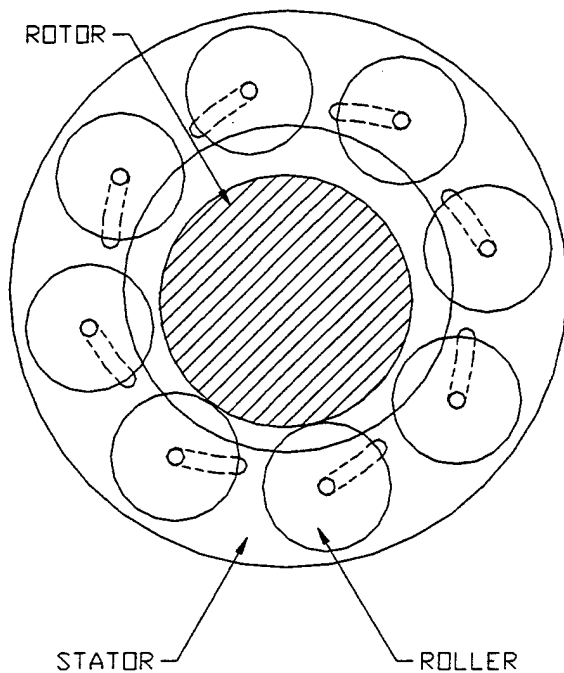
Figure 1: Diagram of the Auxiliary Bearing Model

behavior of a rotor system interacting with this type of self-centering auxiliary bearing during critical operating conditions. Of particular interest is the transient and steady state behavior of such a system. A simulation model was developed to predict the dynamic behavior of such a system. It consists of a shaft coupled with a self-centering bearing. The shaft and the rollers are assumed to be rigid. A number of studies (for a variety of parametric configurations) using this model were performed to evaluate the relative dynamic response characteristics and load capacity. Some insights and observations were made with regard to possible dynamic behaviors.

Acknowledgement

References

Bently, D. E., 1974, ``Forced Subrotative Speed Dynamic Action of Rotating Machinery,'' ASME Paper No. 74-PET-16.

Black, H. F., 1968, ``Interaction of a Whirling Rotor With a Vibrating Stator Across a Clearance Annulus,'' *Journal of Engineering Science*, Vol. 10, No. 1, pp. 1-12.

Childs, D. W., 1979, ``Rub-Induced Parametric Excitation in Rotors,'' *ASME Journal of Mechanical Design, Vol.* 101, pp. 640-644.

Childs, D. W., 1982, ``Fractional-Frequency Rotor Motion Due to Nonsymmetric Clearance Effects,'' *ASME Journal of Engineering for Power*, Vol. 104, pp. 533-541.

Ehrich, F. F., 1966, ``Subharmonic Vibration of Rotors in Bearing Clearance,'' ASME Paper 66-MD-1.

Ehrich, F. F., 1988, ``High Order Subharmonic Response of High Speed Rotors in Bearing Clearance,'' *ASME Journal of Vibration, Acoustics, Stress, and Reliability in Design*, Vol. 110, pp. 9-16.

Ehrich, F. F., 1991, ``Some Observations of Chaotic Vibration Phenomena in High-Speed Rotordynamics,'' ASME Journal *of Vibration, Acoustics, Stress, and Reliability in Design*, Vol. 113, pp. 50-57.

Gelin, Al, Pugnet, J. M., and Hagopina, J. D., 1990, ``Dynamic Behavior of Flexible Rotors with Active Magnetic Bearings of Safety Auxiliary Bearings,'' *Proceedings of 3rd International Conference on Rotordynamics*, Lyon, France, pp. 503-508.

Lawen, James L., and Flowers, George T., "Interaction Dynamics Between a Flexible Rotor and an Auxiliary Clearance Bearing," ASME Design Engineering Division, v. 90, pp. 199-126, 1996.

Yamamoto, T. T., 1954, ``On Critical Speeds of a Shaft,'' *Memoirs of the Faculty of Engineering, Nagoya University* (Japan), Vol. 6, No. 2.

Effects of Flux Saturation in a Magnetic Bearing on Rotor Motion

M. Chinta*

Mechanical Engineering Technology Program

A. B. Palazzolo

Department of Mechanical Engineering

Texas A & M University

College Station, TX 77843-3367

Active magnetic bearings are electro-mechanical systems whose stiffness and damping characteristics can be changed by varying the gains of the feedback controllers. They levitate a rotor by the attractive forces of magnetic fields generated by the electromagnets. Magnetic bearings use ferro magnetic materials such as silicon iron (saturation flux density, $B_{sat} = 1.5$ tesla) and cobalt iron ($B_{sat} = 2.2$ tesla). Such high flux levels make it possible for them to support heavy rotors. They have been used to support shafts with diameters from 14 mm to 1.25 m, and have load capacities up to 300 kN per radial bearing.

The system studied here is an eight-pole (four-electromagnet) radial magnetic bearing with a laminated stator and rotor. The input currents to electromagnets are controlled by two proportional-derivative (PD) current feedback controllers, one for each x and y axes. The current though each magnet is the sum of a bias current and a control current. The magnetic force, F, is directly proportional to the square of the coil current, and inversely proportional to the square of the gap between the stator and rotor.

The magnetic force is directly proportional to the square of the resulting flux density, B. B is linearly proportional to the applied flux intensity, H, for a certain range of B. There is a saturation flux density, B_{sat}, which cannot be exceeded by increasing H, thus limiting F. This becomes a problem for large rotor

---
*Author to whom correspondence should be addressed.

motion that may be caused by large unbalance loads.

The flux saturation levels of various magnetic materials are reported in [1]. The flux saturation was first studied for a magnetic bearing in [2], where the authors present an iterative procedure to estimate the flux density. Peak bearing forces are estimated by considering flux saturation and assuming that control current is equal to bias current [3]. For a magnetic bearing with linear stiffness and damping, the flux saturation was studied using finite element method [4].

In this research, it is assumed that the B-H relation is piecewise linear; the magnetic force is nonlinear in rotor displacement even in the linear portion of B-H curve. The focus of the paper is to investigate the effects of flux saturation nonlinearity on the rigid rotor dynamics.

It was found that for a bearing with hardening spring nonlinearity, the effect of flux saturation is to increase the bearing stiffness. There are also minimum values of B_{sat} below which the bearing cannot provide any stable restoring forces to levitate the rotor.

When the rotor weight was neglected, the rotor did not show any subharmonic motion due to flux saturation nonlinearity. When rotor weight was included, the rotor had period-2 subharmonic for a range of rotor excitation forces.

References

[1] P. E. Kueser, D. M. Pavlovic, D. H. Lane, J. J. Clark, and M. Spewock, *Properties of Magnetic Materials for Use in High-Temperature Space Power Systems*, NASA SP–3043, 1967.

[2] M. S. Sarma and A. Yamamura, "Nonlinear Analysis of magnetic bearings for space technology," *IEEE Transactions on Aerospace and Electronic Systems*, vol. AES–15, no. 1, pp. 134–170, 1979.

[3] E. Maslen, P. Hermann, M. Scott, and R. R. Humphris, "Practical limits to the performance of magnetic bearings: peak force, slew rate, and displacement sensitivity," *ASME Journal of Tribology*, vol. 111, pp. 331–336, 1989.

[4] F. Hsiao and A. Lee, "An investigation of the characteristics of electromagnetic bearings using the finite element method," *ASME Journal of Tribology*, vol. 116, pp. 710–719, 1994.

Analysis of Flexible Multi-Body Systems
with Intermittent Contacts

O.A. Bauchau
Georgia Institute of Technology,
School of Aerospace Engineering.
Atlanta, Georgia, 30332, USA.

1   Introduction

This paper is concerned with the dynamic analysis of flexible, nonlinear multi-body systems undergoing intermittent contacts. Contact can occur between two rigid or deformable bodies of the system, or with an external body. Intermittent contact can be of an accidental nature, such as, for instance, the impact of a member of the system on an unexpected obstacle. Another common source of intermittent contact is the presence of clearance at the joints of a multi-body system. Clearance can be associated with manufacturing imperfections, or caused by unavoidable wear such as, for instance, fatigue or damage induced looseness in revolute joints and bearings. Proper understanding and modeling of the behavior of multi-body systems with clearances is a key step toward health monitoring of such systems. Finally, intermittent contact is sometimes an inherent feature of the system such as, for instance, in the Geneva wheel mechanism, or in cam-follower systems operating at off design conditions resulting in intermittent separation of the cam-follower pair.

The approaches to modeling of intermittent contact fall into two broad categories depending on the assumed duration of contact. In the first approach, contact is treated as a discontinuity, *i.e.* the duration of contact is assumed to tend to zero. The configuration of the system is assumed to be identical before and after impact, and the principle of impulse and momentum is used to compute the momenta after impact. Energy transfer during impact can be modeled in a heuristic manner using the concept of coefficient of restitution. This approach was first proposed by Kane [1], then applied to rigid multi-body systems by Wehage and Haug [2], and extended to flexible systems by Khulief and Shabana [3]. The accuracy of this approach is inherently limited by the assumption of a vanishing impact duration. Furthermore, energy balance is not necessarily satisfied when the principle of impulse and momentum is applied [4].

In the second approach to contact modeling, the impact duration is finite, and the time history of the forces acting between the contacting bodies which can be either rigid or deformable is explicitly computed during the simulation. Of course, a constitutive law describing the force-deformation relationship for the contacting bodies is required if the bodies are deformable. This approach was used by a number of researchers [5, 6, 7], among others. Various types of constitutive laws were used, but the classical solution of the static contact problem presented by Hertz [8] has been used by many investigators. Energy dissipation can be added in an appropriate manner, as proposed by Hunt and Crossley [9].

In this work, the contact event is assumed to be of finite duration. The overall approach to the modeling of intermittent contact is broken into three separate parts: a purely kinematic part describing the configuration of the contacting bodies, a unilateral contact condition, and an optional contact model. The first, purely kinematic part of the problem is developed. The candidate contact points [10], *i.e.* the points of the bodies that are the most likely to come in contact if the bodies were in contact, are defined by a number of holonomic constraints that involve the kinematic variables defining the configuration of the contacting bodies and the parameters that describe the curve defining their outer shape. The knowledge of the location of these candidate contact points leads to the definition of the relative distance q between the bodies. The implementation of these nonlinear holonomic constraints is discussed in detail.

The second part of the model, described in the next section, is the unilateral contact condition which is readily expressed in terms of the relative distance as $q \geq 0$. In previous work, this condition has been

enforced by means of a logical spring-damper system, *i.e.* a spring-damper system acting between the bodies when they are in contact, and removed when they separate. The properties of the spring-damper system can be selected to model the physical characteristics of the contact zone, as was done in ref. [5]. In ref. [7], the logical spring constant is taken to be a large number that enforces the non-penetration condition through a penalty approach, and the logical damper is added to control the spurious oscillations associated with this penalty formulation. In this work an alternate route is followed: the contact condition is enforced through a purely kinematic condition $q - r^2 = 0$, where r is a slack variable used to enforce the positiveness of q. This approach is shown to yield a discrete version of the principle of impulse and momentum.

The last part of the model, is the contact model which takes into account the physical characteristics of the contacting bodies. When these bodies are perfectly rigid this model is not necessary. When the bodies are deformable, their local inter-penetration, or *approach*, is defined, and the contact model consists of a constitutive law that relates this approach to the contact force.

The nonlinear holonomic constraints and the contact model associated with intermittent contacts in multi-body systems will be formulated within the framework of the energy preserving and decaying schemes introduced in [11, 12]. In these schemes, unconditional stability is achieved for nonlinear elastic multi-body systems by combining two features: an energy preservation or decay statement for the elastic bodies of the system, and the vanishing of the work done by the forces of constraint. The use of these unconditionally stable schemes is of particular importance in intermittent contact problems whose dynamic response is very complex due to the large, rapidly varying contact forces applied to the system. Numerical examples are presented. An automated time step size selection procedure developed in [12] is used to obtain accurate solutions in an efficient manner.

2   Conclusions

This paper has presented an analysis methodology for nonlinear, flexible multi-body system undergoing intermittent contact. Contact events are assumed to be of finite duration, and the contact force is explicitly computed as part of the simulation. The overall approach to the modeling of intermittent contact is broken into three distinct parts: a purely kinematic part describing the configuration of the contacting bodies, a unilateral contact condition, and an optional contact model.

The first part of the model involves a number of nonlinear holonomic constraints which are enforced using a Lagrange multiplier technique. These constraints are enforced in such a way that the work they perform vanishes exactly. This feature, together with the energy preserving or decaying statement associated with the elastic bodies, imply the unconditional stability of the time integration process. The unilateral contact condition is transformed into a holonomic constraint by the addition of a slack variable. For a simple case, this procedure was shown to yield a discrete version of the principle of impulse and momentum. The optional contact model describes the relationship between the contact force and the deformation of the contacting bodies.

Several numerical examples were presented and an automated time step size adaptation procedure was used in the simulations. The model allows a detailed analysis of intermittent contact problems. The efficiency and accuracy of the model was demonstrated.

References

[1] T. R. Kane. Impulsive motions. *Journal of Applied Mechanics*, 15:718–732, 1962.

[2] R.A. Wehage and E.J. Haug. Dynamic analysis of mechanical systems with intermittent motion. *ASME J. of Mech. Design*, 1981.

[3] Y. A. Khulief and A. A. Shabana. Dynamic analysis of constrained systems of rigid and flexible bodies with intermittent motion. *ASME Journal of Mechanisms, Transmissions, and Automations in Design*, 108:38–44, 1986.

[4] T. R. Kane. *Dynamics*. Holt, Rinehart and Winston, Inc, New-York, 1968.

[5] Y. A. Khulief and A. A. Shabana. A continuous force model for the impact analysis of flexible multi-body systems. *Mech. Mach. Theory*, 22:213–224, 1987.

[6] H.M. Lankarani and P.E. Nikravesh. A contact force model with hysteresis damping for impact analysis of multi-body systems. *Journal of Mechanical Design*, 112:1990, 369-376.

[7] A. Cardona and M. Géradin. Kinematic and dynamic analysis of mechanisms with cams. *Computer Methods in Applied Mechanics and Engineering*, 103:115–134, 1993.

[8] S.P. Timoshenko and Goodier J.N. *Theory of Elasticity*. McGraw-Hill Book Company, New-York, third edition, 1970.

[9] K.H. Hunt and F.R.E. Crossley. Coefficient of restitution interpreted as damping in vibroimpact. *Journal of Applied Mechanics*, 112:440–445, 1975.

[10] F. Pfeiffer and C. Glocker. *Multi-Body Dynamics with Unilateral Contacts*. John Wiley & Sons, Inc, New-York, 1996.

[11] O.A. Bauchau. Computational schemes for flexible, nonlinear multi-body systems. Part I: Theory. *Multibody System Dynamics*, 1998.

[12] O.A. Bauchau. Computational schemes for flexible, nonlinear multi-body systems. Part II: Applications. *Multibody System Dynamics*, 1998.

DYNAMICS OF SELF-EXCITED OSCILLATORS
WITH 1:2 INTERNAL RESONANCE

G. Verros and S. Natsiavas

Department of Mechanical Engineering

Aristotle University

54006 Thessaloniki, Greece

(Phone: +30 31 996088, Fax: +30 31 996078, e-mail: natsiava@ccf.auth.gr)

ABSTRACT

Modal interactions occurring in the response of nonlinear mechanical systems, due to the presence of an internal resonance, have been the subject of intensive research work, over the last three decades. For such systems, some of the energy supplied to a mode of the system by the excitation may be transferred and activate other modes, participating in the internal resonance. However, most of these studies analyzed systems with stiffness nonlinearity only. On the other hand, many mechanical oscillators may exhibit significant damping nonlinearities, leading to self-excited behavior. For such systems, vibration modes which are not excited directly by external forcing may eventually get excited through ꞁ nonlinearities and mixed-mode response may arise, even in the absence of internal resonance.

The main objective of this study is to present an analysis for the response of a class of two degree of freedom self-excited oscillators, in the presence of 1:2 internal resonance. The normalized equations of motion are first presented in a general weakly nonlinear form. Then, a perturbation methodology is applied, yielding a set of three slow-flow equations for the amplitudes and phases of approximate motions of the system. The stability analysis of these motions is also performed. In the second part of the study, numerical results are obtained for an example mechanical system. First, response diagrams are presented, showing the existence of various solution branches and illustrating the effect of the system parameters on the response. Then, more numerical results are presented, obtained by direct integration in linear damping ranges where the slow-flow equations possess no stable constant solution. These results, demonstrate the existence of periodic and chaotic solutions of these equations. More specifically, for small levels of linear damping, a Hopf bifurcation is found to occur, marking the transition from phase-locked mixed mode response to phase-entrained motions. These motions are found to develop phase drift eventually, through the occurrence of a homoclinic explosion of the slow-flow equations. Moreover, escape phenomena are also observed for certain combinations of the system parameters.

Thursday, July 30
1530-1700
Session 18.

Applying the POD Method for Modal Analysis and Modal Interaction in Coupled Structural/Mechanical Systems

Ioannis T. Georgiou * and Ira B. Schwartz
Special Project in Nonlinear Science, Code 6700.3
Naval Research Laboratory, Washington DC 20375

In phase space, a normal mode of vibration manifests itself as a two-dimensional invariant manifold of motion. The dynamics restricted on the invariant manifold evolve on characteristic time scales. Basic issues arise when trying to associate multi-time and multi-space scales in spatio/temporal data of structural dynamical systems to normal modes. We are developing novel methodologies to relate multi-time and multi-space scales in numerical and experimental spatio/temporal data to normal modes. In particular, we employ the POD (proper orthogonal decomposition) method as a primary tool to extract the dominant normal modes and the associated characteristic multi-time scales in discrete spatio/temporal data of the motion of a coupled nonlinear structure consisting of a linear viscoelastic beam coupled to a pendulum. The POD method reveals that, for weak coupling between the nonlinear pendulum oscillator and the linear continuum, the dynamics are governed by a slow nonlinear normal mode. The POD method identifies both the amplitude dynamics and the spatial distribution of the slow normal mode. Thus, the time scales for a motion due to the slow normal mode reflect the nonlinearity of a single normal mode. The dynamics in the neighborhood of the nonlinear slow normal mode involve interaction between the slow normal mode and the fast linear dynamics of the continuum. Slow/fast modal interaction manifests itself in the distribution of the frequency spectrum content of the amplitudes of the POD modes: They contain mixed time-scales, that is, a sequence of time scales associated with the nonlinear slow normal mode and fast time scales associated with the linear fast normal modes. We have found that during abrupt changes from periodic motions to chaotic motions high frequencies are generated. These high frequencies reflect interaction among active normal modes and the generation through transverse bifurcations of new normal modes. We present numerical and experimental results.

---

* Research Engineer, SAIC-Science Applications International Corporation, McLean, VA 22102

Multi-Body Analysis of a Tilt-Rotor Configuration

G. L. Ghiringhelli, P. Masarati[1] and P. Mantegazza
Politecnico di Milano
and
M. W. Nixon
Langley Research Center

Abstract - This paper describes the capabilities of an aeroelastic rotorcraft code, developed in-house at the Politechnico di Milano, which is based on multi-body dynamics theory. The current investigation is focused on correlation of the multi-body code predictions with experimental results associated with the Wing and Rotor Aeroelastic Testing System (WRATS), a 1/5-scale semi-span aeroelastic model of the V-22 FSD, which has been tested and is currently located at NASA Langley Research Center. Advantages of the multi-body aeroelastic code over existing comprehensive aeroelastic codes include the capability of modeling highly nonlinear phenomenon such as rotor blade motions during wind-up and maneuvers, and a more exact math model of hub components such as pitch links, pitch horns, and and bearings. The simulations addressed in the paper include: 1) correlation of the aeroelastic stability, with particular regard to the proprotor/pylon instability that characterises the tilt rotor, 2) determination of the dynamics of the system and the loads due to typical maneuvers with particular regard to the conversion from helicopter to airplane mode, and 3) determination of stresses in critical components like the pylon downstop.

Introduction - The 1/5-scale aeroelastic model of the V-22 has undergone a long testing campaign. It was built and tested in the period from 1983 to 1988 to support the preliminary design and the full scale development of the tilt rotor aircraft known then as the JVX. The wind tunnel tests began at Langley's TDT on a semispan model and were performed globally in three different facilities including the Boeing Helicopter VSTOL tunnel for both the semispan and the fullspan model configurations. The model returned to Langley in 1993, where is now employed as the Wing Rotor Aeroelastic Testing System (WRATS) under a loan agreement between the US Navy and NASA Langley Research Center.

The numerical simulations are performed by means of a Multi-Body formulation developed at the *Dipartimento di Ingegneria Aerospaziale* of the *Politecnico di Milano*, Italy, which resulted in a proof-of-concept code that is still under development. The proposed approach is based on a "Lagrangian Multipliers" or "Redundant Coordinate Formulation". It is intended for the simultaneous solution of multi-disciplinar problems including non-linear dynamics, aero-servoelasticity, electric and hydraulic networks. It aims at the modeling of complex systems, a clear example of which is the proposed aeroservoelastic model of a tiltrotor aircraft.

---

[1] Corresponding Author, E-mail: *masarati@aero.polimi.it*

The equations of the dynamics of a constrained system are written in form of a system of first order Differential-Algebraic Equations (DAE). For each inertial body it consists in the six equations defining the momentum and the six ones assessing the equilibrium of forces. In this way both the equations and the unknowns have a clear physical meaning, thus leading to an efficient as well as easy-to-implement and easy-to-enhance formulation. Constraint equations are added if needed. They can be both holonomic or non-holonomic and they introduce algebraic unknowns that are analogous to the well known Lagrange multipliers and directly represent the reaction forces and the couples.

Increasingly detailed models are considered in the work. The following sub-models are taken into account: 1) rotor with both rigid and flexible blades, 2) rotor plus clamped wing and conversion mechanisms, with flexible downstop and conversion beam, 3) rotor plus swashplate and control system flexibility, and 4) complete flexible semispan model.

The inertial properties are modeled by means of lumped masses while the "lumped" and "distributed" deformable elements are represented by means of simple rods and flexible rotational hinges, and finite volumes beam elements, respectively. This is a new and original interpretation of the finite volumes concept applied to structural dynamics. It simplifies the determination of the elastic contribution of the beam element to the equilibrium equations and proved to be free from shear locking.

Simple quasi-steady strip-theory is considered for the aerodynamics of both the rotor and the wing. Dynamic inflow is also modeled in order to account for the rotor induced velocity.

The authors wish to aknowledge the NASA Langley Research Center which cooperated in providing data for the correlation studies.

KEYWORDS: TILT-ROTOR, MULTI-BODY DYNAMICS

References

[1] Ghiringhelli, G. L., P. Masarati and P. Mantegazza, 1997, "Multi-Body Aeroelastic Analysis of Smart Rotor Blades, Actuated by Means of Piezo-Electric Devices", *CEAS Int. Forum on Aeroelasticity and Structural Dynamics*, June 17–20, Rome, Italy

[2] Masarati, P. and P. Mantegazza, 1997, "On the C^0 Discretisation of Beams by Finite Elements and Finite Volumes", *l'Aerotecnica Missili e Spazio*, Vol. 75, pp. 77–86

[3] Popelka, D., M. Sheffler, J. Bilger, 1987, "Correlation of Test and Analysis for the 1/5-Scale V-22 Aeroelastic Model" *Journal of the American Helicopter Society*, Vol. 32, (2), Apr

[4] Settle, T. B., and D. L. Kidd, 1992, "Evolution and Test History of the V-22 0.2-Scale Aeroelastic Model", *Journal of the American Helicopter Society*, Vol. 37, (1), Jan

PERIODIC INTERNAL PRESSURIZATION OF A NONLINEAR ELASTIC SPHERE IN AN EXTERNAL FLUID

Henry W. Haslach, Jr.

Dept. of Mechanical Engineering, Univ. of Maryland Baltimore County, Baltimore, MD 21250

haslach@engr.umbc.edu

The elastodynamic behavior of a nonlinear elastic spherical membrane with an internal periodic pressure and lying in an external fluid models a cranial aneurysm. Such a model has independent interest for studying the question of how the material of the membrane affects its dynamic response. Singularities in the potential function for the static loading of the sphere will be reflected in the dynamic behavior. A similar study of how singularities in the potential function for a dissipative mechanical system affect its dynamic response has been made for a rigid body with different types of supports [1]. Here, the external fluid resists expansion of the nonlinear elastic spherical membrane but aids contraction. The system, under periodic loading, is therefore not always dissipative.

The configuration of the system is described by the stretch variable $\lambda = a(t)/A$, where $a(t)$ is the current radius and A is the undeformed radius. The equation of motion, as derived by Shah and Humphrey [2], for an arbitrary material having Cauchy stress, $T(\lambda)$, is

$$\left(\frac{\rho H A}{\lambda^2} + \rho_f A^2 \lambda\right)\frac{d^2\lambda}{dt^2} + \frac{3}{2}\rho_f A^2 \left(\frac{d\lambda}{dt}\right)^2$$
$$+ \frac{2}{A}\frac{T(\lambda)}{\lambda} = P_i(t) - P_\infty,$$

where ρ and ρ_f are the densities of the membrane and of the external fluid respectively, H is the undeformed membrane thickness, $P_i(t)$ is the internal pressure, and P_∞ is the constant pressure of the external fluid infinitely far from the sphere. Both the membrane and the external fluid are assumed incompressible so that their densities are constant.

A comparison is made of membrane material models which do and do not exhibit a static bifurcation with respect to the mean internal pressure. The Fung model for biological materials exhibits no bifurcation, while the neoHookean and some Mooney-Rivlin models for incompressible rubber produce a limit bifurcation, a fold catastrophe in the energy, with respect to static internal pressure changes. The dynamics of the Mooney-Rivlin spherical membrane under constant internal pressure has been studied numerically in a few cases by Akkas [3].

The homogeneous case of constant internal pressure, P_m, in the spherical membrane is described by the vectorfield, with $P = P_m - P_\infty$ and $x_1 = \lambda$,

$$\dot{x}_1 = x_2$$
$$\dot{x}_2 = \frac{x_1^2}{\rho H A + \rho_f A^2 x_1^3}\left[-\frac{3}{2}\rho_f A^2 x_2^2 - \frac{2T(x_1)}{Ax_1} + P\right].$$

This is a family of vectorfields indexed by P. Fixed points $(\lambda(P), 0)$ correspond to the static equilibria, $\lambda(P)$, obtained from

$$P = \frac{2}{A\lambda}T(\lambda).$$

The behavior near the fixed points can be investigated using the Jacobian of the vectorfield, putting $\dot{x}_2 = g(x_1, x_2)$,

$$J = \begin{pmatrix} 0 & 1 \\ g_1 & g_2 \end{pmatrix},$$

where

$$g_1 = \frac{x_1(-2\rho H + \rho_f Ax_1^3)}{A(\rho H + \rho_f Ax_1^3)^2}\left[-\frac{3}{2}\rho_f A^2 x_2^2 - \frac{2T(x_1)}{Ax_1} + P\right]$$
$$+ \frac{x_1^2}{\rho H A + \rho_f A^2 x_1^3}\left[\frac{\partial}{\partial x_1}\left(-\frac{2T(x_1)}{Ax_1}\right)\right];$$
$$g_2 = \frac{-3\rho_f A^2 x_1^2 x_2}{\rho H A + \rho_f A^2 x_1^3}.$$

The Jacobian has eigenvalues at fixed points

$$\frac{1}{2}\left(g_2 \pm \sqrt{g_2^2 + 4g_1}\right).$$

The divergence of the vectorfield,

$$\frac{-x_1^2}{\rho H A + \rho_f A^2 x_1^3}3\rho_f A^2 x_2$$

shows that the system is contracting if $x_2 > 0$ and expanding if $x_2 < 0$. Therefore the system is not always dissipative. Recall that always $x_1 > 0$. The divergence also shows, by the Bendixson theorem, that any periodic orbit must intersect $x_2 = 0$ in phase space.

The Fung model is $T(\lambda) = c(C_1 + C_3)(\lambda^2 - 1)\exp[.5(C_1+C_3)(\lambda^2-1)^2]$. The static equilibria for each P are the solutions of the monotonic, increasing, concave up function, for $F = 2c(C_1 + C_3)/A$,

$$P(\lambda) = \frac{F}{\lambda}(\lambda^2 - 1)\exp[.5(C_1 + C_3)(\lambda^2 - 1)^2].$$

Put $C = \rho H A$ and $D = \rho_f A^2$. The vectorfield is

$$\dot{x}_1 = x_2$$
$$\dot{x}_2 = \frac{x_1^2}{C + Dx_1^3}\left[-\frac{3}{2}Dx_2^2 - \frac{F}{x_1}(x_1^2 - 1)\right.$$
$$\left. \exp[.5(C_1 + C_3)(x_1^2 - 1)^2] + P\right].$$

The vectorfield for each fixed P has a single fixed point. Then, $g_1 < 0$ and $g_2 = 0$ at any fixed point. Since the eigenvalues are purely imaginary, each fixed point is a center.

The Hamiltonian for the undamped Fung system at constant pressure, P, is

$$\frac{1}{2}x_2^2 + \frac{c}{\rho H A^2}\exp[0.5(C_1 + C_3)(x_1^2 - 1)^2] - \frac{P}{3\rho H A}x_1^3.$$

Numerical experiments indicate the existence of an asymptotically stable limit cycle under internal pressures of the form $P = P_m + B\sin(\omega t)$. The linearized vectorfield is of the form of a nonhomogeneous Mathieu oscillator, but this equation may not capture the behavior since it is area preserving, while the Fung model is not.

The incompressible Mooney-Rivlin strain energy for the isothermal equilibrium states of a flat membrane is, in terms of the in-plane stretches,

$$c_1(\lambda_1^2 + \lambda_2^2 + \lambda_1^{-2}\lambda_2^{-2} - 3) + c_2(\lambda_1^{-2} + \lambda_2^{-2} + \lambda_1^2\lambda_2^2 - 3)$$

The material is called neoHookean if $c_2 = 0$. The neo-Hookean static equilibrium states for the sphere are

$$P(\lambda) = \frac{4c_1 H}{A}(\lambda^{-1} - \lambda^{-7}).$$

A limit point occurs at $dP/d\lambda = 0$. For any neoHookean material, the bifurcation is at $\lambda = 7^{1/6} = 1.38309$ when $P_c = 0.61973(4c_1 H/A)$. No equilibria exist for $P > P_c$. The function $T(\lambda)/\lambda$, proportional to $P(\lambda)$, is therefore increasing up to the limit point and is then decreasing.

The undamped Mooney-Rivlin constant pressure system has Hamiltonian, for $\Gamma = c_2/c_1$, and $p = P/F$,

$$\frac{1}{2}x_2^2 - p(x_1 - 1) - \frac{3\Gamma}{4}(1 - x_1^2) + \ln x_1 - \left(\frac{1}{6} + \frac{1}{4}\Gamma x_1^2\right)(1 - x_1^{-6}).$$

The full neoHookean dynamic system, with $C = \rho H A$, $D = \rho_f A^2$, and $F = 4c_1 H/A$ has Jacobian entries

$$g_1 = -\frac{F(7x_1^{-6} - 1)}{C + Dx_1^3} + \left(\frac{x_1^2}{C + Dx_1^3} - \frac{3Dx_1^4}{(C + Dx_1^3)^2}\right)$$
$$(P - F(-x_1^{-7} + x_1^{-1}) - 1.5Dx_2^2)$$
$$g_2 = \frac{-3Dx_1^2 x_2}{C + Dx_1^3}.$$

There are no fixed points if $P > P_c$. On the other hand, if $0 < P < P_c$, there are two fixed points with x_1 corresponding to the static equilibria and $x_2 = 0$. The second two terms in g_1 are zero at the fixed points corresponding to a given $P < P_c$. The fixed point less than $x_1 = 7^{1/6}$ is a center since $g_1 < 0$. The fixed point greater than $x_1 = 7^{1/6}$ is a saddle since $g_1 > 0$. This is as expected from the fact that the left hand equilibrium point is statically stable and the right hand equilibrium point is unstable. As P tends towards P_c, the two fixed points approach $(7^{1/6}, 0)$. They annihilate each other at P_c, a saddle-center bifurcation. As P tends to zero, the left hand equilibrium moves towards $x_1 = 1$ and the right hand towards infinity. For negative P, the saddle fixed point disappears and there is a single fixed point, which is a center. But, there is no local bifurcation at $P = 0$.

A normal form at the bifurcation pressure, P_c, arises from translating the fixed point $(7^{1/6}, 0)$ to the origin and then taking the Taylor series to second order,

$$\dot{y}_1 = y_2$$
$$\dot{y}_2 = \frac{7^{1/3}}{C + \sqrt{7}D}\left(\frac{-6F}{7^{7/6}} + P\right) - 1.5\frac{7^{1/3}}{C + \sqrt{7}D}Dy_2^2$$
$$+ \frac{7^{1/6}(2C - \sqrt{7}D)}{(C + \sqrt{7}D)^2}\left(\frac{-6F}{7^{7/6}} + P\right)y_1 + \left[\frac{7^{-1/6}3F}{(C + \sqrt{7}D)}\right.$$
$$+ \left.\frac{(C^2 - 7^{3/2}CD + 7D^2)}{(C + \sqrt{7}D)^3}\left(\frac{-6F}{7^{7/6}} + P\right)\right]y_1^2$$

This is a saddle-center bifurcation. The undamped system $(D = 0)$ for each $0 < P < P_c$ has a homoclinic loop emanating from the saddle point which surrounds the region of periodic orbits about the center point. The addition of the damping does not change the location or type of the fixed points. A periodic forcing function with large enough amplitude may generate transverse homoclinic points by perturbing the loop.

References

[1] H. W. Haslach, Jr., Dynamical effects of degenerate singularities in the potential for mechanical systems, in *Nonlinear Techniques in Structural Dynamic Systems*, Vol. 9 of *Structural Dynamics Systems, Computational Techniques, and Optimization*, ed. C. T. Leondes, International Series in Engineering, Technology and Applied Science, Gordon and Breach, to appear, 1998.

[2] A. D. Shah and J. D. Humphrey (1998). Finite strain elastodynamics of intracranial saccular aneurysms. To appear.

[3] N. Akkas (1978). On the dynamic snap-out instability of inflated non-linear spherical membranes. *Int. J. Non-Linear Mech.* Vol. 13, pp. 177 - 183.

MOTION REDUCTION IN SYSTEMS WITH UNCONTROLLABLE MODES AND/OR NONCOLLOCATED INPUTS: A PERTURBATION-BASED APPROACH

R. Randall Soper, Walter Lacarbonara, Char-Ming Chin,
Ali H. Nayfeh, and Dean T. Mook

Department of Engineering Science and Mechanics, MC 0219

Virginia Polytechnic Institute and State University, Blacksburg, Virginia USA 24061

A new open-loop control strategy applied to a planar pendulum subjected to the most severe combination of base excitations, horizontal motion at the primary-resonance frequency and vertical motion at the principal-parametric resonance frequency, is developed. The control action is typical of many single-input control systems; the control authority in one direction is high and the control authority in the orthogonal direction is zero in a linear sense. Although the action of the controller is linearly decoupled from part of the system dynamics, effects are transferred to the orthogonal direction through nonlinear coupling. Proper detuning of the control input allows the nonlinear coupling to provide control action in the direction that is uncontrollable in a linear sense. The dynamics at reduced orders, determined by a multiple-scales perturbation analysis, suggest the appropriate form of the control detuning. The normal form of the system provides information about how each parameter of the detuning affects the steady-state pendulation of the system. In this case, heuristic arguments are used to reduce the dimension of the unknown detuning parameters to a manageable size. The maximum pendulation angle of the steady-state motion of the system is one of the appropriate metrics of the system response; here it is used as the cost function for evaluation of the optimal detuning gains. Because the size of the design parameter set has been reduced, a simple grid search is employed to find the optimal control.

This work is not the first to examine the effects of multi-frequency excitation on the steady-state amplitude of dynamic systems by using perturbation methods (Nayfeh, 1984). Also an indirect adaptive quenching algorithm for a nonlinear single-degree-of-freedom system subjected to external and/or parametric disturbances with unknown constant system parameters was developed by using a perturbation-based approach (Heydon et al., 1990). Here the importance of transferring energy to uncontrollable modes via nonlinear coupling (through either plant or actuator action) is recognized and explored for control objectives. Application of perturbation techniques to problems of this type provides a unified approach that may be applicable to a broad class of such systems.

The control strategy is referred to as "open loop" because neither the system states nor a

measured output are employed in direct feedback. However, the approach tacitly assumes direct availability of the disturbance levels and relative phases. In practice, these values could be directly measured or estimated through use of an augmented state observer. Determination of the resonant excitation character could be extracted from base excitation measurements by means of phase-locked loop electronics (Algrain et al., 1997).

References

1. Nayfeh, A. H., "Interaction of Fundamental Parametric Resonances with Subharmonic Resonances of Order One-Half," *Proceedings of the 25th Structures, Structural Dynamics and Materials Conference*, Palm Springs, CA, May 14-16, 1984.

2. Nayfeh, A. H., "Quenching of a Primary Resonance by a Combination Resonance of the Additive or Difference Type," *Journal of Sound and Vibration* **97**, 65-73, 1984.

3. Nayfeh, A. H., "Quenching of Primary Resonance by a Superharmonic Resonance," *Journal of Sound and Vibration* **92**, 363-377, 1984.

4. Heydon, B. D., Nayfeh, A. H., and Bauman, W. T., "An Adaptive Quenching Algorithm for a Nonlinear Single-Degree-of-Freedom Sustem," *Nonlinear Dynamics* **1**, 193-208, 1990.

5. Algrain, M., Hardt, S., and Ehlers, D., "A Phase-Lock-Loop-Based Control System For Suppressing Periodic Vibration in Smart Structural Systems," *Smart Materials and Structures* **6**, 10-22, 1997.

Post-Buckling Analysis of Nonlinear Dynamical Thick Beam Model and Dual Variational Principles

David Yang Gao

Department of Mathematics,
Virginia Polytechnic Institute and State University
Blacksburg, VA 24061, E-mail: gao@math.vt.edu

ABSTRACT

The study of nonlinear dynamic beam theory has a long history. Although many large deformation beam theories have been developed, engineers are still looking for some simple but useful models for general engineering problems. It is known that the effect of transverse shear strain on the bending solutions cannot be neglected when dealing with thick beams or sandwich beams with low shear modulus, because this effect becomes relatively significant. In order to study the shear control of nonlinear thick beams subjected to arbitrary loading systems, a fourth order nonlinear beam model was proposed recently [1]:

$$EI(w_{,xxxx} - \alpha w_{,x}^2 w_{,xx} + \lambda w_{,xx}) = f(x) + E \int_{-h}^{h} y v_{,xxx} dy \qquad (1)$$

$$v_{,xx} + \beta v_{,yy} = y w_{,xxx}, \qquad (2)$$

where $\alpha = 3h(1 - \nu^2) > 0$ and $\beta = (1 - \nu)/2 > 0$ are constants. The shear deformation $v(x, y)$ is assumed to be an odd function of y. Hence, this beam model can only handle special external shear load on the top and bottom of the beam.

In the present paper, a new second order nonlinear dynamical beam theory is proposed as the following:

$$\xi_{,xx} + \beta \xi_{,yy} = -(1 + \nu) w_{,x} w_{,xx} + \rho \xi_{,tt}, \qquad (3)$$

$$(3(1 + \nu) w_{,x}^2 + \beta) w_{,xx} + \frac{1}{2h} \int_{-h}^{h} ((1 + \nu) \xi_{,x} w_{,x} + \beta \xi_{,y})_{,x} dy + f = \bar{\rho} w_{,tt}, \qquad (4)$$

$$\xi_{,y}(x, \pm h, t) = -w_{,x} \pm q^{\pm}(x, t), \qquad (5)$$

where $\xi(x, y, t)$ is horizontal displacement of the beam, $f(x, t)$ is the lateral load on the beam, $q^+(x, t)$ and $q^-(x, t)$ are shear loads on the top $(y = h)$ and bottom $(y = -h)$ of the beam, respectively. In dynamic buckling analysis, if the beam is subjected to a compressive load λ_o at $x = L$, the horizontal displacement can be written as

$$\xi(x, y, t) = -px - \int \frac{1 + \nu}{2} w_{,x}^2 dx + v(x, y, t)$$

where $v(x, y, t)$ is a pure shear deformation. Then the governing equations for the dynamic buckling problem in large deformed thick beam theory are

$$v_{,xx} + \beta v_{,yy} = 0 \quad \forall (x, y) \in \Omega,$$

$$(\frac{3\alpha^2}{2} w_{,x}^2 + \beta - \lambda \alpha) w_{,xx} + \frac{\beta}{2h} v_{,x}(x, y)|_{y=\pm h} + f = \rho w_{,tt}$$

$$v_y(x, \pm h) = -w_{,x}(x) \pm q^{\pm}(x, t) \quad \forall x \in [0, L],$$

where $\alpha = \sqrt{1 - \nu^2}$, and $\lambda > 0$ is a parameter. This is a coupled nonlinear dynamic problem. For a given periodical external load $f(x, t)$ and $\lambda > 0$, this second order nonlinear system may have chaotic solutions. The total potential of this dynamic buckling problem is a nonconvex functional

$$P(v, w) = \frac{E}{2} \int_\Omega [(v_{,x} + \frac{1}{2}\alpha w_{,x}^2 - \lambda)^2 + \beta(v_{,y} + w_{,x})^2] d\Omega - \int_0^L fw \, dx. \qquad (6)$$

If the shear effect is ignored, the total potential $P(w)$ reduces to the well-known van der Waal's double-well energy. The associated dynamical system is a Duffing-type equation.

Based on the general duality theory developed in nonconvex finite deformation mechanics [2], a pure complementary energy extremum principle (involving the Kirchhoff type stress only) is constructed. An interesting triality theorem in dynamical buckling analysis is discovered. The speaker will show that in unstable systems, if the so-called complementary gap function, introduced by Gao and Strang in 1989, is positive, this complementary energy principle gives a global stable buckling state. However, if the gap function is negative, this general complementary energy may have two so-called super-critical points The one which minimizes the pure complementary energy gives another local stable buckling state. The other super-critical point, which maximizes the complementary energy is a unstable buckling state.

References

[1] Gao, David Y. and Russell, David L. (1996), Finite deformation extended beam theory and nonlinear buckling analysis, in *Contemporary Research in the Mathematics and Mechanics of Materials* Ed. by R.C. Batra and M.F. Beatty, CIMNE, Barcelona, Spain, pp. 430-441.

[2] Gao, David Y. (1997), Dual extremum principles in finite deformation theory with applications to post-buckling analysis of extended nonlinear beam model, *Appl. Mech. Reviews*, **50** (11), part 2, November, S64-S71.

AUTHOR INDEX TO SESSION PAPERS